EPIDERMAL ADHESION MOLECULES IN HUMAN WOUNDS AND DEVELOPMENT OF A TISSUE EXPLANT CULTURE SYSTEM TO INVESTIGATE MODIFICATION OF THEIR EXPRESSION.

WILLIAM DYLAN JONES

PhD Thesis

Submitted To The University of Wales College of Medicine

May 2004

ACKNOWLEDGEMENTS

I cannot thank Professor Harding enough for his overwhelming support and encouragement throughout the period of this study. Thanks are also given for his guidance during the writing of the thesis. I also thank Dr Keith Moore for facilitating my access to the laboratories and coordinating my employment during the period of study. His original ideas also formed the basis for the development of the tissue explant culture system and his technical support during the laboratory investigations as well as the writing of the thesis is gratefully acknowledged.

The financial support received from Smith & Nephew, which facilitated my employment with The Wound Healing Research Unit is also gratefully acknowledged. In particular thanks must also be given to Dr Sarah Brown, a statistician working for Smith & Nephew who carried out the analysis of variance on the data from the tissue explant culture system.

I also wish to thank Mr Dean Boyce for his encouragement and his advice in writing the thesis.

Finally, I give thanks to Catrin my wife for her dedicated love and support throughout the period of writing the thesis.

TABLE OF CONTENTS

LIST OF FIGURES AND TABLES III

SUMMARY XI

ABBREVIATIONS XII

1.0 INTRODUCTION 1

1.1 OVERVIEW OF MECHANISMS INVOLVED IN TISSUE REPAIR 1
1.1.1 Haemostasis 8
1.1.2 Inflammation 13
1.1.3 Neutrophils 15
1.1.4 Macrophages: Inflammation , Granulation and Fibrosis 16
1.1.5 T Lymphocytes 24
1.1.6 Angiogenesis 27

1.2 CELL ADHESION MOLECULES 31
1.2.1 Expression of integrins 35
1.2.2 Extracellular structure and ligand interaction 37
1.2.3 Intracellular interactions 38
1.2.4 Integrins in wound healing 39

1.3 MATRIX METALLOPROTINASES 41
1.3.1 Regulation of MMP activity 45
1.3.2 MMPs and Wound Healing 48
1.3.3 MMP-2 (Gelatinase A) and MMP-9 (Gelatinase B) 50

1.4 HYPOXIA AND WOUND HEALING 53

1.5 MODELS OF WOUND HEALING 57

1.6 WOUND HEALING AND AGEING 66

2.0 AIMS OF THIS THESIS 72

3.0 METHODS 73

3.1 IMMUNOHISTOCHEMICAL CHARACTERISATION OF CELL ADHESION MOLECULE EXPRESSION 73
3.1.1 Sources of Tissue 73
3.1.2 A model of normal acute wound healing 73
3.1.3 Additional source of acute wound tissue: The Pilonidal Sinus Excision Wound 74
3.1.4 A model of chronic wound healing 75
3.1.5 Preparation of specimens and cryostat cutting 76
3.1.6 Staining technique 76

3.2.0 Tissue explant culture 78
3.2.1 Explant culture 78
3.2.2 Cytokine analysis by ELISA plate assay 79
3.2.4 Metalloproteinase analysis 80
3.2.5 Immunohistological analysis 86
3.2.6 Microscopy analysis 88

4.0 RESULTS **90**

4.1.0 EPIDERMAL INTEGRIN EXPRESSION AND PROVISIONAL MATRIX DEPOSITION IN A SURGICALLY INDUCED ACUTE WOUND MODEL **90**
4.1.1 Immunolocalisation of $\alpha_5\beta_1$ expression 90
4.1.2 Immunolocalisation of the αV integrin subunit expression 93
4.1.3 Immunolocalisation of $\alpha 2\beta_1$ expression 96
4.1.4 Immunolocalisation of $\alpha_3\beta_1$ expression 100
4.1.5 Immunolocalisation of Serum Fibronectin in a human acute wound 102
4.1.6 Immunolocalisation of cellular fibronectin in a human acute wound 104
4.1.7 Immunolocalisation of Vitronectin within human acute wound tissue 107

4.2.0 β_4, E-Cadherin and Syndecan-1 Expression in Pilonidal Excision Acute Wound Tissue **110**
4.2.1 Immunolocalisation of β_4 integrin subunit expression 110
4.2.2 Immunolocalisation of syndecan-1 expression 113
4.2.3 Immunolocalisation of E-cadherin expression 115

4.3.0 EPIDERMAL INTEGRIN EXPRESSION AND MATRIX PROTEIN EXPRESSION IN CHRONIC WOUNDS **118**
4.3.1 Immunolocalisation of $\alpha_5\beta_1$ within chronic wound tissue 119
4.3.2 Immunolocalisation of $\alpha_2\beta_1$ within chronic wound tissue 121
4.3.3 Immunolocalisation of $\alpha_3\beta_1$ within chronic wound tissue 123
4.3.4 Immunolocalisation of α_V integrin subunit within chronic wound tissue 124
4.3.5 Immunolocalisation of β_4 within chronic wound tissue 125
4.3.6 Immunolocalisation of E-cadherin within chronic wound tissue 127
4.3.7 Immunolocalisation of syndecan-1 within chronic wound tissue 129

4.4.0 TISSUE EXPLANT CULTURE: An *ex vivo* model of wound healing **131**
4.4.1.0: Cytokine/MMP levels present in explant tissue as markers of its inherent variability 133
4.4.1.1 Interleukin-1 (IL-1) 134
4.4.1.2 Interleukin-8 (IL-8) 144
4.4.1.3 Metalloproteinase 2 (MMP-2) 159
4.4.1.4: Metalloproteinase 9 (MMP-9) 171
4.4.1.5 Transforming Growth Factor-β 183
4.4.1.6 Vascular Endothelial Growth Factor 195
4.4.1.7: Histology of control (time 0 hours) and 8hour explant culture tissue 207
4.4.1.8 Analysis of LDH Levels as a Marker of Cell Death 213
4.4.2.0 Effect of changing oxygenation levels on IL-8 and TGF-β levels in wound bed tissue. 214
4.4.2.1 Effect of changing oxygen concentrations on TGF-β Levels 215
4.4.2.2 Effect of changing oxygen concentrations on IL-8 levels 222
4.4.3.0 Stimulation of edge biopsies with LPS 226
4.4.3.1 Effect of LPS on IL-1β and TNFα levels 226
4.4.3.2 Effect of LPS on $\alpha_5\beta_1$ integrin expression. 227

5.0 DISCUSSION **229**

7.0 APPENDICES **263**

Appendix I: Record of Biopsies **263**

Appendix II: Reagent list for quantitation of MMPs by Zymography **265**

8.0 REFERENCES **268**

LIST OF FIGURES AND TABLES

Figure 1.0: Diagramatic representation of the overlapping phases of wound healing (below) and the timing of the influx of cellular constituents into the wound site during each of these phases (above). Reproduced from The Wound Programme, University of Dundee (9) 3

Figure 1.1: Diagrammatic representation of the intrinsic and extrinsic pathways of the clotting cascade. Oral anticoagulants can act on clotting factors II, VII, IX and X shown in grey boxes. PL = -ve charged phospholipid, ATIII = antithrombin III and LMWHs = low molecular weight heparins. Reproduced from (36) 10

Figure 1.3: Diagrammatic representation of the integrin and cadherin classes of adhesion receptors. They are depicted in association with their cytoskeletal components and their typical extracellular ligands. Reproduced from(140,141)Tal-talin, Pax-paxillin, Vin-vinculin, FAK-focal adhesion kinase, Src-tyrosine kinase, CAS-docking protein. 33

Figure 1.4: Diagrammatic illustration of the potential intracellular signalling pathways activated on integrin binding to their ECM Ligand or growth factor. Reproduced from (162). FAK = focal adhesion kinase, MLCK = myosin light chain kinase and PI3K = phosphoinositide-3-kinase. Red boxes = small GTPases, green boxes = protein kinases and yellow boxes cytoskeletal proteins. 39

Table 1.1: List of human MMPs and their substrates. Reproduced from reference (172) 42

Figure 1.5: Diagrammatic representation of the domain structure of the various subtypes of MMPs. Reproduced from reference (172) 44

Table 3.1: List of monoclonal antibodies used to immunolocalise matrix proteins and cell adhesion molecules 78

Figure 3.1: Example of gelatin zymogram run to measure MMP-2/-9 in supernatants from the explant culture of wound bed and edge tissue. STD = Standards. Red box = background analysis. White box = MMP quantitation 84

Figure 3.2: MMP-2 standard curve. Standards ran over a concentration range of 1, 2, 4, 8, 12, 16, 20 and 32ng/ml as depicted by the cleared bands on the Zymogram included below. 85

Figure 3.3: MMP-9 standard curve Standards ran over a concentration range of 1, 2, 4, 8, 12, 16, 20 and 32ng/ml as depicted by the cleared bands on the Zymogram included below. 85

Figure 3.4: Diagrammatic illustration of the Modulator Incubator Chambers - 101™ (Billups-Rothenberg inc., USA) 87

Table 3.2: List of monoclonal antibodies used to immunolocalise leucocyte cells .. 87

Figure 4.1.1: Immunohistochemical localisation of $\alpha_5\beta_1$ integrin in normal skin (scale bar 100μm) 91

Figure 4.1.2: Expression of α5β1 within wound edge epidermis 24 hours post wounding (scale bar = 100μm) 91

Figure 4.1.3: Immunolocalisation of $\alpha_5\beta_1$ expression within wound edge epidermis 72 hours post wounding (scale bar = 100μm). MT = migrating tip, GT = granulation tissue 92

Figure 4.2.1: Immunolocalisation of α_V integrin subunit espression in normal skin (scale bar = 100μm) 94

Figure 4.2.2: Immunolocalisation of α_V integrin subunit expression 48 hours post wounding (scale bar = 100μm). MT - migrating tip, GT – granulation tissue... 95
Figure 4.2.3: Immunolocalisation of α_V integrin subunit expression 96 hours post wounding. (a) Low power image demonstrating both wound edges (scale bar = 100μm). (b) Higher power image of wound edge as indicated by the arrow (scale bar = 200μm)..... 95
Figure 4.3.1: $\alpha_2\beta_1$ expression in normal skin (scale bar = 100μm). 97
Figure 4.3.2: $\alpha_2\beta_1$ expression within acute wound tissue 48 hours post wounding (scale bar = 100μm). GT – granulation tissue, MT – migrating tip 98
Figure 4.3.3: $\alpha_2\beta_1$ expression 72 hours post wounding (scale bar = 100μm). GT – granulation tissue..... 99
Figure 4.3.4: $\alpha_2\beta_1$ expression 96 hours post wounding (scale bar = 100μm). GT – granulation tissue, MT – migrating tip, AE – adjacent epidermis. 99
Figure 4.4.1: $\alpha_3\beta_1$ expression in normal skin (scale bar = 100μm) 101
Figure 4.4.2: Expression of $\alpha_3\beta_1$ in epidermis at the edge of a 96hour acute wound (scale bar = 50μm)..... 102
Figure 4.5.1: Immunolocalisation of Serum Fibronectin in normal skin (scale bar = 100μm). 103
Figure 4.5.2: Immunolocalisation of serum fibronectin within 72 hour acute wound tissue representing its pattern of deposition over the 96 hour healing time course (scale bar = 100μm). WE – wound edge, GT – granulation tissue 104
Figure 4.6.1: Immunolocalisation of cellular fibronectin deposition in normal skin. (scale bar = 50μm)..... 105
Figure 4.6.2: Immunolocalisation of cellular fibronectin deposition within acute wound tissue at 96 hours post wounding (scale bar = 100μm). GT – granulation tissue..... 106
Figure 4.6.3: Higher power image of cellular fibronectin deposition under the migrating epidermis presented previously in figure 4.6.2 (scale bar = 100μm) 106
Figure 4.7.1: Deposition of vitronectin in normal skin. (Scale bar =100μm)..... 108
Figure 4.7.2: Immunolocalisation of vitronectin deposition in a 24 hour acute wound (scale bar = 100μm). WE – wound edge, LE – leading edge..... 109
Figure 4.7.3: Immunolocalisation of vitronectin deposition at the edge of a 96hour acute wound (scale bar = 100μm). LE – leading edge 109
Figure 4.8.1: β4 integrin subunit expression in normal skin (scale bar = 50μm) ... 111
Figure 4.8.2: Low power image of β_4 integrin subunit expression in a section of healing pilonidal sinus wound edge tissue (scale bar = 200μm) AE – adjacent epidermis, WE – wound edge, GT - Granulation Tissue. 112
Figure 4.8.3: Higher power image of figure 4.8.2(scale bar = 100μm) MT – migrating tip, GT – granulation tissue..... 112
Figure 4.9.1: Syndecan-1 expression in normal skin (scale bar = 100μm)..... 114
Figure 4.9.2 Syndecan-1 expression within migrating epidermis at the edge of a healing acute pilonidal sinus wound (scale bar = 100μm). MT – migrating tip, GT – granulation tissue. 115
Figure 4.10.1: Immunohistochemical localisation of E-cadherin using the MCA1482 monoclonal antibody within normal human adult skin (scale bar = 50μm)..... 116
Figure 4.10.2: Low power image of E-cadherin expression within epidermis at the edge of an acute healing pilonidal excision wound (scale bar = 200μm). 117

Figure 4.10.3: High power image of the migrating tip already depicted above in figure 4.10.2 (scale bar = 100μm) 117
Figure 4.10.4: High power image of the adjacent epidermis already depicted in figure 4.10.2 (scale bar = 50μm). 118
Figure 4.11.1: Immunolocalisation of $\alpha_5\beta_1$ within chronic wound tissue at the edge of a chronic non healing leg ulcer (scale bar = 200μm). AE – adjacent epidermis, GT – granulation tissue 120
Figure 4.12.1: Immunolocalisation of $\alpha_2\beta_1$ expression within tissue at the edge of a chronic venous leg ulcer (scale bar =200μm) 122
Figure 4.13.1: Immunolocalisation of $\alpha_3\beta_1$ within chronic wound tissue at the edge of a chronic non healing leg ulcer (scale bar = 200μm). DE – distal epidermis, WE – wound edge 123
Figure 4.13.2: Higher power image of the epidermis at the wound edge presented previously in figure 4.13.1 (scale bar = 100μm) 124
Figure 4.14.1: Immunolocalisation of α_V integrin subunit within epidermis at the edge of a chronic non healing venous leg ulcer (scale bar = 100μm). WE – wound edge 125
Figure 4.15.1: β_4 integrin subunit expression in chronic venous leg ulcer tissue (scale bar = 100μm). GT = Granulation Tissue, MT = Migrating Tip 126
Figure 4.16.1: E-cadherin expression within chronic wound edge epidermis where expression was maintain in the suprabasal layers (scale bar = 200μm) 127
Figure 4.16.2: Chronic wound edge epidermis where expression was decreased to a similar level to that seen at the epidermal edge of acute wounds (scale bar = 50μm) 128
Figure 4.17.1: Low power image of syndecan-1 expression within epidermis at the edge of a chronic venous leg ulcer (scale bar = 200μm). WE – wound edge .. 129
Table 4.1: Descriptive statistic for data on 8 tissue segments from 4 wound edge biopsies. Data is recorded in units of pg/ml/mg of tissue 135
Figure 4.18.1: IL-1 levels in 8 segments from 4 wound edge biopsies 135
Figure 4.18.2: IL-1 levels in tissue segments from 4 individual wound edge biopsies. Each biopsy corresponds to those previously depicted in figure 4.18.1. Data is recorded in units of pg/ml/mg of tissue. 136
Table 4.2: Descriptive statistic characterising data spread around mean IL-1 levels detected in each wound edge biopsy. Data is recorded in units of pg/ml/mg of tissue. 137
Figure 4.18.3: IL-1 mean levels in 4 individual wound edge biopsies 137
Table 4.3: Descriptive statistics characterising data spread around mean IL-1 levels in 12 segments from 4 wound bed biopsies. . Data is recorded in units of pg/ml/mg of tissue. 139
Figure 4.18.4: Scatter graph showing IL-1 levels in segments from n = 4 bed biopsies 139
Figure 4.18.5: Line graphs showing IL-1 levels in 4 individual wound bed biopsies. 140
Table 4.4: Descriptive statistics characterising data spread around mean IL-1β levels present in 4 individual wound bed biopsies. . Data is recorded in units of pg/ml/mg of tissue. 142
Figure 4.18.6: IL-1 mean levels in 4 individual wound bed biopsies 142
Figure 4.18.7 (a): IL-1 levels in n = 4 edge and n = 4 bed biopsies from chronic venous leg ulcers 143

Figure 4.18.7 (b): Il-1 levels in n = 4 edge and n = 4 bed biopsies from chronic venous leg ulcers 143
Figure 4.19.1: Scatter graph displaying IL8 levels present in 10 tissue segments taken from 5 wound edge biopsies 145
Table 4.6: Analysis of variance on IL-8 levels detected in 5 wound edge biopsies. 146
Figure 4.19.2: Line graphs depicting IL-8 levels detected in each of the tissue segments from the 5 individual wound edge biopsies 147
Table 4.7: Descriptive statistics characterising the data spread around the mean IL-8 levels present in 5 wound edge biopsies. . Data is recorded in units of pg/ml/mg of tissue 149
Figure 4.19.3: Line graph depicting mean IL-8 levels present in 5 wound edge biopsies. Log_{10} transformation of the data was applied to account for the wide range in values 149
Table 4.8: Descriptive statistic characterising the data spread around the mean IL-8 levels present in 24 tissue segments taken from 8 wound bed biopsies. Data is recorded in units of pg/ml/mg of tissue 150
Figure 4.19.4: Scatter graph depicting the data spread for IL-8 levels detected in 24 tissue segments taken from 8 wound bed biopsies 151
Table 4.9: Analysis of variance of the IL-8 levels present in the 8 wound bed biopsies. A1 = analysis of biopsies 1-4. A2 = analysis of biopsies 5-8 152
Figure 4.19.5: Line graphs depicting the levels of IL-8 detected in the 3 tissue segments taken from each of the 8 wound bed biopsies. 152
Table 4.10: Descriptive statistics characterising the data spread around the mean IL-8 levels present in the 8 wound bed biopsies. Data is recorded in units of pg/ml/mg of tissue. 154
Figure 4.19.6: Line graphs depicting the mean IL-8 levels present in each of the 8 individual wound bed biopsies. Due to the wide range of the data a Log_{10} was performed on the data 155
Figure 4.19.7 (a): Bar graph depicting overall mean IL-8 levels present in the 8 wound bed and 5 wound edge biopsies. The line plot depicts the overall mean IL-8 levels present in both wound edge and bed biopsies 156
Figure 4.19.7 (b): Box plot allowing a comparison of IL-8 levels present in wound edge and bed biopsies at all time points depicted above in figure 14 (a) 157
Table 4.11: Descriptive statistics characterising the data spread around the mean MMP-2 levels present in 8 tissue segments taken from 4 wound edge biopsies. Data is recorded in units of pg/ml/mg of tissue 160
Figure 4.20.1: Scatter graph depicting the data spread for MMP-2 levels detected in 8 tissue segments from 4 wound edge biopsies 161
Figure 4.20.2: Line graphs depicting MMP 2 levels detected in tissue segments taken from 4 wound edge biopsies 161
Table 4.12: Descriptive statistics characterising the data spread around the overall mean levels of MMP-2 present in 4 wound edge biopsies Data is recorded in units of pg/ml/mg of tissue. 162
Figure 4.20.3: Line graph depicting mean MMP 2 levels present in 4 individual wound edge biopsies 162
Table 4.13: Analysis of variance (ANOVA) on MMP-2 levels detected in 4 wound edge biopsies. 163

Table 4.14: Descriptive statistics characterising the data spread around mean MMP-2 levels present in 8 tissue segments taken from 4 wound edge biopsies Data is recorded in units of pg/ml/mg of tissue. 165
Figure 4.20.4: Scatter graph depicting MMP2 levels detected in 12 segments from 4 wound bed biopsies 165
Figure 4.20.5: Line graphs depicting MMP-2 levels in tissue segments from each of the 4 individual wound bed biopsies 166
Table 4.15: Descriptive statistics characterising the data spread around the mean MMP-2 levels present in each of the 4 wound bed biopsies. Data is recorded in units of pg/ml/mg of tissue. 167
Figure 4.20.6: Line graph depicting mean MMP-2 levels present in 4 individual wound bed biopsies 167
Table 4.16: Analysis of variance on MMP-2 levels present in 4 wound bed biopsies 168
Figure 4.20.7(a): Bar graph depicting overall mean MMP-2 levels present in n = 4 wound bed or n = 4 wound edge biopsies. A plot of overall mean levels present in both wound edge and bed biopsies is also included. 170
Figure 4.20.7(b): Box plot representing overall levels of MMP-2 present in wound edge or bed tissue at all the time points during the 8 hour culture. MMP-2 levels are depicted as mean median values along with the associated range for each dataset 170
Table 4.17: Descriptive statistics characterising the data spread around the mean MMP-9 levels detected in 8 tissue segments taken from 4 wound edge biopsies. Data is recorded in units of pg/ml/mg of tissue 171
Figure 4.21.1: Scatter graph of MMP-9 levels detected in 8 tissue segments taken from 4 wound edge biopsies 172
Figure 4.21.2: Line graph depicting MMP-9 levels present in tissue segments taken from 4 wound edge biopsies 173
Table 4.18: Descriptive statistics characterising data spread around mean MMP-9 levels present in 4 wound edge biopsies. Data is recorded in units of pg/ml/mg of tissue 174
Figure 4.21.3: Line graph depicting mean MMP-9 levels present in each of the 4 individual wound edge biopsies. 175
Table 4.19: Analysis of variance of MMP-9 levels detected in 4 wound edge biopsies. 175
Table 4.20: Descriptive statistic characterising data spread around mean MMP-9 levels present in 12 tissue segments from 4 wound bed biopsies. Data is recorded in units of pg/ml/mg of tissue. 177
Figure 4.21.4: Scatter graph depicting MMP-9 levels present in 12 tissue segments taken from 4 wound bed biopsies. 177
Figure 4.21.5: Line graphs depicting MMP-9 levels present in tissue segments obtained from 4 individual wound bed biopsies 178
Table 4.21: Descriptive statistic characterising data spread around mean MMP-9 levels present in 4 wound bed biopsies. Data is recorded in units of pg/ml/mg of tissue. 179
Figure 4.21.6: Line graph depicting mean MMP-9 levels present in each of the 4 wound bed biopsies 179
Table 4.22: Analysis of variance on MMP-9 levels present in 4 wound bed biopsies. 180

Figure 4.21.7(a): Bar graph depicting mean MMP-9 levels present in 4 wound edge or wound bed biopsies. A plot of mean MMP-9 levels present in both biopsy tissue types is also displayed 182
Figure 4.21.7(b): Overall levels of MMP-9 present in wound edge or bed tissue at all the time points during the 8 hour culture. Mean MMP-9 levels are plotted with their 95% CIs. Box plots represent the range and median values for each dataset 182
Table 4.23: Descriptive statistic characterising data spread around mean TGFβ levels present in 8 tissue segments taken from 4 wound edge biopsies. Data is recorded in units of pg/ml/mg of tissue. 185
Figure 4.22.1: Scatter graph depicting TGFβ levels present in 8 tissue segments taken from 4 wound edge biopsies. 185
Figure 4.22.2: Line graph depicting TGFβ levels present in tissue segments from 4 individual wound edge biopsies 186
Table 4.23: Descriptive statistic characterising data spread around mean TGFβ levels present in 4 wound edge biopsies. Data is recorded in units of pg/ml/mg of tissue 186
Figure 4.22.3: Line graph depicting mean TGFβ levels present in 4 individual wound edge biopsies 187
Table 4.25: Descriptive statistics characterising data spread around mean TGFβ levels present in 8 tissue segments taken from 4 wound bed biopsies. Data is recorded in units of pg/ml/mg of tissue. 190
Figure 4.22.4: Scatter graph depicting data spread of TGFβ levels present in 12 tissue segments taken from 4 wound bed biopsies 190
Figure 4.22.5: Line graphs depicting TGFβ levels present in tissue segments taken from 4 individual wound bed biopsies 191
Table 4.26: Descriptive statistic characterising data spread around mean TGFβ levels present in each of the 4 wound bed biopsies. Data is recorded in units of pg/ml/mg of tissue. 191
Figure 4.22.6: Line graph depicting mean TGFβ levels present in each of the 4 wound bed biopsies 192
Table 4.27: ANOV for TGF-β levels present in wound edge and bed tissue over 8 hours. Note variance component inestimable at 2, 6 and 8 hours 192
Figure 4.22.7: Bar graph depicting overall mean TGFβ levels present in 4 wound edge or wound bed biopsies. A plot of the mean value present in both types of tissue is also displayed 194
Figure 4.22.7 (b): Overall levels of TGFβ present in wound edge or bed tissue at all the time points during the 8 hour culture. Mean TGFβ levels are plotted with their 95% CIs. Box plots represent the range and median values for each dataset 194
Table 4.28: Descriptive statistics characterising data spread around mean VEGF levels present in 8 tissue segments taken from 4 wound edge biopsies. Data is recorded in units of pg/ml/mg of tissue. 196
Figure 4.23.1: Scatter graph depicting data spread of VEGF levels present in 8 tissue segments taken from 4 wound edge biopsies 196
Figure 4.23.2: Line graphs depicting VEGF levels present in tissue segments taken from 4 individual wound edge biopsies 197

Table 4.29 Descriptive statistic characterising data spread around mean VEGF levels present in each of the 4 wound edge biopsies. Data is recorded in units of pg/ml/mg of tissue. 198
Figure 4.23.3: Line graphs depicting VEGF levels present in tissue segments taken from 4 individual wound edge biopsies 199
Table 4.30: Descriptive statistic characterising data spread around mean VEGF levels present in each of the 4 wound bed biopsies. Data is recorded in units of pg/ml/mg of tissue. 200
Figure 4.23.4: Scatter graph depicting data spread of VEGF levels present in 12 tissue segments taken from 4 wound bed biopsies 200
Figure 4.23.5: Line graphs depicting VEGF levels present in tissue segments taken from 4 individual wound bed biopsies 202
Table 4.31: Descriptive statistic characterising data spread around mean VEGF levels present in each of the 4 wound bed biopsies. Data is recorded in units of pg/ml/mg of tissue. 203
Figure 4.23.6: Line graph depicting mean VEGF levels present in each of the 4 wound bed biopsies 204
Table 4.32: Analysis of variance for VEGF levels present in wound edge and bed tissue over 8 hours. 204
Figure 4.23.7(a): Bar graph depicting overall mean VEGF levels present in 4 wound edge or wound bed biopsies. A plot of the mean value present in both types of tissue is also displayed 205
Figure 4.23.7(b): Overall levels of VEGF present in wound edge or bed tissue at all the time points during the 8 hour culture. Mean VEGF levels are plotted with their 95% CIs. Box plots represent the range and median values for each dataset 206
Table 4.33: Power calculations of number of biopsy required for further investigation 206
Table 4.34: Leucocyte cell numbers in chronic wound edge and bed biopsies recorded as mean number of cells per x40 field of view. Figures in parantheses represent the range (R) and standard deviation (SD). NS = not stained 210
Table 4.35: Leucocyte cell numbers in chronic wound edge and bed biopsies recorded as mean number of cells per x40 field of view. Figures in parantheses represent the range (R) and standard deviation (SD). NS = not stained 211
Table 4.36 Leucocyte cell numbers in chronic wound edge and bed biopsies recorded as mean number of cells per x40 field of view. Figures in parantheses represent the range (R) and standard deviation (SD). NS = not stained 211
Table 4.37 Leucocyte cell numbers in chronic wound edge and bed biopsies recorded as mean number of cells per x40 field of view. Figures in parantheses represent the range (R) and standard deviation (SD). NS = not stained 211
Figure 4.24.1: Mean T lymphocyte numbers present in chronic wound edge and bed biopsies identified by their expression of the CD3 surface marker. Cell numbers are recorded as mean number of cells per x40 field of view 212
Figure 4.24.2: CD4 expressing T helper cell numbers and CD8 expressing T suppressor cell numbers present in chronic wound edge and bed biopsies. . Cell numbers are recorded as mean number of cells per x40 field of view. CD4/CD8 ratios are also recorded above each edge or bed biopsy (RT=Ratio). 212
Figure 4.25.1: LDH levels measured over a 12 hour culture period in 4 wound bed tissue segments placed in 0%, 10%, 20% and 95% oxygen 213

Figure 4.26.1: TGF-β levels in 8 individual wound bed biopsies with 4 segments from each allocated for culture in 0%, 10%, 20% and 95% oxygen after 4 hours. In biopsy 3 an extra segment is included providing data on culture in atmospheric air. 218
Table 4.39: Mean TGF-*β* levels at all Oxygen concentrations (95% CIs of the mean). 219
Table 4.40: Mean change in TGF-β levels between 4 and 8 hours for each oxygen concentration adjusting for expression at 4 hours. 220
Table 4.41: Mean change in TGF-β levels between 4 and 8 hours at each oxygen concentration. 220
Table 4.42: Mean change in TGF-β levels between 4 and 12 hours at each oxygen concentration, adjusting for expression at 4 hours 220
Table 4.43: Mean change in TGF-β levels between 4 and 12 hours at each oxygen concentration, without adjusting for expression at 4 hours 220
Figure 4.26.2: Scatter graph depicting the spread of TGF-β levels present in 32 segments taken from 8 biopsies cultured over 12 hours. One tissue segment from each biopsy was allocated for culture with either 0%, 10%, 20% or 95% oxygen after the 4 hour control period 221
Figure 4.27.1: IL-8 levels in 6 individual wound bed biopsies with 4 segments from each allocated for culture in 0%, 10%, 20% and 95% oxygen after 4 hours. In biopsy 2 & 3 an extra segment is included providing data on culture in atmospheric air. 223
Table 4.44: Mean IL-8 levels at all Oxygen concentrations (95% CIs of the mean). 224
Table 4.45: Mean change in IL-8 levels between 4 and 8 hours at each oxygen concentration 224
Table 4.46: Mean change in IL-8 levels between 4 and 12 hours at each oxygen concentration 225
Figure 4.27.2: Scatter graph depicting the spread of IL-8 levels present in 24 segments taken from 6 biopsies cultured over 12 hours. One tissue segment from each biopsy was allocated for culture in either 0%, 10%, 20% or 95% oxygen after the 4 hour control period. 225
Table 4.47: Levels of IL-1β and TNFα present in a wound edge biopsy split into a control T0 histology tissue segment a T24hr tissue segment cultured in normal medium and T24hr tissue segment cultured in medium containing LPS. The level of $\alpha_5\beta_1$ integrin expression in the wound edge epidermis was also recorded. + = limited expression +++ = marked expression ± = no change 227
Figure 4.28.1: $\alpha_5\beta_1$ immunoreactivity within wound edge tissue taken from chronic VLU (reactivity indicated by arrows). a) T0hr control (scale bar = 100μm). b) T24hr placed in normal culture medium (scale bar =50μm) c) T24hr stimulated with LPS (scale bar = 25μm) 228

SUMMARY

When cutaneous injury involves disruption of the basement membrane, keratinocytes must disassemble their complex attachment to it, enabling lateral migration over a wound surface consisting of a new provisional matrix. Integrin cell adhesion molecules have already been characterised as prime mediators of this process in experimental human wounds. However, very little is known about the role played by integrins as well as other epidermal adhesion molecules such as syndecans in more complex chronic wounds.

In this study, a human model of rapidly healing surgically induced wounds and pilonidal excision wound tissue was used to establish the previously documented expression of epidermal adhesion molecules in the acute healing process. Chronic venous leg ulcer wound tissue was then taken as representing the process of chronic wounding and used to investigate its effect on these adhesion molecules.

Differences were found between the expression of adhesion molecules in acute and chronic wounds. In particular $\alpha_5\beta_1$ expression was decreased in chronic wound epidermis. As a result, a tissue explant culture system was developed to investigate the possibility of modifying its expression on chronic wound keratinocytes. Characterisation of venous leg ulcer explant tissue within this system highlighted the inherent heterogeneity of the tissue, leading to a large degree of variability in the levels of analytes such as IL-8 measured within it. Pilot experiments with two biopsies suggested that $\alpha_5\beta_1$ expression could be up regulated on chronic wound keratinocytes in response to an inflammatory stimulus. However, further development of this system will be required to reduce the variability within it, before real changes in cell behaviour in response to exogenous stimuli can be demonstrated. Given the difficulties in extrapolating data from animal to human tissue, development of models such as this could prove invaluable in trying to understand the complexities of chronic wounds.

ABBREVIATIONS

2D	Two-dimensional
3D	Three-dimensional
A2	Arachidonic Acid-2
ADP	Adenosine diphosphate
ATIII	Antithrombin-III
bFGF	Basic Fibroblast Growth Factor
CAM	Cell Adhesion Molecules
CD	Cluster of Differentiation
CFU-GEMM	Colony forming unit-granulocyte, erythrocyte, macrophage, megakaryocyte
CFU-GM	Colony forming unit-granulocyte macrophage
CI	Confidence Interval
CTGF	connective tissue growth factor
Cyr61	cysteine rich 61
DPX	Mounting medium (solution of polystyrene/plasticizers in xylene)
ECM	Extracellular Matrix
EGF	Epidermal Growth Factor
ELISA	Enzyme-Linked Immunosorbent Assay
FGF	Fibroblast Growth Factor
GM-CSF	Granulocyte macrophage-colony stimulating factor
HA	Hyaluronic Acid
ICAM	Intracellular adhesion molecule
IFNy	Interferon
Ig	Immunoglobulin
IGF	Insulin-Like Growth Factor
IL	Interleukin (i.e. IL-1β)
KD	Kilo Daltons
LDH	Lactate Dehydrogenase
LFA	Lymphocyte function associated antigen
LMWH	Low Molecular Weight Heparin
LPS	Lypopolysacharide
LTB4	Leukotriene B4
Mac-1	Macrophage antigen-1
mmHg	Millimetres of Mercury
MMP	Metalloproteinase
N-CAM	Neuronal Cell Adhesion Molecule
NMR	Nuclear magnetic resonance
PAF	Plasminogen Activating Factor
PCPE	procollagen C-proteinase enhancer
PDGF	Platelet Derived Growth Factor
PDGF-AA	Platelet Derived Growth Factor-AB
PDGF-AB	Platelet Derived Growth Factor-AA
PDGF-BB	Platelet Derived Growth Factor-BB
PLF	proliferin family
RECK	reversion-inducing cysteine-rich protein with Kazal motifs
RPMI	Roswell Park Memorial Institute medium
RT	Room Temperature
SCID	Severe combined immunodeficiency
SD	Standard deviation

SDS PAGE	Sodium Dodecyl Sulphate Polyacrylamide Gel Electrophoresis
Self-MHC	Major Histocompatability Complex
TBS	Tris Buffered Saline
TFPI-2	tissue factor pathway inhibitor 2
TGF	Transforming Growth Factor
Th	T-helper lymphocyte
TIMP	Tissue Inhibitor of Metalloproteinase
TNF alpha	Tumour Necrosis Factor alpha
TPA	12-O-tetradecanoylphorbol-13-acetate
TRE	TPA responsive element
UPA	Urokinase Plasminogen Activator
VEGF	Vascular Endothelial Growth Factor
VLA	Vascular leucocyte antigen
VLU	Venous Leg Ulcer
WHRU	Wound Healing Research Unit

1.0 INTRODUCTION

1.1 OVERVIEW OF MECHANISMS INVOLVED IN TISSUE REPAIR

Over the past 4 decades, an enormous amount of knowledge has been collected regarding the process of wound healing. This is probably due to the simultaneous increase in the awareness of the clinical problem and the expansion of new knowledge in the fields of molecular and cellular biology. Application of the scientific knowledge gained has allowed significant strides to be made in understanding the molecular and cellular processes that must interact to produce the living tissue, required for effective wound healing. However, a full understanding of these molecular and cellular processes can not be gained without first considering the anatomy and physiology of the skin, the phases of the healing process and the different types of wounds and their repair.

It is important to establish that, depending on the type and extent of tissue injury, a wound can travel either through the reparative or, in some cases, the regenerative process. Unlike many other species, man's primary mode of healing, when tissue loss is significant, is by repair. Repair is the process in which new tissue, different to that already present (i.e. scar tissue) is synthesised. In contrast, regeneration is the process where new tissue identical to that already present is synthesised, to replace the damaged tissue (1). In adult humans, only hepatic and epithelial tissues have the potential for regeneration, but in most cases tissue healing is via repair (2). However, when tissue damage is superficial (i.e. restricted to the epithelium and not involving vessel interruption), the requirement for connective tissue synthesis is absent. The re-epithelialisation that occurs in such a wound can therefore be thought of as regeneration as opposed to repair.

Injury to any tissue is known to initiate a complex cascade of biochemical and cellular events, each in turn helping to clear damaged cells and other unwanted elements, to protect viable tissues and to reconstitute the area. The extent and timing of these events are controlled by a multiplicity of mediators which have been under intense investigation during the last ten years (3).

Wound healing is a process with both microscopic and macroscopic markers. It is easier to understand the overall process of wound healing if it is broken down into distinguishable components. The process of wound healing has classically been sub-divided into three overlapping phases, originally described by Clark (1). The three overlapping phases of wound healing are inflammation, granulation tissue production and matrix formation, and remodelling. These are illustrated in figure 1.0 along with the timing of the influx of the major cell types involved in each of the phases. The inflammatory phase begins at the moment of injury and normally extends to approximately day four to six post injury (1). The quality of healing is a reflection of the quality of the inflammatory response. Furthermore, the quality and extent of the inflammatory response is also dependent on the severity of the injury and the ability of the individual's body to respond and support the healing process at the moment of injury (4;5). This is born out by the deleterious effects which immunocompromised and physiologically challenged states have on the normal healing process (5-8).

It is important to bear in mind, that although macroscopically a wound may appear quiescent, there are numerous biochemical and immunological events taking place during the early inflammatory response associated with a newly created wound. It is essential to establish that the quality of the inflammatory response and the subsequent phases of healing are reliant on the influx of several cell types into the wound environment. In fact, the greatest number of differing cells, enter the wound

during this initial phase. Due to the overlapping nature of the healing process, several of the cell types remain within the wound throughout the subsequent phases of healing (see figure 1.0 below).

Figure 1.0: *Diagramatic representation of the overlapping phases of wound healing (below) and the timing of the influx of cellular constituents into the wound site during each of these phases (above). Reproduced from The Wound Programme, University of Dundee* (9)

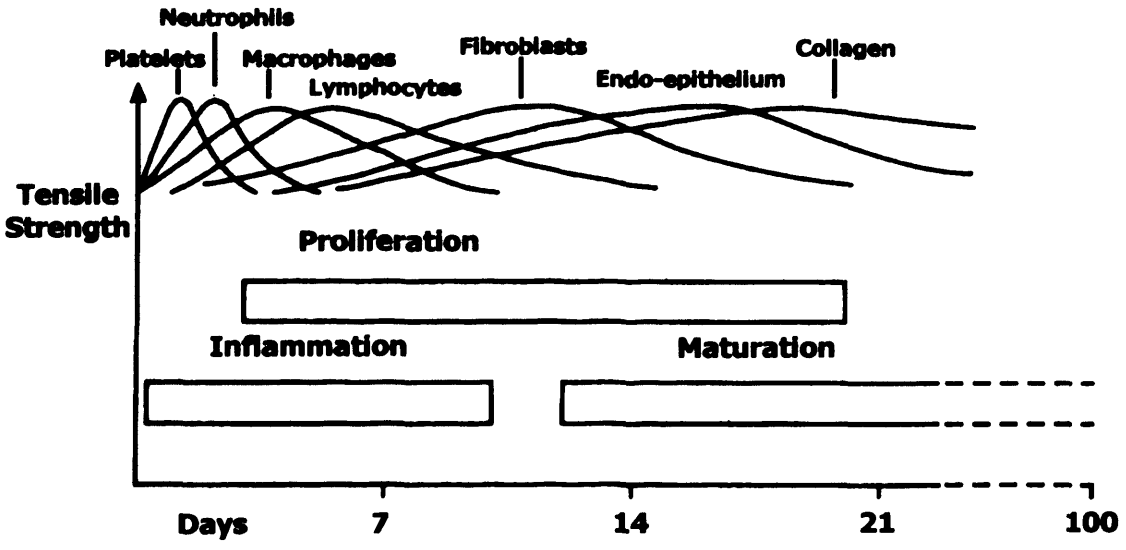

During the early inflammatory phase, it is important that effective haemostasis takes place, as it heralds the release of vasoactive substances with the ability to influence the ensuing inflammatory response. Following tissue injury, blood vessel disruption allows the extravasation of blood constituents with concomitant platelet aggregation, blood coagulation and generation of bradykinin and complement-derived anaphylatoxins (10;11)

Platelets have been shown to function in a number of other ways through the release of a variety of biologically active molecules such as PDGF and EGF which stimulate

cell migration and growth into the injured site (12). Other functions include increasing vascular permeability via serotonin release, leukocyte accumulation via release of chemotractants, fibroplasia, collagen synthesis and angiogenesis (3). It is evident that the platelets play a critical role in the initiation of inflammation and hence the subsequent process of wound healing.

Traditionally, the neutrophil has been considered to be the first leucocyte to infiltrate an area of tissue inflammation and injury, but small numbers of macrophages also begin to appear from the circulation during this early phase of healing (3;13). The neutrophils enter a site of tissue injury early in the first 24 hours and remain there between 6 hours and several days (8). The major function of neutrophils during this early inflammatory phase is to rid the wound site of contaminating bacteria, whereas the presence of monocytes and their subsequent conversion to macrophages seems critical to the initiation of tissue repair (12). After the first few days of tissue injury, if bacterial contamination is minimal, neutrophil infiltration will cease, their numbers will decline and effete neutrophils will be phagocytosed by tissue macrophages (14).

As a result of the changing characteristics of the cellular influx, an arbitrary division can be drawn between an early and late inflammatory response with accumulation of macrophages and lymphocytes marking the later response. However elevated bacterial counts may prolong the early inflammatory response, increasing the risk of tissue damage resulting from the reactive oxygen intermediates, proteolytic enzymes and cationic proteins released by the phagocytic activity of the neutrophil (1;15). Heavy bacterial contamination of the wound will therefore interfere with the progression to the next phase of wound healing.

Accumulation of the macrophage population continues regardless of whether the neutrophil infiltrate resolves or persists, allowing the macrophage to progressively become the predominant wound phagocyte. It was thought for many years that the primary function of the macrophage was the removal and degradation of injured tissue debris along with phagocytosis of pathogenic organisms. In 1975 evidence emerged to suggest a role for macrophages in the orchestration and execution of both the proteolytic and reparative phases of wound healing (16). Further investigation into the role played by wound macrophages over the last two decades has revealed that they are able to secrete a plethora of biologically active substances crucial to wound healing (8;12). Consequently, it has been suggested that this allows them to play a pivotal role in the transition between wound inflammation and wound repair. These biologically active substances or monokines are important in the proliferation of fibroblasts, smooth muscle cells and endothelial cells and include factors such as tumour necrosis factor (TNF) -α, interleukin (IL) -1, transforming growth facator (TGF) -β, platelet derived growth factor (PDGF) and vascular endothelial growth factor (VEGF) (17;18).

Its influence on angiogenesis is certainly one of the main reasons why the macrophage is so important in the early stages of healing as this effects the restoration of nutrient supply to newly forming granulation tissue. Many of the other monokines and growth factors released by the macrophage are also important in the initiation and propagation of granulation tissue and hence the transition from the first to the second phase of wound healing

The granulating phase of wound healing begins on approximately day 4 post-injury and extends to around 21 days (1). This phase involves the synthesis of granulation tissue, restoring some of the body's structural integrity and allows the wound to

gradually gain in its ability to withstand outside pressure. Granulation tissue consists of a dense population of macrophages, fibroblasts and neovasculature embedded in a loose matrix of collagen, fibronectin and hyaluronic acid (12). It has a granular appearance when incised and visually examined, which reflects the presence of multiple newly formed blood vessels (1). The observation that macrophages, fibroblasts and blood vessels move into the wound space as a unit highlights the interdependence of cells involved in the process of tissue repair.

The cell most closely associated with the granulation phase of healing is the fibroblast, as its greatest burst of activity occurs in this phase. It undergoes an alteration in cell phenotype making it more motile and capable of depositing several types of extracellular materials essential to wound healing, namely tropocollagen and the proteoglycans of ground substance (19). The connective tissue matrix laid down by the fibroblasts acts as an essential substrate on which macrophages, new blood vessels and fibroblasts themselves can migrate into the wound space. Tropocollagen is secreted into the extracellular matrix as the precursor to collagen where it polymerises to form various types of collagen. In the early granulation tissue these include collagens IV, V and VI, which are then gradually replaced by collagen I predominantly, and to a lesser degree by collagen III (19). Type I collagen is in fact the most abundant in the body and is found in fibrous connective tissue, skin, tendon, ligaments and bone (20). The fibroblast also produces elastin, a "rubber-like" material found in the skin, lung, blood vessels, and bladder which aids in maintaining tissue shape (20). The third fibrous components of the connective tissue produced by the fibroblast are the structural glycoproteins such as laminin and fibronectin which are known to be active in cell-to-matrix interactions (19). The ability of fibronectin to simultaneously bind connective tissue cells and the ECM, along with the ability of

cells to rapidly adhere and detach from a fibronectin substratum, makes it an ideal matrix for fibroblasts to move through (21). The ground substance produced by fibroblasts is composed of glycosaminoglycans, most notably hyaluronic acid and proteoglycans which are hydrophilic substances, causing them to attract large amounts of water and sodium (20).

The signals that induce fibroblast proliferation and migration into a wound space include chemotactic factors, growth factors, changes in structural molecules, and loss of nearest neighbour cell-to-cell attachment. The first cell components thought to release substantial amounts of preformed growth factors into a wounded area are platelets which store in their granules PDGF, EGF, TGF (-α and -β) and FGF (22). With the subsequent arrival and activation of macrophages, which foregoes the granulation phase of healing, a source for the continual synthesis and release of growth factors is put into place. Macrophages produce PDGF, TGF-α and -β, and FGF-like peptides making them an important cellular link between the earlier inflammatory stages and the following phases of wound healing (23). There has been intense investigation into the interplay of fibroblast growth and chemotactic factors *in vitro* and also *in vivo,* where combinations of growth factors have been added to wounds (24-26). From these studies, it is clear the signals for fibroblast migration and proliferation are complex and interrelated. In addition to their ability to synthesize and secrete structural macromolecules, they also possess a contractile capacity (27). Many if not all the fibroblasts that migrate into the wound space retract their endoplasmic reticula and Golgi apparati to perinuclear locations, forming large actin bundles that course through the peripheral cytoplasm oriented parallel to the long axes of the cells (27;28). These actin rich fibroblasts or myofibroblasts have been suggested to be largely responsible for wound contraction as they are the most

numerous cellular constituent of granulation tissue and have been shown to align within the wound forming cell-to-cell links along the lines of contraction.

Matrix formation and remodelling is classed as the third phase of wound healing. It does in fact overlap with the previous phase, and has been suggested to begin simultaneously with granulation tissue formation. However, after the dissolution of granulation tissue, the matrix structure and composition is constantly altered (29). Elimination of most fibronectin and slow accumulation of large fibrous bundles of type I collagen give the residual scar increasing tensile strength. In fact, the composition and structure of the extracellular matrix changes continuously from the time of its first deposition at the wound margin along with the developing granulation tissue and subsequently more centrally as the granulation tissue grows into the wound space (23). This essentially means that the composition and structure of the extracellular matrix depends on both the time lapse since tissue injury and the distance from the wound margin. In this phase of wound healing there does not seem to be a specific prominent cell activity as fibroblasts continue to function along with proteolytic enzymes working to eliminate collagen fibers not required in the remodelled tissue and to modify those already there (28). The focus of this phase of healing is to increase the organization of the matrix previously laid down by the fibroblasts in order that the damaged tissue can regain its functional status (3).

1.1.1 Haemostasis

The process of haemostasis involves a cascade of enzymatic reactions that result in the formation of a fibrin plug to affect the cessation of blood loss from the injured site. However, haemostasis is also responsible for much wider effects than simply

damming up the injured site. Activation of platelets, a key event during the process of haemostasis, induces platelet release of vasoactive molecules (i.e. serotonin), inflammatory mediators (i.e. prostaglandins) and growth factors (i.e. PDGF) (30). These molecules are involved in promoting the inflammatory response and driving the subsequent phases of wound repair. Platelets are therefore a key link between the initial response to blood vessel injury and the inflammatory phases of wound repair. The fibrin clot also provides the initial structural support to the disrupted tissue at the wound site as well as providing a scaffold for the inward migration of the early cellular components involved in the initial phases of wound repair (31). The early provisional matrix therefore consists of the fibrin clot.

Haemostasis is initiated when disruption of tissue at the injured site provides a surface for the adsorption of the numerous proenzymes involved in haemostasis, which normally circulate in a sea of enzyme inhibitors. Adsorption onto a surface, by a concentration effect, creates a microenvironment relatively free of protease inhibitors (32). This allows the small amount of spontaneous activation normally occurring within the vasculature to be amplified into the full blown clotting cascade termed haemostasis. The last step in this clotting cascade is the conversion of soluble fibrinogen to insoluble strands of fibrin, turning the fluid blood into a solid gel or clot.

The clotting cascade consists of two main pathways (see figure 1.1). One of the pathways is traditionally termed the intrinsic pathway, due to the components involved being present within the blood. The other pathway has been termed the extrinsic pathway as some of the components arise from the surrounding cells and tissues (33). The extrinsic pathway is the most important pathway in the body and is thus termed the *in vivo* pathway, whereas the intrinsic pathway is better termed the

contact pathway as it is activated when shed blood is exposed to an artificial surface such as glass.

Figure 1.1: *Diagrammatic representation of the intrinsic and extrinsic pathways of the clotting cascade. Oral anticoagulants can act on clotting factors II, VII, IX and X shown in grey boxes. PL = -ve charged phospholipid, ATIII = antithrombin III and LMWHs = low molecular weight heparins. Reproduced from (34)*

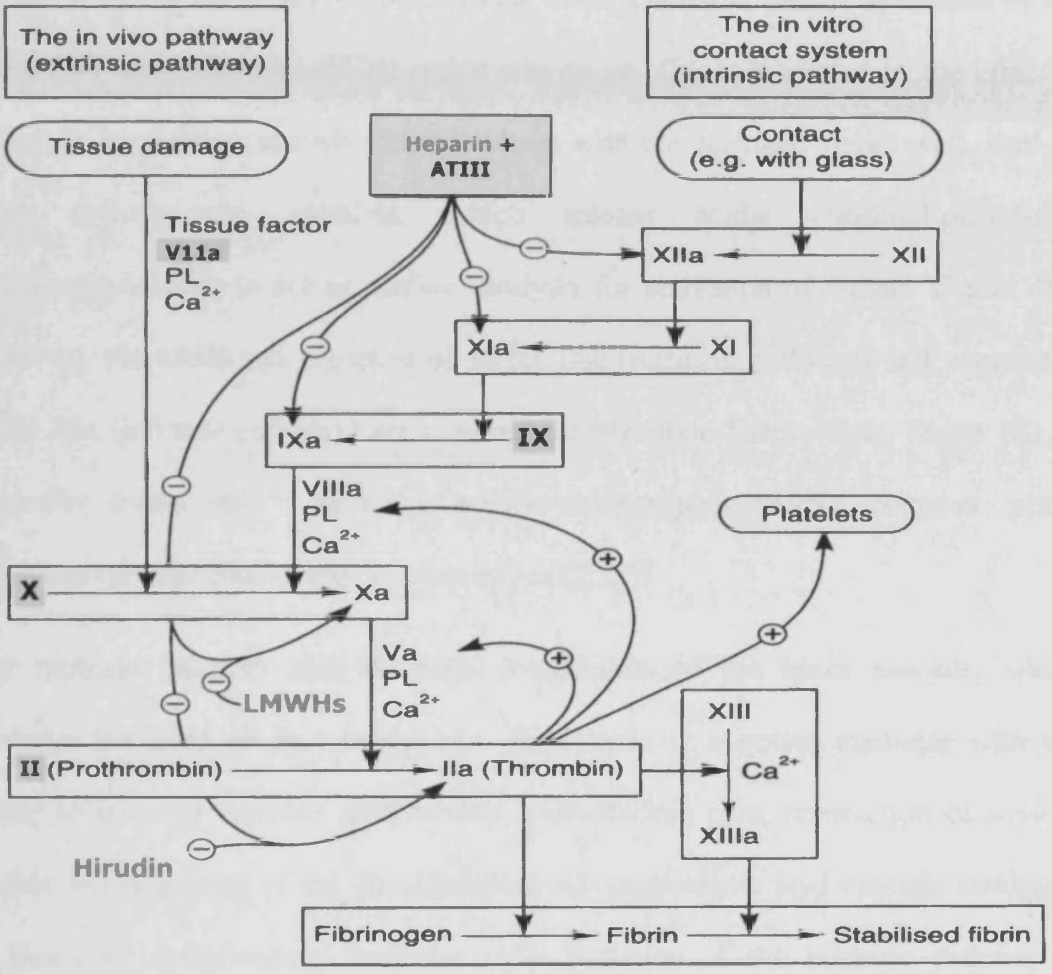

The extrinsic pathway is activated when damage to blood vessels exposes blood to tissue factor (thromboplastin), constitutively produced by cells beneath the endothelium. Factor VII present in plasma binds to tissue factor and in the presence of calcium undergoes an active site transition causing autocatalytic activation to factor VIIa, forming a tissue factor-VIIa complex.(32). This complex activates a

limited amount of factor X and IX (intrinsic pathway) producing factors Xa and IXa. Factor Xa in the presence of factor Va, phospholipid and calcium, converts prothrombin to thrombin leading to the end point of coagulation, the conversion of fibrinogen to fibrin (illustrated in figure 1.1). At this point rapid inactivation of the complex can occur by binding of TFPI to factor Xa. However, if enough thrombin is produced by the factor Xa-VIIa-IXa-tissue factor complex, further activation by the alternative molecules factor VIII and V will occur. This is mediated by the effect of thrombin on platelets and platelet interaction with the damaged vessel wall. Both of these activate the platelets, which release acidic phospholipids (i.e. phosphotidylserine) to act as surface catalysts for activation of factors V and VIII. However, the additional presence of factor IXa (intrinsic pathway) and sometimes factor XIa (intrinsic pathway) are required for persistent haemostasis. Factor IXa in particular forms into a factor IXa-VIIIa-calcium-phospholipid complex which maintains the coagulative state (reviewed in (32;33))

The intrinsic pathway also contains components of the kinin cascade, which produces the final product bradykinin. Bradykinin is a potent mediator with the ability to increase vascular permeability, vasodilation, pain, contraction of smooth muscle and activation of the phospholipase A2- arachidonic acid cascade making it an important inflammatory mediator (32). Initiation of the intrinsic pathway is induced by contact of factor XII (Hageman factor) with a negatively charged surface such as glass ex vivo, but *in vivo* is likely to be a biologically active material such as lipid A of gram-negative bacterial endotoxin. Interaction of factor XII with a negatively charged surface leads to its cleavage and activation. Activated factor XII can activate factor XI which itself activates factor IX. This is the point at which the intrinsic pathway converges with the extrinsic pathway by the activation of factor X

through the formation of the above mentioned factor IXa-VIIIa-calcium-phospholipid complex (see figure 1.1) (reviewed in (32-34)).

As previously mentioned, the coagulation cascade is normally kept under strict control by elements within the blood itself such as protease inhibitors and by the actions of the endothelial cells lining the vasculature. One of the most important of the protease inhibitors is antithrombin III, which neutralises all of the serine proteases in the cascade, whereas another inhibitor heparin cofactor II inhibits only thrombin. Normally the endothelial lining the vasculature expresses surface heparan sulphate, a glycosaminoglycan related to heparin and a cofactor for the inhibitory antithrombin III. The endothelium is also able to directly inhibit platelet aggregation by producing prostacyclin, nitric oxide, converting ADP (platelet agonist) to adenosine, synthesising plasminogen activator (initiating clot lysis) and expressing thrombomodulin, a receptor for thrombin (34). Binding of thrombin to thrombomodulin activates protein C (vitamin K-dependent anticoagulant, aided by protein S co-factor), which then inactivates factors Va and VIIa.

Clot lysis results from a fibrinolytic cascade that is set in motion concomitantly with the coagulation cascade. The fibrinolytic cascade involves several endogenous plasminogen activators including tissue type plasminogen activator (tPA), urokinase-type plasminogen activator (uPA), kallikrein and neutrophil elastase (34). Plasminogen is a serum β-globulin which is deposited on fibrin strands within a clot into which plasminogen activators can diffuse from the blood where they are unstable. Plasmin is cleaved from plasminogen by the action of these serine proteases, which then digests fibrin as well as fibrinogen and factors II, V and VIII (35). The action of plasmin is localised to the clot because the plasminogen activators are predominantly active on plasminogen adsorbed to fibrin and any

escaping plasmin is inactivated by circulating inhibitors such as plasminogen activator inhibitor (PAI-1) (34).

1.1.2 Inflammation

The inflammatory response plays a vital part in the host reaction to injury, infection, trauma and other similar insults. Over the years, inflammation has received much attention for its role in wound healing, where its presence is thought to be a prerequisite to successful tissue repair. This is exemplified by the fact that alterations and impairments of wound healing are well recognised in conditions such as diabetes, jaundice and advanced age, where underlying immune function are affected (35). In addition, many factors known to impair the immune response, such as chemotherapeutic drugs, immunosuppressive drugs and radiotherapy, can also result in a delayed or defective wound healing response (7;14). However, it is only more recently that the full extent of the involvement of the inflammatory response has been recognised. There is an emerging understanding of a continuing role for an increasing number of the cellular components of inflammation in the latter stages of healing.

It is well documented that neutrophils provide the early response to tissue injury and play a key role in the defence against bacterial infection together with the macrophage. In addition, the macrophage has long been recognised to play a role in orchestrating and driving the subsequent phases of wound repair following the initial inflammatory response. However more and more information is emerging about the involvement of other cellular components such as lymphocytes and mast cells in wound healing (36;37). A picture emerges of inflammation as a complex integrated response to injury. It involves various cellular constituents of the immune system

acting to limit local tissue damage, spread of infection and promote the involvement of cells outside the immune system in an integrated healing response.

The classic signs of an acute inflammatory response were described by Celsus over 2000 years ago as redness (rubor), tumour (swelling), heat (calor), pain (dolor), and functio laesa (loss of function) (38). Our understanding of the inflammatory response allows us to explain these macroscopic signs in terms of microscopic cellular constituents and the physiological effects on the surrounding tissue of inflammatory mediators such as cytokines, which are released by them.

Redness is caused by vasodilation resulting from release of vasoactive mediators (i.e. bradykinin). These are released directly from damaged blood vessels or indirectly from the complement anaphylatoxins C3a and C5a which induce mast cell degranulation and release of histamine (1;37). This increases the volume of blood locally and decreases its flow, hereby giving rise to the macroscopically observed redness. At the same time, vascular permeability is increased by the aforementioned vasoactive substances as well as by other inflammatory mediators, such as prostaglandin release by platelets, leading to oedema and localised swelling (30). The increase in vessel permeability allows the infiltration of inflammatory cells with further release of inflammatory mediators and amplification of the inflammatory response. The overall increase in fluid and cellular contents of the inflammatory site increases its metabolic activity and therefore increases local tissue temperature. Inflammation also causes pain as a result of inflammatory mediators (i.e. bradykinin and prostaglandins) and neurotransmitters (i.e. serotonin) released by inflammatory cells or damaged endothelial cells (39;40). These mediators give rise to pain by sensitising the free nerve endings peripheral nociceptive (pain) nerve fibres. In addition neuropeptides such as substance P released from primary afferent nerve

fibres in the periphery and in the dorsal horn of the spinal cord cause peripheral sensitisation to pain (39;40).

As already described above, the inflammatory response to injury is initiated by the release of potent inflammatory mediators during the heamostatic process. Other sources of inflammatory mediators during this initial stage are activation of resident tissue macrophages (5% of total number, 95% exudative macrophages) and locally involved endothelial cells (23;41). At the onset of inflammation, neutrophils tend to infiltrate the wound site in greater numbers due to their constitutive higher numbers in the general circulation. However, migration of macrophages does happen concurrently, although initially in lower numbers (23). A number of the inflammatory mediators act as general chemoattractants for leucocytes as well as increasing cell adhesion expression to facilitate transmigration across the endothelium. These include fibrinopeptides arising from the action of thrombin on fibrin, C5a from the complement cascade, PAF released by activated endothelial cells or neutrophils and LTB_4 released by activated neutrophils (42). Once the initial wave of infiltrating cells are resident within the inflammatory site, they express an extensive repertoire of chemokines, working to attract and activate additional inflammatory cells. This further amplifies the initial inflammatory response and the macrophage is particularly effective in this role (1). One of the chemokines specific for neutrophils is IL-8 secreted by macrophages in response to bacterial lipopolysacharide (LPS), Tumour Necrosis Factor (TNFα) and IL-1β (43).

1.1.3 Neutrophils

Neutrophils start to accumulate within minutes of an injury, peaking in number between 24 and 48 hours post injury (13;23). Their activation by chemokines and

inflammatory mediators increases the expression of surface adhesion molecules which mediate their adhesion to the endothelium and subsequent transmigration (44-47). Their role in wound healing was previously thought to be limited to eliminating contaminated bacteria but more recent evidence has emerged to suggest a role as a source of cytokines/growth factors (48). However, experiments where neutrophils have been depleted have shown no detrimental effect on wound healing except when bacterial colonisation was a factor (49;50). Neutrophils are the archetypal phagocytic cell, utilising enzymatic and oxygen radical mechanisms to destroy the phagocytosed bacteria (51). When activated, neutrophils also produce elastase and collagenase molecules to facilitate their movement through blood vessels and basement membranes (42). It is clear that proteolytic enzymes and oxygen radical molecules contained by neutrophils have the potential to cause immense tissue damage. Unfortunately tissue damage does occur when neutrophils are persistently activated in heavily contaminated wounds or when the inflammatory response is misdirected against host tissue, as in immune complex disease.

1.1.4 Macrophages: Inflammation , Granulation and Fibrosis

Having originally been identified as phagocytic cells, macrophages have turned out to be a versatile cell type with an enormous repertoire of functions depending on their tissue location and activation status (41). Macrophages are resident in most tissues, their functions including antigen presentation, antibacterial activity, antitumour activity and secreting a plethora of growth factors, cytokines and proteolytic enzymes. Examples of tissues containing specialised macrophage phenotypes include connective tissue (histiocytes), liver (Kupffer cells), lung (alveolar macrophages) and central nervous system (microglia) (52).

Macrophages are believed to originate from a pleuripotent stem cell in the bone marrow, which can potentially give rise to myeloid or lymphoid stem cells. Lymphoid stem cells give rise to the lymphocyte cell lineage and thus the various lymphocyte subsets. Myeloid stem cells otherwise known as CFU-GEMM (colony forming unit-granulocyte, erythrocyte, macrophage, megakaryocyte) give rise to cells of the megakaryocyte (platelet), erythroid (red blood cells), and granulocytic-monocytic (neutrophils-macrophage, CFU-GM) cell lineages (53). In the presence of the right growth factor the CFU-GM has been shown to give rise to monoblasts; the first cells from the myeloid lineage committed to macrophage differentiation. A monoblast then gives rise to two promonocytes with a t1/2 of 16hrs, each remaining in the bone marrow and dividing to give rise to two more monocytes, which are then released into the circulation (54;55). Monocytes circulate in the blood for up to 3 days leaving the vasculature randomly under steady state conditions. When disease is present bone marrow production is increased along with extravasation and accumulation within the affected tissue, reducing circulation time dramatically. This therefore provides a large capacity for recruitment into inflamed tissues (41).

The number of macrophages present in skin is low and therefore cutaneous inflammation relies heavily on the recruitment of monocytes from the circulation. Systemic administration of hydrocortisone, known to induce monocytopaenia, by Leibovitch and Ross resulted in a 66% reduction in macrophage numbers associated with an experimentally induced cutaneous wounds in guinea pigs (16). This also ties in with the theory originally put forward by Daems that normally monocytes rapidly migrate through the vasculature of tissues and organs performing a surveillance role (56). It is only under inflammatory or other relevant stimulatory conditions that

monocytes are retained within tissues. In the tissues, they differentiate into tissue macrophages with specialised effector functions specific for the local tissue requirements (53). Differentiation is guided by monocyte contact with inflammatory stimuli such as bacterial contamination or activated complement components as well as interaction with the local cytokine/growth matrix protein milieu encountered at each specific inflammatory site (55;57;58). However the diverse host defence mechanisms carried out by differentiated macrophages, ranging from elimination of pathogenic organisms and neoplastically transformed cells to tissue remodelling, has led to two proposals for the functional diversity generated within the macrophage cell population. One proposal suggests that diversity is generated by functionally distinct and committed subpopulations of macrophages. The individual pools make up a total population of macrophages from which specific effector cell functions can be recruited when required at specific tissue sites. An alternative proposal receiving more experimental support, suggests that macrophages are drawn from a relatively homogenous pool of pluripotential cells (59). These cells develop specific effector functions by responding to stimuli or conditions prevailing at each tissue site, and then differentiating into the appropriate effector cells, thus deriving their heterogeneity from each cell's adaptability (58). Therefore, at a wound site there is a reciprocal flow of information between the monocyte/macrophage population and the surrounding wound tissue (60-62). Macrophage activation by the wound matrix and soluble mediators held within it, will direct differentiation towards a phenotype capable of reciprocally instructing resident cells to steer an appropriate functional course towards successful tissue repair.

As already stated, monocyte recruitment to the site of tissue injury along with neutrophils is initiated by the products of the clotting cascade, complement cascade

and a host of inflammatory mediators released by other locally activated cells such as platelets and endothelial cells. Monocyte recruitment persists until the later stages of wound repair even if neutrophil accumulation has diminished (13). Once resident within the tissue, monocytes are activated, becoming inflammatory monocytes that secrete a plethora of biologically active molecules, to amplify the inflammatory cascade further and recruit more cells to the site. Some of the earliest inflammatory molecules to be released by resident macrophages and newly activated monocytes are TNFα, IL-1β and IL-6 which mediate many of the localised and systemic effects of acute inflammation (48;63). Both TNFα and IL-1β increase cell adhesion molecule expression and permeability of local endothelium. They also act in an autocrine and paracrine manner to activate macrophages and other local cells to produce chemokines to attract further inflammatory cells to the wound site (46). TNFα and IL-1β also have systemic effects such as increasing the core temperature by acting on the hypothalamus and IL-6 is mainly involved in stimulating the release of acute phase proteins by the liver to produce the acute phase response (46).

Monocytes, like neutrophils are known to have specific chemoattractants including fragments of collagen, elastin and fibronectin, enzymatically active thrombin and TGFβ (1). In addition they are stimulated to produce colony stimulating factor–1, a cytokine which promotes monocyte survival locally and increases haematopoiesis in the bone marrow (64). Initially macrophages assist neutrophils in removing potential pathogenic organisms but are particularly effective in debriding the wound site removing tissue debris and effete neutrophils

As healing progresses, macrophages become more involved in new tissue formation (granulating phase) and later in tissue remodelling. Succesful removal and

breakdown of damaged ECM at an inflammatory site is an integral part of the initiation of tissue reconstruction. To meet this requirement monocytes and macrophages secrete a host of tissue degrading enzymes including metalloproteinases, serine proteases, cysteine proteases and acid hydrolases. Some of these enzymes also play a part in the later stages of tissue remodelling and scar formation. The spectrum of proteolytic enzymes secreted by monocytes differs from that of macrophages (65;66). Monocytes are a significant source of MMP-9, which degrades cleaved native collagen peptides (gelatins), along with a serine protease identical to neutrophil elastase, neutral pH-optimum cathepsin G (cysteine protease) and acid-optimum cathepsin L (cysteine protease), involved in degrading elastin (67-70). Therefore monocytes are thought to be involved in the initial debridement of damaged tissue and do not contribute significantly to tissue remodelling which requires their differentiation into macrophages (58). As well as secreting a broader spectrum and in some cases greater quantities of proteolytic enzymes macrophages are capable of directing their secretion by fibroblasts (71-73). The action of serine/cysteine proteases and MMPs are opposed by the action of plasma-derived protease inhibitors and tissue iniibitor of metalloproteinases (TIMPs) respectively. It is probably the balance between the proteolytic enzymes and their inhibitors in relation to the ongoing level of matrix synthesis, which ultimately determines whether there is overall tissue synthesis or breakdown. The role of the MMPs and their endogenous inhibitors in wound healing is dealt with in more detail in section 1.3

Macrophage-derived growth factors are essential for the transition between the inflammatory phase and reparative phase of wound repair, a fact which is exemplified by the defective wound repair seen in macrophage-depleted animals.

Many of these growth factors are pleiotropic in their effect and utilise many varied mechanisms to effect the increase in matrix mass. These include increased collagen synthesis by fibroblasts, increased synthesis of other matrix components (i.e. glycosaminoglycans and fibronectin), decrease synthesis of proteolytic enzymes (MMPs) and increase synthesis of proteolytic inhibitry enzymes such as the TIMPs (12).

The best understood of these growth factors are TGFβ, PDGF, IGF-1, FGF, and TGFα. One of the most intensely studied of these growth factors is TGFβ which showed promising results by accelerating wound healing in animal models but to date has not been proven to work in human chronic wounds. During the fibroproliferative phase of wound healing macrophages become the major source of this growth factor (74). It is secreted in a latent form associated with a binding protein. This latent form creates an extracellular pool of TGFβ, which can be activated on demand by proteolytic cleavage or extracelular matrix binding (75-77). Secreted TGFβ can also bind to matrix protein from where it can be cleaved by macrophages in a plasmin-dependent action (76;77).

TGFβ is now thought to be a key factor in the switching of macrophage roles from the early inflammatory phase, where they engage in phagocytosis and tissue debridement, to the fibrogenic reparative phases, where they orchestrate matrix synthesis (78). TGFβ has been shown to prime macrophages to express increased levels of inflammatory and fibrogenic factors such as lysosomal hydrolase β-glucoronidase and PDGF respectively in response to phagocytic stimuli such as that supplied by the bacterial product β 1-3 glucan (59;79-81). This further amplifies the inflammatory response but TGFβ can also have inhibitory effects on macrophage

function. It has been demonstrated that TGFβ can have significant inhibitory effects on the cytocidal effects of macrophages (eliminating pathogens) mediated by the production of reactive oxygen and nitrogen intermediates (82). This could act as a modulating stimulus involved in the directed differentiation of macrophages toward a specific functional phenotype as discussed earlier.

By utilising the mechanisms outlined above for increasing matrix mass TGF-β is a potent inducer of *de novo* matrix synthesis and in particular is affective in stimulating collagen synthesis(83). It has been shown to have a direct effect on collagen synthesis by fibroblasts *in vitro* and shown to inhibit their expression of MMP-1 and MMP-2 as well as increasing the expression of TIMPS (83;84). TGF-β activity is also a key determinant of the length of the fibrotic response and has been implicated in conditions where their is increased production of scar tissue (30;85;86).

Macrophages also become a major source of PDGF during the later stages of matrix synthesis and remodelling after initial release by platelets described previously. PDGF is secreted as either a homodimeric complex (PDGF-AA or PDGF-BB) or a heterodimeric complex (PDGF AB) but its receptor is not expressed by macrophages, and therefore they act solely as a source of this growth factor (86). Although originally identified as a mitogen for fibroblasts, smooth muscle cells and glial cells, like TGF-β it has pleiotropic effects including leucocyte and fibroblast chemotaxis. Evidence from *in vitro* experiments has demonstrated PDGF can stimulate production of fibronectin and HA by fibroblasts, contraction of collagen matrix and release of collagenase by fibroblasts, making it an important factor in the reparative stages of wound healing (87;88). This has been exemplified by *in vivo* studies demonstrating marked effects of exogenous application of PDGF augmenting

healing of incisional wounds in animals, such as increasing wound breaking strength by 150-179% in comparison to control wounds (89;90).

Insulin-like growth factor (IGF-1, somatomedin) mediates the action of growth hormone in targeted tissues such as the liver or bone, promoting protein synthesis and cellular growth. However increased amounts of IGF-1 have been shown to be present in wounds and again the macrophage acts as the cellular source (17). Macrophages are stimulated to secrete IGF-1 by exposure to hyaluronic acid mediated by CD44 the cell surface receptor for HA and in a TNFα dependent manner (80). In view of this, IGF-1 could serve as another factor linking the functional transition of macrophages from the early inflammatory phase to matrix synthesis and remodelling (58). Contact with HA would stimulate macrophage TNFα production enhancing the inflammatory response but also stimulating IGF-1 production in readiness for subsequent tissue reconstruction

In addition to their effects on matrix synthesis and remodelling, macrophages are important sources of angiogenic growth factors such as FGF and TGFα (3). FGF has two functionally identical forms, acidic FGF and basic FGF, and both are growth factors for vascular endothelial cells, fibroblasts and smooth muscle cells (3;18). Once secreted, FGF binds to the ECM and becomes functionally active when cleaved from the ECM (91;92). Macrophages play an important part in this process by releasing uPA which has been shown to cleave bFGF from cell derived matrices a process which was enhanced by TGFβ (76). TGFα shares almost 40% sequence homology with EGF and utilises the EGF receptor to exert a cellular response, acting as a growth factor for endothelial cells, epithelial cells and fibroblasts (93).

1.1.5 T Lymphocytes

The role of the lymphocyte in wound healing is less well documented, but in recent years, evidence has accumulated in human wounds to indicate a putative role. Indirect evidence is provided in that agents known to enhance T-lymphocyte function, such as arginine, lead to increased wound breaking strength and collagen deposition, whereas agents that suppress T lymphocyte function, such as cyclosporine A markedly impair wound healing (94;95). More direct evidence for lymphocyte involvement in the control of wound repair is provided however by *in vivo* lymphocyte depletion studies in a murine model. Depletion of all T lymphocytes produced a marked decrease in wound breaking strength and also a decrease in the hydroxyproline content of subcutaneously implanted polyvinyl alcohol sponges, used as an index of wound collagen deposition (14;96). In contrast, selective depletion of the $CD8^+$ T suppressor/ cytotoxic lymphocyte subset resulted in enhancement of wound healing whereas depletion of the $CD4^+$ T helper subset had no effect on wound breaking strength or collagen deposition (97). Since the $CD4^+$ lymphocyte subpopulation is now recognised to be functionally heterogenous, the lack of effect of depletion of the total $CD4^+$ population may indicate the existence of subsets of $CD4^+$ T cells which have counterregulatory actions. Most recently human *in vivo* data has emerged from the laboratory at WHRU and others demonstrating the presence of differing lymphocyte subsets during the time course of wound healing and their persistence during the latter phases of tissue synthesis and remodelling (36;98).

Work carried out in the WHRU laboratory has demonstrated a characteristic accumulation of lymphocytes and macrophages at the wound margin and in the bed of both chronic non-healing and healing surgical wounds. The $CD4^+$:$CD8^+$ T-

lymphocyte ratio of perivascular infiltrates at the margin of a healing pilonidal sinus excision wound was found to be 3.3 ± 0.3 at 7 days after surgery followed by a decrease to 2.1 ± 0.3 as healing progressed to wound closure (36). The majority of chronic venous leg ulcer tissue examined was found to have a low $CD4^+$:$CD8^+$ ratio identical to that of the almost closed healing wound (99). This observation may be significant if $CD8^+$ lymphocytes act to inhibit healing in accordance with experimental murine data (97). In contrast to T-lymphocytes, B-lymphocytes were found to be absent early in healing of surgical wounds and from chronic wounds. However within surgical wounds, their numbers increased as healing progressed so that they comprised 30% of the total wound margin lymphocyte population prior to wound closure (36).

Although there is a marked lymphocyte infiltrate within the chronic wound, healing does not progress (99). It is possible that this may be due to the lymphocyte population having an inappropriate composition and / or function.

Although the role of lymphocytes in human wound healing has not been defined, their role in other inflammatory conditions is well documented. Studies of their cytokine secretion profiles show that both $CD4^+$ and $CD8^+$ T lymphocytes are heterogenous (14). The nature of an immune response is controlled by the T lymphocyte subpopulation activated upon recognition of antigen in association with self-MHC determinants (100). $CD4^+$ T lymphocytes are currently believed to consist of at least three distinct subpopulations termed Th1, Th2, and Th0 cells (101). Th0 cells produce cytokines characteristic of both Th1 and Th2 cells, and will eventually differentiate into either Th1 or Th2 cells (102). Th1 lymphocytes secrete the cytokines IFNγ, IL-2, IL-3, TNF-α, TNF-β, GM-CSF, promote cellular immune responses and are considered to be proinflammatory (100;101). Th2 lymphocytes

produce, IL3-6, IL-10, IL-13 and GM-CSF, and promote antibody production (14;100;103). Th1 and Th2 cellular functions are mutually inhibitory. Many experimentally induced and naturally occurring immune responses show patterns of cytokine production clearly indicative of Th1 or Th2 dominance. Th1 cells have been associated with autoimmune diseases such as Hashimoto's Thyroiditis, Graves' disease and rheumatoid arthritis (104). Th2 cells have been associated with strong antibody responses, allergy and reactions to parasites (which involve IgE production) and some autoimmune disorders (100). It is currently believed that multipotent Th0 cells differentiate into either Th1 or Th2 cells depending on the nature of the antigenic stimulus and the cytokine environment in which stimulation by antigen occurs.

Although the differentiation of the naive $CD4^+$ Th0 subsets is influenced by the dose of antigen, the type of antigen presenting cell and the major histocompatibility complex class II haplotype, the most potent differentiation inducing stimuli are cytokines themselves (104). This has been demonstrated to be a consequence of IL-12 and IL-4 action, which via specific transcription factors promote IFNγ and IL-4 production, inducing Th1 or Th2 differentiation respectively (105). This is critically relevant to wound healing as the chronic wound is an environment full of cytokines and growth factors with the potential to influence the differentiation of the Th0 to Th1 or Th2 cells. In addition there are now numerous examples of experimental models in which modulation of the Th1/Th2 balance may be achieved by administration of recombinant cytokines or cytokine antagonists to alter the outcome of disease (101). T lymphocytes may also therefore serve as targets for therapy in chronic wounds since specific inactivation or induction of either Th1 or Th2

lymphocyte subsets may alter the development of the immune response within chronic wound tissue.

Heterogeneity is also found within the $CD8^+$ lymphocyte subset. The majority of $CD8^+$ lymphocytes are termed cytotoxic T lymphocytes which produce IFNγ but recent evidence has indicated the existence of non-cytotoxic $CD8^+$ T cells which produce IL-4 (103). It has therefore been suggested that there may exist functionally distinct subsets of $CD8^+$ T cells which produce different profiles of cytokines and which may play an important part in regulating the pattern of cytokine secretion by $CD4^+$ T cells.

Although the presence of both $CD4^+$ and $CD8^+$ lymphocytes has previously been recognised in chronic wound tissue, it is still not understood why these cells are continually recruited to the wound site and what role they play in the maintenance of chronicity. Their presence may be due to non-specific recruitment by the inflammatory reaction or alternatively to the existence of a specific immune response to antigenic stimuli within chronic wound tissue.

1.1.6 Angiogenesis

The study of angiogenesis is currently one of the most rapidly advancing areas of biological research following the discovery by Folkman in 1971 that tumour growth was dependent on new blood vessel formation (106;107). It is involved in a number of normal biological processes (i.e. development of bone and placental tissue), including those involved in the regeneration and restoration of damaged tissue such as wound repair (108;109). In fact, genes involved in angiogenesis have also been consistently found to be involved in wound healing (109). Interestingly the nature of angiogenesis involved in physiological processes where it occurs in short bursts and

is self limiting, can be distinguished from its involvement in pathological processes where it often persists indefinitely (110).

Angiogenesis constitutes the sprouting of new capillaries from pre-existing vessels in a complex process involving multiple interactions between endothelial cells, surrounding pericytes, smooth muscle cells, ECM, and angiogenic cytokines/growth factors (111). This occurs in a series of sequential steps in response to angiogenic stimuli such as VEGF, bFGF and TNFα released by inflammatory cells such as mast cells and macrophages (112). Endothelial cells lining existing microvessels respond to these factors by proliferating, increasing CAM expression and secreting proteolytic enzymes, which allows them to migrate through the basement membrane into the interstitial stroma, breaking it down as they go (110;113). Proliferation occurs at the base of the developing sprout as opposed to the tip and eventually the endothelium aligns in a bipolar fashion to form a lumen. These newly formed hollow micro vascular sprouts then proceed to anastomose with each other, forming a capillary through which blood can flow (111).

During the last decade, studies investigating the increase in erythropoietin levels in response to hypoxic stimulation revealed a mechanism involving transcriptional regulators termed hypoxia inducible factors (HIFs) through which oxygen availability could directly regulate the angiogenic response (114-116). HIFs are heterodimers made up of α and β subunits, which exist as a series of isoforms encoded by distinct genetic loci (117). HIF-β subunits are constitutive nuclear proteins whereas HIF-α subunits are inducible by hypoxia. In addition, among the three HIF-α isoforms, HIF-1α and HIF-2α are able to interact with hypoxia response elements (HREs) to induce transcriptional acvtivity (115). This allows HIFs to

upregulate a number of angiogenic genes, the most marked being an up to 30 fold induction of VEGF, which can occur within minutes (115;118). It is now thought that the HIF-α subunits are themselves regulated by a multistep process of post-translational modifications leading to changes in activity, abundance, mRNA splicing and subcellular localisation (119). They are directly linked to the availability of oxygen through a series of non-haeme, iron-dependent oxygenases that hydroxylate specific HIFα residues in an oxygen-dependent manner (119). These pathways provide mechanisms by which the availability of molecular oxygen when coupled to HIF hydroxylase activity can then be linked to HIF-dependent transcription and angiogenic growth factor expression.

Accumulating knowledge about the complexity of angiogenesis has led to a greater understanding of the angiogenic mechanisms involved in wound healing. Potent angiogenic factors including FGF-1, FGF-2, PDGF, TGFα and TGFβ are released from disrupted cells at the wound site in addition to a rapid induction of VEGF in response to localised tissue hypoxia (92). VEGF is released largely by macrophages and activated epidermal cells at the wound site (120). In fact macrophages play a central role in regulating angiogenesis during wound healing by releasing a host of other pro-angiogenic factors such as PDGF, bFGF and aFGF, partly in direct response to changes in oxygen tension (41). As well as this, a number of lesser known angiogenic factors including Del-1 an ECM protein, and members of the Cyr61, CTGF and NOV (CCN) family, namely connective tissue growth factor (CTGF) and cysteine rich 61 (Cyr61), have been shown to be pro-angiogenic through their binding to $\alpha_v\beta_3$ integrin (121). In addition, members of the proliferin family (PLF) acting through the mannose-6-phosphate receptor have also been shown to promote angiogenesis (122).

Binding of the above angiogenic factors to their respective receptors leads to the activation of endothelial cells. Endothelial cells respond by increasing their proliferation, expressing CAMs such as $\alpha_1\beta_1$ $\alpha_2\beta_1$ $\alpha_5\beta_1$ and $\alpha_v\beta_3$ and releasing MMPs (i.e. MMP-2, MMP-9 and MT1-MMP), which facilitates their migration and invasion into the surrounding stroma (112). bFGF and VEGF are thought to be the major factors in this process. In addition VEGF, also known as vascular permeability factor, induces vascular permeability allowing leakage and deposition of plasma proteins such as fibrin and fibronectin into the surrounding stroma (123).

Endothelial cells utilise the integrin CAMs to bind to matrix proteins facilitating their migration into and through the surrounding provisional wound matrix. The classification and functional roles of the CAMs is dealt with in more detail in section 1.2. Studies on chick chorioallontoic membrane and full thickness cutaneous wound models in Yorkshire pigs have demonstrated $\alpha_v\beta_3$ to be one of the key adhesion molecules in this process (92;124;125). Clark, using the pig wound model demonstrated $\alpha_v\beta_3$ to be most heavily expressed at the tips of capillary sprouts, whereas β_1 integrins were expressed along the whole length of the wound neovasculature (124). More recently the relationship between the α_v integrins VEGF and bFGF was revealed when-$\alpha_v\beta_3$ antibodies blocked bFGF induced angiogenesis whereas anti-$\alpha_v\beta_5$ antibodies blocked VEGF mediated angiogenesis (126;127). Furthermore, *in vitro* studies have shown that blocking $\alpha_5\beta_1$ blocks bFGF-induced angiogenesis as apposed to VEGF-induced angiogenesis and that $\alpha_5\beta_1$ can also potentiate the action of $\alpha_v\beta_3$ (128). $\alpha_v\beta_3$ has also been shown to bind MMP-2 which is thought to involve its activation and its localisation to the surface of invading endothelial cells (129).

Once angiogenesis is established within a wound, filling it with granulation tissue, then this response must be limited and eventually shut down as part of the resolution of the healing response. It is thought that this occurs mainly via directed apoptosis of the unwanted neovasculature which is regulated by a variety of angiogenesis inhibitors including thrombospondins 1 and 2, angiostatin, endostatin, tumstatin and angiopoeitin 2 (129-131). Interestingly, recent studies have suggested that the anti-angiogenic effects of thrombospondins, tumstatin and endostatin may be mediated by binding to $\alpha_v\beta_3$ (112;113;129). Again there may be specific pathways involved since endostatin can block bFGF- but not VEGF-induced angiogenesis (132). Essentially, hypoxia-induced angiogenesis is shut down when tissue oxygen levels rise. However, it is now thought that angiogenesis is controlled by a net balance between molecules that have positive and negative regulatory activity. This has given rise to the idea of an angiogenic switch that characterises the endothelial activation status dependent on the balance between these regulatory molecules (133).

To date the best studied of all the angiogenic factors important in wound healing is VEGF. Its key role in angiogenesis during wound healing has been exemplified by attempts to introduce it exogenously to animal wounds. This has resulted in enhanced wound healing in a diabetic mouse model and increased strength of fascial repair in normal mice (134;135).

1.2 CELL ADHESION MOLECULES

Interaction with their environment and each other, requiring adhesive properties, is of fundamental importance to cells and is mediated by specific cell surface receptors or adhesion molecules (40). Cell adhesion molecules (CAMs) are transmembrane proteins which provide anchorage, cues for migration, and signals for cell growth

and differentiation (35). The functioning of multicellular organisms requires specific cell-cell and cell-matrix adhesion, and it is clear that many of the molecules used by early metazoans have been preserved through evolution (136). Without intercellular adhesion the formation of multilayered covering epithelia, epithelial gland formation or development of complex organ systems would be impossible (137). Most cells will express many different CAMs, but the localization and pattern of CAMs may be altered by the type of tissue, the position of a cell within a tissue and the state of cellular differentiation.

There are two principle types of cell adhesion which CAMs can participate in, namely cell adhesion to matrix proteins and cell-to-cell adhesion (35). Figure 1.3 illustrates the overall organisation of a cell to extracellular matrix (ECM) interaction, classically undertaken by the integrin molecules, and a cell-to-cell interaction commonly facilitated by the cadherin molecules. The application of molecular biology and molecular analyses over the last decade, now allows us to think of cell adhesion in terms of well defined molecules and thus made their classification easier. (40). The majority of adhesion molecules fall into 4 major families which are now well characterised and understood. These are the Cadherins, Immunoglobulin superfamily, Selectin and Integrin family of adhesion receptors (39). More recently knowledge is gathering on other families of adhesion receptors such as the syndecans and other membrane bound proteoglycans (41).

Figure 1.3: Diagrammatic representation of the integrin and cadherin classes of adhesion receptors. They are depicted in association with their cytoskeletal components and their typical extracellular ligands. Reproduced from(138;139)Tal-talin, Pax-paxillin, Vin-vinculin, FAK-focal adhesion kinase, Src-tyrosine kinase, CAS-docking protein.

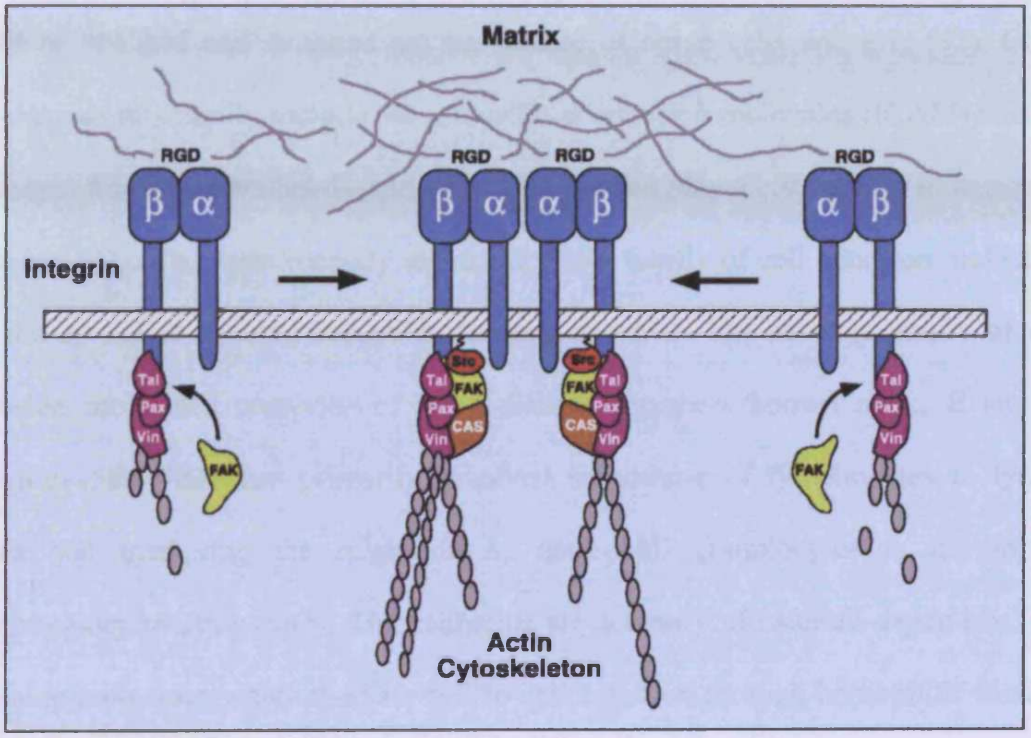

Cadherin

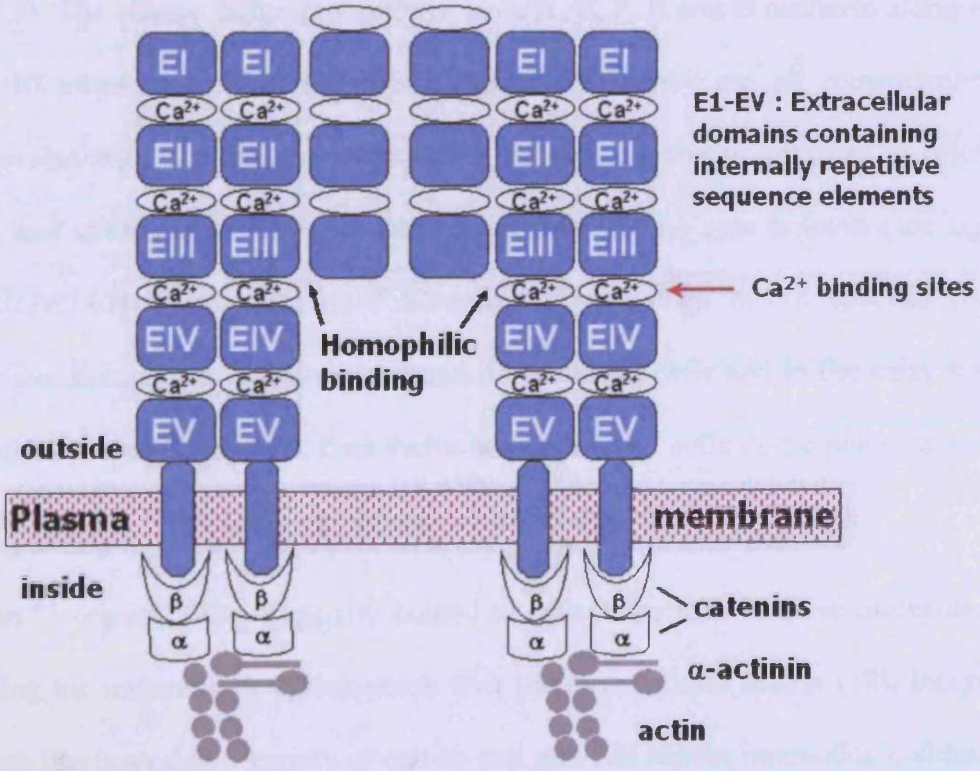

The members of the immunoglobulin super gene family of cell adhesion molecules are large plasma membrane glycoproteins which function primarily in cell-to-cell adhesion in a Ca^{2+} independent manner. The prototype of this family is the neural-CAM or N-CAM and is found on the surface of nerve cells and glia (42). Other members of this family include the intracellular adhesion molecules (ICAM) and the leucocyte function associated - antigens (LFA) which play a critical role in leucocyte adhesion (43). The most recently identified major family of cell adhesion molecules are the so called homing receptors, termed selectins. The selectin family of cell adhesion molecules comprise of three distinct members known as L, E and P-selectins (58). They are primarily involved in homing of lymphocytes to lymph nodes and mediating the migration of neutrophil granulocytes in developing inflammatory reactions (44). The cadherins are a family of calcium-dependent, cell adhesion molecules which mediate cell-to-cell adhesion through homophilic binding (i.e. cadherin bound to cadherin on an apposed cell in a Ca^{2+} dependent manner-see figure 1.3). The classic cadherin family include N, E, P, R and B cadherin along with around 10 other molecules described to date (27). They are all transmembrane glycoproteins with extracellular domains containing sequences involved in calcium binding and cytoplasmic domains which link them to the cytoskeleton (see figure 1.3) (27;29;140) They are highly homologous and each has a specific tissue distribution. E-cadherin is primarily found on epithelial cells and in the early stages of mammalian embryogenesis, P-cadherin is localised on cells in the placenta and in the epidermis and N-cadherin on nerves, heart and eye lens cells (27;29).

The term "integrins" was originally coined to reflect the role of these molecules in integrating the intracellular cytoskeleton with the extracellular matrix (38). Integrins have been implicated in a variety of cell-to-cell and cell matrix interactions, although

they appear to be the primary mediators of cell-to-extracellular matrix adhesion (52;58). Among the extracellular matrix ligands for integrins are fibronectin, fibrinogen, laminin, various collagens, entacin, tenascin, thrombospondin, von Willebrand factor and vitronectin (38). Although binding of the majority of integrins is to ligands that are components of extracellular matrices, certain integrins can bind soluble ligands such as fibrinogen or counter-receptors on adjacent cells (38).

The integrins have been characterized as non covalently associated, heterodimeric, transmembrane glycoproteins, consisting of an α and a β chain (141;142). This is illustrated in figure 1.3. At present there over 20 members of the integrin family selected from among 20 α and 8 β subunits that heterodimerise to produce the functional receptors (143;144). Association of these 20 α and 8 β could in theory give more than 100 integrin heterodimers, but in practice the diversity appears to be much more restricted (58). Many α subunits can only associate with a single β subunit allowing subfamilies with shared or common β subunits to be defined (i.e.β_1, β_2, β_3, β_4) (35). However, each β subunit can combine with a different α subunit and depending on the particular subunit pairing the intact heterodimer can recognize either one or multiple ligands present in the ECM or on the surface of opposing cells (145;146). In parallel with this, work carried out on defining the integrin ECM ligands and counter-receptors has made it clear that several different integrins bind to the same ligand, although the same recognition sequence is not always recognized or utilized (143).

1.2.1 Expression of integrins

The complement of integrins expressed by different cell types varies greatly with some integrins being clearly cell type specific. Examples of this are gpIIb/IIIa,

expressed exclusively by megakaryocytes and platelets along with $\alpha_6\beta_4$, which is specific for epithelial cells and tumours derived from them (143). The β_1 integrins also known as VLA subfamily, due to the late appearance of $\alpha_1\beta_1$ and $\alpha_2\beta_1$ on T lymphocytes, are expressed on a variety of cell types, including fibroblasts, leucocytes, platelets, monocytes, endothelial cells and most epithelial cell types (147). They serve as extracellular matrix binding proteins and specific binding can be found with the collagens, laminin, fibronectin and vitronectin, but they are also known to participate in cell-to-cell binding, in particular $\alpha_2\beta_1$ and $\alpha_3\beta_1$ (147).The β_1 chain has been localized by immunohistochemial studies on almost all epithelial cell types with reactivity occurring not only on the basal surfaces but also on lateral and apical surfaces (148;149).

The most extensively studied integrin group on leucocytes is the β_2 subfamily, but $\alpha_1\beta_1$, $\alpha_2\beta_1$, $\alpha_4\beta_1$ and $\alpha_4\beta_7$ integrins also occur on lymphocytes (150-152). Expression of the β_2 leucocyte integrins is found mainly on leucocytes and haemopoietic precursor cells. The leucocyte function associated molecule (LFA-1) with an $\alpha_L\beta_2$ chain occurs on almost all leucocytes but not on some tissue macrophages (153). The macrophage receptor Mac-1 with an $\alpha_M\beta_2$ chain has been detected on granulocytes, monocytes and some lymphocytes (147).

The α_V integrin subunit can associate with five different β subunits to form the functional heterodimers which mainly bind to vitronectin and fibronectin. However the $\alpha_V\beta_3$ integrin interacts with a variety of proteins involved in blood coagulation and is the only α_V integrin expressed on endothelia (154). The other α_V integrin heterodimers are expressed on a variety of epithelial cells of both normal and

neoplastic phenotype. The expression on these cells appears to be limited to the basal surface in contact with the basement membrane (147).

1.2.2 Extracellular structure and ligand interaction

The integrin chains all consist of a large extracellular domain, a membrane spanning domain, and an intracellular domain (155). All the α chains have a long extracellular domain of approximately 1000 kD containing several cation binding sites. The α subunits all contain a seven-fold repeat of a homologous segment. The last three or four of these repeats contains the sequences Asp-x-Asp-x-Asp-Gly-x-x-Asp or related sequences, that are thought to be involved in the divalent, cation-binding properties of these subunits (155;156). Similarly the β chains have long extracellular domains of approximately 750 kD with repetitive amino acid sequences containing a high number of cysteine residues believed to be internally disulphide bonded (156;157). Electron microscope studies suggest that the N-terminal extracellular domains of the α and β subunits combine to form a globular head configuration containing the ligand recognition sites (157;158). Connected to this are two extended tails containing the C-terminal portions of α and β subunits and their transmembrane domains.

It is this globular head structure made up of the N terminal extracellular regions of both subunits that is important in specific ligand recognition (156). This is based on the fact that the proteolytic and recombinant truncated fragments of $\alpha_{IIb}\beta_3$ integrin containing the N terminal halves of the α and β subunits, can bind their corresponding ligands. It is also known that high affinity ligand recognition requires both subunits and therefore may involve multiple ligand contact points (157).

Despite the diversity of integrin ligands, progress has been made in understanding the structural basis for ligand recognition by integrins. Several approaches to identify and characterize ligand binding sites have been implemented, including high resolution X-ray and NMR analysis, molecular modeling, crosslinking and site directed mutagenesis (159). It is evident from these studies that integrins possess multiple sites of ligand interaction. However, selectiveness of binding or recognition is still not fully understood.

1.2.3 Intracellular interactions

In view of the fact that the response of cells to adhesion includes spreading cytoskeletal organization, polarization, migration, proliferation and activation of specific gene expression, it is evident that cell adhesion involves a lot more than just cell attachment (160). As integrins have been analyzed in molecular detail, many of them have proved to be transmembrane proteins and evidence has accumulated to indicate that their cytoplasmic domains interact specifically with a variety of cytoskeletal proteins (155).

It was known for a number of years that sites of cell adhesion were also sites of intracellular cytoskeleton concentration (38). A picture has now emerged of integrins together with their cytoskeletal components being able to regulate or modulate signalling cascades initiated by other receptors. In this way integrin mediated cell adhesion has been shown to have profound effects in terms of amplitude and or duration, on signalling processes associated with receptor tyrosine kinases, G protein-coupled receptors and cytokine receptors (30;161;162). Therefore, via their integrin cell adhesion complexes, cells are able to integrate positional information concerning cell-to-cell or cell matrix contacts with information about the availability

of growth or differentiation factors. It is beyond the scope of this text to give a detailed account of the rapidly increasing intracellular events associated with integrin signaling processes. However, a summary of the more commonly known associations is illustrated in figure 1.4. It is evident from this summary that integrins can have profound effects on cellular proliferation, survival and motility.

Figure 1.4: *Diagrammatic illustration of the potential intracellular signalling pathways activated on integrin binding to their ECM Ligand or growth factor. Reproduced from (163). FAK = focal adhesion kinase, MLCK = myosin light chain kinase and PI3K = phosphoinositide-3-kinase. Red boxes = small GTPases, green boxes = protein kinases and yellow boxes cytoskeletal proteins.*

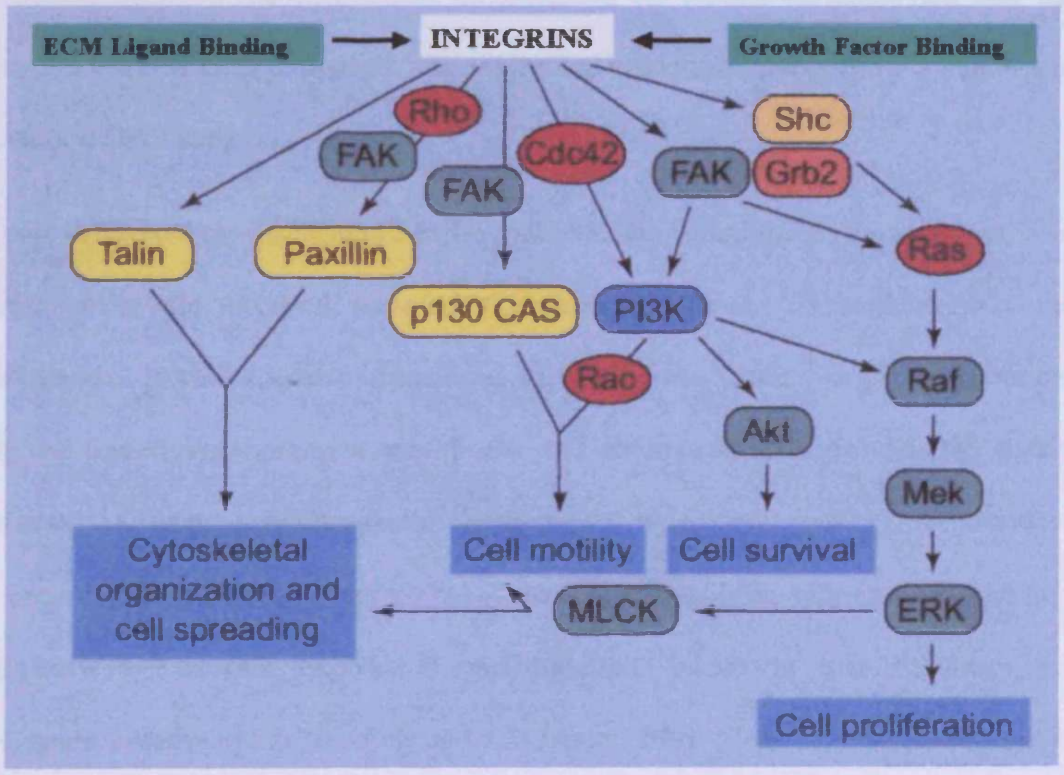

1.2.4 Integrins in wound healing

Wound repair is a complex process, which requires continual interaction among cells, cytokines and matrix. In view of this essential interaction, it is clear that integrins play an important role in all phases of wound repair. Initially the platelet

integrins are important in mediating their interaction with the provisional matrix proteins, which is essential for stable clot formation. During the subsequent phases of healing, the β_2 integrins play a critical role in leukocyte accumulation within the wound, in the process of neovascularisation and in the later stages during wound contraction, $\alpha_2\beta_1$ and $\alpha_5\beta_1$ integrins probably provide the linkage between fibroblasts and the ECM (164). Since the focus of this present study will be the keratinocyte integrins, it is significant that in the context of wound repair these are the best studied. To date, a number of epidermal wound healing studies have demonstrated a correlation between the appearance of integrins on wound keratinocytes and the appropriate ECM ligand beneath the migrating epidermis, suggesting a functional interaction (165-168).

As part of the cutaneous wound healing process, the function of keratinocytes is to rapidly cover the exposed underlying connective tissue. To achieve this, the keratinocytes at the wound margin need to disassemble their complex attachment with the underlying basement membrane and migrate over a provisional matrix consisting of fibrinogen, vitronectin, tenascin and type 1 collagen (1). Exposure of the wound margin keratinocytes to these new ligands has been suggested to lead to a modulation of integrin expression and function, which in turn regulates the subsequent keratinocyte spreading and migration (166). More recently, evidence is starting to emerge of a dynamic interplay between new matrix proteins such as laminin 5 laid down by the migrating keratinocytes, growth factors released at the migrating front and the integrins expressed by the keratnocytes themselves (169-172). This will be dealt with in the discussion in the context of the results of the current study.

1.3 MATRIX METALLOPROTINASES

Matrix metalloproteinases (MMP) are zinc and calcium dependent proteases, which cleave within their target polypeptides making them endopeptidases (173). To date there are 23 known human MMPs (listed in table 1.1) but the discovery of these proteases was made over forty years ago by Gross and Lapiere who demonstrated the involvement of a collagenase in the involution of tadpole tails (174). MMPs are actually one subfamily (termed matrixins) out of four making up the metzincin superfamily of proteases, the other three being the serralysins, adamalysins and astracins. This subclassification is based on structural homology within the subfamilies (175).

Traditionally the MMPs have been classified into the collagenases (MMP-1, 8, 13), gelatinases (MMP-2 and 9), stromelysins (MMP-3, 10, 11) and matrilysins (MMP-7 and 26) based on their substrate specificity (176) (see table 1.1). They were also assigned numbers according to the chronology of their discovery. As the list of non-ECM substrates cleaved by them grows and knowledge of the degree of overlap in substrate specificy has been gained, this classification system has become somewhat misleading in its nomenclature. More recently, identification of their genetic diversity was facilitated by the human genome project but use of the more traditional names remain useful as they often reflect a distinct function, structural feature or location (173).

Table 1.1: List of human MMPs and their substrates. Reproduced from reference (173)

Protein name*	Alternative names	Collagenous substrates	Non-collagenous ECM substrates	Non-structural ECM component substrates
MMP-1	Collagenase-1	Collagen types I, II, III, VII, VIII, X, and gelatin	Aggrecan, casein, nidogen, serpins, versican, perlecan, proteoglycan link protein, and tenascin-C	α_1-antichymotrypsin, α_1-antitrypsin/ α_1-proteinase inhibitor, IGFBP-3, IGFBP-5, IL-1β, L-selectin, ovostatin, recombinant TNF-α peptide, and SDF-1
MMP-2	Gelatinase-A	Collagen types I, IV, V, VII, X, XI, XIV, and gelatin	Aggrecan, elastin, fibronectin, laminin, nidogen, proteoglycan link protein, and versican	Active MMP-9, active MMP-13, FGF R1, IGF-BP3, IGF-BP5, IL-1β, recombinant TNF-α peptide, and TGF-β
MMP-3	Stromelysin-1	Collagen types II, IV, IX, X, and gelatin	Aggrecan, casein, decorin, elastin, fibronectin, laminin, nidogen, perlecan, proteoglycan, proteoglycan link protein, and versican	α_1-antichymotrypsin, α_1-proteinase inhibitor, antithrombin III, E-cadherin, fibrinogen, IGF-BP3, L-selectin, ovostatin, pro-HB-EGF, pro-IL-β, pro-MMP-1, pro-MMP8, pro-MMP-9, pro-TNFα, and SDF-1
MMP-7	Matrilysin-1, neutrophil collagenase	Collagen types I, II, III, V, IV, and X	Aggrecan, casein, elastin, enactin, laminin, and proteoglycan link protein	β_4 integrin, decorin, defensin, E-cadherin, Fas-L, plasminogen, pro-MMP-2, pro-MMP-7, pro-TNFα, transferrin, and syndecan
MMP-8	Collagenase-2	Collagen types I, II, III, V, VII, VIII, X, and gelatin	Aggrecan, laminin, and nidogen	α_2-antiplasmin and pro-MMP-8
MMP-9	Gelatinase-B	Collagen types IV, V, VII, X, and XIV	Fibronectin, laminin, nidogen, proteoglycan link protein, and versican	CXCL5, IL-1β, IL2-R, plasminogen, pro-TNFα, SDF-1, and TGF-β
MMP-10	Stromelysin-2	Collagen types III, IV, V, and gelatin	Fibronectin, laminin, and nidogen	Pro-MMP-1, pro-MMP-8, and pro-MMP-10
MMP-11	Stromelysin-3		Laminin	α_1-antitrypsin, α_1-proteinase inhibitor, and IGFBP-1
MMP-12	Macrophage metalloelastase		Elastin	Plasminogen
MMP-13	Collagenase-3	Collagen types I, II, III, IV, V, IX, X, XI, and gelatin	Aggrecan, fibronectin, laminin, perlecan, and tenascin	Plasminogen activator 2, pro-MMP-9, pro-MMP-13, and SDF-1
MMP-14	MT1-MMP	Collagen types I, II, III, and gelatin	Aggrecan, dermatan sulphate proteoglycan, fibrin, fibronectin, laminin, nidogen, perlecan, tenascin, and vitronectin	$\alpha_v\beta_3$ integrin, CD44, gC1qR, pro-MMP2, pro-MMP-13, pro-TNFα, SDF-1, and tissue transglutaminase
MMP-15	MT2-MMP	Collagen types I, II, III, and gelatin	Aggrecan, fibronectin, laminin, nidogen, perlecan, tenascin, and vitronectin	Pro-MMP-2, pro-MMP-13, and tissue transglutaminase
MMP-16	MT3-MMP	Collagen types I, III, and gelatin	Aggrecan, casein, fibronectin, laminin, perlecan, and vitronectin	Pro-MMP-2 and pro-MMP-13
MMP-17	MT4-MMP	Gelatin	Fibrin and fibronectin	
MMP-19	RASI-1	Collagens types I, IV, and gelatin	Aggrecan, casein, fibronectin, laminin, nidogen, and tenascin	
MMP-20	Enamelysin		Aggrecan, amelogenin, and cartilage oligomeric protein	
MMP-21				α_1-antitrypsin
MMP-23	CA-MMP	Gelatin		
MMP-24	MT5-MMP	Gelatin	Chondroitin sulfate, dermatin sulfate, and fibronectin	Pro-MMP2 and pro-MMP-13
MMP-25	Leukolysin, MT6-MMP		Collagen type IV and gelatin	Fibrin and fibronectin Pro-MMP-2
MMP-26	Matrilysin-2, endometase	Collagen type IV and gelatin	Casein, fibrinogen, and fibronectin	β_1-proteinase inhibitor
MMP-28	Epilysin		Casein	

*Although there are 23 human MMPs, 29 numbers have been used in the literature. The symbols MMP-4, MMP-5, MMP-6 and MMP-29 are redundant in humans and are no longer in use; MMP-18 corresponds to a *Xenopus laevis* collagenase, for which no human ortholog is known, and a human protein published as MMP-18 is now called MMP-19. Two nearly identical human genes found in a segment of chromosome 1 that is duplicated were called *MMP21* and *MMP22* but are now referred to as *MMP23A* and *MMP23B*.

The MMP genes are structurally similar and a number of them (MMP1, MMP3, MMP7, MMP8, MMP10, MMP12, MMP13, MMP20 and MMP26) are found in a cluster on human chromosome 11 (11q21-23), which suggests that they evolved by duplication of a common ancestral gene (173;177). This is further reflected in their similar mechanisms of catalysis and regulation. In particular they require zinc at their catalytic site and are synthesised as zymogens (proMMPs) containing a cysteine switch motif PRCGXPD in the propeptide that maintains them in their zymogen form (outlined in figure) (112;177).

Most of the known MMPs are secreted, apart from a subset termed membrane-type MMPs (MT-MMPs), containing a single transmembrane domain, ensuring their cell surface expression, followed by a cytoplasmic tail. The basic structure of the MMPs, otherwise termed the minimal domain MMP structure, consists of a secretory signal sequence, a pro-domain that maintains the zymogen status and a catalytic domain (see figure). The catalytic domain consists of a consensus motif, which contains three histidines providing a zinc binding site, in addition to a conserved 'Met-turn' motif, which resides below the active site zinc ion (175;177;178). Two of the MMPs (MMP-7 and 26), only contain this mimimal domain structure and have been termed the minimal domain MMPs or matrilysins (179;180). Other MMPs contain additional features such as a carboxy terminal hemopexin-like domain conferring a degree of substrate specificity, a furin protease cleavage site in the pro-domain or a fibronectin-like repeat sequence in the catalytic domain (175). There are seven MT-MMPs all possessing furin-cleavage recognition sites between their pro and catalytic domains. Four of them (MT1-, MT2-, MT3- and MT5-MMP) have a transmembrane domain and short cytoplasmic tail making them type I transmembrane proteins (181).

Figure 1.5: Diagrammatic representation of the domain structure of the various subtypes of MMPs. Reproduced from reference (173)

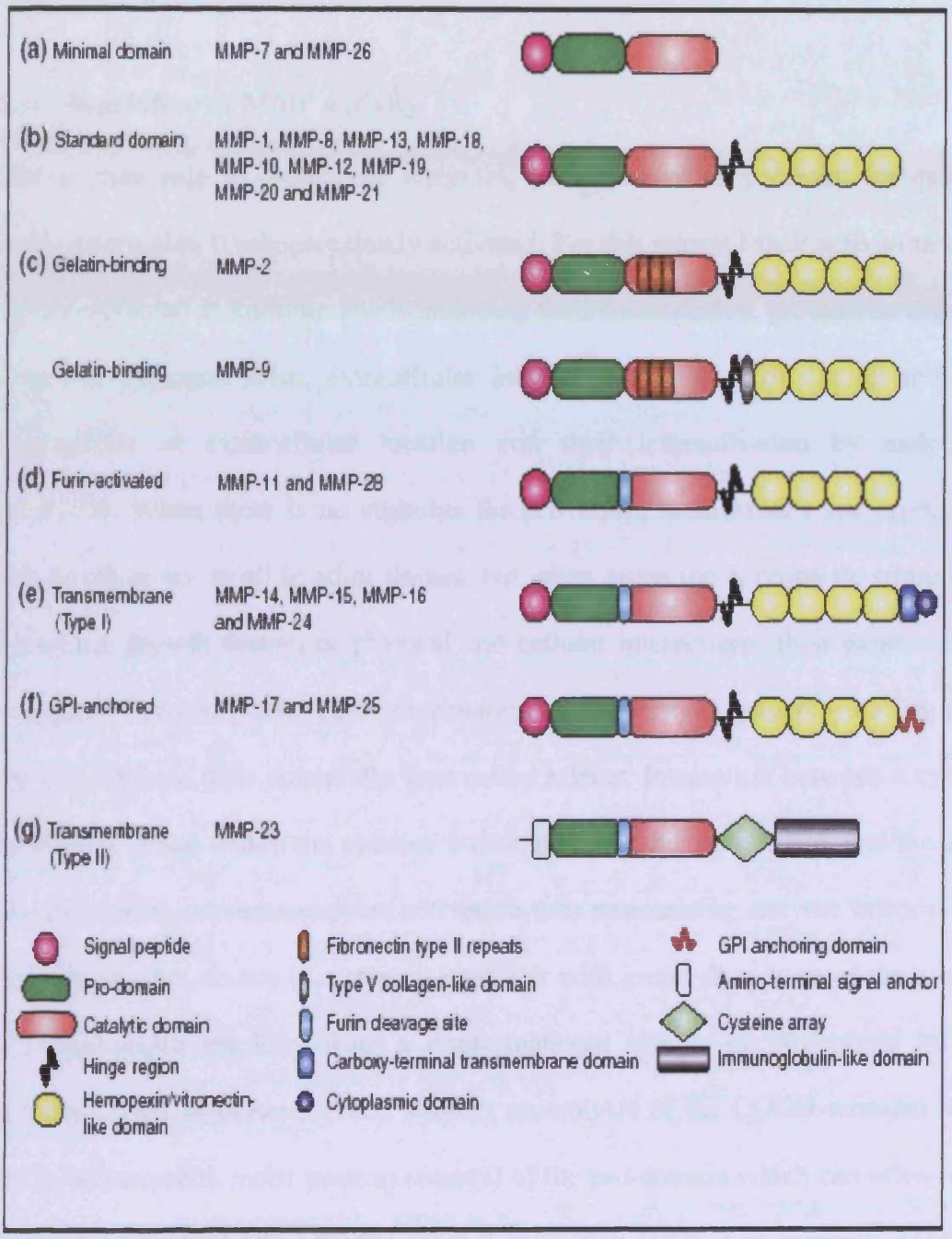

However, MMP-23 has an NH_2-terminal signal anchor positioned intracellularly in a type II transmembrane orientation (182;183). The other two (MT4- and MT6-MMP) are bound to the membrane via a glycosylphosphatidylinositol moiety at their COOH

termini (184). Apart from MMP-23 and MT4-MMP they are all capable of activating MMP-2 (177).

1.3.1 Regulation of MMP activity

Due to their role as proteolytic enzymes, MMPs have the potential for extensive tissue destruction if inappropriately activated. For this reason MMP activation is very tightly regulated at multiple levels including their transcription, proteolytic activation from the zymogen form, extracellular inhibition by a host of natural inhibitors, intracellular or extracellular location and their internalisation by endocytosis (173;175). When there is no stimulus for activation, most MMPs are expressed at low levels or not at all in adult tissues, but when given the appropriate stimuli from cytokines, growth factors or physical and cellular interactions, their expression can be rapidly induced (185). Their expression as inactive zymogens plays a key role in the limitation of their potentially destructive effects. Interaction between a cysteine-sulphydryl group within the cysteine switch motif of the pro-domain, and the active-site zinc atom, prevents enzyme activation thus maintaining enzyme latency (173). Activation often occurs in a stepwise manner with initial disruption of the cysteine-zinc interaction resulting from a conformational change or proteolysis by other proteases such as plasmin (186). Further proteolysis of the COOH-terminal side of the cysteine switch motif leads to removal of the pro-domain which can often require the involvement of other MMPs for full activation (177). For example, MMP-2 is activated by MT-MMPs such as MMP-14 (181).

A number of MMPs (proMMP-1, proMMP-3, proMMP-7, proMMP-9, proMMP-10 and proMMP-13) are activated by plasmin, which is generated from plasminogen by tissue plasminogen activator bound to fibrin and from urokinase plasminogen

activator bound to a specific cell surface receptor (187). As both plasminogen and urokinase plasminogen activator are membrane associated, they are able to localise the activation of MMPs to prevent unwanted tissue destruction and producing directed ECM remodelling.

Once MMPs are activated, there are four classes of inhibitors present in the extracellular spaces and body fluids known to have broad inhibitory activity against many of them (188). These include the tissue inhibitors of metalloproteinases (TIMPs), membrane anchored molecules termed reversion-inducing cysteine-rich protein with Kazal motifs (RECK) and in the circulation the protease inhibitor α2-macroglobulin (188;189). The fourth class includes a number of proteins containing sequences with some similarity to the N-terminal sequence of the TIMPs. These are the netrins such as the small inhibitor derived by proteolysis of the procollagen C-proteinase enhancer (PCPE) and a serine proteinase inhibitor termed tissue factor pathway inhibitor 2 (TFPI-2) (190). In addition thrombospondin-1 and 2 have also been shown to inhibit the activity of MMP-2 and more specifically thrombospondin-1 inhibits proMMP-2 and proMMP-9 activation (191).

TIMPs are the most extensively studied of all the MMP inhibitors. This may be a reflection of their ability to inhibit all MMPs tested to date apart from TIMP-1, which fails to inhibit MT1-MMP (177). They are secreted proteins with a molecular weight of ~21kDa, which are variably glycosylated and are made up of a three-loop N-terminal domain and an interacting three-loop C-subdomain (192). To date there are four mammalian TIMPs that have been cloned, purified and characterised. They are thought to regulate MMP activity during tissue remodelling (192). Although they are secreted, they may also be found at the cell surface in association with membrane-bound proteins as, for example, TIMP-2, TIMP-3 and TIMP-4 can bind

MT1-MMP (188). TIMPs bind to MMPs in a 1:1 stoichiometric ratio and reversibly block MMP activity but differ in their expression patterns and affinity for various MMPs (193). Essentialy, TIMP-1 and -2 inhibit a broad range of MMPs, Timp-3 preferentially inhibits MMP-1, -3, -7 and -13 and TIMP-4 is more restricted to MMP-2 and –7, with lesser activity towards MMP-1, -3 and -9 (175). More recently, evidence has emerged that they may also have additional functions to MMP inhibition such as the involvement of TIMP-2 in activation of MMP-2 (175).

In normal tissues MMPs are only expressed when and where needed for processes such as embryonic development, wound healing, uterine and mammary involution, cartilage-to-bone transition during ossification, and trophoblast invasion into the endometrial stroma during placental development (112;175). Aberrant expression of MMPs has however been associated with pathological conditions such as periodontitis, pulmonary fibrosis, rheumatoid arthritis, and tumour cell invasion and metastasis (194-197).

A key step in the degradation of the ECM is the extracellular secretion of MMPs and indeed the collagenases (MMP-1, 8, 13 and 14) are the only MMPs that can efficiently degrade the fibrillar collagens (types I, II and III) in their triple helical domains (198). This initial cleavage renders these molecules thermally unstable allowing them to unwind to form gelatin, which can then be degraded by other MMPs, the major gelatinises being MMP-2 and 9 (173).

Classicaly the MMPs have been thought of as molecules purely involved in matrix degradation and remodelling. However, the ECM is no longer thought of as simply an extracellular scaffold but in addition, a reservoir for biological molecules (e.g. growth factors) and a source of signals for directing cell migration and activation. In

line with this, the view of the biological roles of MMPs has also changed and their interaction with the ECM is now thought to influence cell behaviour. For example, MMPs can release several growth factors (i.e. TGFβ and FGF-1) by cleaving either the growth-factor binding protein or the matrix molecule to which these proteins attach (199). Furthermore, growth factor precursors such as members of the EGF family have been shown to be activated and released by MMP mediated proteolytic cleavage (HB-EGF cleaved by MMP-3 and MMP-7) (200). In fact, MMP substrates include a number of non-ECM molecules such as cell surface receptors (i.e. CD44 cleaved by MMP-14) and adhesion receptors (i.e. E-cadherin cleaved by MMP-3) (see table 1.1) (201;202). As a result of these interactions with non-ECM substrates, they are now thought to be involved in a variety of physiological and pathological processes that were previously unrecognised (191;203).

1.3.2 MMPs and Wound Healing

Given the complex interactions between different cell types, matrix components and biological factors it is not surprising that MMPs have been found to play a crucial role in many of the key processes involved in wound healing. ECM degradation/ remodelling by MMPs is required at many stages of normal wound healing, including provisional matrix degradation, cell migration, angiogenesis, and matrix remodelling of the granulation tissue. Several MMPs have been implicated in these stages of wound healing, during which they are strictly, spatially and temporally regulated. Furthermore, wound healing models have demonstrated MMP inhibitors such as TIMP-1 to inhibit processes such as keratinocyte migration thus delaying wound closure (204). Similarly, lack of MMP activation has been shown to impair wound healing as demonstrated by the poor wound healing response seen in

plasminogen-deficient mice (205). Complete blocking of keratinocytes migration in these knockout mouse models treated with additional MMP inhibitors suggests a degree of synergism between these two classes of proteolytic enzymes (206).

MMPs are produced by a broad range of cells, including normal epithelial cells, fibroblasts, myofibroblasts, chondrocytes, osteoclasts, endothelial cells and leucocytes (176). For example collagenase-1 (MMP-1), stromelysin-2 (MMP-10) and gelatinase B (MMP-9) are all expressed by migrating keratinocytes. A great deal of evidence is now accumulating on the role of MMPs in angiogenesis another vital process in wound healing. Not only are they involved in the degrading of basement membrane and other ECM components allowing endothelial detachment and migration into new tissue but also in release of ECM-bound proangiogenic factors (bFGF, VEGF, and TGFβ) (112). They are also capable of generating endogenous angiogenesis inhibitors such as the cleavage of plasmin by MMPs releasing angiostatin (113). Indeed, MMP inhibitors have been shown to inihibit angiogenesis in animal models (207).

During the last ten years there has been an increasing interest in the role of MMPs in chronic wounds. Early studies showing their elevated levels in granulation tissue of chronic pressure ulcers and chronic leg ulcers suggested that a highly ptoteolytic environment was contributing to the chronicity of these wounds (208). Subsequent studies have shown decreased levels of TIMPs with corresponding increased levels of MMPs to be present in chronic wounds (209;210). This evidence implies that the ratio of MMPs to their corresponding inhibitors is more important in determining whether there is ECM or growth factor degradation than their individual levels.

1.3.3 MMP-2 (Gelatinase A) and MMP-9 (Gelatinase B)

MMP-2 and MMP-9 are the major gelatinises. However, despite this relative specificity they are also able to degrade collagens IV, V, VII and X, fibronectin, vitronectin and laminins (211). In addition MMP-2 can assist the collagenases (i.e. MMP-1 and MMP-8) in degrading the interstitial collagens (types I-III), the initial rate limiting step in ECM degradation, as these collagens constitute the ECM's major structural components (212). The gelatinases can then continue degrading these denatured collagen fragments (gelatins) along with the stromelysins (MMP-3, -10, -11). Structurally they differ from other MMPs in having three repeats of a type II fibronectin-like domain inserted between their catalytic and homeopexin-like domains allowing them to bind with gelatin, collagens and laminin (213).

MMP-2 has a Mr of 72kD and is expressed mainly in dermal fibroblasts and endothelial cells (214). It is unique among MMPs as it does not contain sequences within its propeptide susceptible to proteolytic activation but alternatively has a recently characterised, distinctive cell surface mechanism of activation. This involves intracellular processing of MT1-MMP and transport to the cell membrane where it binds TIMP-2 via its catalytic domain. Interaction of pro-MMP-2 with TIMP-2 then allows a nearby MT1-MMP to partially activate the pro-MMP-2, which completes its activation by autocatalysis (215;216). Several other MT-MMPs have been implicated in its activation including MT2, MT3, MT5 and MT6-MMP (177). MMP-2 inhibition can be carried out by any of the four TIMPS, thrombospondin-2 and the cell surface receptor known as RECK (188).

Regulation of MMP-2 differs fundamentally from the other MMPs. This is reflected in its constitutive level of expression allowing it to play a housekeeping role in dissolution of damaged collagens and remodelling of newly synthesised matrixes

(110). The presence of a noncanonical TATA box in its promoter region directing its basal level of secretion is consistant with this role. In addition, The MMP-2 promoter region lacks the 12-O-tetradecanoylphorbol-13-acetate (TPA) responsive element (TRE) sequence as well as the known transactivator sequences AP-1 and PEA-3, which may explain the lack of MMP-2 upregulation by agents such as PMA, TNF- or IL-1 (217). The promoter also lacks the upstream TGF-β inihibitory element, which correlates with evidence that MMP-2 transcription is not suppressed by TGF-β (217).

The MMP-9 proenzyme has an Mr of 92 kD and its secretion has been associated with eosinophils, neutrophils, macrophages, monocytes, alveolar macrophages, cultured keratinocytes and other transformed and tumour derived cells (218-221). This proenzyme includes a propeptide element with an M_r of 10 Kd involved in maintaining enzyme latency and lost on full activation (222). Unlike MMP-2, the MMP-9 promoter region contains two putative TREs that may serve as the binding sites for the transcription factor AP-1. Other regulatory binding sites demonstrated to be present in the promoter region are the SP-1 and nuclear factor kappa B (NF-kB) transcription factors. In addition, a consensus sequence for a TGFβ inhibitory element has been identified but its role in MMP-9 inihibition is still not entirely clear as other evidence suggests a role for TGFβ in upregulating MMP-9 synthesis (222-225). However, the above regulatory binding sites may be implicated in the activation of MMP-9 expression induced by several growth factors and cytokines including IL-1β, EGF, and TNFα (226-228). In addition to being activated by several growth factors and cytokines, MMP-9 has also been implicated in the activation of TGFβ, VEGF and IL-8 as well as downregulation of IL-2 receptor α (199;229).

MMP-9 inhibition is carried out by the TIMPs, more specifically TIMP-1 and like MMP-2, its cell surface inhibition is carried out by RECK (173;188). In fact, MMP-9 binds several cell surface receptors such as CD44, ICAM and the α2 chain of type IV collagen which localises to the cell surface of MCF10A human breast epithelial cells (230-232). The association with CD44 can lead to activation of latent TGF-β suggesting that cell surface location of MMP-9 provides a mechanism to direct and localise its activity to the pericellular environment (199). Given the range of cell types expressing MMP-9 and its ability to degrade/remodel the ECM, it is not surprising that it has been implicated in several developmental, repairative or pathological processes. These include regulation of bone development, trophoblast invasion during embryo implantation, stromal cell expression during tumour cell infiltration, penetration of the vascular endothelial wall during tumour metastsis, angiogenesis, rheumatoid arthritis and several processes involved in wound repair (175;233).

Studying the complex interacations between different cell types, matrix components and biological factors involved in the various phases of wound healing has revealed a key role for the gelatinases in many of these processes. A study of the temporal and spatial expression patterns of MMPS during healing of murine excisional skin wounds suggested that MMP-9 levels were increased during active re-epithelialisation, whereas MMP-2 levels and its cell surface activator MT1-MMP were detected exclusively and at high levels in the granulation tissue during the later phases of wound repair (234). Similarly, in a study of human mucosal wounds, MMP-9 was prominent in keratinocytes during wound resurfacing while MMP-2 was localised to the stroma (214). In fact, elevated levels of gelatinases have been found

in a number of wound types including acute surgical wounds, blisters, experimental corneal wounds, burns injuries and venous leg ulcers (209;235-238).

The role of gelatinases in chronic human wounds in conjuction with MMPs in general has been increasingly investigated during the last decade. Yager and co-workers demonstrated elevated levels of the gelatinases in decubitus ulcer fluid compared to mastectomy drain fluid and Bullen and co-workers demonstrated elevated levels of MMP-9 in chronic wounds in conjuction with decreased levels of TIMPs (209;239). More recently Trengrove and co-workers demonstrated that high levels of MMPs including MMP-2 and -9 decreased on transition of a chronic wound from a non healing to a healing phase (240). This was supported by Wysocki and co-workers who demonstrated concomitantly raised levels of MMP-9 and urokinase plasminogen activator (uPA) in chronic wounds, which decreased on healing. They suggested a possible proteolytic cascade initiated by the plasminogen activator-plasmin (PA-plasmin) system leading to activation of MMP-9 was present in chronic wounds (221). It is clear fom the cumulative evidence, that levels of gelatinases and their endogenous inhibitors, the TIMPs, plays a key role in the pathophysiology of chronic wounds. However, it remains unclear whether this is a causative role or a result of the disordered inflammatory response characteristic of these wounds.

1.4 HYPOXIA AND WOUND HEALING

Disruption of blood supply that occurs in damaged or inflamed tissues often leads to the formation of areas of low oxygen tension or hypoxia. Normally the oxygen tension within healthy tissues is of the order of 20-70 mmHg, equivalent to 2.5-9% oxygen saturation (30). However, when there is inadequate tissue perfusion within wounds, multiple transient or chronic areas of hypoxia can develop. In this setting

oxygen levels less than 10 mmHg equivalent to <1% saturation have been reported (12;33;72).

There are a number of underlying causes such as diabetes, peripheral vascular disease, radiation injury, pressure injury and venous stasis known to be responsible for creating and perpetuating chronic wounds (75). The common feature to all of these conditions is inadequate tissue oxygenation, which is a known impediment to normal wound healing (75;76). However this is a paradox in itself since there is now an emerging view that while detrimental to wound healing, low oxygen tension may provide a stimulus for certain cellular activities. This is understood from the perspective that in acute wounds hypoxia is temporary while in chronic wounds persistent hypoxia may actually be part of the pathogenesis of the wound. Evidence continues to accumulate suggesting that oxygen is an important independent control for many cellular activities and for the expression of several eukaryotic genes (84). It is now known that several genes important in tissue repair particularly VEGF can be directly influenced by low oxygen tension via HIFs, which is dealt with in more detail in section 1.1.6. Fibroblast replication, longevity and clonal expansion are all enhanced in hypoxia, and as early as 1985 macrophages were shown to excrete an angiogenic factor only when exposed to low oxygen tension (30;48;77-79). The effect on macrophages was reversible and the threshold for production of the angiogenic factor was 15-20mmHg. Similarly hypoxia has been shown to upregulate the synthesis of TGFβ, endothelin-1, platelet derived growth factor B chain and vascular endothelial growth factor (80-83).

The role of hypoxia in chronic venous leg ulcer wounds is particularly complicated since oxygen levels within these wounds is perplexingly low in spite of the fact that limb amputation is rarely necessary (84). One of the ways in which hypoxia can

contribute to the chronicity of venous leg ulcers is by predisposing them to wound infection as oxygen is bacteriocidal to some anaerobes (241-243). Oxygen also improves the bacteriocidal function of phagocytes and may reduce production of toxins by clostridia (244)

It may be for these reasons that hyperbaric oxygen (100% oxygen greater than atmospheric pressure) has been used in the treatment of chronic wounds (245). However there is not a universal agreement on the use of hyperbaric oxygen in the treatment of leg ulceration. Furthermore, its use is only effective when inhaled, as oxygen applied directly to the wound has not been shown to penetrate beyond the immediate surface of the wound (246). In spite of this, several small studies have demonstrated a benefit from hyperbaric oxygen therapy in treating diabetic foot ulcers and patients who smoked but did not show signs of peripheral vascular disease (245;247)

The role of oxygen in the enhancement of growth factor action within wound tissue may explain its beneficial effect on chronic wounds. In fact, hyperbaric oxygen is one of the treatments along with growth factors and compression bandaging for venous ulceration, which have been used clinically to enhance the rate of healing in chronic wounds (75). Treatment with hyperbaric oxygen to reverse ischaemic conditions in a rabbit dermal ulcer model enhanced the effect of bFGF (76). Furthermore treatment of an aged rabbit dermal ear ulcer model with hyperbaric oxygen showed an equivalent beneficial healing response to treatment with $TGF\beta_3$ (75).

Investigators have also focused on the effect of hypoxia on macrophage activity. Macrophages are known to accumulate in or adjacent to poorly vascularised,

diseased or damaged tissue. These tissues include avascular and necrotic sites in breasts (248) and ovarian carcinomas (249), hypoxic areas of dermal wounds (250), avascular locations in atherosclerotic plaques (41), the synovium in joints with rheumatoid arthritis (251) and ischaemic sites in proliferative retinopathy (252). It is thought that by altering gene expression and adapting their metabolic activity macrophages are able to continue functioning under such extreme conditions. In fact hypoxia can also induce marked changes in their secretory activity, promoting the release of both pro-angiogenic and inflammatory cytokines by macrophages *in vitro* and *in vivo* (for reviews see (41)). However, maintaining phagocytic and bacteriocidal functions under hypoxic conditions is more difficult for macrophages as they require oxygen to generate the respiratory burst associated with these functions. This is directly through the production of reactive oxygen species such as superoxide and indirectly by regulating intravacuolar pH to levels optimal for lysosomal enzyme activity (253). It is not surprising therefore that a number of studies have reported an inhibitory effect of hypoxia on the phagocytic activity of macrophages *in vitro* or *in vivo* (254-256).

It is worth noting that relatively few studies have shown the aforementioned effects of hypoxia without the presence of additional co-stimuli. For example *in vitro* studies have shown LPS and IFNγ to enhance the response of macrophages to hypoxia (257-259). In summary, the response of macrophages to hypoxia promotes the accumulation, survival and activation of macrophages and other leukocytes at diseased sites. Furthermore, it stimulates neovascularisation by the mechanisms already described in section 1.1.6 to re-establish full perfusion and tissue oxygenation. This sequence of events, resulting from the stimulation of macrophages by hypoxia is particularly evident in wound healing and solid tumours.

1.5 MODELS OF WOUND HEALING

The biological complexity of the healing process has made finding a model that can accurately and reliably reproduce the events of wound healing in human tissue extremely difficult. For this reason both *in vivo* and *in vitro* models of wound healing tend to focus on specific phases of this process such as the inflammatory response and the synthetic or remodelling phases. The validity of any model is however founded on the same basic principles. It must provide reproducible, quantifiable data that recapitulates as closely as possible the specific or multiple events and conditions within a human wound. The following section attempts to provide a brief overview of the use of *in vivo* and *in vitro* models of wound healing, allowing later comparison with the tissue explant model developed within the current study.

In vivo Models

In vivo models of tissue repair can involve both animal and human models. The use of experimental animal models for scientific research has encompassed a range of living organisms from unicellular protozoans to chimpanzees (144). Specific animal models are normally characterised by an inherited, naturally acquired or induced pathological process that, in one or more respects, closely resembles the same phenomenon in humans (143;144). When considering the choice of animal model for the study of tissue repair, the following factors have been proposed to be important (144):-

- accurate reproduction of the specific wound lesion
- possibility for multiple investigations
- exportability

- ability to obtain multiple biopsy samples
- compatibility with animal facilities
- ease of handling
- availability in more than one species
- time required to obtain useful results.

There is an obvious advantage to choosing human tissue in that it will more accurately reflect the complex nature of human wounds encountered in clinical practice. However human wound healing studies are limited by the ability to excise and analyze tissue, which is particularly difficult when creating skin wounds in normal healthy subjects. Creation of any skin wound or excision of existing wound tissue in human subjects carries ethical implications.

Choosing the type of *in vivo* model can be directed by the specific phase of the healing response that the investigator wants to study. Several models have been developed for the study of angiogenesis. These include a rabbit ear chamber (148;149), the Algire chamber (transparent plastic window placed in the dorsal subcutaneous tissue of a mouse), the hamster cheek pouch, the rabbit corneal pocket and the chick chorioallantoic membrane assay (CAM)(reviewed in (144)). The rabbit ear chamber provides a method for vision, photography and quantification of capillaries filling an artificially defined wound during measurable changes in the oxygen environment (33). The Algire chamber provides similar methods of measuring angiogenesis. However, these models possess little resemblance to clinical wounds. Furthermore the tissues are not utilised in the context of their normal physiology since the cornea is normally avascular and CAM is a tissue that grows very rapidly compared to most other tissues (144).

Various histological approaches to quantifying angiogenesis have also been used based on applying specific staining techniques to serial tissue sections (151;152). These do not allow dynamic investigation and it has been shown that endothelial cell counts from histological sections can provide a misleading index of angiogenesis (144;150). Epithelialisation and dermal reconstitution have also been evaluated using serial sections of wound tissue (153).

Models developed for the study of granulation tissue formation and wound contraction are based on artificial types of wounds using implanted foreign material. Alternatively, tissue models directly related to the pathogenesis of specific wounds such as excisional, incisional or burn wounds have been used. Artificial wounds are created by implanting a chamber, sponge or tube into a subcutaneous pocket (reviewed in (144) and (48)). This creates a dead space in which granulation tissue can develop at the periphery and in the case of the chambers, the central reservoir is filled with wound fluid. The use of tubes involves less trauma and can therefore be used in humans. The validity of these artificial models was supported by the finding that collagen deposition within polyvinyl alcohol (PVA) sponges correlates with incised wound tensile strength during healing (154). The dead space created within these artificial wounds provides a site of easy access to the wound where putative agents such as growth factors and function blocking antibodies can be added (163). In addition the artificial wounds can be retrieved allowing investigators to determine cellular infiltration, protein content, and deposition of extracellular matrix (154). Although they provide information on granulation tissue formation and its tensile strength, artificial wounds do not address the problem of chronic or non healing wounds. Furthermore, they cannot provide information on epithelialisation.

Questions have also been raised about physical characteristics such as pore size, a property which can itself affect the rate of cellular infiltration (260).

Tissue models of wound healing are based on the removal of normal or wounded tissue at single or multiple time points. Although discontinuous as a measurement, when repeated samples are taken over a timecourse, a dynamic element of monitoring can be achieved. Excisional wound models lend themselves to the study of wound healing in animals as they can be accurately reproduced and allow multiple investigation since the wounds can be made anywhere on the body surface. Excision of a small amount of tissue from human skin, normally by biopsy, is one of the few available tissue models of healing in humans. Scalpels, scissors or dermatomes have been used mainly in rats, hamsters, rabbits and pigs to create full or partial thickness excision wounds. Study of this excision tissue allows multiple processes to be evaluated including epithelialisation, contraction, dermal reconstitution, inflammation, chemotaxis, angiogenesis, matrix production/organisation and cosmetic and functional outcome (144)

Excisional models can be used to study the effect of dressings or externally applied biological agents and recapitulates the loss of tissue often resulting from the inciting insult involved in creating a wound *in vivo.* However extrapolating data from excisional wound studies in animals to humans can be a problem as many of the animal species used (mouse, rat, rabbit and hamster), have a subcutaneous panniculus carnosus muscle, which enhances wound closure by contraction. The pig is the laboratory species considered to be the closest approximation of skin structure to humans but displays a rapid healing course with contraction formation (63). For this reason the rabbit ear model is considered the best approximation to human

wound healing, where this is by epithelialisation and granulation tissue formation, as this model heals without contraction (46).

In considering their application as tissue models of wound healing incisional wounds possess the same properties as those already described for excisional wounds i.e. they can be accurately reproduced and can involve multiple investigations. Incisional wound models have been used in skin and other organs available for surgery such as retina, tendons and anastomosis of internal viscera with the main outcome measurements being wound strength collagen content and histology (144). The advantage of incisional wound models, particularly in human tissue, is that they show good approximation to surgically inflicted wounds seen in clinical practice.

Regeneration of the superficial layers of the skin has been extensively studied using suction blister wound models (64;261), tape stripping models (31) and partial thickness dermatome excision models (165;166). Because these wounds are superficial, they can be used in human studies. However, their obvious limitation is that no information can be gained concerning matrix deposition. Furthermore, in the case of the blister and tape stripping models, the epidermal regeneration occurs without the disruption of the basement membrane, an event that normally occurs in the majority of cutaneous wounds seen in clinical practice.

The *in vivo* models dealt with so far all possess the ability to model one or more elements of an acute wound, which follows an increasingly understood biological pathway towards undelayed wound closure. However it is well known that human skin is unique and highly variable according to age, sex, race and region of the body (167;168). For this reason there is no one single model that can fully represent the biological phenomenon of the human wound healing process. This is particularly true

when dealing with complex chronic or difficult to heal wounds. Some authors question the use of animal models suggesting that many of the apparent abnormalities presented in animal experiments seem to reflect the unique biological phenomenon of the particular species being studied, the unnatural means by which the disease was induced or only the stressful environment of the laboratory (65).

The complexities of understanding normal wound healing is further compounded when this process is delayed or affected by an underlying pathological process. Examples of complex wounds include burns, diabetic ulcers, venous ulcers and pressure sores. A number of animal models have been developed to study all aspects of diabetes including wound healing and can be divided into induced or genetic diabetic models. Administration of streptozotocin or alloxan to experimental animals has been used to induce insulin-dependent diabetes, creating an animal model in which impaired wound healing could be studied (160;162). Genetic strains of diabetic animals include db/db mice and rats, ob/ob mice, BB rats and non-obese diabetic mice (NOD) (30;161). Other methods of models of impaired wound healing include radiation-impaired models, steroid-impaired models and adriamycin-impaired models (chemotherapeutic agent). A fundamental criticism of such models is that healing impairment is often accomplished by the introduction of toxic agents, which have complicated systemic side effects (55).

Ischaemia is a common factor in the pathogenesis of the complex wounds listed above and numerous animal species have been used to develop models that reflect this. An example is a bipedicled H-flap on the back of rats where the central cross bar is rendered ischaemic by transecting the central vein (57). The perfusion and biochemical properties of the wounds have been well characterised but the central ischaemic area becomes revascularised and only one wound per animal is created.

An alternative model is an ischaemic rabbit ear dermal ulcer model, which attempts to simulate the chronic venous leg ulcer (59). Again, a central area of ischaemia is attained by transecting the central and caudal arteries and then a full thickness wound created at this site, which heals by new tissue formation and minimal contraction. As described for other excisional wounds all phases of wound healing can be analysed histologically in this model.

Another factor frequently present in complicated wounds is advanced age. In view of this Ashcroft and co-workers used an established aged mouse colony to study the healing of incisional wounds by immunohistochemical methods (54). Other investigators have applied the above H-flap model and rabbit ear dermal ulcer model to aged animals combining the elements of ischaemia and age frequently underlying human chronic wounds (16). Studies with aged animals are however limited by the high cost and reduced availability of the animals and also the increased death rate compared to young animals (55).

***In vitro* Models**

In simple terms *in vitro* models are less expensive and carry minimal ethical considerations when compared with *in vivo* models. In general they take less time and can easily generate large sample numbers. They lack the inherent heterogeneity of *in vivo* wound studies, which makes it easier to study the mechanism of action of single compounds. However *in vitro* models themselves can differ in their level of complexity, ranging from single cell systems to multicellular three-dimensional (3D) matrices or even organ culture. Supplementing the culture medium or replacing it with wound fluid from different wound types at different stages of healing, can act to

mimic more closely the wound environment, in particular the inflammatory response (144).

Single cell systems or monolayers can be grown directly on the culture surface of culture dishes or on other substrates such as collagen, fibrin, fibronectin, vitronectin or laminin (60;262). The creation of a wound is mimicked by mechanically creating a defect in the monolayer with instruments such as pipette tips or needles (156). These single cell systems can be used to study migration (263), proliferation (30;157) and protein synthesis (158;159).

3D matrices are commonly composed of type I collagen or fibrin and are thought to be more representitive of wound physiology than 2D systems. Composition of the gel matrix can be modified by incorporating different types of collagen, fibronectin or glycosaminoglycans, which provides a closer representation of the early provisional wound matrix (66). Migration of fibroblasts into collagen gels has been extensively studied by Schor and co-workers (69). It has also been carried out with fibroblasts isolated from biopsy wound tissue (68). Cell proliferation and migration can also be studied in this system. It also lends itself well to studying wound contraction as it better represents the scaffolding nature of wound matrix.

More recently multicellular systems have been developed where keratinocytes are co-cultured with fibroblasts incorporated into a 3D gel matrix (61;62). Again, this is a closer approximation to the biological properties of a typical wound and in particular allows the study of cell-to-cell interactions. They are however difficult to assemble and require experience. Commercially available skin equivalents also allow the study of cell interactions within a multicellular environment through the creation

of wounds of varying depths within them (62). Migration, proliferation, protein synthesis and wound contraction can all be measured within these 3D systems.

The closest approximation to the 3D multicellular nature of human skin is probably achieved by organotypic cultures. Intact human skin can be studied in culture as skin explants, which unlike living skin equivalents have all the cellular elements including skin appendages present. Explant tissue can either be cultured at the air-liquid interface or submerged in the culture medium and healing can be studied directly from explants placed directly onto plastic dishes (62;67;70;145;264). In addition, there has been studies of full thickness incisional wounds made in explant tissue, where the development of tensile strength was monitored (67). Furthermore standardised burn wounds have been created on skin explants allowing assessment of re-epithelialisation, which is the process most often analysed in organotypic culture systems (71). The major drawback for tissue explant systems is the inability to modify the composition of their cellular and matrix constituents i.e. they lack the ability of the *in vivo* wound to recruit new cells. However the ability to study wound cells in the context of their multicellular 3D interaction present *in vivo*, was the basis for the development of the current tissue explant culture system described in this thesis.

1.6 WOUND HEALING AND AGEING

Ageing has long been recognised as one of the major factors affecting wound healing and is often implicated in the impaired healing of chronic wounds such as venous leg ulcers. It is still not entirely clear whether this is an effect of age on its own, or co-existing pathological states such as diabetes and peripheral vascular disease often occuring in elderly individuals. This is borne out by the fact that most chronic wounds occur in aged patients with varying degrees of local tissue ischaemia resulting from either increased venous pressure (secondary to venous insufficiency), arterial occlusion (secondary to peripheral vascular disease), pressure causing pressure sores or local complications of diabetes (265;266). However, there is evidence to support the view that healthy aged humans can mount an adequate healing response, for example following surgery, using the same processes as younger individuals (267-270).

Understanding the cellular and molecular mechanisms underpinning the healing response in aged humans was initially complicated by the lack of well-characterised animal models. In addition, many of the studies carried out in aged humans that demonstrated impaired wound healing, as represented by measures such as wound dehiscence, infection and decreased tensile strength, were carried out on individuals with significant co-morbidity (271). It was therefore difficult to attribute the effect purely to the ageing process. Over the last decade, better-characterised ageing animal models have contributed to a clearer understanding of the specific effects ageing can have on the healing response.

Ashcroft and co-workers using a well-characterised ageing mouse colony, demonstrated an association of ageing with reduced deposition of ECM components, upregulation of angiogenesis and an altered inflammatory response (272). These

were detected as a reduced immunostaining for fibronectin, laminin and collagen along with a delayed monocyte/macrophage and B-lymphocyte infiltration. Conversely, there was an increase in heparan sulphate within the wounds associated with an increase in blood vessel staining. In contrast to these findings, Smith and co-workers found an increase in macrophage numbers infiltrating aged murine skin wounds (273). However, these macrophages displayed decreased phagocytic activity and a non-significant trend towards producing lower levels of MIP-2, MIP-1α, MIP-1β and eotaxin chemoattractants, which the investigators associated with an impaired healing response.

In another study, Swift and co-workers also demonstrated delayed re-epithelialisation and collagen synthesis in excisional wounds created in aged mice (273). In addition, there was significantly less bFGF and VEGF present in aged mice, which was partly explained by a decrease in macrophage production of VEGF. Consistent with this Ashcroft and co-workers also demonstrated an initial delay in appearance of PDGF A and B isoforms, PDGF-α and β- receptors and EGF and its receptor in their ageing mouse colony (274). This was coupled to a later increased level of TGF-β3 and bFGF in the wounds of aged animals, in comparison to an overall increase in TGF-β1 and 2 isoforms in the wounds of younger animals. The evidence accumulated here indicates that ageing in animals is associated with clear biochemical changes that may go someway to explaining the impaired healing response frequently encountered in ageing humans.

Human studies on ageing have also revealed clear effects of factors associated with ageing on the healing response. Ashcroft and co-workers investigated the inflammatory response and endothelial CAM profile in cutaneous punch biopsies

taken from healthy human subjects ranging in age from 19-96 years (275). They demonstrated a delayed appearance of monocytes/macrophage and lymphocyte appearance in the aged subjects associated with delayed expression of ICAM-1 and VCAM-1. Despite a delayed appearance of macrophages, a higher proportion of mature macrophages were present in the older subjects, which could have a bearing on the inflammatory mediator profile secreted by these cells. These findings are consistent with the altered inflammatory response demonstrated in ageing mice and may be the consequence of an altered endothelial CAM expression profile present in elderly individuals.

In addition, this group have demonstrated clear differences in the balance of proteolysis both in the normal skin of aged human subjects and during their response to cutaneous wounding (276). These included age-related increases in MMP-2 and –9 in response to wounding on a background of increased levels of MMP-2 present in normal aged skin. Furthermore, in a separate study they also demonstrated levels of TIMP-1 and –2 to be higher in normal young skin as compared to aged skin. This was mirrored by a significant increase in their expression during the early phases of healing in the young subjects (up to day 3 post wounding), which was absent in the older individuals. This data supports the view that there is an age related change in the proteolytic balance within normal skin, resulting in dermal tissue breakdown that may lead to impaired wound healing and predipose elderely individuals to developing chronic wound states.

More recently an understanding of how the changes in hormonal levels with age and differences between the male and female sexes may have implications for wound healing has been gained. Oestrogen has been shown to reverse the age-related delay in the cutaneous wound healing of post-menopausal women through administration

of systemic hormone replacement therapy (277). This was associated with an increase in TGF-β1 that was postulated to be responsible for the observed accelerated wound healing. Interestingly, the delayed wound healing seen in ageing healthy human females was associated with improvement in both microscopic and macroscopic scar quality, which was directly attributed to decreased levels of TGF-β1 detected within the wounds (277). Following on from this work, Ashcroft and co-workers investigated the effects of topical oestrogen on cutaneous wound healing in healthy elderly men and women (278). They demonstrated accelerated wound healing in males and females in response to topical oestrogen therapy characterised by increased collagen and fibronectin levels and increased wound strength in the later phases of healing. This was associated with decreased wound elastase levels, which may have been related to the decreased neutrophil numbers and decreasd fibronectin degradation also detected. The response to oestrogen by males was however significantly less than that in females within this study and led the investigators to investigate the role of the male sex hormone testosterone. Using a hairless mouse model, they demonstrated that reducing testosterone levels (by castration or androgen receptor (AR) blockade) stimulated the healing response by removing its direct stimulatory effect on macrophage TNF-α production, and its consequent pro-inflammatory effect (54). The authors speculated that the effect of reduced systemic oestrogen levels on delayed healing in the elderly may be excarcerbated in elderly males by the additional inhibitory effects of testosterone which may be masked in younger males by higher local oestrogen levels. They also suggested that this may explain other data indicating that being male is a significant risk factor for delayed healing in age-related chronic wound repair (279).

Interestingly, studies investigating the role of ageing in wound healing have also added to the knowledge about factors affecting scarring. Ashcroft and co-workers noted that despite a decrease in the level of collagen within wounds created in their ageing mouse colony, the collagen architecture had the basket-weave appearance of normal skin and was associated with a better macroscopic scar appearance (54). As already mentioned, they also observed the delayed wound healing in ageing healthy human females to be associated with improvements in both microscopic and macroscopic scar quality (277). It would seem therefore that a delayed healing response in aged skin is paradoxically associated with improved scarring and a better cosmetic appearance. The association between improved scarring and a dampened down inflammatory response found in age related studies on wound healing, is also found in studies on foetal wound healing. The onset of scarring during foetal wound repair, occuring around the mid to early third trimester, corresponds with the emergence of an acute inflammatory response. More specifically an age-dependent defect in the ability of foetal neutrophils to phagocytose bacteria has been demonstrated and they have been found to be present in decreased numbers in scarless foetal wounds (280). It would seem therefore that as the immune system develops and its ability to mount an acute inflammatory response increases, scar formation ensues at the repair site. It is only with the decline in immune function with age, termed immunosenescence, that this fibrotic response is curtailed.

Another similarity between data from age-related and foetal wound healing studies is the relative proportion of TGF-β isoforms present during the healing response. The TGF-β1 and TGF-β2 isoforms are known to have pro-fibrotic functions and to promote scar formation (281-283). They also enhance tissue repair by attracting monocytes and fibroblasts, increasing extracellular matrix deposition and modulating

protease expression (90;284;285). In line with this, treatment of adult rat wounds with neutralising antibody to TGF-β1 and -β2 reduces scar formation and the delayed wound healing with improved scar quality seen in ageing healthy human females, was similarly attributed to decreased levels of TGF-β1 (277;286). Furthermore, increased levels of TGF-β3 and bFGF have been found at later time points in the wounds of aged animals, in comparison to an overall increase in TGF-β1 and 2 isoforms in the wounds of younger animals (274). Treatment of adult rat wounds with exogenous TGF-β3 also reduces scar formation (287). It therefore appears that it is the relative proportion of TGF-β isoforms, and not the absolute amount of any one isoform, that may determine the wound repair outcome. Interestingly, this situation is mirrored in foetal wound healing as in scarless foetal wounds, TGF-β3 expression is increased while TGF-β1 levels are unchanged. In contrast, foetal wounds which have developed scarring, have increased TGF-β1 levels and decreased TGF-β3 levels.

More recently, studies have confirmed the key role played by TGF-β in the fibrotic response and uncovered some of the downstream factors under its regulation. For example CTGF is selectively and rapidly induced in mesenchymally derived cells by the action of TGF-β (288;289). It is thought that it represents a downstream effector molecule for the profibrotic activities of TGF-β in the maintenance and repair of connective tissues and within fibrotic disease settings such as scleroderma and keloid scarring (288;290). Consequently, researchers are now hoping to develop agents to target key regulatory molecules such as CTGF to inhibit the fibrotic response and subsequent development of scarring.

2.0 AIMS OF THIS THESIS

The expression pattern of the integrin cell adhesion molecules has been well characterised in normal skin and in human acute experimental wounds. However, little work has been done to characterise their expression in chronic wounds, in particular in chronic venous leg ulcers. In addition, human data on the epidermal expression of syndecan-1 and E-cadherin in acute or chronic wounds is lacking.

The primary aim of this study was therefore to confirm the established expression pattern of the integrin molecules and characterise the expression of syndecan-1 and E-cadherin in normal and acutely wounded human skin. Comparison of these expression patterns would be made to those found in chronic venous leg ulcers. Thus defective expression of any of these molecules in chronic wound epidermis could be detected and their role in the delayed epithelialisation of these wounds further investigated.

A secondary aim was to develop and characterise a tissue explant model of chronic wound tissue. It would then be utilised to investigate the possibility of modulating $\alpha_5\beta_1$ integrin expression found to be defective in some early observations in chronic venous leg ulcers.

Characterisation of the behaviour of chronic venous leg ulcer tissue in culture conditions would also allow the possibility of developing the system as a testing bed for the addition of potential therapeutic agents.

3.0 METHODS

3.1 IMMUNOHISTOCHEMICAL CHARACTERISATION OF CELL ADHESION MOLECULE EXPRESSION

3.1.1 Sources of Tissue

Sections 3.1.2-3.1.4 describe the methods of obtaining clinical tissue. Two sources of acute wound tissue were utilised, as only a limited amount was available from normal healthy volunteers as part of the model of normal acute wound healing. After an initial panel of integrin antibodies was run in tissue from the acute wound model, expression of the β_4 integrin subunit, E-cadherin and syndecan-1 adhesion molecules was studied in pilonidal wound excision tissue.

3.1.2 A model of normal acute wound healing

Following informed patient consent, an acute surgical wound was created on the forearms of eight healthy adult human volunteers. This was achieved by instilling up to 5ml of 1% lignocaine local anaesthetic into the subcutaneous tissues, and taking a single 3mm punch biopsy from the anterior forearm of each subject. This acted as the zero time biopsy and source of normal skin. Each wound was then allowed to heal normally under an adhesive polyurethene dressing (Opsite, Smith & Nephew) for a period of either 24, 48, 72 or 96 hours. At each time point, a second 6mm punch biopsy was taken to include the original biopsy site. The technique for taking biopsies is described in the following section on the additional source of acute wound tissue, the pilonidal excision wound. Individual volunteers selected to be re-biopsied at the same time points were matched for sex and age. The overall age range for the study volunteers was 21-48 years

3.1.3 Additional source of acute wound tissue: The Pilonidal Sinus Excision Wound

Patient selection

Patients with acute surgical wounds after having excision of a pilonidal sinus were recruited from surgical firms at the University Hospital of Wales, Cardiff Royal Infirmary, Llandough Hospital (South Glamorgan) and the Royal Gwent Hospital (Newport, Gwent). These patients were recruited as part of a concurrent study within the laboratory subsequently published in the literature (36). In this study patients had undergone surgical excision of a pilonidal sinus within one week of evaluation and fully informed consent was obtained from all patients. At recruitment to the study, a detailed clinical history was obtained from each patient to detect any past or current illness that may influence healing. Based on this exclusion criteria were: age below eighteen; pregnancy; serious coexisting illness; treatment with steroids; treatment with immunosuppressants; chronic renal failure; known malignancy.

An alternative source of normal tissue was used for comparison with the pilonidal sinus excision tissue. After gaining prior permission from the operating surgeons, who then gained consent from the appropriate patients under their care, freshly excised skin from mastectomy operations at Llandough Hospital was collected from theatre. 6mm biopsies were imediately taken, snap frozen in liquid nitrogen and prepared for cryostat cutting as detailed below.

Biopsy technique

Biopsies were taken from the excision site edge, incorporating epidermis and dermis at the wound edge with adjacent granulation tissue. Location of the biopsy was noted to avoid repetition of the same biopsy site. Prior to biopsy, 3-5 mls of 1% lignocaine was instilled into the area. A 6mm disposable sterile biopsy punch was pushed into

the tissue with a gentle rotatory movement to the full length of the 6mm blade. The tissue was then removed by means of a 'scooping' action in order to minimise tissue damage by handling with forceps. Bleeding was usually slight and controlled if necessary with gentle pressure with a gauze swab for one to two minutes.

Biopsy frequency

The following biopsy regime was followed for the original study carried out by Boyce *et al* (36). However, in the current study this pilonidal excision tissue was used when available and was no longer required as part of the original study. For this reason it did not include any early (within 1 week post operation) or later (day 42 post operation) time point tissue.

In the original study, the first biopsy was taken within 7 days of operation at the next available outpatients appointment and nominated as the day 0 postoperative biopsy. Using this fixed time point subsequent biopsies were taken at day 7, day 21 and day 42 post wounding, providing the wound had not healed. Day 7 and day 21 time point biopsies from 4 individual subjects were included in the current study. Patient details can be found in appendix I

3.1.4 A model of chronic wound healing

As a model of chronic wound healing a standard wound type was again selected: the chronic venous leg ulcer. Eight patients, each with a venous ulcer were included for study. None of these ulcers had made significant progress towards healing for at least six months prior to biopsy. All had duplex ultrasonography to prove their diagnoses, and were free from clinical signs of infection. A single 6mm punch biopsy was obtained from each ulcer edge, again incorporating epidermis and dermis at the ulcer edge with adjacent granulation tissue, using the technique described above for

pilonidal excision tissue. This was also the technique used when harvesting tissue for the tissue explant culture system described later.

3.1.5 Preparation of specimens and cryostat cutting

Each biopsy was mounted on its side in Cryo-M-Bed embedding medium (Bright Instrument Co.Ltd., Cambridgeshire, UK) on a cork board, so that a cross section of epidermis and dermis was outermost. It was then snap frozen in liquid nitrogen at –170°C.

Snap frozen tissue samples stored in liquid nitrogen at –170°C were placed on a pre-cooled chuck (-20°C) in the cryostat cutting chamber using embedding medium. The tissue was supported by building up the embedding medium around the sample within the cryostat. 6um sections were taken and mounted onto poly-L-lysine (Sigma-Aldrich Ltd. Dorset, UK) coated slides. These were wrapped in foil and stored at –22°C.

3.1.6 Staining technique

Tissue sections were allowed to reach room temperature and the foil removed prior to fixing the sections in dry acetone (Fisher Scientific Ltd., Loughborough, UK) at 20°C for 15 minutes. Excess acetone was removed by air drying the sections for 10 minutes at room temperature. Sections were washed twice in TBS for five minutes each time. They were then incubated for twenty minutes with normal blocking serum (Dako Ltd. High Wycombe, UK). Excess blocking serum was removed and the primary antibodies (Dako Ltd. High Wycombe, UK) were applied at the working dilution of monoclonal antibody.

The sections were incubated for 30 minutes at room temperature in a humid atmosphere. Sections were washed three times for five minutes at room temperature in TBS buffer pH 7.4. The biotinylated secondary antibody was applied to the sections, which were then incubated within a humid container for thirty minutes. Preparation of the 'ABC' (Avidin-Biotin Complex) histochemical staining reagent (Vector Laboratories, Peterborough, UK) was also carried out at this point. Sections were washed for five minutes three times in TBS. The ABC histochemical staining reagent was applied to the sections, which were then incubated in a humid container for thirty minutes.

The sections were washed for five minutes, three times in TBS and the DAB substrate (0.005%) (Dako Ltd. High Wycombe, UK) applied to the sections for 10 minutes at room temperature. The sections were rinsed in TBS, followed by tap water, counterstained in heamatoxylin for thirty seconds and then washed again in tap water. The sections could be differentiated in 1% alcohol if the counterstain was too intense. The sections were dehydrated by passing through 70% alcohol, then 100% alcohol (BDH Laboratory Supplies, Poole, UK) twice, for five minutes each time. Excess xylene was blotted off and the sections were mounted in DPX (DBH Laboratory Supplies. Poole, UK) under cover slips and evaluated by light microscopy.

Monoclonal antibody panel

Antibodies used and relevant dilutions are shown in table 3.1 below.

Table 3.1: *List of monoclonal antibodies used to immunolocalise matrix proteins and cell adhesion molecules*

Antigen	Dilution	Antigen	Dilution
$\alpha_5\beta_1$	1/250	E-Cadherin	1/200
α_V	1/1000	Syndecan-1	1/200
$\alpha_2\beta_1$	1/500	Serum Fibronection	1/100
$\alpha_3\beta_1$	1/100	Cellular Fibronectin	1/1000
β_4	1/400	Vitronectin	1/1000

3.2.0 Tissue explant culture

3.2.1 Explant culture

Biopsy tissue was weighed aseptically and dissected into approx. 5mg fragments. Each fragment was placed in 0.2ml of RPMI 1640 medium supplemented with 10% foetal calf serum (FCS) (Life Technologies Ltd., Renfrewshire, UK), penicillin (100IU/L)(Sigma-Aldrich Ltd, Dorset, UK), streptomycin (100IU/L) (Sigma-Aldrich Ltd, Dorset, UK) and fungisone (25μ/ml) (Sigma-Aldrich Ltd, Dorset, UK). This was held in one well of a 96 well culture plate. Tissue was cultured at 37°C with a humidified atmosphere of 5% CO_2 in air. The culture supernatant was removed and

replaced at 2, 4, 6 and 8 hours unless otherwise stated. Supernatants were frozen in aliquats at –22°C for ELISA and metalloproteinase assay while supernatants for LDH assay were stored overnight at 4°C.

3.2.2 Cytokine analysis by ELISA plate assay

Twin site sandwich Quantiqine® ELISA plate assay kits (R & D Systems Europe Ltd.) were set up as per the manufacturers instructions. This was done to assay the levels of human IL-1β, IL-8, TGF-β_1 and VEGF. An additional activation step using 1N HCL at a concentration of 0.2ml per 1ml of supernatnant as indicated by the manufacturer was included for TGFβ_1. Levels of TGF-β1 measured in the culture supernatants therefore included activated latent TGF-β1. ELISA plates were read at a wavelength of 450nm using a Labsystems Multiskan MS plate reader (Process Analysis & Automation Ltd., Farnborough, UK.) The absolute cytokine concentration was determined by use of a calibration curve prepared using standards provided by the kit manufacturer. Culture medium assayed as controls, did not contain detectable levels of IL-1β, IL-8 or VEGF but did contain detectable levels of TGF-β1. Levels of TGF-β1 detected in the medium controls (resulting from the supplementation of the culture medium with foetal calf serum containing TGF-β1), were subtracted from the levels detected in the supernatants to control for this.

3.2.3 LDH Assay

Culture supernatants stored overnight at 4°C were assayed for the levels of LDH using a standard quantitative calorimetric kit (Sigma-Aldrich Ltd, Dorset, UK). The assay was prepared in a 96 well plate using the reagents supplied in the kit as per the manufacturers instructions. The absolute LDH concentration was determined by use

of a calibration curve prepared using standards supplied by the kit manufacturer. LDH concentration in the samples and standards was quantified using a using a Labsystems Multiskan MS plate reader (Process Analysis & Automation Ltd., Farnborough, UK.) set at a wavelength of 450nm.

3.2.4 Metalloproteinase analysis

Frozen aliquots of culture supernatant were tested for MMP-2 and MMP-9 levels using a modification of a sodium dodecyl sulphate polyacrylamide gel electrophoresis (SDS PAGE) method to allow their analysis by gelatin zymography. Essentially this involved initial protein separation of the samples by SDS PAGE for 2 hours at a constant voltage of 120V, followed by 8% gelatin zymography.

Protocol for the Preparation and Running of Gelatin Zymograms:

A discontinuous gel system was used with two types of gel known as a stacking gel and a separating or resolving gel. The lower gel (resolving gel) was a 10% SDS PAGE gel, containing 8% gelatin. The upper (stacking) gel was a 5.0% SDS PAGE gel. The gels were set up as described below and ran using a Bio-rad Mini Protean II electrophoresis system (Bio-rad Laboratories Ltd. Hemel Hempstead, UK).

Gelatin Preparation:

A solution of type A gelatin was made up to a concentration of 20mg/ml ddH_20 (G-2625 Sigma, Dorset, UK)

Gel former preparation:

All components were cleaned thoroughly with Lipsol (detergent). Then the glass was soaked along with the spacers in 100% alcohol and wiped dry. The former was then

placed in a former holder extension and glass plates were inserted into the former. Spacers were inserted between the plates – ensuring they were tight to the edge. The top screws were tightened (finger tight), the former was removed and then the bottom screws were tightened while ensuring the bottom edges of the plates were flat to prevent gel leakage when pouring. This arrangement was then clipped into a pouring stand.

Resolving Gel:

Gel apparatus were assembled (as above) and resolving gel components were mixed (appendices II). Temed was added last and the resolving gel poured into the former using a 10ml syringe or Pasteur as soon as possible. The resolving gel was poured to within 1cm of the top of the gel former. After pouring, water-saturated butanol (50:50 mix at RT) was immediately pipetted onto the surface of the resolving gel. The gel was allowed to set for 45 minutes. Toward the end of the setting period, the stacking gel was prepared. Once the resolving gel had set, the butanol was poured off into a sink, and the gel washed with water and excess water above the gel was soaked up with filter paper squares.

Stacking Gel:

Stacking gel components were mixed (appendics II), Temed added last, and the gel poured into the former (between plates) using a 10 ml syringe or Pasteur as soon as possible. A comb was placed into the gel ensuring no bubbles. The gel was allowed to set for 45 minutes. It was then fitted to the running block. Central and side chambers were filled with running buffer (appendices II). The comb was then removed and wells cleaned out using running buffer applied from a 10 ml syringe and large needle.

Sample preparation

15μl of sample and 15μl of sample loading buffer (appendics II) were mixed (30μl) and 20μl of the mixture loaded. Four fold dilutions of the culture supernatants were made to generate final band intensities that fell close to the optimal ranges produced by the standard curves.

Loading samples

Wells had a 20μl capacity. A Hamilton syringe (or sloping yellow tip micropipette) was used to load the sample. High molecular weight standard (Sigma [SDS-6H], Dorset, UK) was prepared with bromophenol blue as indicated in the supplied instructions and 10μl was added to one well – usually the last well on the right hand side.

Running the gel

The gel was run at 120V until the bromophenol blue had left the end of the gel and then run for an additional 30 minutes. If better definition was required, gels could be run cold using chilled running buffer but then a longer running time was allowed.

Developing the gel

The running buffer was discarded and the equipment dismantled. Screws were undone and glass plates containing gel slid out from the holder. The gel was then freed from the plates and immersed in 2.5% Triton exchange buffer (appendices II) for 30 minutes. This was repeated with fresh exchange buffer for a further 30 minutes.

Incubation

Gels were placed in incubation buffer (appendices II), covered with foil wrap and incubated at 37°C over night to allow MMP digestion of the gelatin substrate.

Staining the gel

Gels were uncovered after overnight incubation and stained in Coomassie blue staining solution (appendices II) for 30 minutes.

The gels were then washed in distilled water and placed in destaining solution (appendices II) for 2 hours. The destain was then refreshed and the gels left at RT overnight.

Drying the gel

The gels were placed on filter paper; Saran Wrap was layed over and then flattened down over the gel. Gels were then dryed for 45 minutes using a Biorad model 583 vacuum assisted gel dryer (Bio-rad Laboratories Ltd. Hemel Hempstead, UK) at 85°C.

Quantification by Densitometry

Once dryed the gels were scanned into Microsoft photoshop using a standard flatbed scanner. Images were saved as TIFF files and imported into the Molecular Analyst® software package (version 1.2. Bio-rad Laboratories Ltd. Hemel Hempstead, UK) held on a 486 Research Machines personal computer.

The Molecular Analyst® software allowed the cleared gelatin bands representing active and latent MMP activity to be selected with boxes, as depicted by the white box in figure 3.3. Likewise, areas of backgound stain could be selected with boxes,

depicted by the red box in figure 3.3. The software was then able to quantify the relative pixel intensity of the bands by generating densitometry values which were compared with the standard bands run at an MMP concentration of 10ng/ml.

Figure 3.1: *Example of gelatin zymogram run to measure MMP-2/-9 in supernatants from the explant culture of wound bed and edge tissue. STD = Standards. Red box = background analysis. White box = MMP quantitation*

The proportionality of this relationship was confirmed by generating standard curves for MMP-2 and –9 depicted in figures 3.2 and 3.3 respectively. Four fold dilutions of the culture supernatants were made to bring the amount of sample loaded on each gel within this standard range. Background levels and values obtained for culture medium controls run on each gel were subtracted from the sample values. Culture medium was run on each gel to control for the presence of MMPs in the FCS added to the medium. Total MMP-2 and –9 activity were then calculated from the sum of the active and latent forms quantified by densitometry of the gelatin zymograms. These values were then related to the weight of tissue in each biopsy or tissue segment and recorded in units of pg/ml/mg.

Figure 3.2: *MMP-2 standard curve. Standards ran over a concentration range of 1, 2, 4, 8, 12, 16, 20 and 32ng/ml as depicted by the cleared bands on the Zymogram included below.*

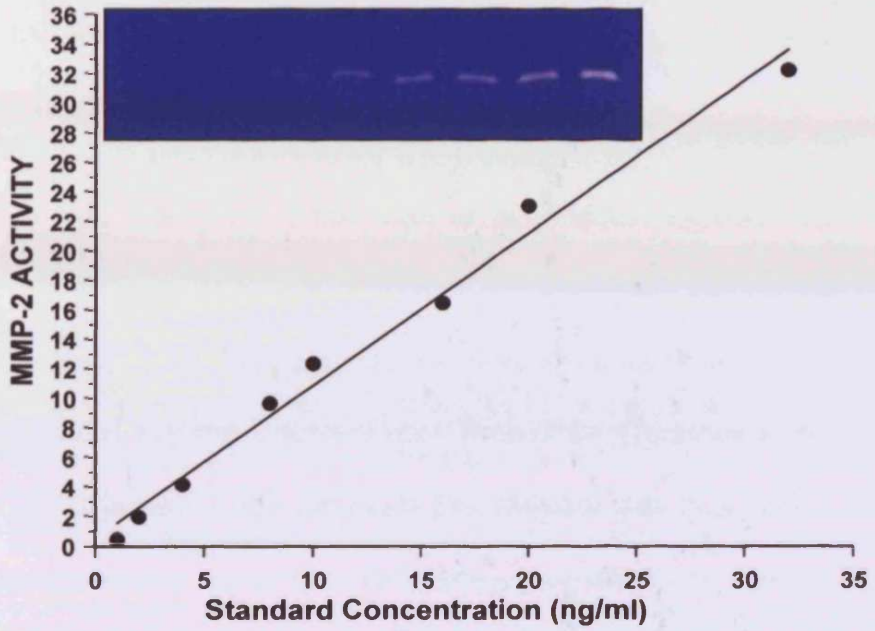

Figure 3.3: *MMP-9 standard curve Standards ran over a concentration range of 1, 2, 4, 8, 12, 16, 20 and 32ng/ml as depicted by the cleared bands on the Zymogram included below.*

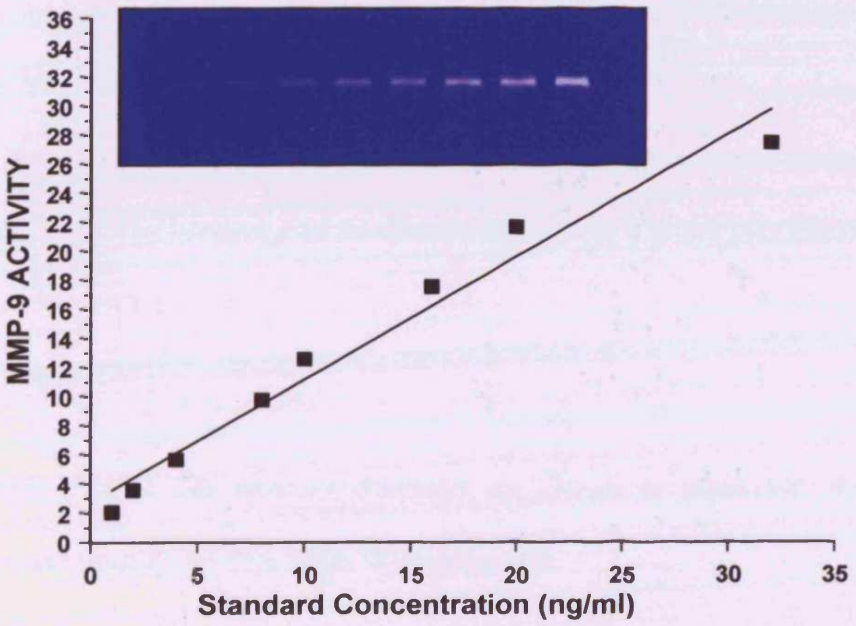

Oxygenation Experiments

Controlled oxygenation of the culture environment was achieved using the Modulator Incubator Chambers - 101™ (Billups-Rothenberg inc., USA) (see figure 3.4). 96 well plates containing the tissue for culture were placed in these gassing chambers. The gassing chambers were then flooded with either, 0%, 10%, 20% or 95% oxygen depending on the level of oxygenation required. This was delivered from compressed gas bottles containing a pre-analysed gas mixture of oxygen and CO_2 balanced with nitrogen (B.O.C. Special Gases, Cardiff). The manufacturer recommended that the chambers were flushed for 4 minutes to ensure the required level of oxygenation was achieved. The chamber was then sealed and placed in a standard incubator at 37°C. The gassing procedure was repeated each time the supernatant was replaced at the specified time intervals

3.2.5 Immunohistological analysis

A control sample time zero hours and two samples (see below) cultured for 8 hours were snap frozen in liquid nitrogen. Tissue sections were then prepared from them using the methods outlined in section 3.1.5. The frozen tissue sections were stained with a panel of monoclonal antibodies using the procedures already outlined in section 3.1.6 The histology of the tissue cultured for 8 hours was then compared with the time 0 control tissue

Monoclonal antibody panel

Antibodies used and relevant dilutions are shown in table 3.2. Antibodies were purchased from Dako Ltd. High Wycombe, UK.

Figure 3.4: Diagrammatic illustration of the Modulator Incubator Chambers - 101 ™ (Billups-Rothenberg inc., USA)

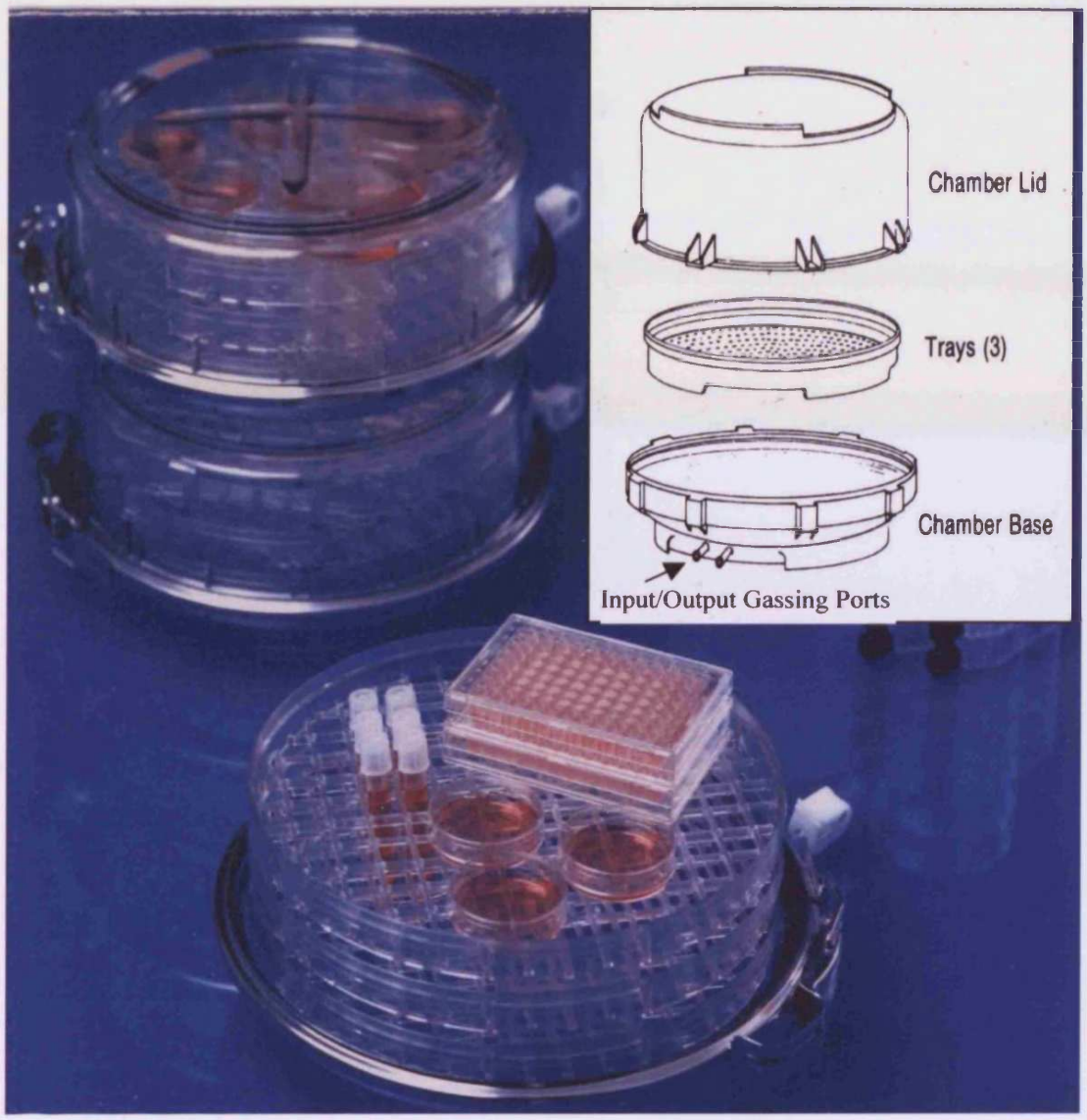

Table 3.2: List of monoclonal antibodies used to immunolocalise leucocyte cells

Antigen	Cellular Distribution	Dilution	Working Concentration
CD3	T lymphocytes	1 in 50	0.29mg/ml
CD4	T helper/inducer lymphocytes	1 in 10	1.9mg/ml
CD8	T suppressor/cytotoxic lymphocytes	1 in 30	0.35mg/ml
CD68	Macrophages, monocytes	1 in 50	0.31mg/ml
CD35	Macrophages, monocytes, B lymphocytes, neutrophils (C3b receptor)	1 in 30	0.49mg/ml

3.2.6 Microscopy analysis

Qualitative assessment

The following features were considered in identifying cell types, in addition to their immunolocalisation by specific monoclonal antibody staining.

Polymorphonuclear Neutrophils: small cells with multilobed dark nuclei and scant cytoplasm.

Macrophages: cells with eccentric 'kidney' shaped nuclei, sometimes containing cytoplasmic granules and vaculoes.

Fibroblasts: large cells, difficult to identify with haematoxylin staining only. Often enlarged and orientated into bundles.

Capillary endothelial cells: large cells with elliptical nuclei orientated within tubular vessel like structures.

Quantitative assessment.

Using the cellular features described above in conjuction with the immunohistochemical labelling of the appropriate cell surface marker (see table 3.2, antibody panel) the relevant cells were identified within the prepared tissue sections. The lymphocytic infiltrates were counted using x40 magnified fields of view. Each tissue section was systematically quantified by selecting an initial x40 field of view in the most lateral and superior edge of a tissue section and moving sequentially down and across the remaining tissue in ordered columns. This counting was facilitated by a video projection of the microscope image onto a video monitor and computer screen. A computer software programme developed by Dr Peter Plassmann (University of Glamorgan) enabled accurate labelling of each positive cell without

duplication. This was achieved by visualising each cell on the computer screen and then labelling them with the computer mouse. The software programme would then total the number of cells counted in each field of view. The number of cells in each field of view was summatted for the whole section and then divided by the number of fields viewed to give a mean number of cells counted per field of view.

4.0 RESULTS

4.1.0 EPIDERMAL INTEGRIN EXPRESSION AND PROVISIONAL MATRIX DEPOSITION IN A SURGICALLY INDUCED ACUTE WOUND MODEL

The immunolocalisation of the integrin molecules within the epidermis of normal adult human skin was used to characterise their normal expression and as a control of their expression in wounded skin. Normal skin was obtained from the time zero 3mm punch biopsies taken from the upper forearms of healthy adult volunteers as part of the model of surgically-induced acute wound healing described in the methodology. This model provided acute wound tissue in the form of a 6mm punch biopsy taken from the aforementioned 3mm biopsy site at 24, 48, 72 or 96 hours post wounding. Immunolocalisation of epidermal integrin expression in acute wound tissue over this time course would allow study of the changes in their expression pattern induced by a normal healing response. Immunolocalisation of the appropriate antigens is characterised by the positive brown staining depicted in the following figures.

4.1.1 Immunolocalisation of $\alpha_5\beta_1$ expression

Figure 4.1.1 illustrates the immunolocalisation of the human $\alpha_5\beta_1$ integrin within a frozen section of normal skin using the PID6 anti-$\alpha_5\beta_1$ monoclonal antibody. Anti-$\alpha_5\beta_1$ reactivity was not observed within the extracellular matrix or in the cells of the epidermis. However, anti-$\alpha_5\beta_1$ reactivity was observed throughout the dermal layer and appeared to be localised to cell membranes and processes, giving rise to a fibrillar staining pattern. The anti-$\alpha_5\beta_1$ reactivity was also localised to the membranes of a large number of endothelial cells within the dermis.

***Figure 4.1.1**: Immunohistochemical localisation of $\alpha_5\beta_1$ integrin in normal skin (scale bar 100μm)*

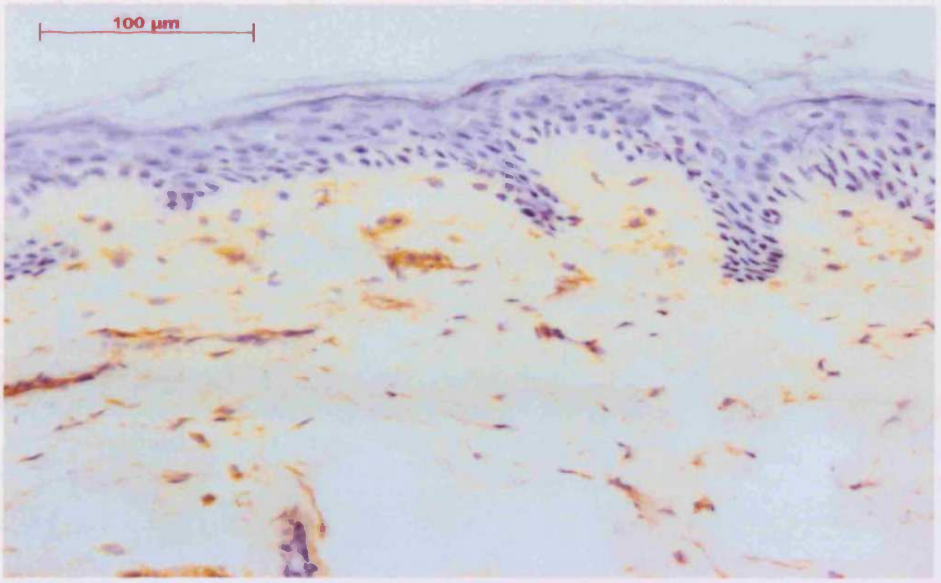

***Figure 4.1.2:** Expression of α5β1 within wound edge epidermis 24 hours post wounding (scale bar = 100μm).*

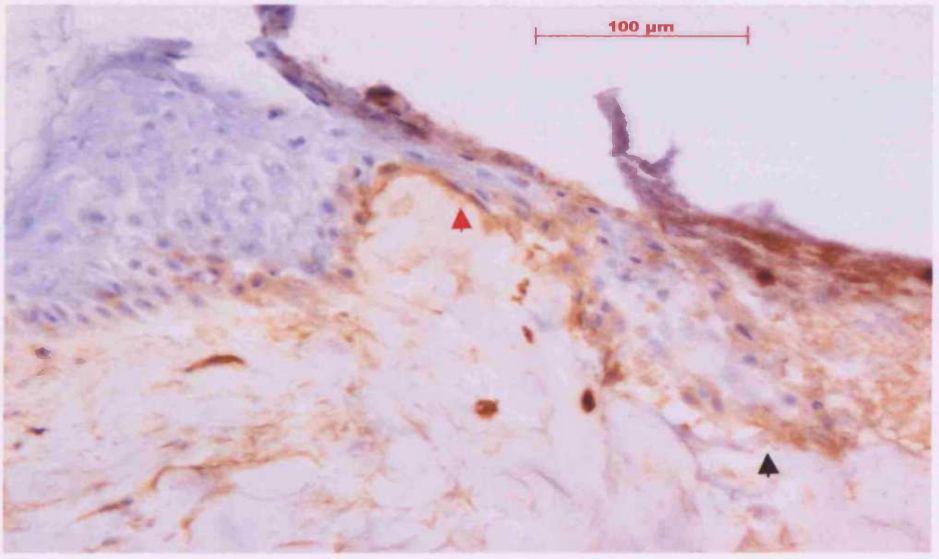

Figure 4.1.2 illustrates the immunolocalisation of $\alpha_5\beta_1$ integrin in a 6μm frozen section of 24 hour acute wound tissue. A weak pericellular anti-$\alpha_5\beta_1$ reactivity was localised to the membranes of basal keratinocytes at the wound edge (black arrow),

which extended a short distance into the adjacent epidermis (red arrow). Anti-$\alpha_5\beta_1$ reactivity was not detected within the adjacent normal epidermis.

At 48 hours post wounding, immunolocalisation of $\alpha_5\beta_1$ expression was again limited to the migrating keratinocytes in contact with the wound matrix. This expression was increased over that seen at 24 hours post wounding and had a pericellular distribution. Expression was maintained on migrating keratinocytes within the epidermis of acute wound tissue at 72 hours post wounding. This was again strictly limited to the basal keratinocytes in contact with the wound and had a pericellular distribution, which can be clearly seen in figure 4.1.3 to label the migrating epidermal tongue (see arrow).

Figure 4.1.3: *Immunolocalisation of $\alpha_5\beta_1$ expression within wound edge epidermis 72 hours post wounding (scale bar = 100μm). MT = migrating tip, GT = granulation tissue*

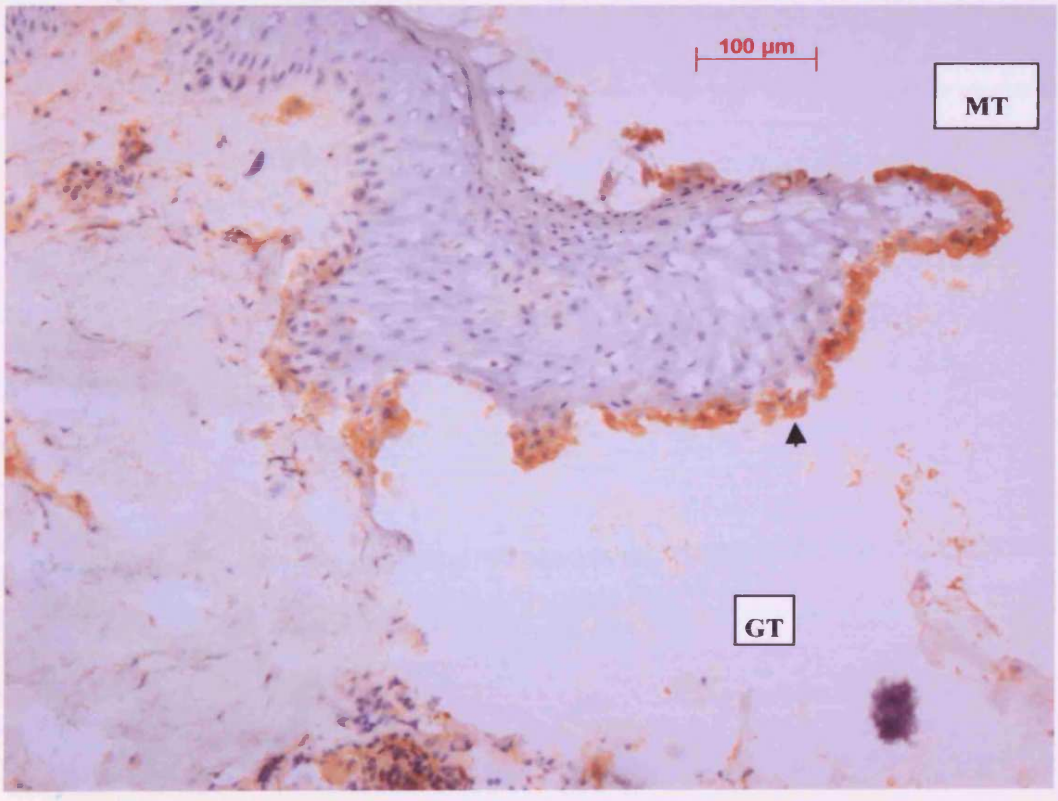

No change in the cellular localisation or distribution of $\alpha_5\beta_1$ expression was observed within the epidermis of acute wound tissue 96 hours post wounding. However the level of anti-$\alpha_5\beta_1$ reactivity was slightly decreased compared to that seen at 48 and 72 hours post wounding. Except for some limited expression in epidermis immediately adjacent to the wound at 24 hours post wounding, $\alpha_5\beta_1$ expression was not detected in epidermis adjacent or distal to the wound edge during the rest of the healing time course. Expression was detected in the dermis and wound matrix with the same fibrillar pattern described in normal skin (see figure 4.1.1).

4.1.2 Immunolocalisation of the αV integrin subunit expression

Probing 6μm frozen sections of normal skin and acute wound tissue with the VNR147 monoclonal antibody allowed immunolocalisation of the α_V integrin subunit expression. Immunolocalisation of the α_v integrin subunit within normal skin is illustratred in figure 4.2.1. Anti-α_V reactivity was localised to the membrane of basal and adjacent suprabasal layer keratinocytes. The α_V staining pattern appeared to have a pericellular distribution and showed the greatest intensity around the basal keratinocytes. Anti-α_V reactivity was also observed throughout the dermal layer. This α_V immunoreactivity was localised to cell membranes and processes giving rise to a fibrillar staining pattern.

***Figure 4.2.1**: Immunolocalisation of α_V integrin subunit espression in normal skin (scale bar = 100μm).*

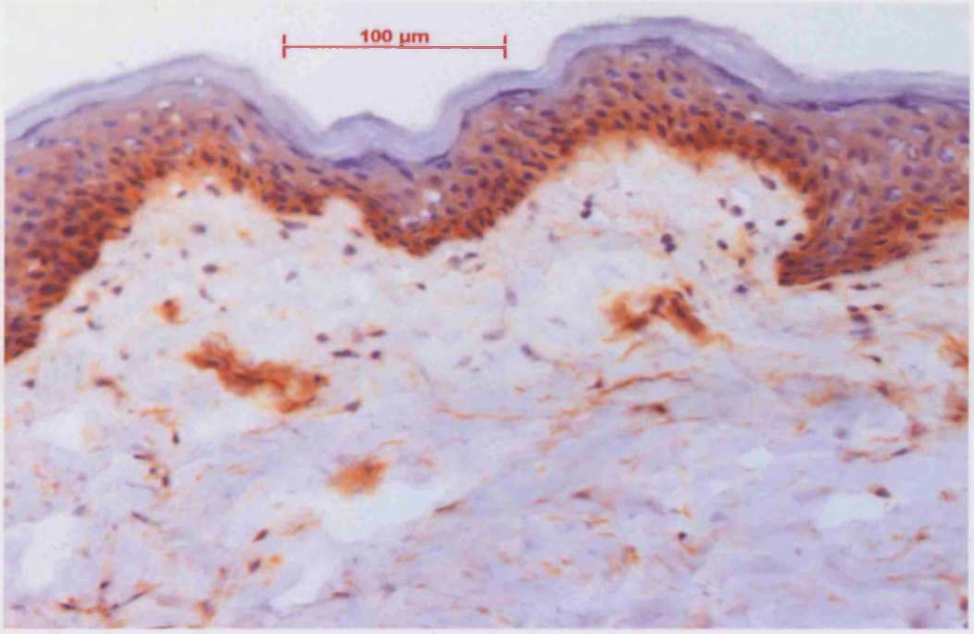

At 24 hours post wounding anti- α_V reactivity was localised in a pericellular distribution to basal keratinocytes in contact with the wound matrix. Greatest staining intensity was observed along their basal membrane. Anti-α_V reactivity was also localised to the membranes of basal and suprabasal keratinocytes present in the adjacent normal epidermis and had not changed from that described previously for normal skin (see figure 4.2.1) with staining intensity being strongest on the basal keratinocytes. Dermal expression was only observed in the adjacent normal skin, having the same expression pattern as previously described in relation to figure 4.2.1.

***Figure 4.2.2**: Immunolocalisation of α_V integrin subunit expression 48 hours post wounding (scale bar = 100μm). MT - migrating tip, GT – granulation tissue*

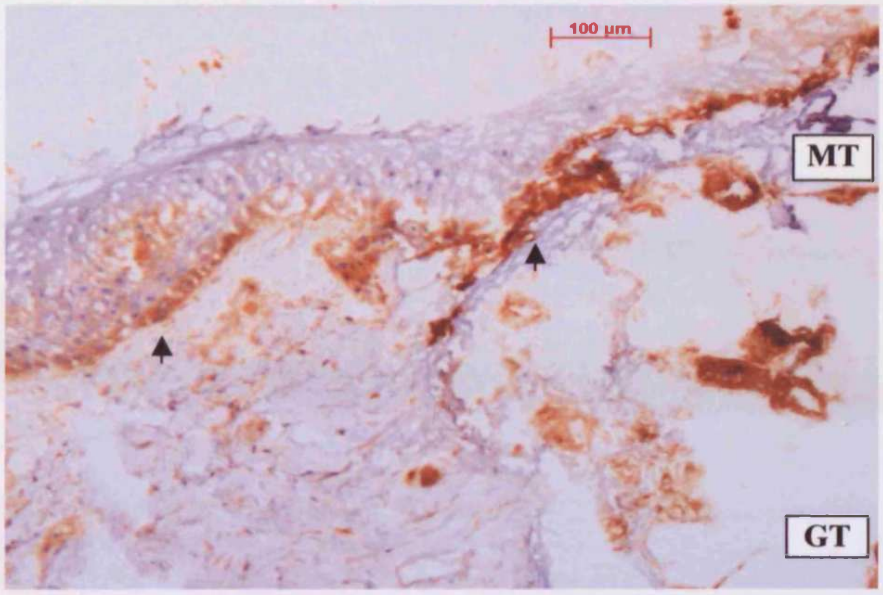

***Figure 4.2.3**: Immunolocalisation of α_V integrin subunit expression 96 hours post wounding. (a) Low power image demonstrating both wound edges (scale bar = 100μm). (b) Higher power image of wound edge as indicated by the arrow (scale bar = 200μm)*

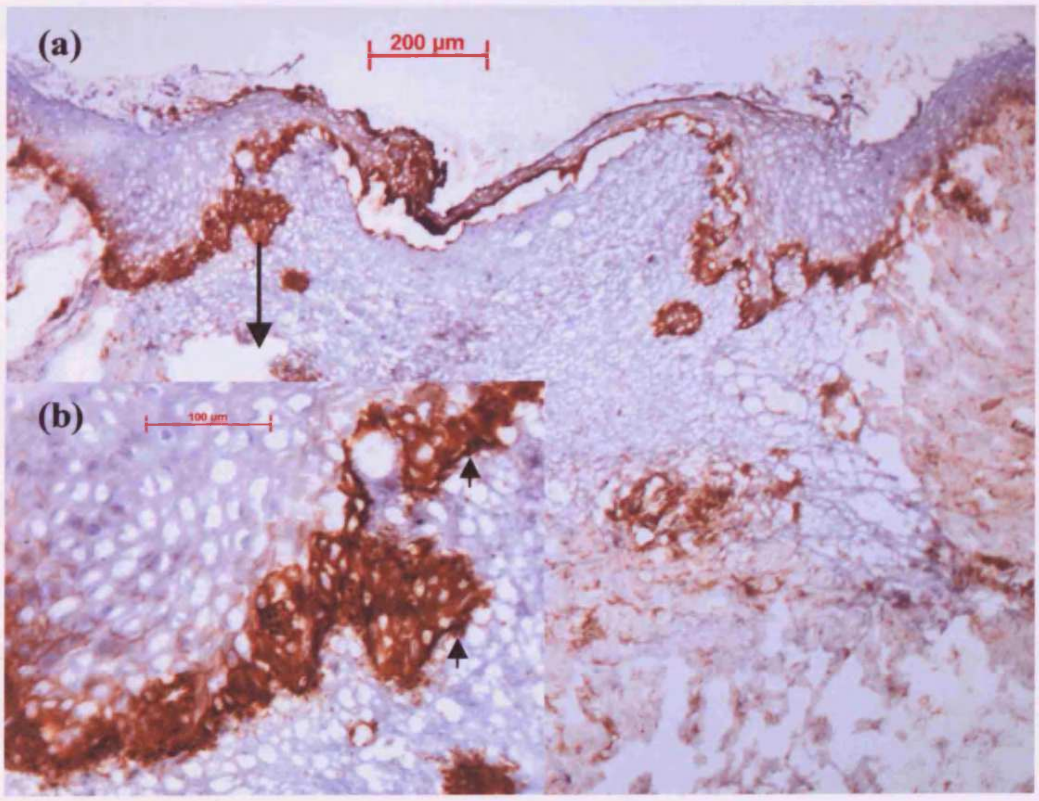

Figure 4.2.2 illustrates the immunolocalisation of the α_V integrin subunit in 48 hour acute wound tissue. Anti-α_V reactivity was detected on the membranes of basal keratinocytes in contact with the wound matrix. This reactivity displayed a pericellular distribution and had the greatest staining intensity along their basal membranes. The staining intensity observed on basal keratinocyte in contact with the wound matrix appeared to be increased compared to that observed at 24 hrs post wounding and over that in the adjacent epidermis (see arrows). At 72 hours post wounding a further increase in staining intensity on basal keratinocytes in contact with wound matrix was seen with expression again being concentrated along their basal membranes. This increased intensity on basal keratinocytes migrating over the wound matrix was maintained at 96 hours post wounding and is demonstrated in figure 4.2.3 (see arrows figure 4.2.3 (b)). Throughout the healing time course keratinocytes in the adjacent epidermis showed no changes in their expression of the α_V subunit from that already described in normal skin. This was also true of α_V expression in the dermal layer.

4.1.3 Immunolocalisation of $\alpha 2\beta_1$ expression

In figure 4.3.1 immunolocalisation of $\alpha_2\beta_1$ integrin with the PIE6 monoclonal antibody in frozen sections of normal skin is demonstrated. Anti-$\alpha_2\beta_1$ reactivity was detected on basal layer keratinocytes and within the first two suprabasal layers of normal skin. The immunoreactivity had a pericellular distribution and was concentrated to the lateral and apical membranes of the basal keratinocytes. Weak anti-$\alpha_2\beta_1$ reactivity was also observed around the blood vessels of the dermis. This

immunoreactivity was localised to the membrane of the endothelial cells and the immune cells migrating out of the vessels.

Figure 4.3.1: *$\alpha_2\beta_1$ expression in normal skin (scale bar = 100μm).*

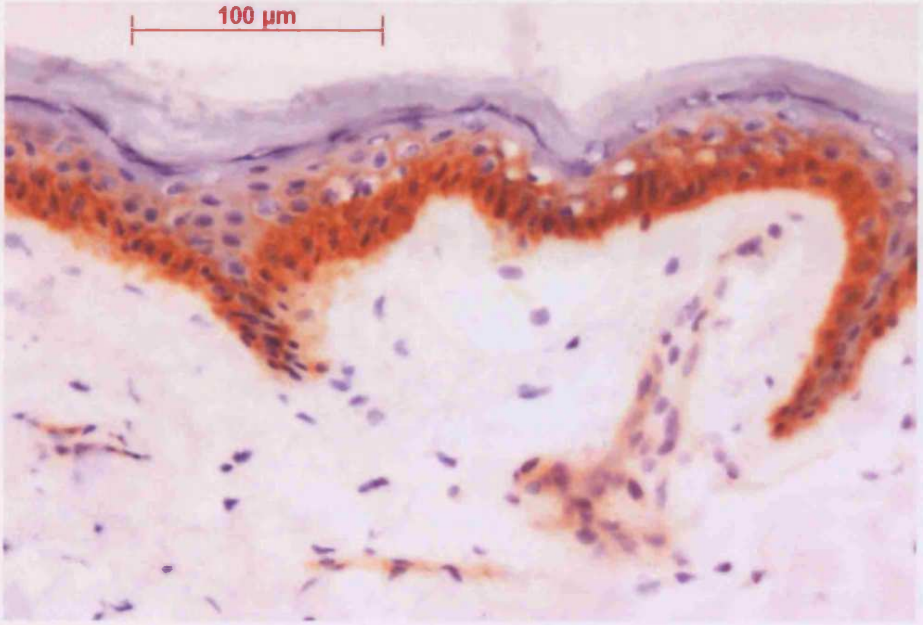

Anti-$\alpha_2\beta_1$ reactivity was detected on keratinocytes of the basal and first two suprabasal layers of epidermis at the edge of 24 hour acute wound tissue. This immunoreactivity had a pericellular distribution, but had a stronger intensity on basal layer keratinocytes, which was concentrated on their lateral and apical membrane. This was particularly marked on basal keratinocytes at the tip of the advancing edge of epidermis. In addition, staining intensity on these keratinocytes was also strong on their basal membranes.

Figure 4.3.2: *$\alpha_2\beta_1$ expression within acute wound tissue 48 hours post wounding (scale bar = 100μm). GT – granulation tissue, MT – migrating tip*

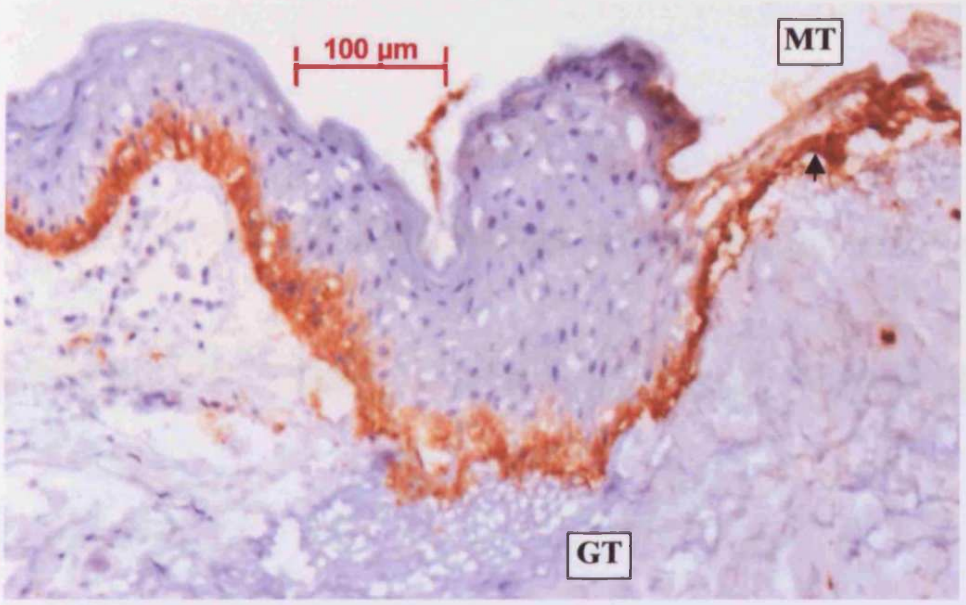

Figure 4.3.2 demonstrates the pattern of anti-$\alpha_2\beta_1$ detected at the wound edge of tissue 48 hours post wounding which was similar to that already described for tissue 24 hours post wounding. At 48 hours post wounding, anti-$\alpha_2\beta_1$ reactivity was detected on basal keratinocytes and a small number of suprabasal keratinocytes within the migrating epidermis in contact with the wound. The increased staining intensity within the migrating epidermis was now limited to a small number of keratinocytes at the very tip of the advancing epidermis (see arrow figure 4.3.2). Keratinocytes behind the advancing tip displayed the same staining intensity as those in the epidermis adjacent to the wound edge which was similar to that observed in the adjacent epidermis at 24hours post wounding. At 72 hours post wounding the distribution of expression within the migrating epidermis in contact with the wound matrix had not changed except for an increase in the number of suprabasal cells expressing $\alpha_2\beta_1$. Intense staining was still observed on keratinocytes at the leading edge of the migrating epidermis indicated by the arrow in figure 4.3.3.

Figure 4.3.3: *$\alpha_2\beta_1$ expression 72 hours post wounding (scale bar = 100μm). GT – granulation tissue.*

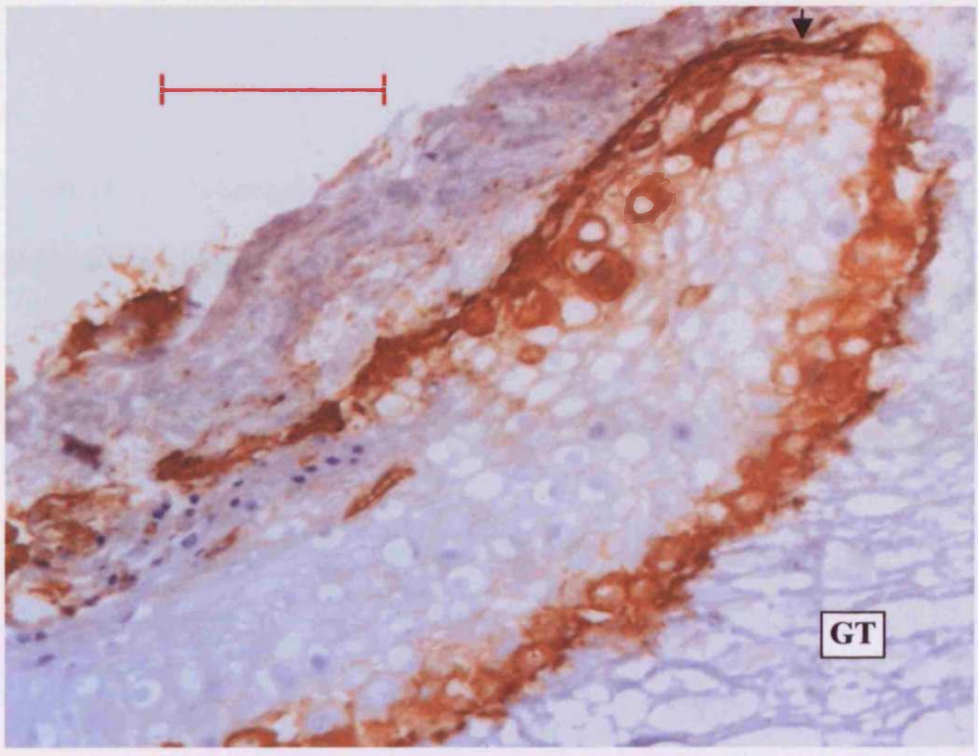

Figure 4.3.4: *$\alpha_2\beta_1$ expression 96 hours post wounding (scale bar = 100μm). GT – granulation tissue, MT – migrating tip, AE – adjacent epidermis.*

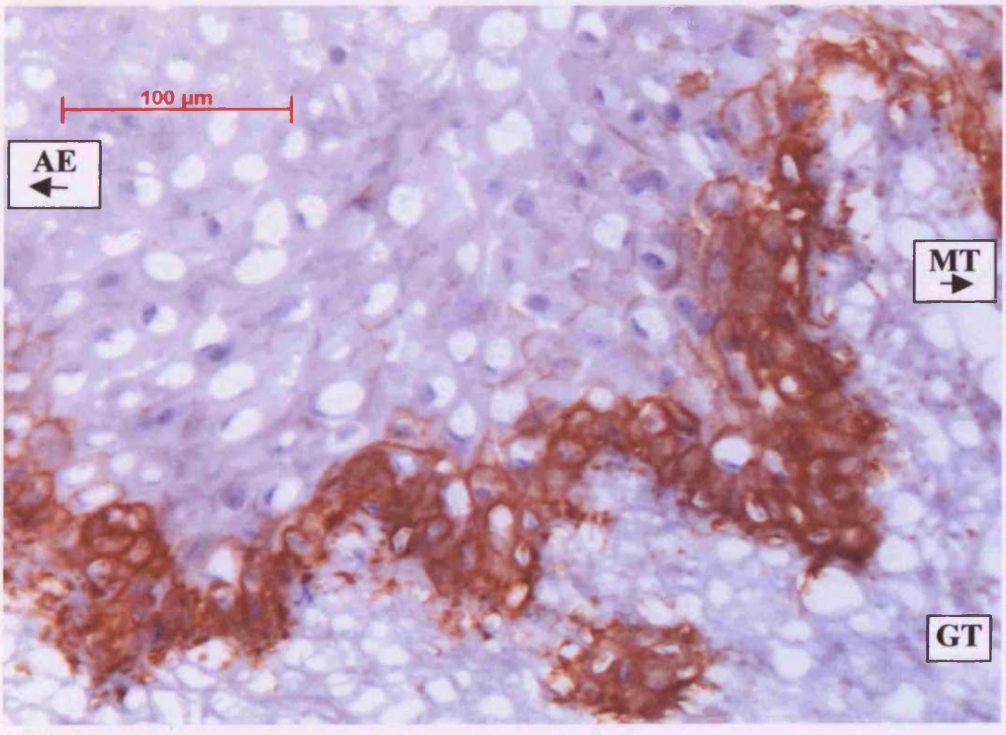

At 96 hours post wounding an increased number of suprabasal keratinocytes were observed to express $\alpha_2\beta_1$ in the already migrated epidermis behind the leading edge as shown above in figure 4.3.4. This expression again displayed a lateral/apical membrane distribution. Throughout the healing time course $\alpha_2\beta_1$ expression did not change within the adjacent normal epidermis from that described in normal skin. This was also true of expression observed within the dermal layer.

4.1.4 Immunolocalisation of $\alpha_3\beta_1$ expression

Figure 4.4.1 illustrates frozen sections taken from normal skin, probed with the GR3 anti-α_3 monoclonal antibody to immunolocalise $\alpha_3\beta_1$ integrin expression. Anti-α_3 reactivity was detected on basal keratinocytes and on cells of the first two suprabasal epidermal layers. This anti-α_3 reactivity displayed a pericellular distribution but was concentrated on the basolateral membranes of basal keratinocytes. In addition, weak anti-$\alpha_3\beta_1$ reactivity was observed to be localised to the cell membrane of endothelial cells and immune cells migrating out of blood vessels within the dermal layer.

Anti-α_3 immunoreactivity within 24 hour acute wound tissue was detected on basal and suprabasal keratinocytes. This was observed within the epidermis at the wound edge and in the adjacent non wounded epidermis (figure 4.4.2). Immunoreactivity in the adjacent normal skin displayed the same staining pattern as previously described for normal skin and did not change throughout the following 72 hours. However, anti-$\alpha_3\beta_1$ reactivity detected in wound edge epidermis was decreased in intensity and the number of individual suprabasal cells observed to express $\alpha_3\beta_1$ was slightly increased (figure 4.4.3).

Figure 4.4.1: *$\alpha_3\beta_1$ expression in normal skin (scale bar = 100μm)*

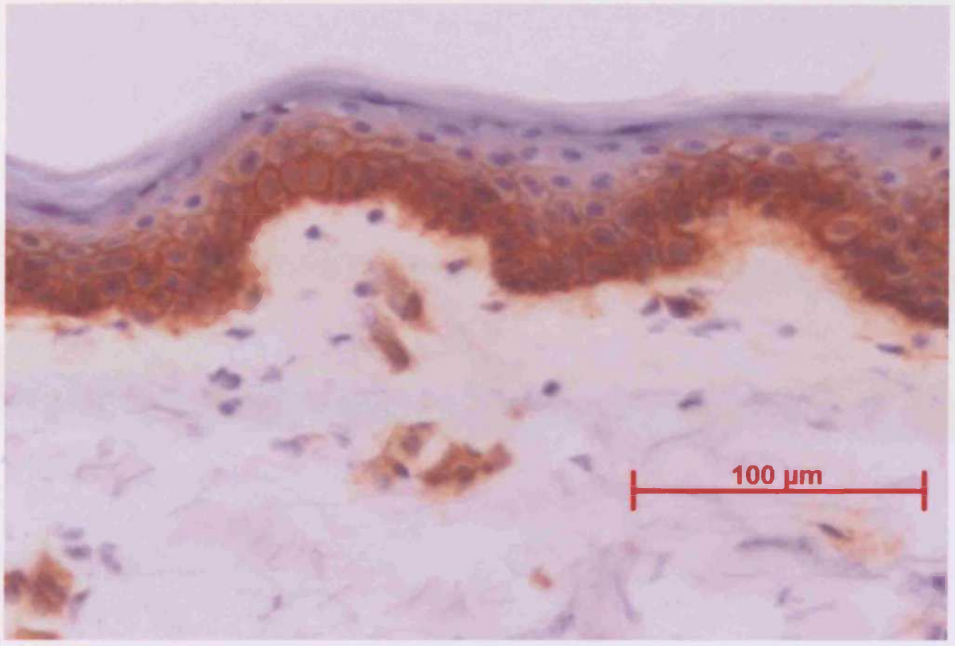

This expression pattern within the migrating epidermis did not change dramatically at 48, 72 and 96 hours post wounding except for a continuous increase in the number of suprabasal cells expressing $\alpha_3\beta_1$. Anti-α_3 reactivity within the dermal layer was detected around the blood vessels and a small number of inflammatory cells. This immunoreactivity did not change throughout the healing time course and gave an intense staining pattern on the membranes of endothelial cells while inflammatory cells were stained with less intensity.

Figure 4.4.2: *Expression of $\alpha_3\beta_1$ in epidermis at the edge of a 96hour acute wound (scale bar = 50μm)*

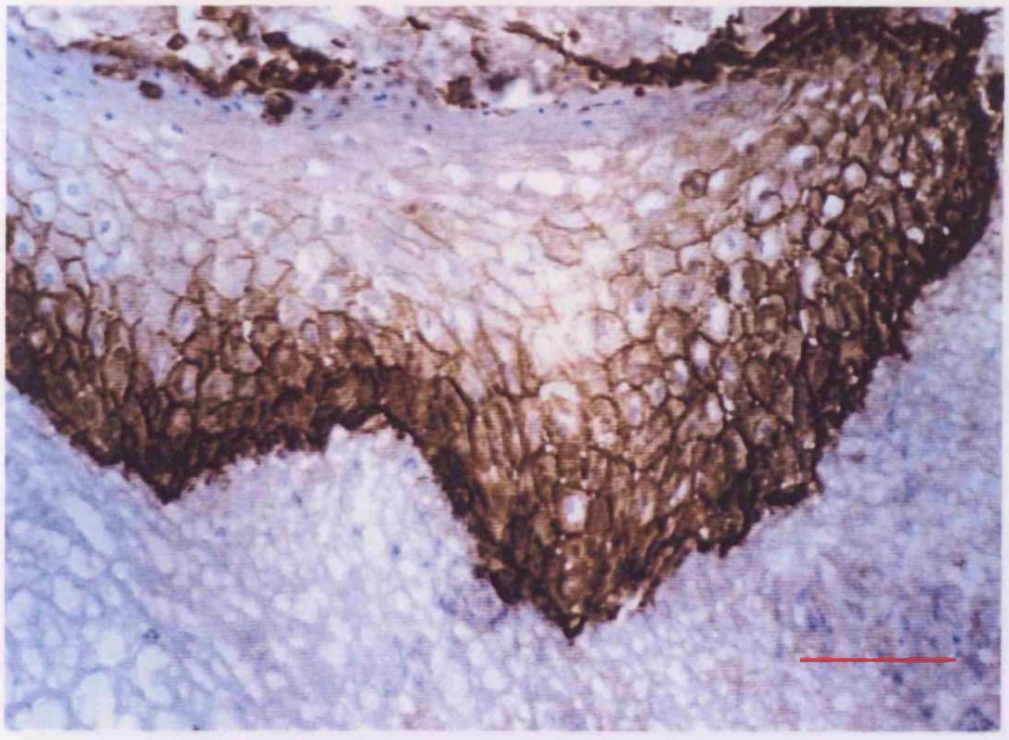

4.1.5 Immunolocalisation of Serum Fibronectin in a human acute wound

Illustrated in figure 4.5.1 is the immunolocalisation of serum fibronectin within a frozen section of normal skin using the anti serum fibronectin monoclonal antibody. Anti serum fibronectin reactivity was detected throughout the dermal layer giving a homogenous granular staining pattern with greatest intensity in the upper dermis directly under the epidermis. This immunoreactivity did not appear to have any cellular association. Immunoreactivity was also observed as a dense homogenous staining pattern around the blood vessels present within the dermal layer. Again, this did not appear to have any cellular association. Weak anti-serum fibronectin reactivity was observed discontinuously throughout the epidermis and appeared to be

associated the nuclei. However, this was considered to be non-specific binding, which was a known characteristic of this particular antibody.

Figure 4.5.1: *Immunolocalisation of Serum Fibronectin in normal skin (scale bar = 100μm).*

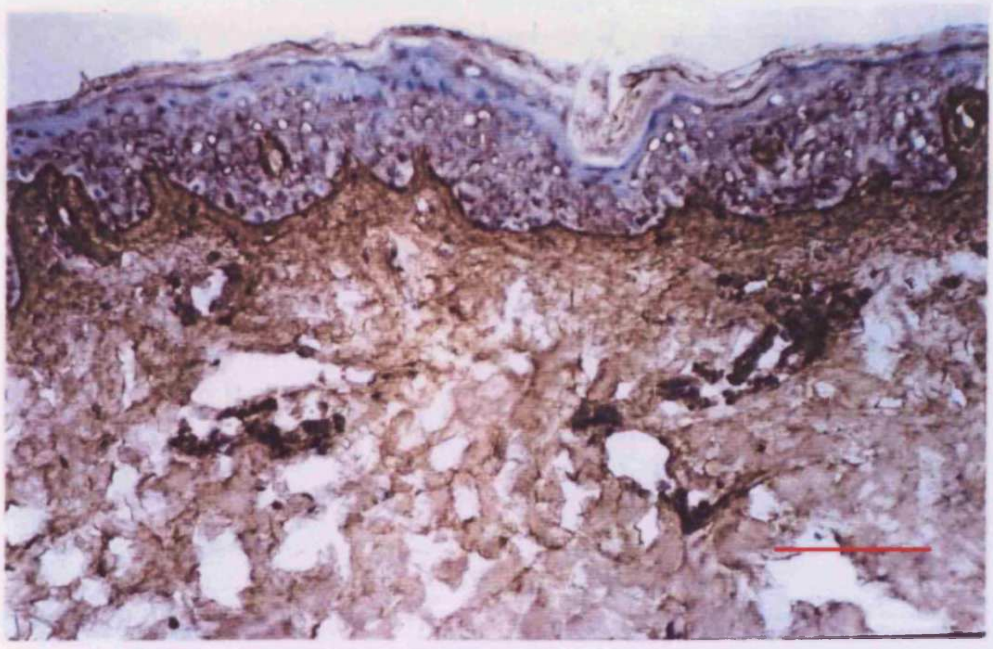

Immunolocalisation of serum fibronectin within frozen sections of acute wound tissue over the 96 hour healing time course was also achieved using the anti serum fibronectin monoclonal antibody. Serum fibronectin immunoreactivity was detected throughout the dermal layer of 24 hour acute wound tissue. This immunoreactivity was observed to have a similar staining pattern to that observed in normal skin. Immunoreactivity was also detected throughout the wound bed in a homogeneous granular staining pattern and was particularly noticeable near to the edge of the wounded epidermis. At 48 hours post wounding there was an overall increase in staining intensity observed throughout the dermis and wound bed. In addition, a dense homogenous granular immunohistochemical staining pattern was observed within the wound matrix in contact with the epidermis at the wound edge (see arrows

figure 4.5.2). Figure 4.5.2 represent the pattern of serum fibronectin deposition within acute wound edge tissue at 72 hours post wounding which was similar to that previously described for 24 hour and 48 hour wound tissue. There was however a further increase in the staining intensity of wound matrix directly in contact with migrating epidermis at the wound edge. Staining of wound tissue at 96 hours did not differ from that seen at 72 hours post wounding.

Figure 4.5.2: *Immunolocalisation of serum fibronectin within 72 hour acute wound tissue representing its pattern of deposition over the 96 hour healing time course (scale bar = 100μm). WE – wound edge, GT – granulation tissue*

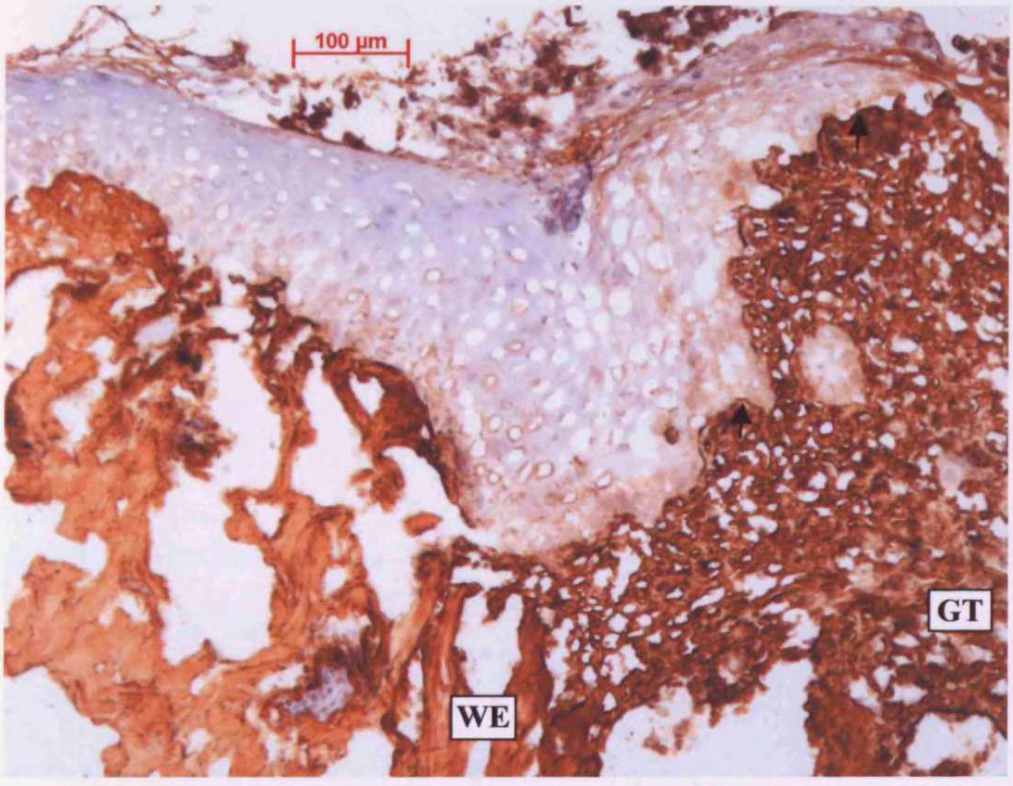

4.1.6 Immunolocalisation of cellular fibronectin in a human acute wound

Figure 4.6.1 illustrates a frozen section of normal skin probed with an anti-cellular fibronectin monoclonal antibody. Weak anti-cellular fibronectin reactivity was

detected throughout the upper dermis but in particular directly underneath the epidermis. This was observed as a fibrillar staining pattern associated with cell membranes and processes. Cellular fibronectin immunoreactivity was also detected around the blood vessels within the dermal layer. This reactivity had a weak homogenous granular staining pattern, which appeared to be associated with the dermal membrane of endothelial cells.

Figure 4.6.1: *Immunolocalisation of cellular fibronectin deposition in normal skin. (scale bar = 50μm)*

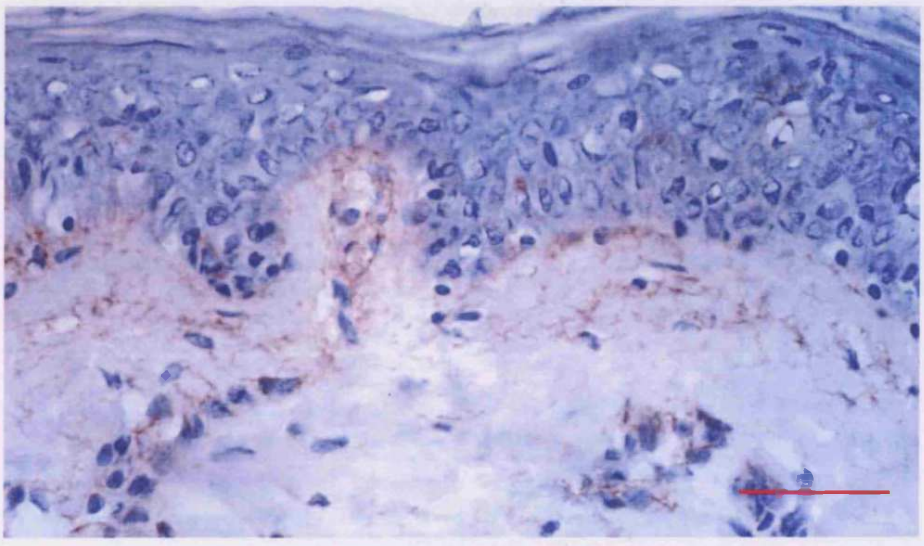

Cellular fibronectin was also immunolocalised within frozen sections of acute wound tissue over the 96 hour healing time course using the anti cellular fibronectin monoclonal antibody. Anti cellular fibronectin reactivity within 24hour acute wound tissue was detected throughout the upper dermis, displaying the same staining pattern as seen in normal skin. However, an increased amount of cellular fibronectin reactivity was observed under the epidermis both at the wound edge and in the adjacent normal skin. Cellular fibronectin deposition over the 96 hour healing time course is represented by the staining pattern observed in 96 hour wound tissue depicted in figure 4.6.2.

Figure 4.6.2: *Immunolocalisation of cellular fibronectin deposition within acute wound tissue at 96 hours post wounding (scale bar = 100μm). GT – granulation tissue*

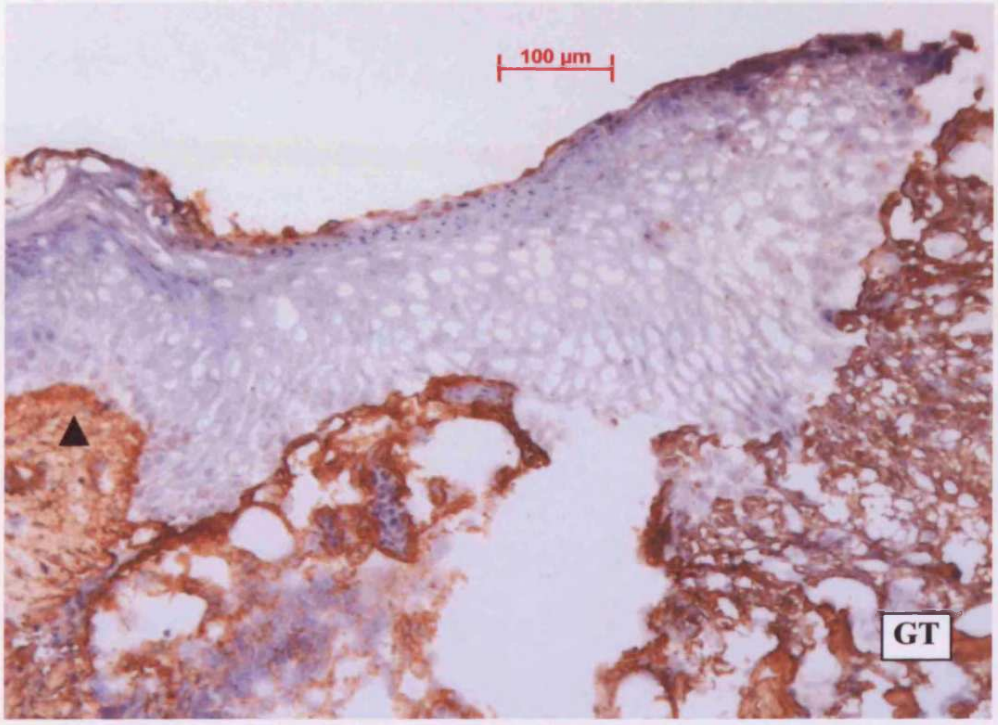

Figure 4.6.3: *Higher power image of cellular fibronectin deposition under the migrating epidermis presented previously in figure 4.6.2 (scale bar = 100μm)*

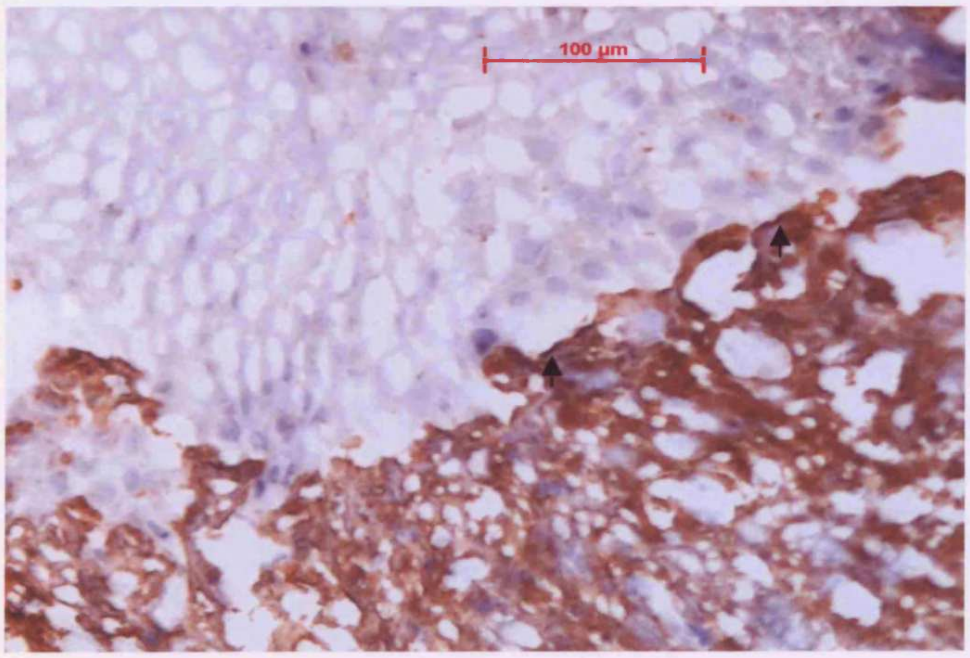

At 48 hours post wounding a further increase in immunoreactivity was detected in the upper dermis directly under the epidermis near to the wound edge. This had the same staining pattern observed in normal skin. However, immunoreactivity was also detected within the wound matrix in contact with the migrating epidermis at the wound edge. This immunoreactivity was observed to have a strong homogenous granular staining pattern which was seen more clearly in the 96 hour healing time depicted in figure 4.6.3 (see arrows figure 4.6.3). Anti-cellular fibronectin reactivity was also markedly increased around the blood vessels present within the dermis and had the same staining pattern previously described for normal skin. The only change in staining pattern seen at 72 hours post wounding was an increased staining intensity in the upper dermis near to the wound edge. This was further increased in 96hour acute wound tissue with no other changes seen at this healing time point (see arrowhead figure 4.62).

4.1.7 Immunolocalisation of Vitronectin within human acute wound tissue

Immunolocalisation of vitronectin within a frozen section of normal skin using the 1.110 anti-vitronectin monoclonal antibody is illustrated in figure 4.7.1. Anti vitronectin immunoreactivity was observed throughout the dermal layer but to a greater degree in the upper epidermis. This reactivity was observed as a fibrillar staining pattern, which was associated with cell membranes and processes. Furthermore, a discontinuous granular staining pattern was observed directly under the epidermis, which appeared to be associated with the basement membrane zone. The blood vessels present within the dermis were observed to have a surrounding weak anti-vitronectin immunreactivity, which was seen as a weak homogenous granular staining pattern. This anti-vitronectin reactivity did not appear to have a

cellular association. Weak anti vitronectin immunoreactivity was also discontinuously present within the epidermis and again did not appear to have a cellular association.

Figure 4.7.1: *Deposition of vitronectin in normal skin. (Scale bar =100μm)*

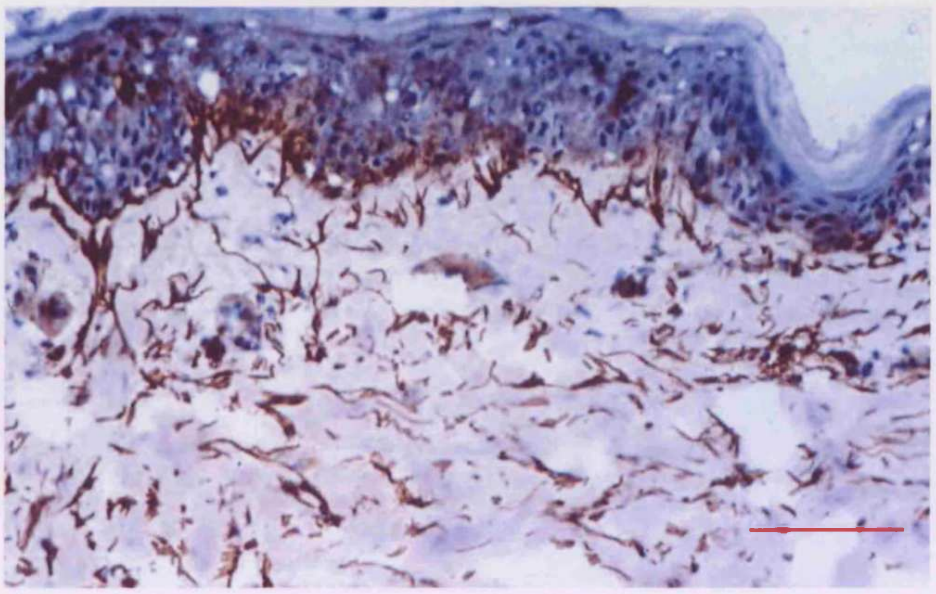

The 1.110 anti-vitronectin monoclonal antibody was used to immunolocalise vitronectin deposited within acute wound tissue over the 96 hour healing time course. Figure 4.7.2 illustrates immunolocalisation of vitronectin within frozen sections of 24 hour acute wound tissue. Anti-vitronectin reactivity gave a staining pattern within the dermis of skin adjacent and distal to the wound consistent with that described in normal skin. However there did appear to be an overall increase in the level of anti-vitronectin reactivity. Anti-vitronectin reactivity was also detected in the wound matrix directly in contact with the epidermis at the wound edge and was observed to have a homogenous granular staining pattern, which is clearly indicated by arrows in figure 4.7.2.

Figure 4.7.2: *Immunolocalisation of vitronectin deposition in a 24 hour acute wound (scale bar = 100μm). WE – wound edge, LE – leading edge*

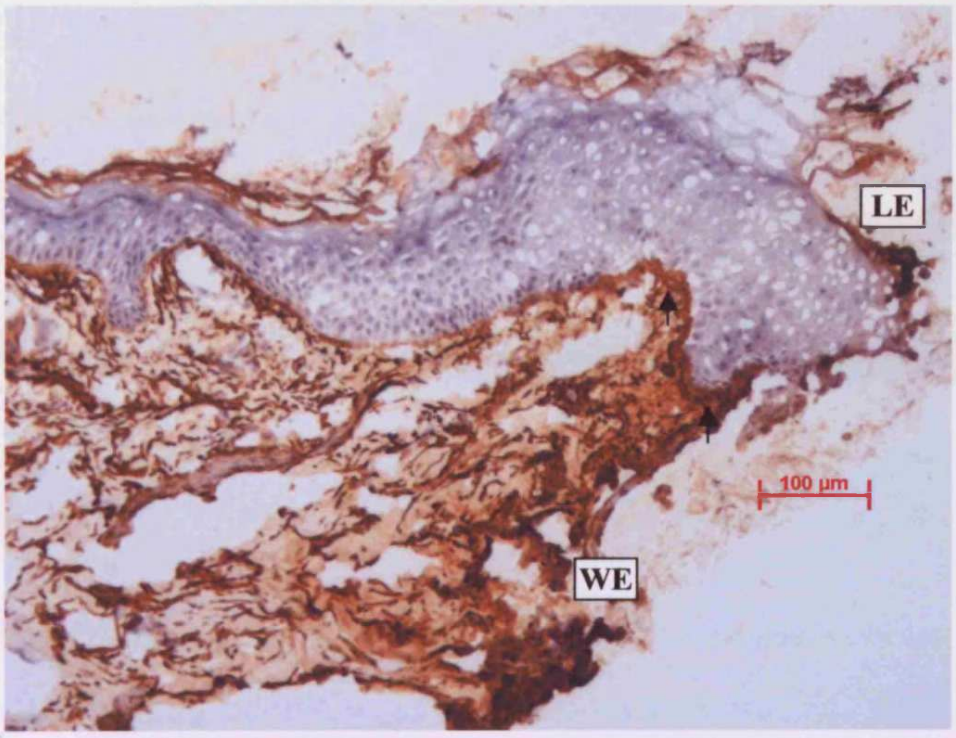

Figure 4.7.3: *Immunolocalisation of vitronectin deposition at the edge of a 96hour acute wound (scale bar = 100μm). LE – leading edge*

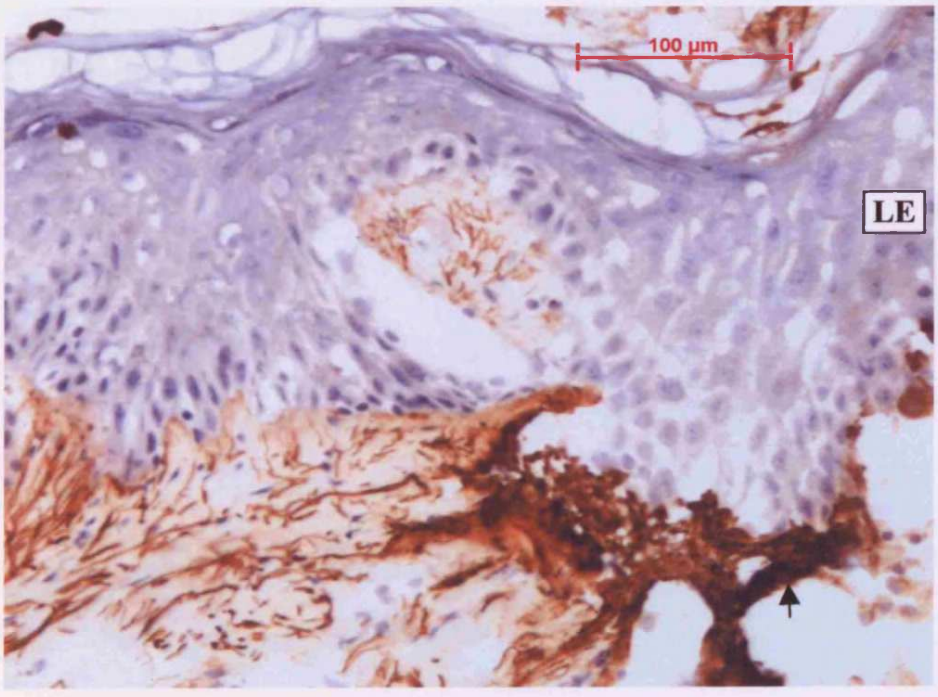

This staining pattern was increased in intensity at 48 hours post wounding and was seen as a linear labelling of the wound matrix directly underneath the migrating epidermis. The linear labelling of the provisional wound matrix was maintained throughout the following 48 hours and was seen to have the greatest staining intensity at 96 hours post wounding (see arrows figure 4.7.3). No other changes in the pattern of anti vitronectin reactivity were observed within the acute wound tissue during the remaining 48 hours of the 96 hour healing time course.

4.2.0 β_4, E-Cadherin and Syndecan-1 Expression in Pilonidal Excision Acute Wound Tissue

Due to the limited amount of tissue obtained from the surgically-induced acute wound model and unavailability of specific antibodies during the initial phase of the study, investigation of β_4, E-cadherin and syndecan-1 expression was carried out using an alternative source of acute wound tissue. An alternative source of tissue already established in other immunohistochemical investigations carried out within the laboratory was the pilonidal excision wound. A description of this source of tissue and retrieval method can be found in the methodology. In total four pilonidal excisional wounds were studied. An alternative source of normal skin was used which is also detailed in the methodology.

4.2.1 Immunolocalisation of β_4 integrin subunit expression

Probing of normal skin with the 3E1 anti-β_4 monoclonal antibody allowed immunolocalisation of β_4 integrin subunit expression within this tissue. β_4 expression was immunolocalised to the basal layer and first suprabasal layer of normal skin. This is illustrated in figure 4.8.1 in which expression is seen to be distributed

pericellularly and concentrated strongly along the basal membrane of the basal layer keratinocytes. The concentration of anti-β_4 reactivity on the basal membrane results in a continuous linear labelling of the dermal epidermal junction or basement membrane zone (see arrows).

Figure 4.8.1: *β4 integrin subunit expression in normal skin (scale bar = 50μm)*

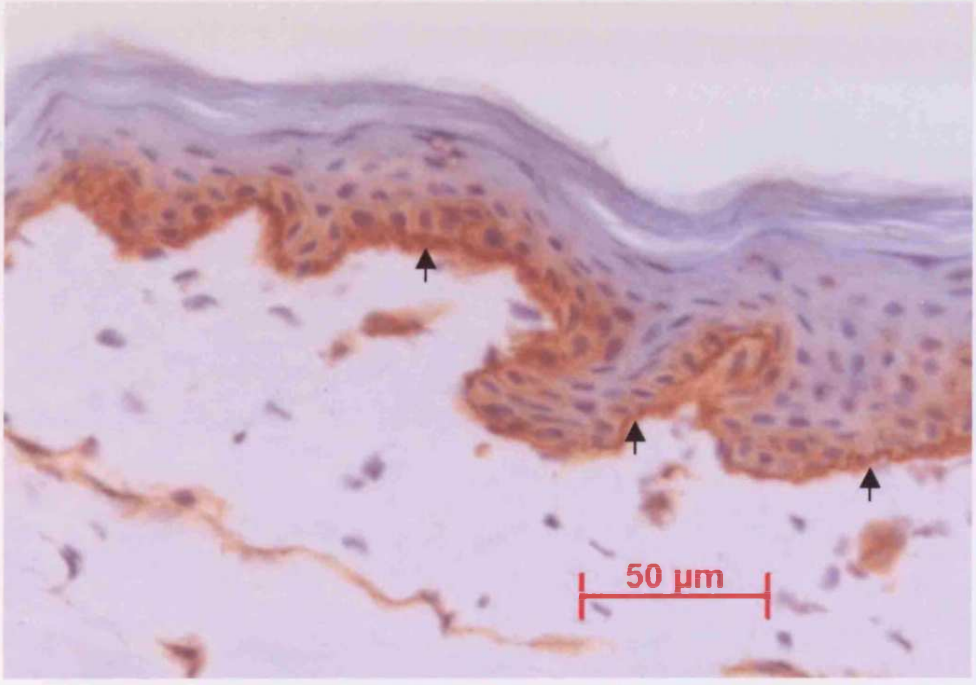

Figure 4.8.2 illustrates the immunolocalisation of the β_4 subunit within a 2 week old healing pilonidal sinus excision wound using the 3E1 monoclonal antibody. Expression of the β_4 subunit was observed in the epidermis of the adjacent normal skin and in the migrating epidermis in contact with the wound matrix. Distribution of β_4 expression in the adjacent normal epidermis was consistent with that already described for normal skin (see figure 4.8.1). However, expression within the migrating epidermal tongue was consistently observed to be present on an increased number of suprabasal keratinocytes (see arrowhead figure 4.8.2).

Figure 4.8.2: *Low power image of β_4 integrin subunit expression in a section of healing pilonidal sinus wound edge tissue (scale bar = 200μm) AE – adjacent epidermis, WE – wound edge, GT - Granulation Tissue.*

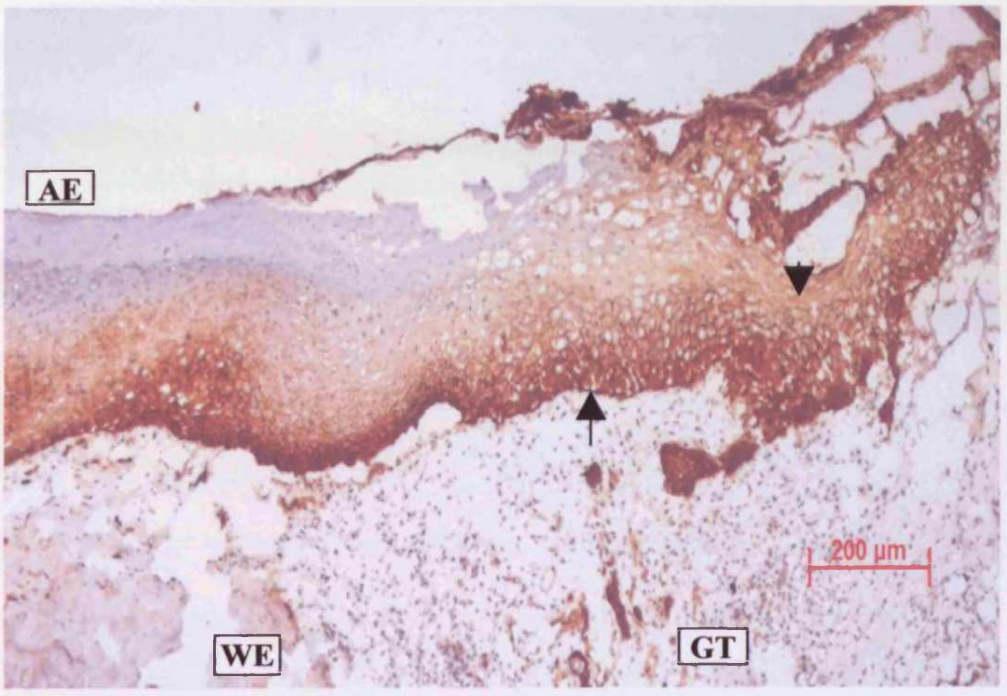

Figure 4.8.3: *Higher power image of figure 4.8.2(scale bar = 100μm) MT – migrating tip, GT – granulation tissue*

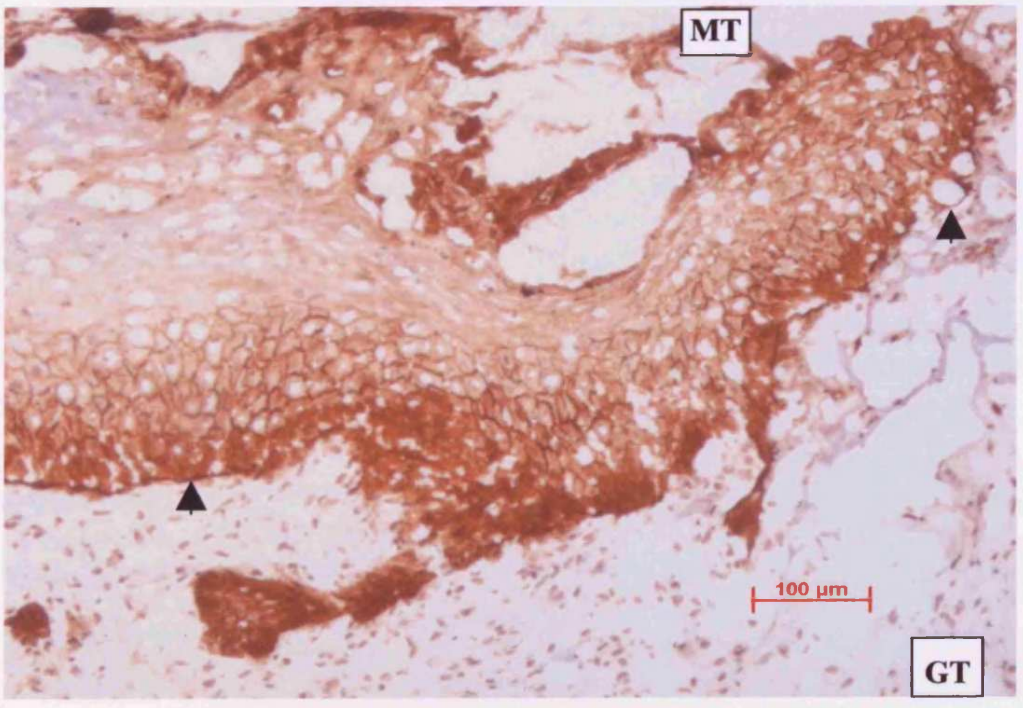

This expression had a pericellular membrane distribution and at the very tip of the migrating epidermal tongue was present on almost all keratinocytes (figure 4.8.3). Suprabasal expression also extended a short distance into the adjacent normal epidermis. Basal keratinocytes within the migrating epidermal tongue also had a pericellular membrane staining pattern, but as in normal skin this was heavily polarised towards the basal membrane. The exception to this was found towards the tip of the migrating epidermis where staining of the basal membrane was decreased or often absent, particularly at the leading edge. This resulted in a discontinuous labelling of the dermal epidermal junction (see arrows in figure 4.8.3). Unfortunately, no comment can be made on the temporal dimensions of these changes in β_4 expression as tissue representing the onset of healing and closure of the wound was not available.

4.2.2 Immunolocalisation of syndecan-1 expression

The expression pattern of syndecan-1 within normal skin was determined using the U266 monoclonal antibody. Using this antibody syndecan-1 expression was immunolocalised to basal and suprabasal keratinocytes with a pericellular membrane staining pattern as seen in figure 4.9.1. In addition, anti-syndecan-1 immunoreactivity gave rise to a homogenuous staining of the keratinocyte cytoplasm in both basal and suprabasal epidermal layers. Specific pericellular membrane staining was more prominent in the suprabasal layers.

Syndecan-1 expression was also observed on endothelial cell membranes within the dermis. This was mainly associated with a small number of relatively smaller capillaries and was not generally present on the endothelial cells of the larger vessels.

Figure 4.9.1: *Syndecan-1 expression in normal skin (scale bar = 100μm)*

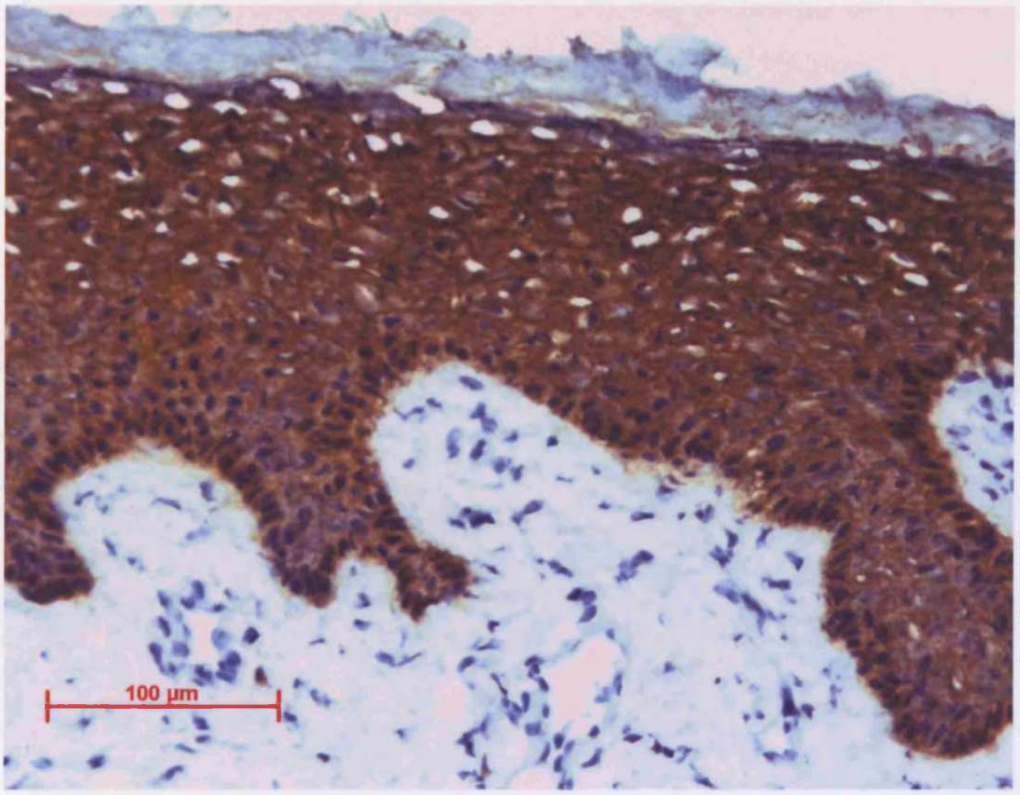

Pilonidal sinus excision wound tissue was also probed with the U266 monoclonal antibody. In this tissue, syndecan-1 expression was detected throughout the epidermis both in the adjacent normal skin and at the healing margin with the same pericellular membrane distribution described for normal skin (see figure 4.9.1). Homogenous staining of the keratinocyte cytoplasm described in normal skin was also present in the acute wound tissue. However, within the migrating epidermis, expression was observed to be stronger in the basal layer when compared to normal skin (see arrow figure 4.9.2) and suprabasal expression was slightly weaker towards the leading edge (see arrowhead figure 4.9.2). This expression pattern was observed within early healing tissue 2 weeks post wounding and in later tissue samples up to 6 weeks post wounding. Unfortunately, tissue representing the onset of healing and

wound closure was not available. Small blood vessels at the wound margin were also observed to express syndecan-1 in association with their endothelial cell membranes.

Figure 4.9.2 *Syndecan-1 expression within migrating epidermis at the edge of a healing acute pilonidal sinus wound (scale bar = 100μm). MT – migrating tip, GT – granulation tissue.*

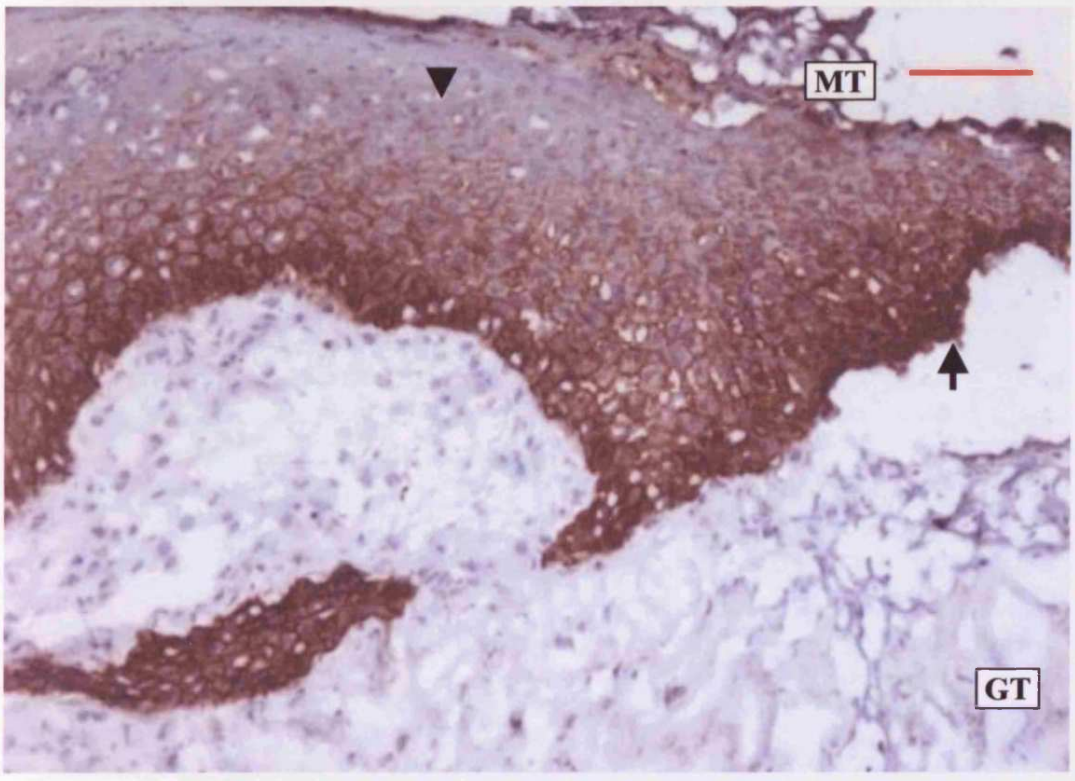

4.2.3 Immunolocalisation of E-cadherin expression

Normal skin was probed with the MCA1482 anti-E-cadherin monoclonal antibody. Using this antibody expression of E-cadherin was detected throughout all layers of the epidermis with exception of the stratum corneum, as illustrated in figure 4.10.1 Expression on suprabasal keratinocytes had a pericellular membrane distribution in contrast to basal layer keratinocytes where expression was limited to the lateral and apical membranes. Weak expression was present within the dermal layer and was associated with endothelial cell membranes.

Figure 4.10.1: *Immunohistochemical localisation of E-cadherin using the MCA1482 monoclonal antibody within normal human adult skin (scale bar = 50μm).*

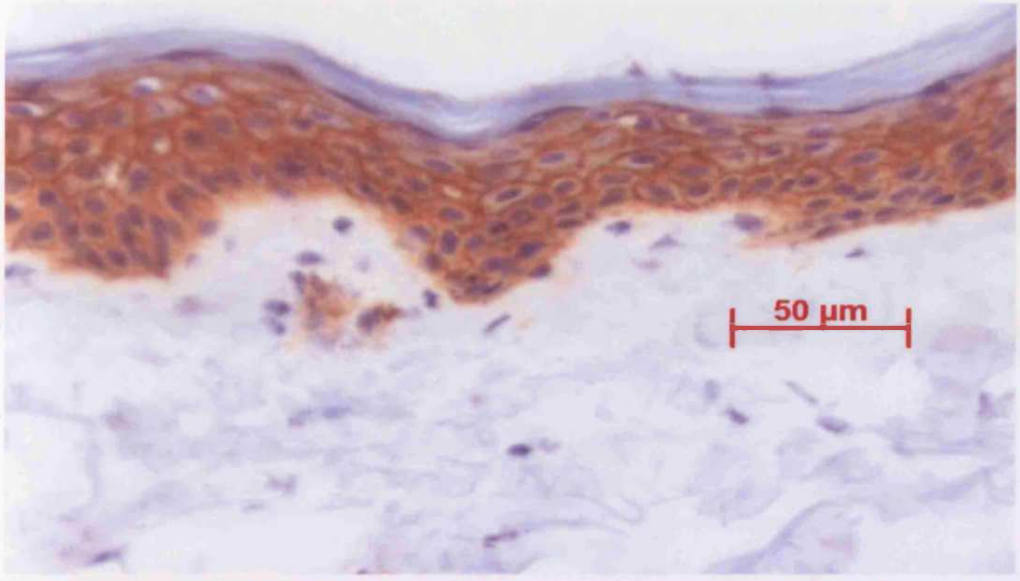

In figure 4.10.2 Immunolocalisation of E-cadherin expression within epidermis adjacent to the wound edge of an acute pilonidal excision wound can be seen to be consistent with that already described in normal skin (see figure 4.10.1 and 4.10.4) Expression was also present within the migrating epidermal tongue. However, this was progressively lost from the upper suprabasal layers on moving from the original wound edge towards the migrating tip (see arrow head figure 4.10.2). When present, E-cadherin expression had a pericellular membrane distribution except in the basal layer where it was limited to the apical and lateral cell membranes.

E-cadherin expression was maintained on basal layer keratinocytes along the whole length of the migrating epidermis. This made it the only layer at the migrating tip in which expression was observed, although at this location it was comparatively weak (see figure 4.10.3). Dermal blood vessels were again observed to express E-cadherin in the adjacent non-wounded skin, which was localised to their endothelial cell membranes. However, E-cadherin expression was not observed within the dermal wound matrix.

Figure 4.10.2: *Low power image of E-cadherin expression within epidermis at the edge of an acute healing pilonidal excision wound (scale bar = 200μm).*

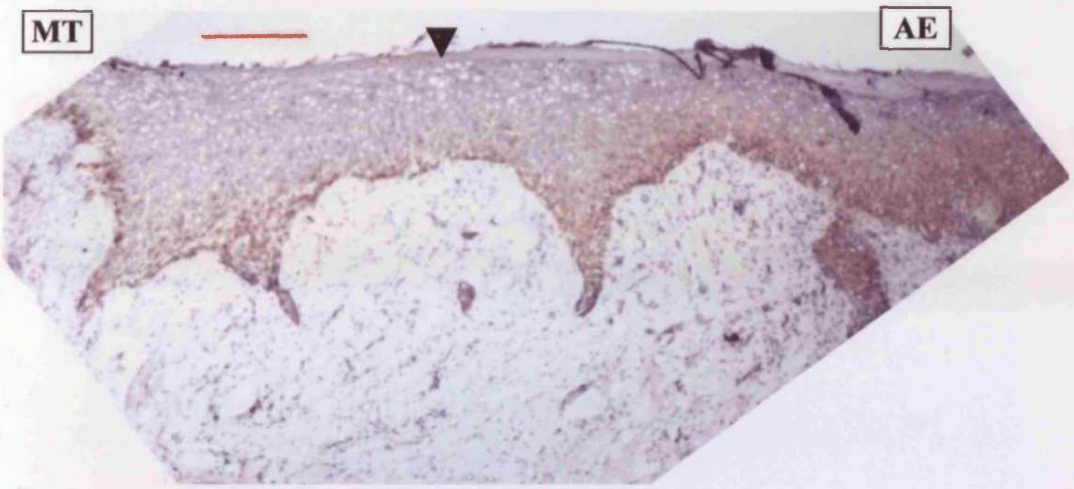

Figure 4.10.3: *High power image of the migrating tip already depicted above in figure 4.10.2 (scale bar = 100μm)*

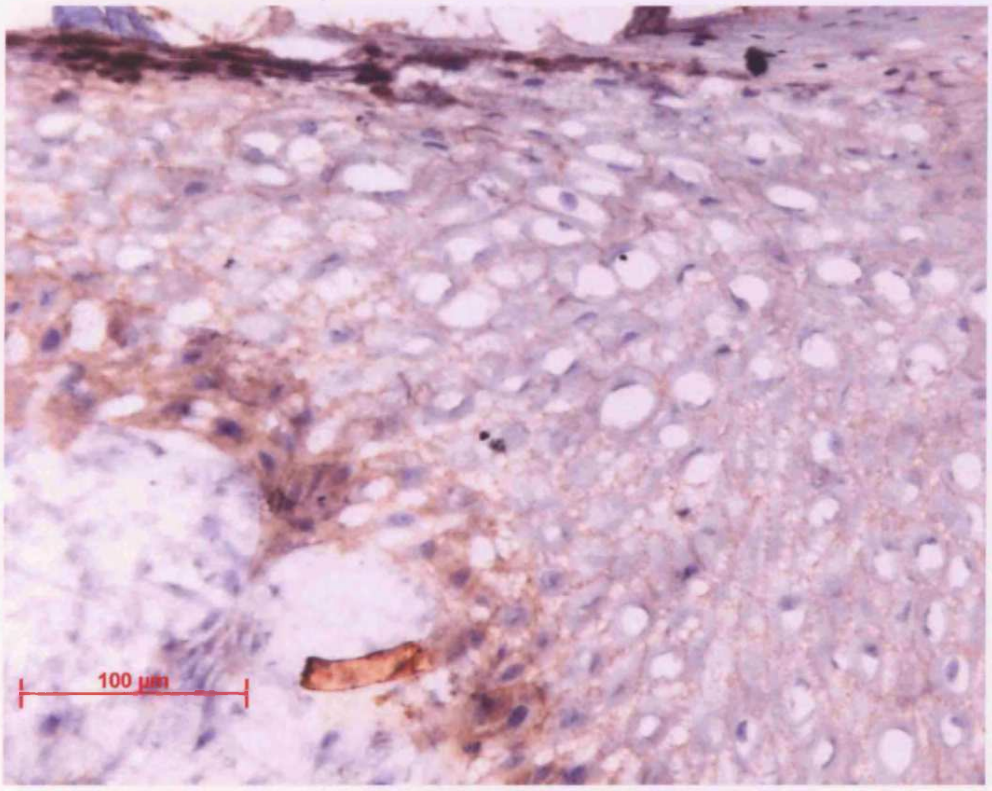

Figure 4.10.4: *High power image of the adjacent epidermis already depicted in figure 4.10.2 (scale bar = 50μm).*

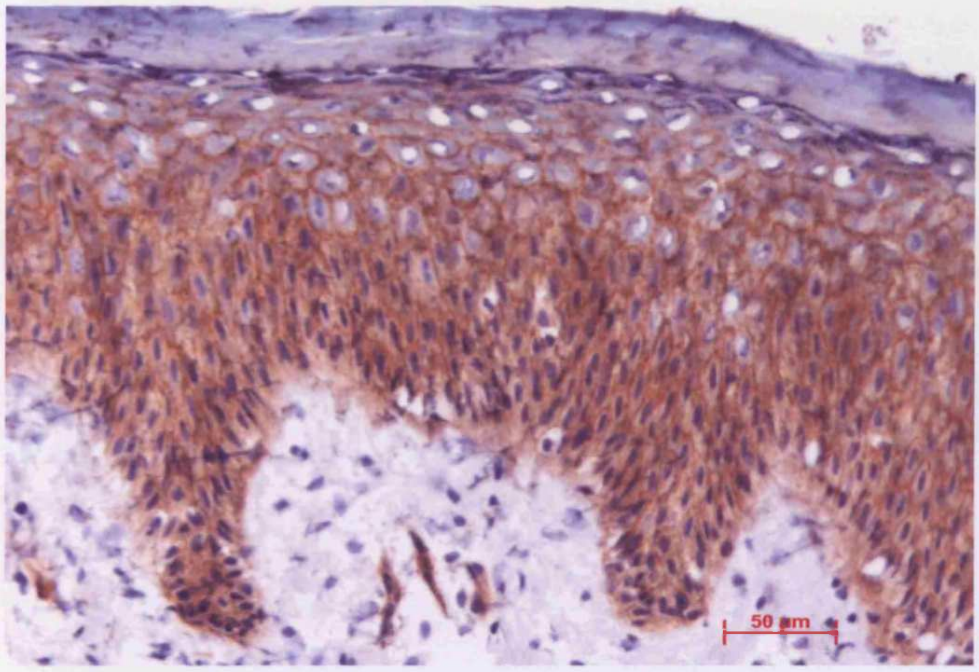

4.3.0 EPIDERMAL INTEGRIN EXPRESSION AND MATRIX PROTEIN EXPRESSION IN CHRONIC WOUNDS

The integrin adhesion molecules and extracellular matrix proteins were immunolocalised within frozen sections of chronic wound tissue. Chronic non-healing venous leg ulcers were used as a source of chronic wound tissue in which the expression of the integrins and ECM proteins could be characterised. This could then be compared to their expression in normal acute wound healing tissue. The sampling of chronic wound tissue is described in the methods section.

4.3.1 Immunolocalisation of $\alpha_5\beta_1$ within chronic wound tissue

Immunolocalisation of the $\alpha_5\beta_1$ integrin within frozen sections taken from chronic wound tissue was achieved using the PID6 anti $\alpha_5\beta_1$ monoclonal antibody. Anti $\alpha_5\beta_1$ reactivity was detected within wound edge epidermis on basal layer keratinocytes and discontinuously on the first suprabasal layer keratinocytes as seen in figure 4.11.1 and 4.11.2. Immunoreactivity could also be detected on basal keratinocytes distal to the wound edge although it appeared to be decreased in intensity compared to the wound edge. The immunoreactivity detected in the distal epidermis is marked with an arrowhead in figure 4.11.2 and represented in higher power in figure 4.11.3. The anti-$\alpha_5\beta_1$ immunoreactivity had a pericellular membrane distribution and appeared to be more intense on the basal keratinocytes in contact with the wound (see arrow figure 4.11.1 and 4.11.2). Periodic changes in the expression of $\alpha_5\beta_1$ were observed in chronic wound edge epidermis when repeat samples were taken from the same wound. This was not carried out using a specific time course and the interval between 2 biopsies in some cases was a number of weeks or months.

$\alpha_5\beta_1$ immunoreactivity was also detected in the dermis and was localised to cell membranes and processes of inflammatory cells. It was possible that some immunoreactivity could be attributed to fibroblast cell membranes, as they are known to express $\alpha_5\beta_1$ but these cells could not be identified directly within the tissue section. The amount of anti-$\alpha_5\beta_1$ immunoreactivity detected in the dermis was observed to be markedly increased in comparison to that observed in normal skin and acute wound tissue. In particular there was an increase in the number of inflammatory cells displaying anti-$\alpha_5\beta_1$ reactivity.

Figure 4.11.1: *Immunolocalisation of $\alpha_5\beta_1$ within chronic wound tissue at the edge of a chronic non healing leg ulcer (scale bar = 200μm). AE – adjacent epidermis, GT – granulation tissue.*

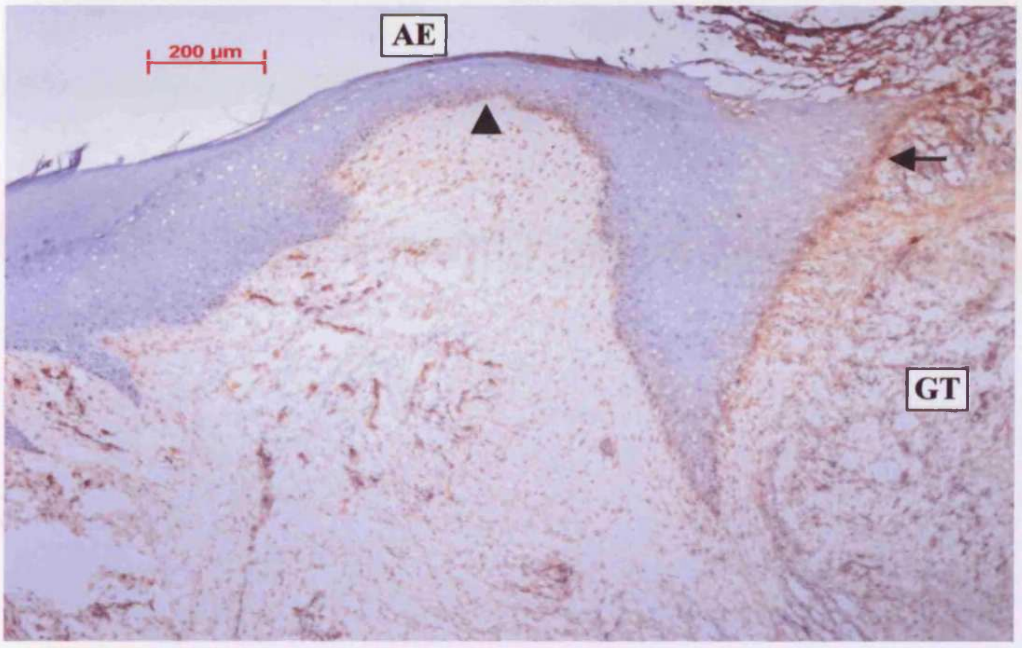

Figure 4.11.2: *Higher power presentation of the leading epidermal edge seen in figure 4.11.1 (scale bar = 100μm)*

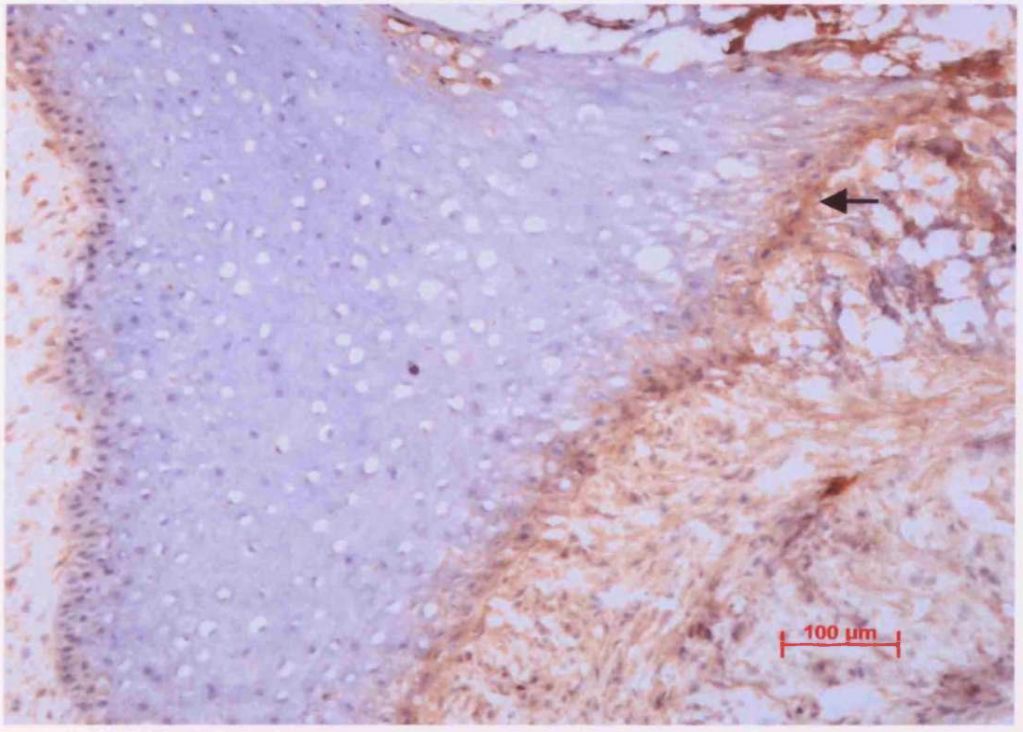

Figure 4.11.3: *Higher power presentation of epidermis away from the wound edge marked with an arrowhead in figure 4.11.1 (scale bar = 50μm)*

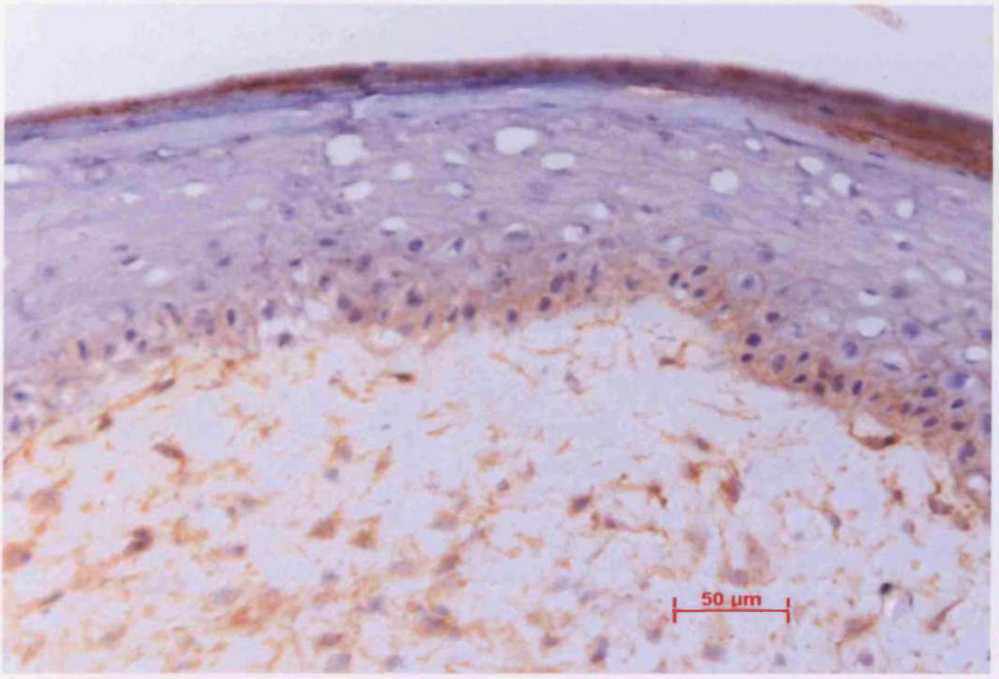

4.3.2 Immunolocalisation of $\alpha_2\beta_1$ within chronic wound tissue

Figure 4.12.1 and 4.12.2 illustrate the immunolocalisation of $\alpha_2\beta_1$ integrin in frozen tissue sections taken from a sample of chronic wound margin tissue using the PIE6 monoclonal antibody. Anti-$\alpha_2\beta_1$ reactivity was detected on basal and suprabasal keratinocytes within the epidermal layer. The $\alpha_2\beta_1$ immunoreactivity was localised to the membranes of these keratinocytes with a pericellular distribution that was concentrated on the lateral and apical membranes in the distal epidermis. However, within the epidermis in contact with the wound bed, staining was most intense on the basal keratinocytes and was concentrated on their basolateral membranes with a similar intensity to that observed in 24 hour acute wounds (figure 4.12.1 arrow and in higher power in figure 4.12.2). Furthermore, an increased number of suprabasal keratinocytes were observed to express $\alpha_2\beta_1$ within the epidermis at the wound edge as indicated by the arrowhead in figure 4.12.2.

Figure 4.12.1: *Immunolocalisation of $\alpha_2\beta_1$ expression within tissue at the edge of a chronic venous leg ulcer (scale bar =200μm)*

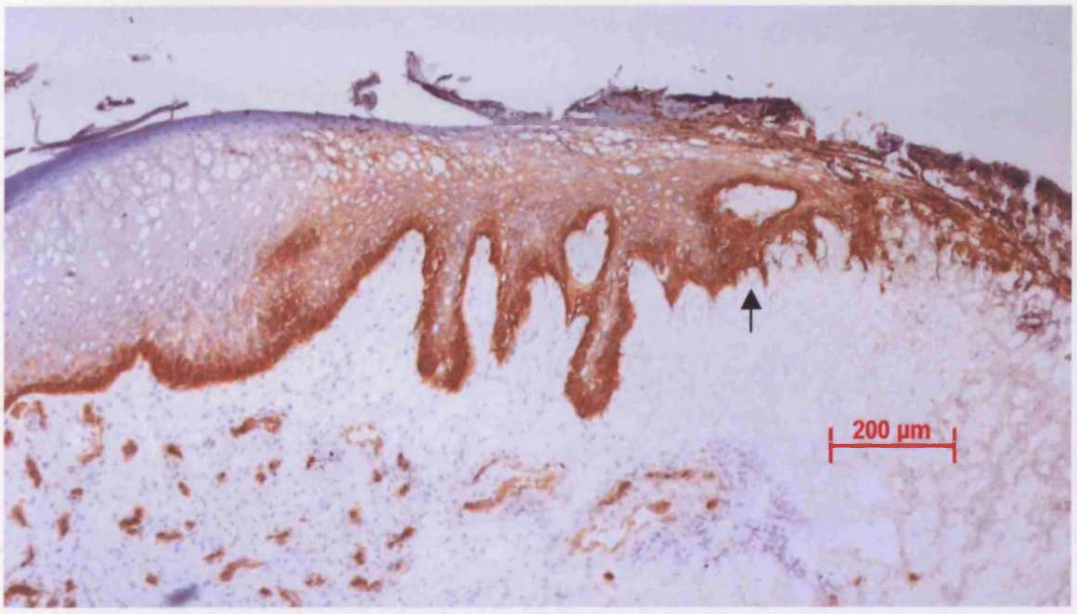

Figure 4.12.2: *Higher power image the wound edge epidermis previously presented in figure 4.12.1 (scale bar = 100μm).*

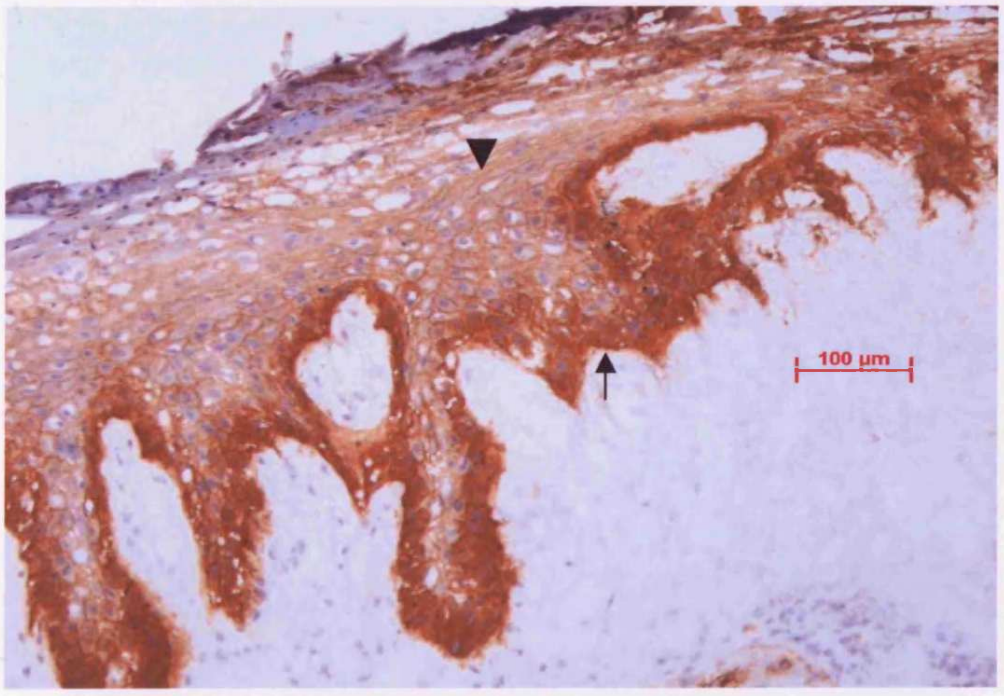

4.3.3 Immunolocalisation of $\alpha_3\beta_1$ within chronic wound tissue

$\alpha_3\beta_1$ was immunolocalised within frozen sections of chronic wound tissue using the GR3 anti-α_3 antibody. Anti-α_3 reactivity was detected on basal and suprabasal keratinocytes of the epidermis at the wound edge and in the epidermis away from the wound edge (see figure 4.13.1). Immunoreactivity was localised to the pericellular membrane of basal and suprabasal keratinocytes with greatest staining intensity along the basal membrane of the basal keratinocytes. Overall, it appeared that staining intensity was greatest at the wound edge. Furthermore, the number of suprabasal cells expressing $\alpha_3\beta_1$ also increased towards the epidermal wound edge (see figure 4.13.2). Immunoreactivity was also detected around the blood vessels present in the dermis where it was localised to the endothelial cell membranes.

Figure 4.13.1: *Immunolocalisation of $\alpha_3\beta_1$ within chronic wound tissue at the edge of a chronic non healing leg ulcer (scale bar = 200μm). DE – distal epidermis, WE – wound edge*

Figure 4.13.2: *Higher power image of the epidermis at the wound edge presented previously in figure 4.13.1 (scale bar = 100μm)*

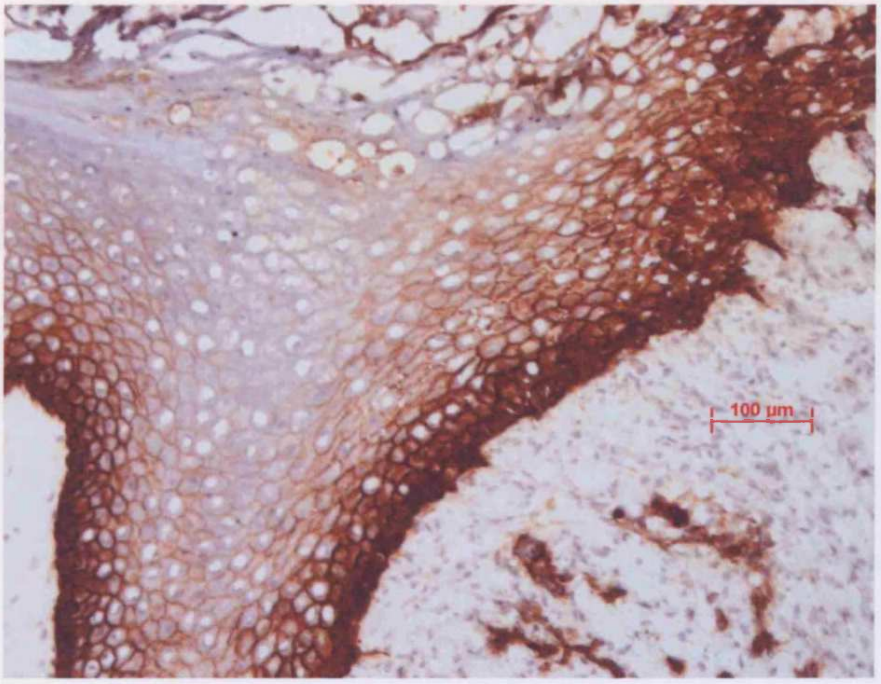

4.3.4 Immunolocalisation of α_V integrin subunit within chronic wound tissue

In Figure 4.14.1 immunolocalisation of the α_V integrin subunit in frozen sections taken from chronic wound tissue using the VNR147 anti-α_V monoclonal antibody can be seen. Anti-α_V reactivity could be detected on basal and a large number of suprabasal keratinocytes (arrowhead) along the whole length of the epidermis. Immunoreactivity had a pericellular membrane distribution, which had the greatest intensity on basal keratinocytes with overall staining intensity being greatest at the wound edge (see arrows).

Figure 4.14.1: *Immunolocalisation of α_V integrin subunit within epidermis at the edge of a chronic non healing venous leg ulcer (scale bar = 100μm). WE – wound edge*

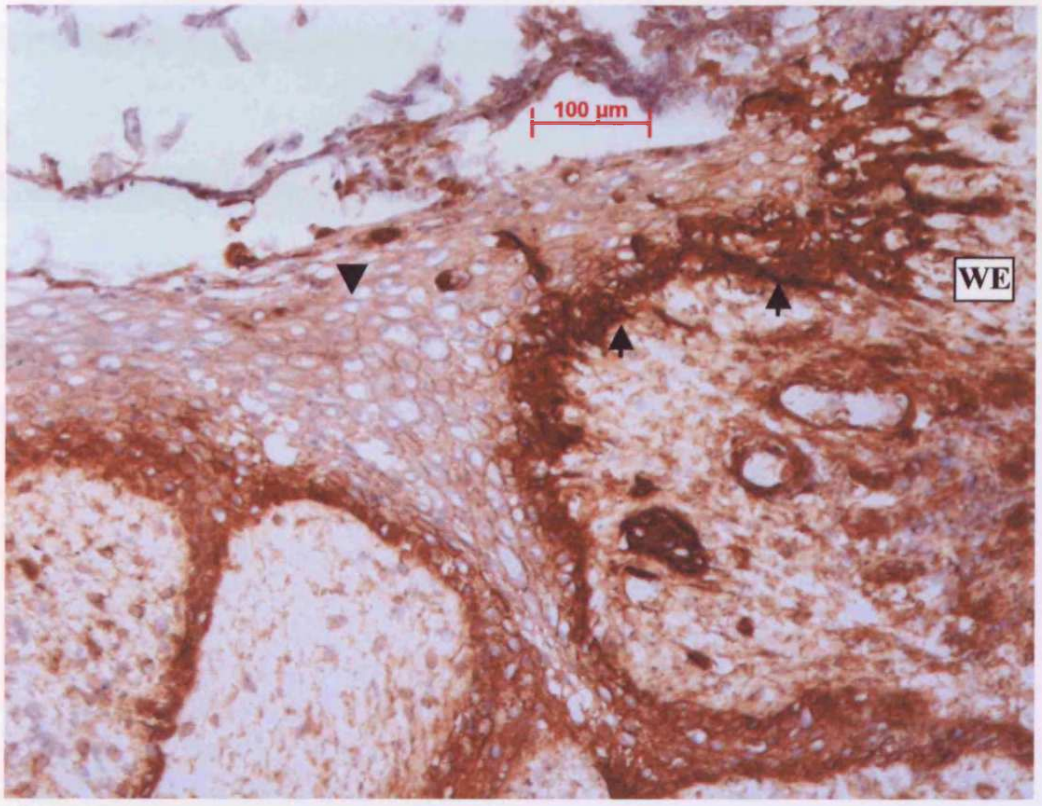

A large degree of α_V immunoreactivity was also detected in the dermis. This immunoreactivity was associated with the membranes of inflammatory and endothelial cells, along with possibly fibroblasts, although these could not be identified directly within these sections.

4.3.5 Immunolocalisation of β_4 within chronic wound tissue

Immunolocalisation of the β_4 integrin subunit within chronic wound tissue was achieved using the 3EI anti-β_4 subunit monoclonal antibody. Anti-β_4 reactivity was demonstrated on basal and suprabasal keratinocytes with a pericellular membrane distribution (see figure 4.15.1). Immunoreactiviy was strongest within the basal

layer, which was concentrated on the keratinocyte basal membrane, again giving a characteristic linear labelling to the dermo-epidermal junction (see arrowheads figure 4.15.1). This extended along the whole of the epidermis and was frequently present towards the tip of the migrating epidermis. An increased number of suprabasal keratinocytes were observed to express β_4 within the migrating epidermal tongue. Increased numbers of suprabasal keratinocytes were also observed to express β_4 subunit in the adjacent non-wounded epidermis when compared to normal skin. This may have been related to the overall increase in epidermal cell numbers, as a consequence of the characteristic hyperplasia often observed at the margin of venous leg ulcers (291;292). Lower levels of immunoreactivity were present in the dermis and wound bed and was associated with endothelial cell membranes.

Figure 4.15.1: *β_4 integrin subunit expression in chronic venous leg ulcer tissue (scale bar = 100μm). GT = Granulation Tissue, MT = Migrating Tip.*

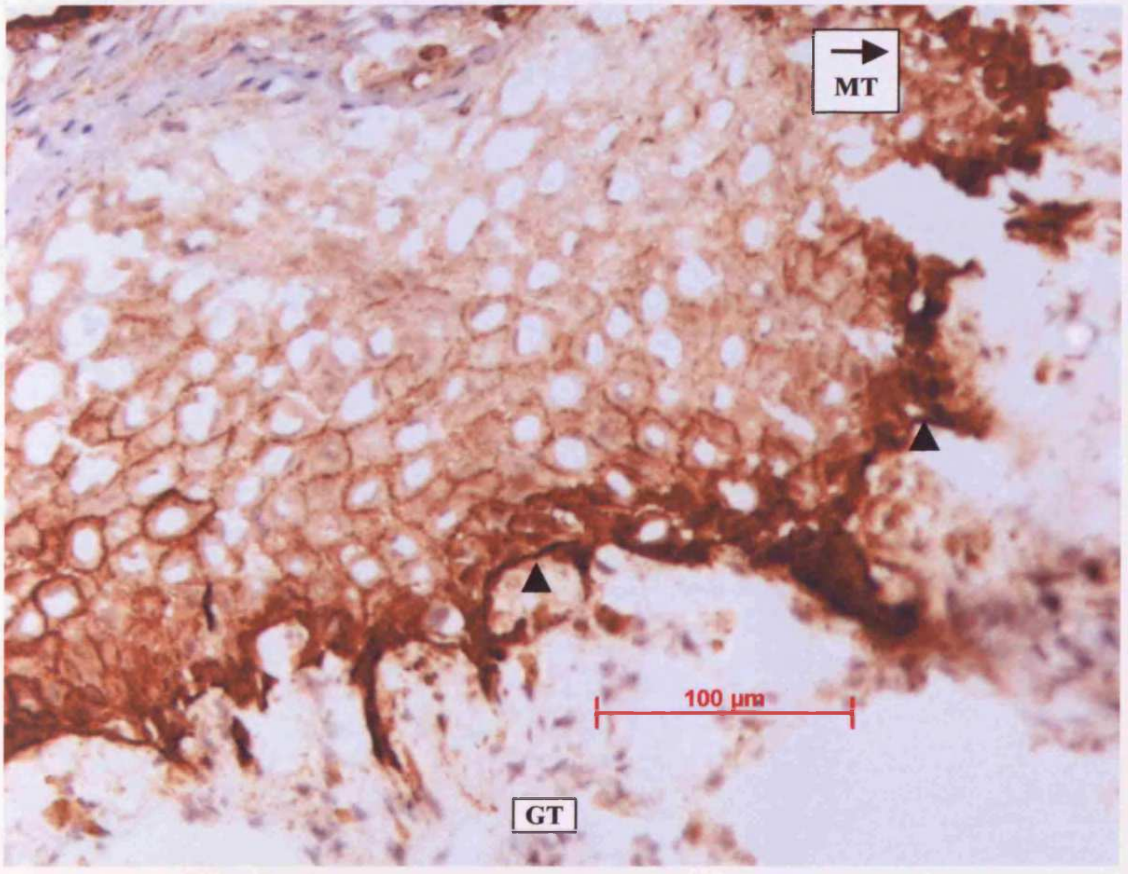

4.3.6 Immunolocalisation of E-cadherin within chronic wound tissue

Probing of chronic wound tissue with the MCA1482 monoclonal antibody allowed immunolocalisation of E-cadherin within chronic venous leg ulcer tissue. Immunolocalisation of E-cadherin expression within the epidermis of this tissue was observed to have a pericellular membrane distribution, except on basal layer keratinocytes where it was localised to their lateral and apical membranes (figure 4.16.1). In 4 of the 6 biopsies studied, expression was present throughout the epidermis including the wound edge (see arrow figure 4.16.1).

***Figure 4.16.1**: E-cadherin expression within chronic wound edge epidermis where expression was maintain in the suprabasal layers (scale bar = 200μm)*

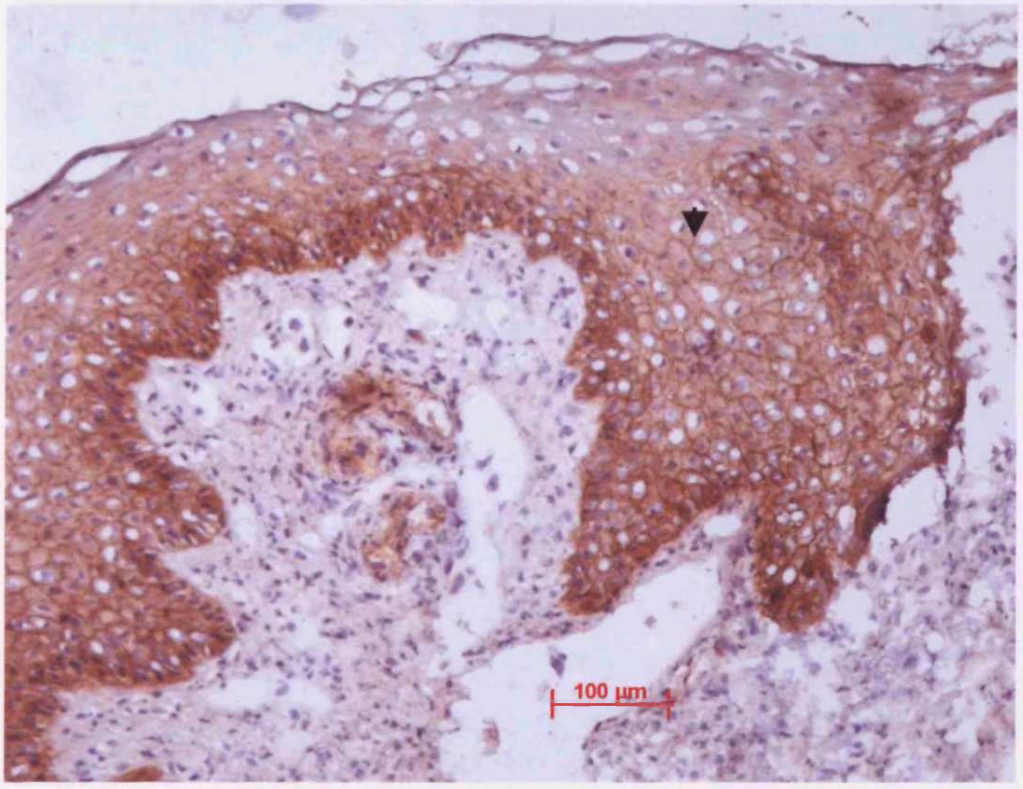

Figure 4.16.2: *Chronic wound edge epidermis where expression was decreased to a similar level to that seen at the epidermal edge of acute wounds (scale bar = 50μm)*

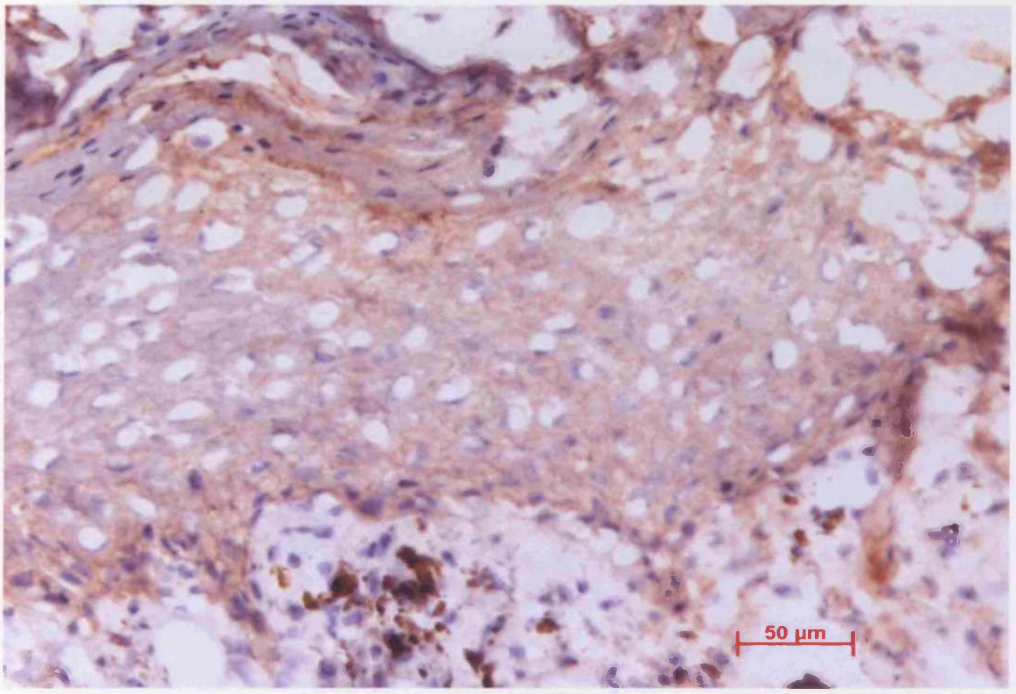

In 2 of the biopsies upper suprabasal expression was progressively lost towards the tip of the migrating epidermis, similar to that observed in acute wound epidermis (see figure 4.16.2). Only a small number of blood vessels within the dermis were observed to express E-cadherin, which was associated with their endothelial cell membranes.

4.3.7 Immunolocalisation of syndecan-1 within chronic wound tissue

The U266 anti-syndecan-1 monoclonal antibody was used to immunolocalise syndecan-1 expression within chronic wound tissue. In figure 4.17.2 the expression is immunolocalised to keratinocyte membranes in a pericellular distribution and homogeneously within the cytoplasm as described in acute wound tissue. This expression was present throughout the epidermis at the wound edge and in the adjacent skin as demonstrated in figure 4.17.1. However, the amount of anti syndecan-1 reactivity within the cytoplasm of keratinocytes was increased over that seen in acute wound tissue (see arrowhead figure 4.17.2). Strong expression was often maintained in the suprabasal layers at the wound edge and increased basal layer expression as in acute wounds was not consistently found in the chronic wound edge epidermis.

Figure 4.17.1: *Low power image of syndecan-1 expression within epidermis at the edge of a chronic venous leg ulcer (scale bar = 200μm). WE – wound edge*

Figure 4.17.2: *Higher power image of the epidermis towards the edge of the wound presented in figure 4.17.1 (scale bar = 100μm). WE – wound edge*

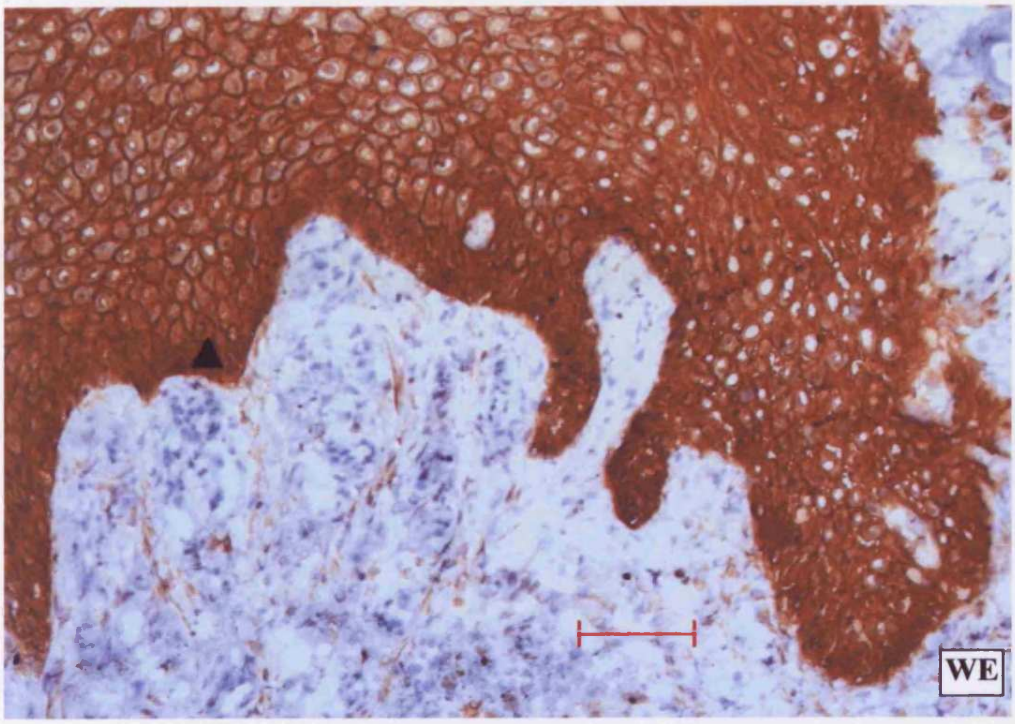

4.4.0 TISSUE EXPLANT CULTURE: An *ex vivo* model of wound healing

To develop a wound model capable of analysing the effect of treatment on chronic wound tissue, an initial analysis of the effect of tissue culture on chronic wound biopsy tissue was required. The aim of this initial phase of the investigation was to evaluate the degree of inherent variability in the behaviour of chronic wound tissue when placed in a tissue culture environment. This variability was assessed in terms of the levels of cytokines and metalloproteinase enzymes released by the tissue into the culture supernatant as a measure of the biological activity of the tissue as a whole. Biopsies were taken from the wound edge and bed of chronic venous leg ulcers, placed in culture media for up to eight hours, during which culture supernatants were removed for analysis and replaced with fresh media every 2 hours. Wound edge biopsies were divided into 3 segments with one control segment being frozen immediately for histology and the other 2 segments placed in culture. Wound bed biopsies were divided into one control segment and three test segments.

The specific cytokines and MMPs analysed were chosen on the basis of the following factors:-

a) Measurable levels would have to be present in the supernatant.
b) The biochemical molecule chosen for analysis would need to be produced by multiple cells and not a specific subset as it would then better represent the biological activity of the tissue as a whole.
c) Availability of an assay system for the chosen biochemical molecule that did not require large amounts of supernatant for each analysis as 200μl was the maximum amount of supernatant available for analysis at each time point.

d) Whether the biochemical molecule could provide clues as to the nature of the overall process going on within the tissue i.e. acute/chronic inflammation, tissue degradation or synthesis.

The biochemical molecules chosen on the above criteria were IL-1, IL-8, TGF-β, VEGF, MMP-2 and MMP-9. Pilot experiments were carried out to determine the detectable levels of cytokines or MMPs in the supernatant and the volume of supernatant required to carry out a test for each. From these experiments IL-8, MMP-2, MMP-9 and TGF-β were chosen to investigate the inherent variability of this wound model, although the data colleted for IL-1 and VEGF are included for completion.

The inherent variability of this system was tested by applying a repeated measures analysis to the wound edge and bed biopsies separately. This was to determine the within biopsy variation (i.e between segments from an individual biopsy or intra-biopsy variation) or the between biopsy variation (inter-biopsy) over the eight hour culture period. In addition, an analysis of variance model was applied to each cytokine or MMP at each time point. This was to quantify the variability between biopsies, or segments within a biopsy both in terms of the actual variability and as a percentage of the total variation. Terms entered into the model corresponded to biopsy and segment within a biopsy.

In addition, as data was available for both, a comparison was done of the levels of analytes present in wound edge and bed tissue. Comparisons were done on the data collected for wound tissue at the 2 and 4 hour time points during the 8 hour culture period. The 2 and 4 hour time points were considered the best approximation to the level of analytes present in the wound tissue prior to removal from the wound. It was

believed that *de novo* production by cells within the biopsy tissue would not make a significant contribution to the overall levels up to 4 hours after removal from the body.

The variation in levels of cytokines found in each biopsy will be presented in the following section. Variation between each individual biopsy will be referred to as inter-biopsy variation and variation between tissue segments within a biopsy will be referred to as intra-biopsy variation. A list of biopsies and the wound from which they were taken is recorded in the appendix I. Reference to these tables will allow comparison of different analyte levels measured in the same biopsy tissue.

4.4.1.0: Cytokine/MMP levels present in explant tissue as markers of its inherent variability

Wound edge and wound bed biopsies were taken from chronic venous leg ulcers (VLUs). One control segment was taken from each biopsy and frozen for histology. Wound edge tissue was further divided into 2 segments but wound bed tissue was further divided into 3 segments. These additional tissue segments were placed in culture for 8hrs. Culture supernatants removed from the wound edge and bed tissue segments were removed every 2 hours and assayed by ELISA for the levels of IL-1, IL-8, TGF-β and VEGF. In addition, levels of MMP-2 and -9 present in the culture supernatants were quantified by Zymography. The following sections describe the levels of each of these analytes detected in the culture supernatants at 2 hour intervals during the 8 hour culture period and are recorded as pg/ml/mg of tissue present.

4.4.1.1 Interleukin-1 (IL-1)

IL-1 levels in 8 tissue segments from 4 wound edge biopsies

The spread of data obtained from the total of 8 segments taken from 4 wound edge biopsies is graphically displayed in figure 4.18.1. Table 4.1 summarises the descriptive statistics used to outline the spread of the data presented in figure 4.18.1.

The large values for the range suggest a large variation in the overall levels of IL-1 measured in wound edge tissue segments. This data is also widely spread around the mean as demonstrated by large standard deviation (SD) values and wide confidence intervals (CI) at the 95% level. The mean IL-1 values seen in table 4.1 appear to rise in the last 4 hours of culture. However the mean is susceptible to the influence of extreme values and the apparent increase is probably due to the simultaneous increase in the range seen in table 4.1. The source of the extreme values was found to be biopsy 3 in which tissue segment 2 is seen to have values approaching 3 SDs from the mean at 6 and 8 hours. At more than 3 SDs from the mean it would statistically be considered as being outlying data. Biopsy 3 is seen more clearly in figure 4.18.2 (c). The effect of these outlying values is also seen in the increase in SD value and widening of the 95% CI in the last 4 hours of culture. The median is not affected by extreme values and in this case can be seen to change very little during the 8 hour culture period indicating that IL-1 levels are not affected by the time in culture. The overall spread of the data seen in figure 4.1.11 suggests a substantial inter- and intra-biopsy variation to be present. This can be observed more clearly in figures 4.18.2 and 4.18.3

Figure 4.18.2 a-d is a graphical representation of the levels of IL-1 produced by the 2 segments of edge tissue in each of the 4 individual wound edge biopsies shown in figure 4.18.1. These graphs illustrate the presence of a large intra-biopsy variation in the levels of IL-1. This is particularly clear in biopsies 1 and 3 figure 4.18.2(a)&(c). Biopsy 3 has already been identified as a source of variability within this dataset due to the extreme values present in tissue segment 2 at 6 and 8 hours.

Table 4.1: *Descriptive statistic for data on 8 tissue segments from 4 wound edge biopsies. Data is recorded in units of pg/ml/mg of tissue*

Wound Edge	2hrs	4hrs	6hrs	8hrs
Mean	5.15	5.85	10.57	10.31
Median	2.83	5.25	6.85	6.83
S.D.	5.95	6.34	12.49	12.16
Range	16.03(0.12-16.16)	19.26(0.18-19.44)	36.33(0.15-36.48)	36.33(0.15-36.48)
CI(95%) ±	4.97	5.30	10.45	10.17

Figure 4.18.1*: IL-1 levels in 8 segments from 4 wound edge biopsies*

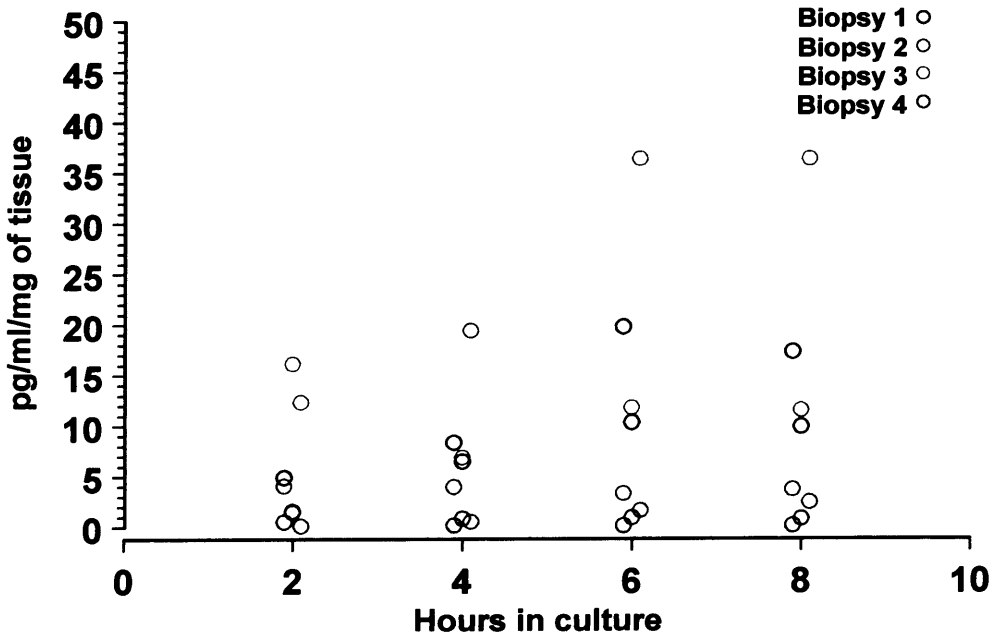

Figure 4.18.2: *IL-1 levels in tissue segments from 4 individual wound edge biopsies. Each biopsy corresponds to those previously depicted in figure 4.18.1. Data is recorded in units of pg/ml/mg of tissue.*

(a) Biopsy 1

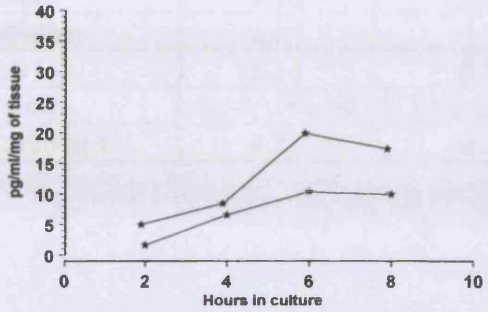

(b) Biopsy 2

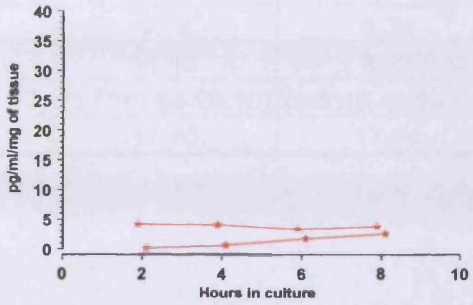

(c) Biopsy 3

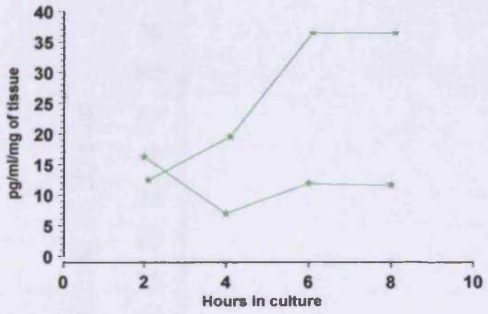

(d) Biopsy 4

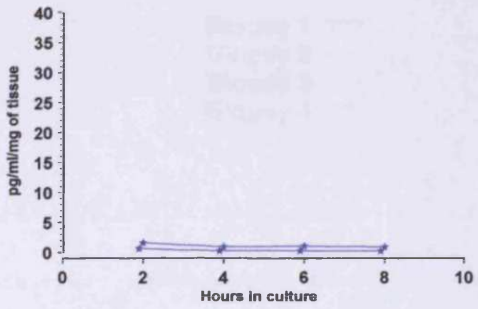

Figure 4.18.3 represents the mean level of IL-1 measured from both segments of wound edge tissue in each individual wound edge biopsy during the 8 hour culture period. Large values for the range recorded in table 4.2 demonstrate the presence of a substantial inter-biopsy variation in the level of IL-1. Again this data is spread widely around the mean at 2, 4, 6 and 8 hours characterised by large SD values and wide CI recorded in table 4.2. This inter-biopsy variation is probably in part a reflection of the high level of intra-biopsy variation noted above in figures 4.1.11 and 4.1.12. Again the median values recorded in table 2 indicate no affect of time in culture on the IL-1 levels.

Table 4.2: *Descriptive statistic characterising data spread around mean IL-1 levels detected in each wound edge biopsy. Data is recorded in units of pg/ml/mg of tissue.*

Wound Edge	2hrs	4hrs	6hrs	8hrs
Mean	5.15	5.85	10.57	10.31
Median	2.68	4.85	8.79	5.39
SD	6.14	5.70	11.12	8.37
Range	13.27(1-14.26)	12.66(0.51-13.17)	23.61(0.54-24.15)	23.55(0.48-24.02)
CI(95%) ±	9.77	9.07	17.70	17.14

Figure 4.18.3: *IL-1 mean levels in 4 individual wound edge biopsies*

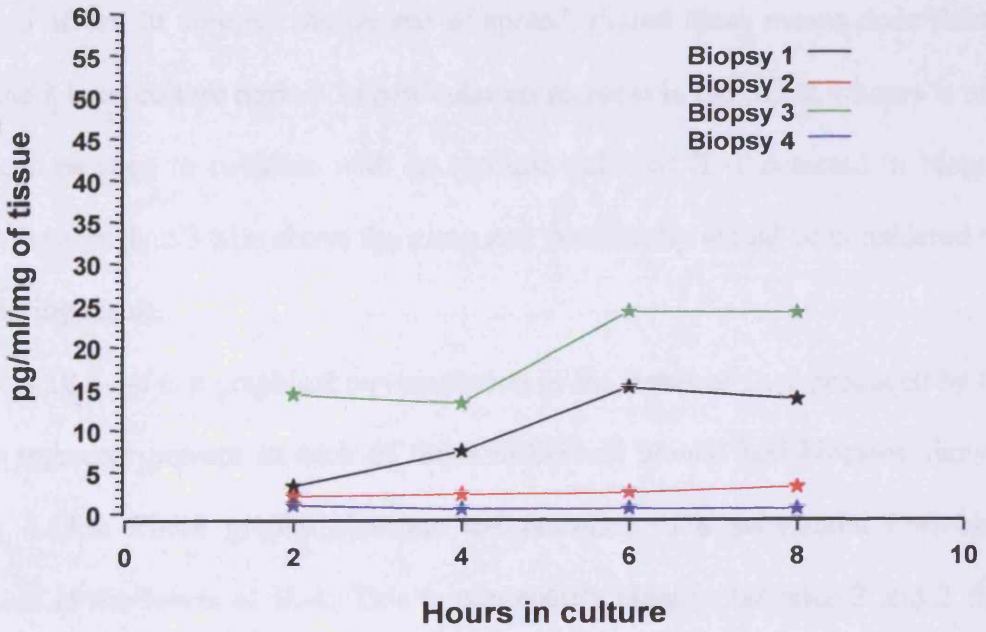

IL-1 levels in 12 tissue segments taken from 4 wound bed biopsies

The spread of data obtained from the total of 12 segments obtained from 4 biopsies is graphically displayed in figure 4.18.4 and table 4.3 summarises the descriptive statistics used to outline the data spread around the mean.

Evidently from the values for the range the data levels of IL-1 in tissue segments from wound bed biopsies is spread widely at each 2 hour time point. Again large standard deviations and wide confidence intervals demonstrate the data to be spread widely around the mean. However, the mean and median values seen in table 4.3 do not fluctuate dramatically over the 8 hour culture period suggesting time in culture to have no affect. In contrast the degree of spread around these means does fluctuate over the 8 hour culture period. In particular an increase in the SD at 4 hours is noted. This can be seen to coincide with an extreme value of IL-1 detected in biopsy 2, which is more than 3 SDs above the mean and statistically would be considered to be an outlying result.

Figure 4.18.5 a-d is a graphical representation of the levels of IL-1 produced by the 3 tissue segments present in each of the 4 individual wound bed biopsies shown in figure 4.18.4. These graphs illustrate the presence of a substantial intra-biopsy variation in the levels of IL-1. This is particularly clear in biopsies 2 and 3 figure 4.18.5 (b) & (c). Figure 4.18.5 (b) highlights the possible outlying level of Il-1β measured at 4hrs in one of the segment taken from biopsy 2. It shows a large departure (> 3 SDs from the mean) from the rest of the measurements observed at the other time points for that particular wound bed segment.

Table 4.3: *Descriptive statistics characterising data spread around mean IL-1 levels in 12 segments from 4 wound bed biopsies. . Data is recorded in units of pg/ml/mg of tissue.*

Wound Bed	2hrs	4hrs	6hrs	8hrs
Mean	14.93	18.60	14.14	17.71
Median	7.83	4.32	4.26	7.47
S.D.	16.97	35.30	18.41	21.47
Range	49.87(0.46-50.32)	125.61(0.91-126.52)	50.19(0.33-50.52)	56.83(0.56-57.39)
CI(95.0%) ±	10.78	22.43	11.70	13.64

Figure 4.18.4: *Scatter graph showing IL-1 levels in segments from* n = 4 bed *biopsies*

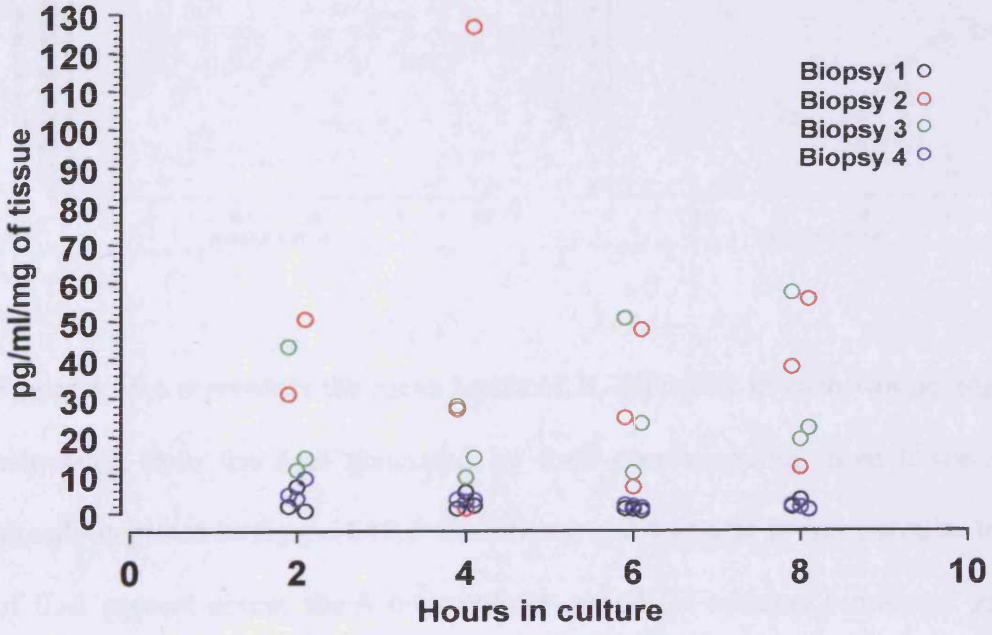

Figure 4.18.5: Line graphs showing IL-1 levels in 4 individual wound bed biopsies.

(a) Biopsy 1

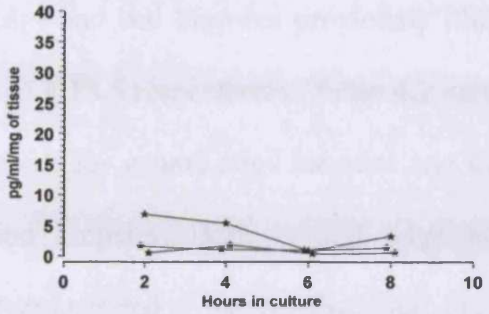

(b) Biopsy 2

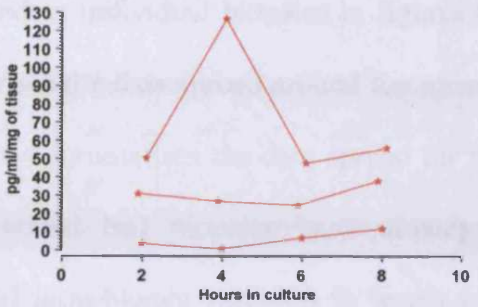

(c) Biopsy 3

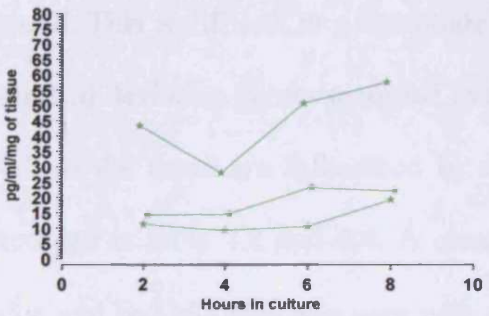

(d) Biopsy 4

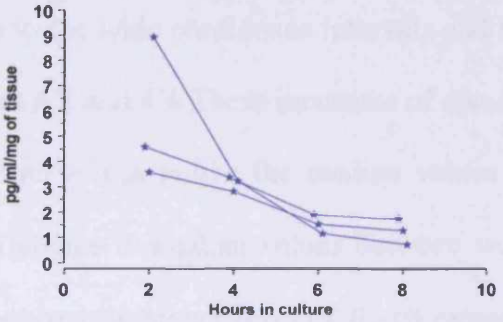

Figure 4.18.6 represents the mean levels of IL-1 present in each wound edge biopsy calculated from the data generated by their corresponding three tissue segments already depicted in figure 4.18.5. Biopsies 1 and 4 appear to have similar low levels of IL-1 present across the 8 hour culture period. In contrast biopsies 2 and 3 had around three times as much IL-1 present, with similar levels found in both biopsies except at 4 hours. However this is related to the outlying result referred to earlier in figure 4. Overall there was a wide variation in the levels of IL-1 present in each biopsy. Large values for the range along with large SD values and wide CIs recorded in table 4.4, indicated a wide spread around the overall mean bed biopsy level, which

is depicted in figure 4.18.7 below. A large inter and intra-biopsy variation in IL-1 levels was therefore present in both wound edge and wound bed tissue.

Figure 4.18.7 (a) represents the overall mean level of IL-1 present in all of the wound edge and bed biopsies previously illustrated as individual biopsies in figures 4.18.3 and 4.18.6 respectively. Table 4.2 summarises the data spread around the mean IL-1 levels for wound edge biopsies and table 4.4 summarises the data spread for wound bed biopsies. Both wound edge and wound bed biopsies have already been demonstrated to have substantial inter and intra-biopsy variation in levels of IL-1 present within them. From the mean levels depicted in figure 4.18.7 (a) there appears to be an overall higher level of IL-1 present in wound bed tissue over the 8hr culture period. This is difficult to substantiate due to the wide confidence intervals and large standard deviation values recorded in tables 4.2 and 4.4 These measures of spread as well as the mean are influenced by extreme values unlike the median values also recorded in table 4.2 and 4.4. A clear difference in median values between wound edge and bed biopsies was seen with a consistently higher level of IL-1β present in wound bed tissue. This is further emphasised in figure 4.18.7 (b) where the mean and median values present in wound edge or bed tissue at all the 2 hourly sampling time points is plotted. The mean level of IL-1 produced by both wound edge and bed tissue is also displayed in figure 4.18.7 (a) as an indication of the overall levels of IL-1 likely to be measured in wound tissue by this explant tissue method. The combined data for wound edge and bed had values for the range of 27.27(1-28.27), 50.95(0.51-51.46), 27.51(0.54-28.05) and 36.63(0.48-35.10) pg/ml/mg of tissue at 2, 4, 6 and 8 hours respectively.

Table 4.4: *Descriptive statistics characterising data spread around mean IL-1β levels present in 4 individual wound bed biopsies. . Data is recorded in units of pg/ml/mg of tissue.*

Wound Bed	2hrs	4hrs	6hrs	8hrs
Mean	14.93	18.60	14.14	17.71
Median	14.24	10.13	13.91	17.26
SD	12.51	22.91	15.08	18.79
Range	25.31 (2.96-28.27)	48.76 (2.70-51.46)	27.36 (0.69-28.05)	33.89 (1.22-35.10)
95% CI ±	19.90	36.45	24.00	29.91

***Figure 4.18.6**: IL-1 mean levels in 4 individual wound bed biopsies*

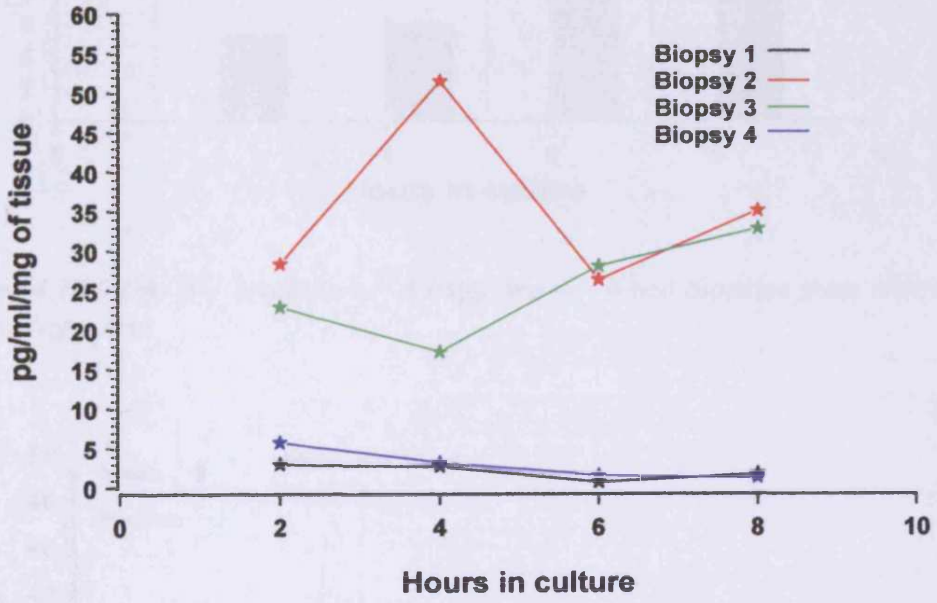

Figure 4.18.7 (a): *IL-1 levels in* n = 4 edge *and* n = 4 bed *biopsies from chronic venous leg ulcers*

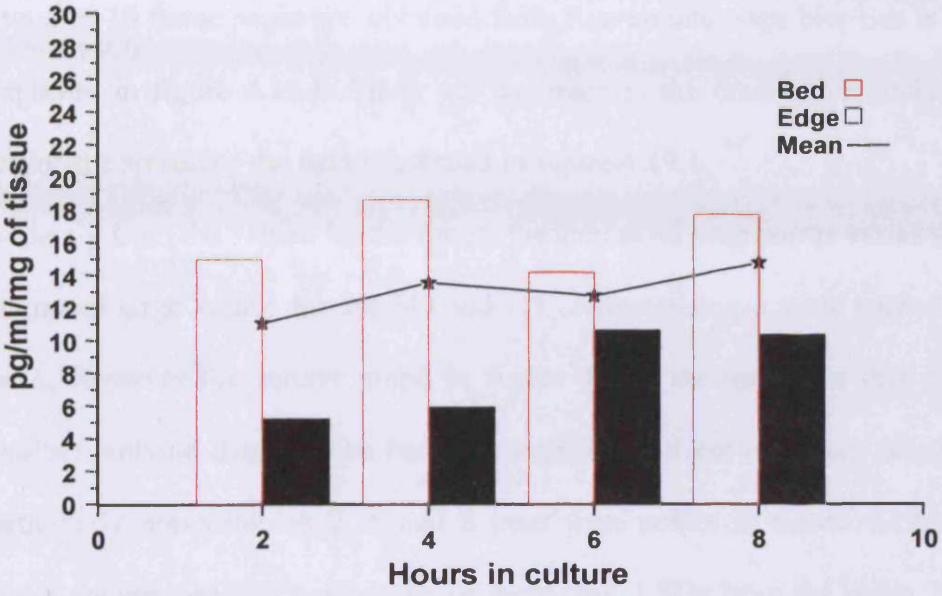

Figure 4.18.7 (b): *Il-1 levels in* n = 4 edge *and* n = 4 bed *biopsies from chronic venous leg ulcers*

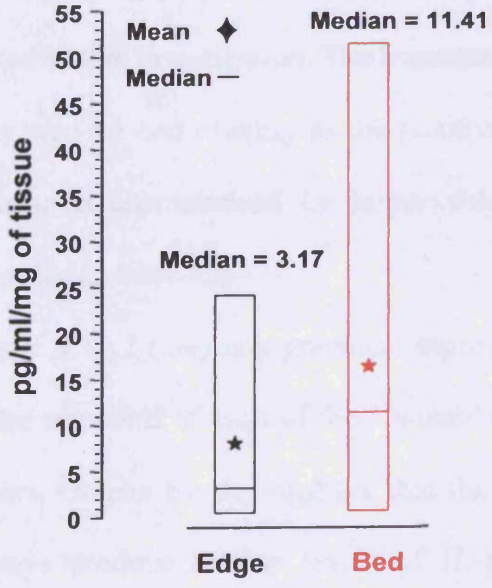

4.4.1.2 Interleukin-8 (IL-8)

Analysis of IL-8 levels in n = 5 edge biopsies cultured for 8 hours

The spread of data obtained from analysis of IL-8 levels in culture supernatants from a total of 10 tissue segments obtained from five wound edge biopsies is graphically displayed in figure 4.19.1. Table 4.5 summarises the descriptive statistics used to outline the spread of the data illustrated in figure 4.19.1.

Evidently from the values for the range, the data at all time points varies widely, with additional large values for the SD and C.I characterising a wide spread around the mean. However the scatter graph in figure 4.19.1 demonstrates that a number of possible outlying data may be having a significant effect on these values. These are particularly noticeable at 2, 6 and 8 hour time points in figure 4.19.1 where the values are approaching a departure of more than 3 SDs from the mean. Notably this effect is not seen at 4 hours where much smaller values are seen for the SD and CI. It should be noted that the CIs at 2, 6 and 8 hours included a possible mean IL-8 value of 0 pg/ml/mg of tissue although IL-8 was found to be present in all the wound tissue tested in this investigation. The presence of possible outlying data at 2, 6 and 8 hours may also be contributing to the positive skewness of the data spread at these time points, as characterised by larger values of the mean compared to the median recorded in table 4.5.

Figure 4.19.2 (a-e) is a graphical representation of the levels of IL-8 present in the tissue segments of each of the 5 wound edge biopsies taken from chronic venous leg ulcers. Graphs a-e demonstrate that the individual segments within a biopsy do not always produce similar levels of IL-8 over the 8 hour culture period. This is particularly evident in graphs (a) and (b) where large intra-biopsy variation is evident. The possible outlying data described in figure 4.19.2 correspond to an IL-8

level of 83763 pg/ml/mg of tissue detected in one of the edge segments from biopsy one at 6 hours along with a level of 39254 pg/ml/mg of tissue detected in the other segment at 8 hours (see figure 4.18.2 (a)). In addition an IL-8 level of 22187 pg/ml/mg of tissue detected in biopsy 3 at 2 hours could represent an outlying piece of data.

Table 4.5: *Descriptive statistics characterising the data spread around the mean IL-8 levels present in 10 tissue segments from 5 wound bed biopsies. Data is recorded in units of pg/ml/mg of tissue.*

Wound Edge	2HRS	4HRS	6HRS	8HRS
Mean	3038.59	1140.81	11579.50	6236.22
Median	951.52	1247.82	1191.33	1547.16
SD	6768.69	559.17	26004.43	11797.93
Range	22008 (179-22187)	1640 (365-2005)	83403 (361-83764)	38706 (548-39254)
CI (95%) ±	4842.04	400.01	18602.46	8439.74

Figure 4.19.1: *Scatter graph displaying IL8 levels present in 10 tissue segments taken from 5 wound edge biopsies*

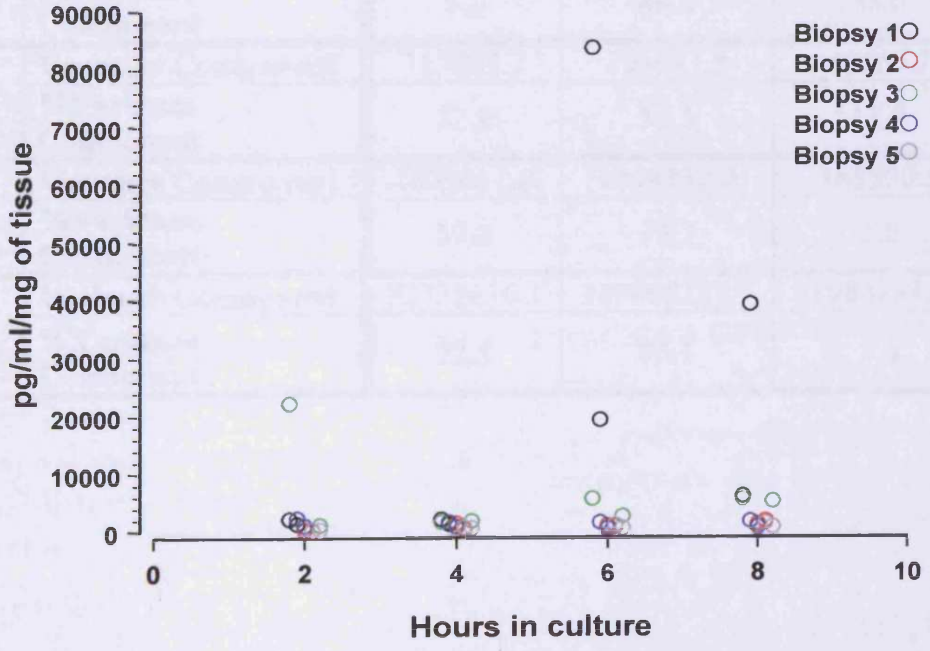

Analysis of variance was applied to the data illustrated in figure 4.60. A statistically significant difference ($p = 0.023$) in IL-8 levels was detected between each segment and there was an observed interaction between segments and time in certain biopsies. The extent of the variability between segments generally increased over time from 40% at 2 hours to 76% at 8 hours (table 4.6). This larger variability at 8 hours is particularly apparent in biopsy 1 figure 4.60 (a). Despite the observed interaction between segments and time, a consistency was observed in IL-8 levels between segments within certain biopsies, e.g. 2, 4 and 5 figure 4.60 (b, d and e). Significant interaction between biopsies and time was also seen ($p = 0.0002$), implying that the IL-8 levels detected between biopsies varied over the 8 hours which is evident in the mean biopsy profiles plotted in figure 4.61.

Table 4.6: *Analysis of variance on IL-8 levels detected in 5 wound edge biopsies.*

Wound Edge Source		**Biopsy**	**Segment**	**Replicates**
2hrs	**Variance Component**	832881.0	25982691.1	38184373.4
	%Variance Component	1.2	40.0	58.8
4hrs	**Variance Component**	113985.2	191021.8	40665.7
	%Variance Component	32.9	55.3	11.8
6hrs	**Variance Component**	1891611.6	1244352.9	165550.3
	%Variance Component	57.3	37.7	5.0
8hrs	**Variance Component**	32321136.2	109468235.7	1986233.4
	%Variance Component	22.5	76.1	1.4

Figure 4.19.2: *Line graphs depicting IL-8 levels detected in each of the tissue segments from the 5 individual wound edge biopsies*

(a) Biopsy 1

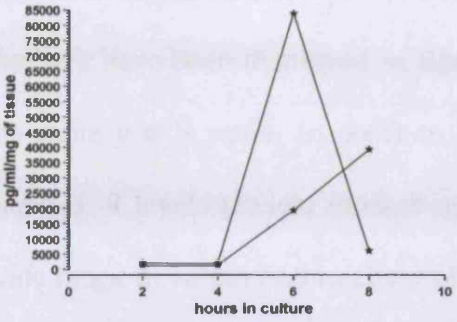

(b) Biopsy 2

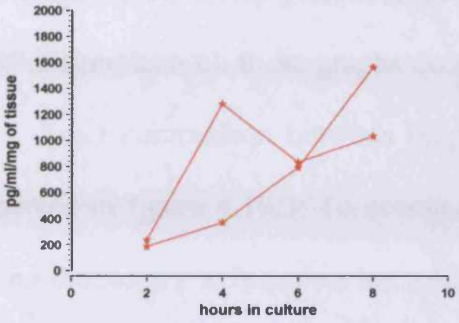

(c) Biopsy 3

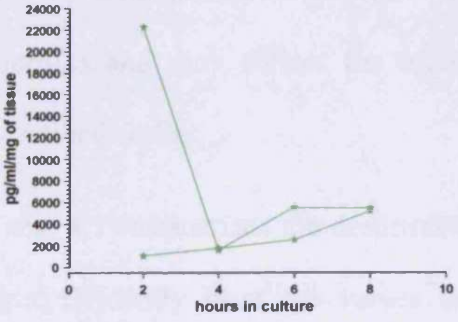

(d) Biopsy 4

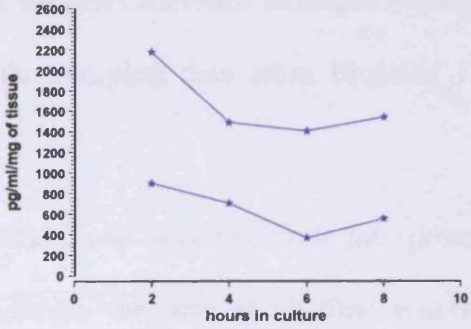

(e) Biopsy 5

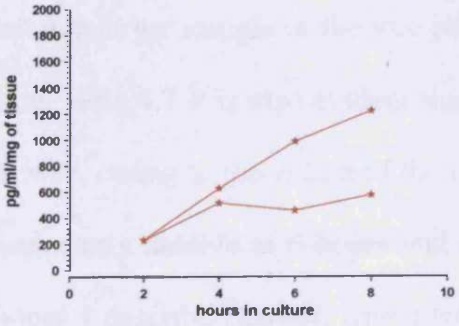

IL-8 mean levels in each individual edge biopsy

Figure 4.19.3 is a graphical representations of mean IL-8 levels present in each of the 5 wound edge biopsies. This was calculated from the levels present in the 2 tissue segments originally taken from them. Although actual levels present in each tissue segment have been displayed in figure 4.19.2 (graphs a-e), these graphs do not have the same y axis scale. In order to make a direct comparison between biopsies the mean IL-8 levels present in each are displayed in figure 4.19.3. To account for the wide range in values and to allow plotting on the same y axis scale a $\log_{10}$ of the data was performed. For example biopsy 1 in figure 4.19.3 shows an approximate tenfold difference in IL-8 production at 6 hours and an approximate fourfold difference in IL-8 levels at 8 hours. However this is the largest difference recorded between edge biopsies and may reflect the effect of the outlying data from biopsies 1 and 3 described earlier.

Table 4.7 summarises the descriptive statistics used to demonstrate the spread of the data. Evidently from the values for the range, the data at all time points varies widely, with additional large values for the SD and C.I characterising a wide spread around the mean. The confidence intervals at 2, 6 and 8 hours include 0 indicating that in a larger sample or the true population, lack of IL-8 production is a possibility. From table 4.7 it is also evident that the data spread at each time point is positively skewed, owing to the values of the means being much larger than the median. This is particularly notable at 6 hours and may reflect the presence of the outlying data in biopsy 1 described earlier, which would affect the mean much more than the median value.

Table 4.7: Descriptive statistics characterising the data spread around the mean IL-8 levels present in 5 wound edge biopsies. . Data is recorded in units of pg/ml/mg of tissue.

Wound Edge	2HRS	4HRS	6HRS	8HRS
Mean	3039	1141	11580	6236
Median	1531	1090	880	1295
SD	4834	469	22355	9357
Range	11395 (205-11400)	1046 (567-1614)	50773 (719-51492)	21755 (895-22649)
CI	6003	582	27757	11618

Figure 4.19.3: Line graph depicting mean IL-8 levels present in 5 wound edge biopsies. Log_{10} transformation of the data was applied to account for the wide range in values

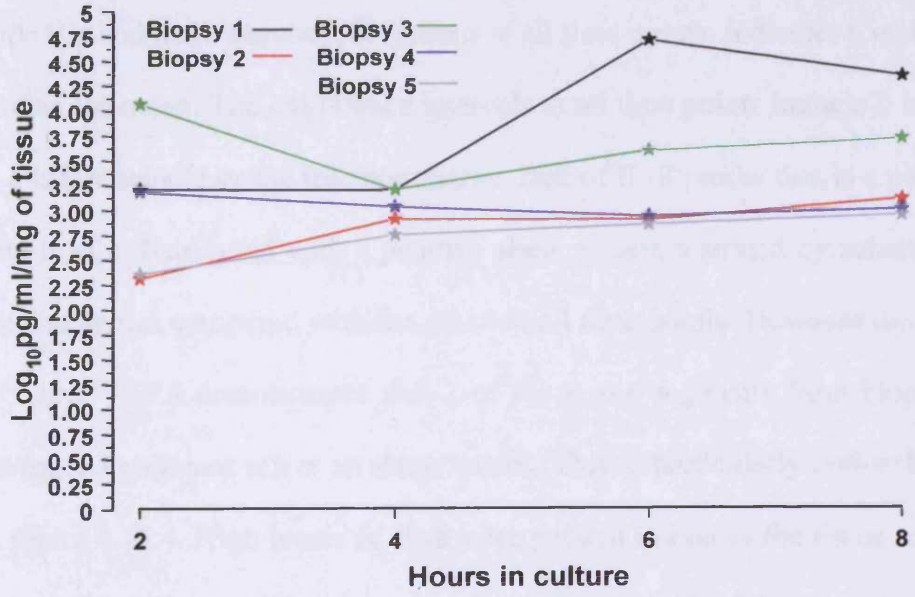

<u>IL-8 levels in 24 tissue segments from 8 wound bed biopsies</u>

The data spread for the IL-8 levels detected in a total of 24 tissue segments obtained from 8 individual wound bed biopsies is graphically displayed in figure 4.19.4. Table 4.8 summarises the descriptive statistics used to outline the spread of the data graphically presented in figure 4.19.4.

Table 4.8: *Descriptive statistic characterising the data spread around the mean IL-8 levels present in 24 tissue segments taken from 8 wound bed biopsies. Data is recorded in units of pg/ml/mg of tissue.*

Wound Bed	2hrs	4hrs	6hrs	8hrs
Mean	3306.87	4571.64	4116.44	5493.28
Median	1331.77	1554.92	1605.29	1461.92
SD	5273.72	8382.31	7382.95	12208.22
Range	24018 (148-24166)	37105 (192-37297)	35450 (0-35450)	59687 (366-60053)
CI(95%)	2226.89	3539.54	3117.54	5155.07

Large values for the range, indicate a high degree of variability in the levels of IL-8 present in wound bed tissue. The variation has elements of both inter and intra-biopsy variation and is more clearly depicted in figures 4.19.5 and 4.19.6 below. The wide CIs and large standard deviations at all time points, indicates a wide data spread around the mean. The confidence intervals at all time points include 0 indicating that in a larger sample or the true population, lack of IL-8 production is a possibility. The data is also distributed with a positive skew as demonstrated by substantially lower median values compared with the mean at all time points. However the scatter graph in figure 4.19.4 demonstrates that 2 of the tissue segments from biopsy 2 may be having a significant effect on these values. This is particularly noticeable at 8 hours in figure 4.19.4. High levels of IL-8 were present in one of the tissue segments from biopsy 2, which overall contained higher levels over the 8 hour culture period. This is more clearly demonstrated in figure 4.19.5 (b). The levels in this tissue segment could statistically be considered as outlying data as they were consistently more than 3 SDs from the mean throughout the 8 hour culture period.

Figure 4.19.4: Scatter graph depicting the data spread for IL-8 levels detected in 24 tissue segments taken from 8 wound bed biopsies

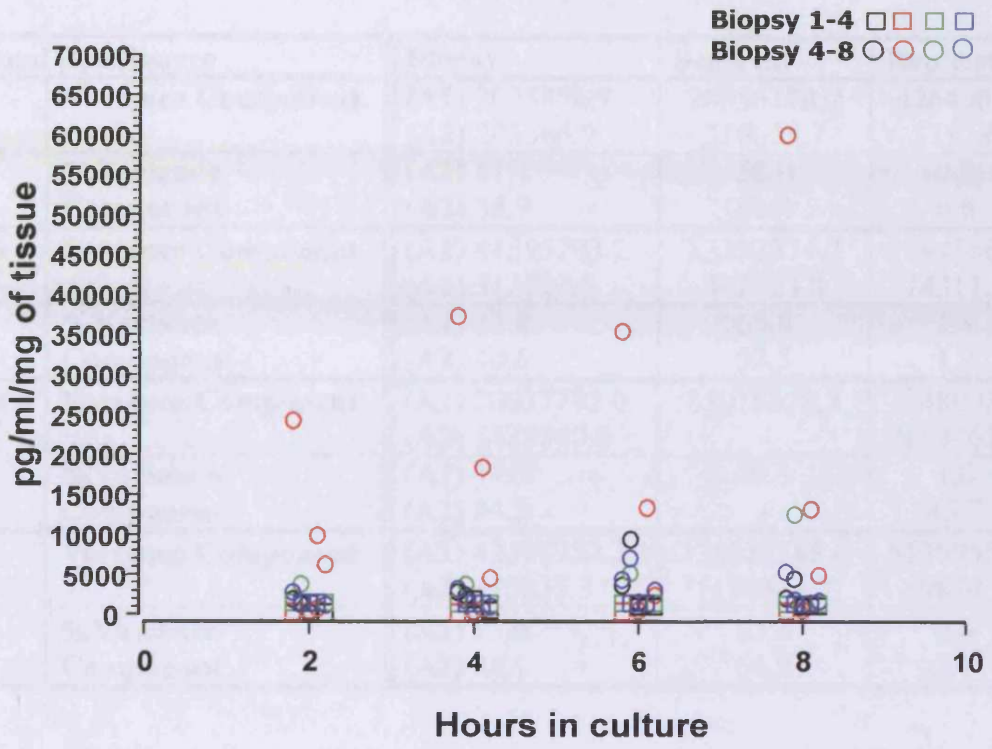

Figure 4.19.5 (a-h) is a graphical representation of the mean levels of IL-8 present in the 3 tissue segments taken from each of the 8 individual wound bed biopsies previously depicted in figure 4.19.4. In a number of the biopsies the segments within an individual biopsy differ in their production of IL-8 over the 8 hour culture period. This is an illustration of the wide data spread around the mean IL-8 levels detected in each wound bed biopsy previously summarised statistically in table 4.7. The y axis have a different scale for each biopsy to highlight the magnitude of the intra-biopsy variation in IL-8 levels. This makes comparing the IL-8 levels in one biopsy with another more difficult and therefore figure 4.19.6 illustrates this more clearly.

Table 4.9: Analysis of variance of the IL-8 levels present in the 8 wound bed biopsies. A1 = analysis of biopsies 1-4. A2 = analysis of biopsies 5-8

Wound Bed Source		Biopsy	Segment	Replicates
2hrs	Variance Component	(A1) 2023876.7 (A2) 203566.9	28555178.7 316035.7	426490.2 3217.6
	%Variance Component	(A1) 41.1 (A2) 38.9	58.0 60.4	0.9 0.6
4hrs	Variance Component	(A1) 41595793.2 (A2) 312522.7	83392374.7 442423.8	1794556.8 14311.7
	%Variance Component	(A1) 32.8 (A2) 40.6	65.8 57.5	1.4 1.9
6hrs	Variance Component	(A1) 20937792.0 (A2) 3438840.0	85015378.7 -	1048005.4 2893462.6
	%Variance Component	(A1) 19.6 (A2) 54.3	79.5 -	1.0 45.7
8hrs	Variance Component	(A1) 42393253.7 (A2) 615835.3	235627185.6 1170343.7	5536955.8 19879.5
	%Variance Component	(A1) 15.0 (A2) 34.1	83.1 64.8	2.0 1.1

Figure 4.19.5: Line graphs depicting the levels of IL-8 detected in the 3 tissue segments taken from each of the 8 wound bed biopsies.

(a) biopsy 1

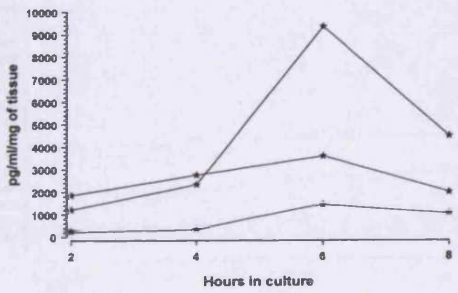

(b) biopsy 2

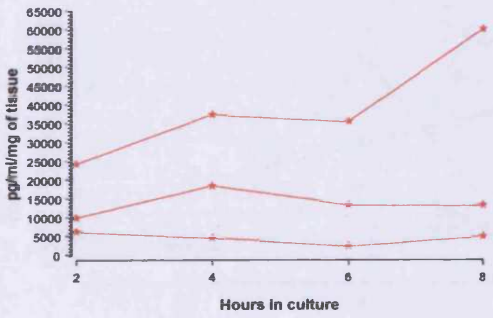

(c) Biopsy 3

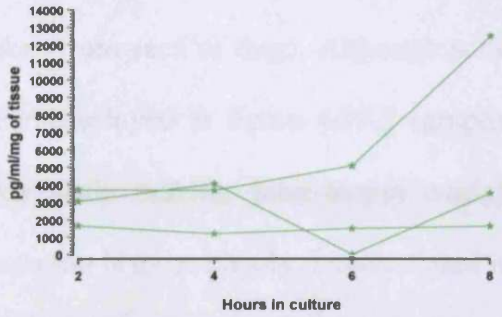

(d) Biopsy 4

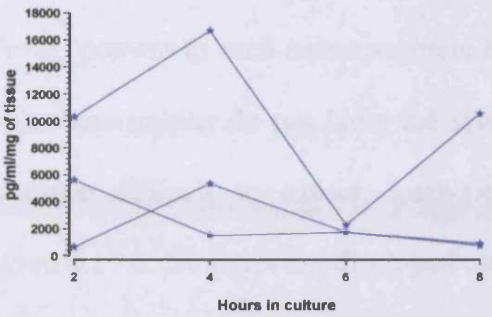

(e) Biopsy 5

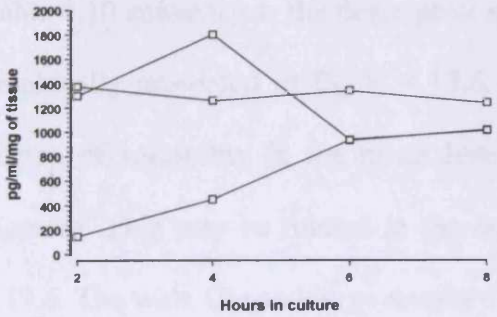

(f) Biopsy 6

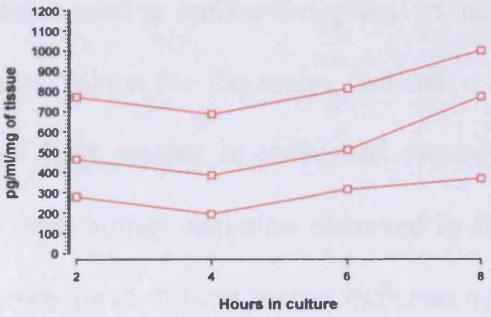

(g) Biopsy 7

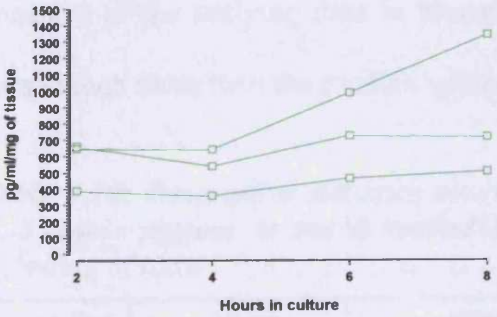

(h) Biopsy 8

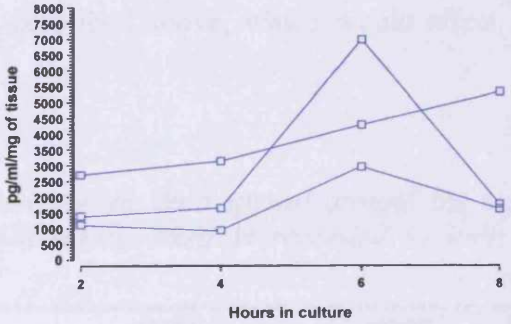

Figure 4.19.6 is a graphical representations of mean IL-8 levels present in each of the 8 wound bed biopsies calculated from the levels detected in the 3 tissue segments taken from each of them. Although actual levels present in each tissue segment have been displayed in figure 4.19.5 (graphs a-h), these graphs do not have the same y axis scale making inter-biopsy variation more difficult to assess. Inter-biopsy variation is more clearly demonstrated in figure 4.19.6. Biopsies are displayed on the same y axis after performing a $\log_{10}$ transformation of the data to account for the wide range. For example biopsy 2 had an average IL-8 level that was at least 4 times higher than the other bed biopsies.

Table 4.10 summarises the descriptive statistics used to outline the spread of the data graphically presented in figure 4.19.6. Large values for the range, indicate a high degree of variability in the mean levels of IL-8 present in individual wound bed biopsies. This may be related to the large inter-biopsy variation observed in figure 4.19.6. The wide CIs and large standard deviations at all time points, indicates a wide data spread around the mean. From table 4.10 it is evident that the data spread at each time point is positively skewed owing to the values of the means being much larger than the median. This is particularly notable at 8 hours and may reflect the presence of the outlying data in biopsy 2 described above, which would affect the mean much more than the median value.

Table 4.10: *Descriptive statistics characterising the data spread around the mean IL-8 levels present in the 8 wound bed biopsies. Data is recorded in units of pg/ml/mg of tissue.*

Wound Bed	2HRS	4HRS	6HRS	8HRS
Mean	3307	4572	4116	5493
Median	1390	1830	2044	2681
SD	4402	6684	5468	8483
Range	12911(501-13412)	19620(419-20038)	16470(543-17012)	25318(713-26031)
CI (95%) ±	3680	5588	4571	7092

Figure 4.19.6: Line graphs depicting the mean IL-8 levels present in each of the 8 individual wound bed biopsies. Due to the wide range of the data a Log_{10} was performed on the data

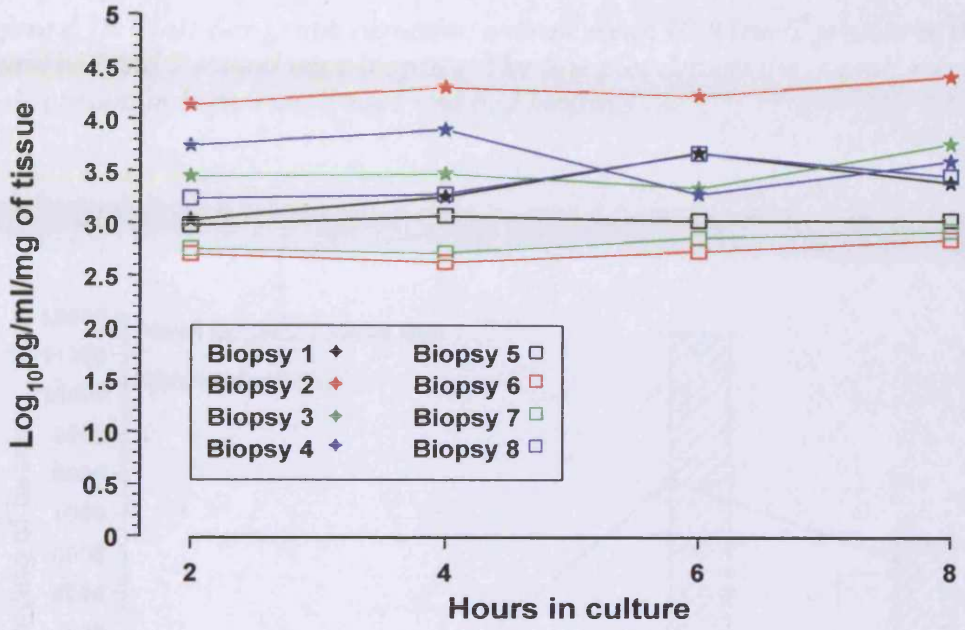

Analysis of variance was applied to the wound bed data in two stages where analysis 1(A1) was carried out on biopsies 1-4 and analysis two (A2) on biopsies 5-8. A highly significant difference between segments within biopsies overall was found (A1: p=0.0001, A2: p=0.011), which is apparent in figure 4.19.5. There was also an observed interaction between segments and time. The variability between segments and the corresponding percentage variation increases over time (table 4.9). This divergence in the difference in IL-8 levels present in different segments is depicted in figure 4.19.5. Significant interaction was also seen between biopsies and time, implying that the extent of difference in IL-8 expression between biopsies varies over time (A1: p = 0.003). This is apparent in the mean biopsy profiles graphically represented in figure 4.19.7 and statistically summarised in table 4.10. There were also differences between biopsies overall whereby biopsy 2 is observed to have a

markedly higher IL-8 level than other biopsies. Low levels of variation between replicate samples for each segment were recorded in table 4.9, indicating that duplicate samples were sufficient to obtain an estimate of measurement error

Figure 4.19.7 (a): *Bar graph depicting overall mean IL-8 levels present in the 8 wound bed and 5 wound edge biopsies. The line plot depicts the overall mean IL-8 levels present in both wound edge and bed biopsies.*

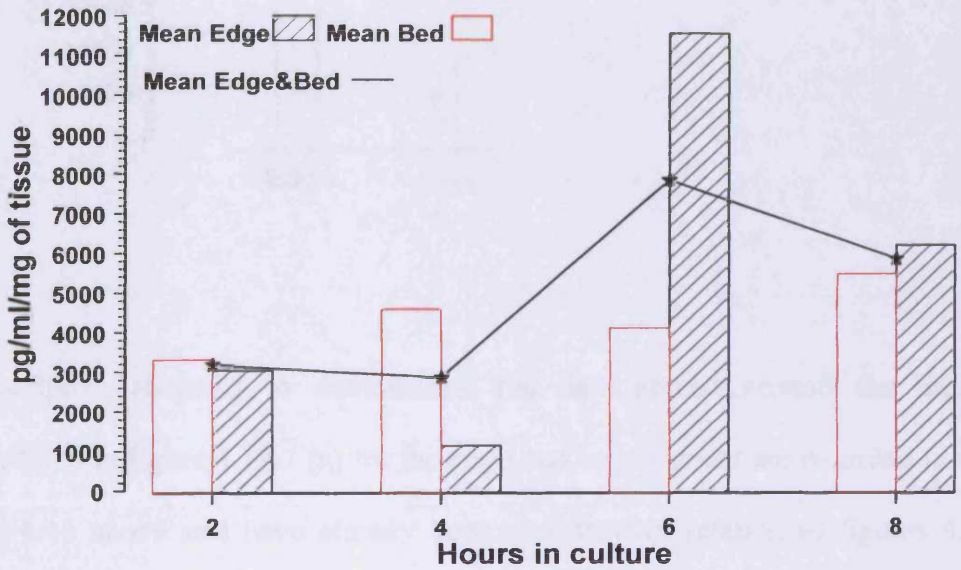

Figure 4.19.7 (a) illustrates the mean levels of IL-8 present in all the bed or edge biopsies over the 8 hour culture period. There doesn't appear to be an obvious difference between the mean IL-8 levels present in wound bed and edge biopsies. However the mean is susceptible to be affected by extreme or outlying values, which in this case have already been described to be present in both types of wound tissue. The median values recorded in tables 4.10 and 4.7 are less affected by outliers and in this case suggest a higher level of IL-8 to be present in wound bed tissue.

Figure 4.19.7 (b): Box plot allowing a comparison of IL-8 levels present in wound edge and bed biopsies at all time points depicted above in figure 14 (a)

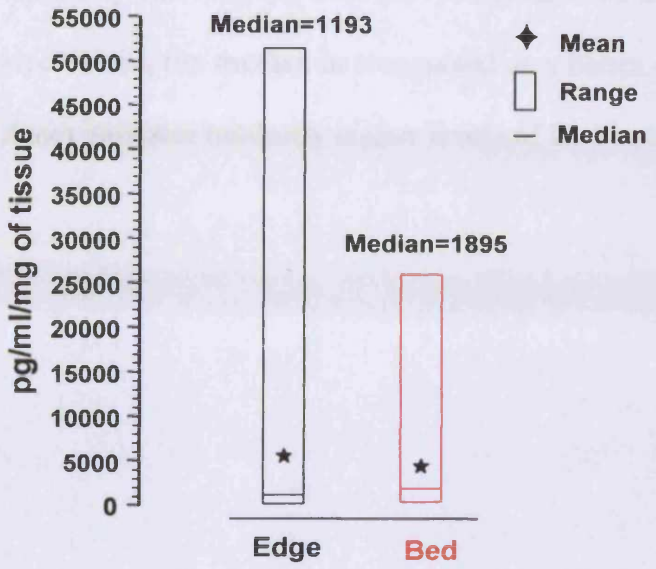

Descriptive statistics to demonstrate the data spread around the mean levels displayed in figure 4.19.7 (a) for the edge and bed biopsies are recorded in tables 4.7 and 4.10 above and have already been described in relation to figures 4.19.3 and 4.19.6. The mean level of IL-8 produced by both edge and bed biopsies is also displayed in figure 4.19.6 (a) as an indication of the approximated levels of IL-8 that is expected to be detected in this culture/assay system. This mean level had a range of 13207.72 (204.62-13412.34), 19620.07 (418.86-20038.92), 50949.37 (542.59-51491.96) and 25318.45 (712.74-26031.19) at 2, 4, 6 and 8 hours respectively.

A further comparison of wound edge and bed tissue is depicted in figure 4.19.7 (b). Mean IL-8 levels present in the 5 wound edge or 8 wound bed biopsies at all time points during the 8 hour tissue culture have been plotted along with the corresponding value for the median and range. Large values for the range depicted in

figure 4.19.7 (b) along with large SD values (edge SD = 12044.45 bed SD = 6173.29) indicate that the data was not normally distributed which may have been influenced by the outlying data previously described. Since the mean is affected by extreme values, the median is recognised as a better comparison for these 2 datasets and again indicates modestly higher levels of IL-8 to be present in wound bed tissue.

4.4.1.3 METALLOPROTEINASE 2 (MMP-2)

Determination of MMP-2 Levels in 8 Segments from 4 Wound Edge Biopsies

MMP-2 levels were quantified in the culture supernatants of 4 wound edge biopsies cultured for 8 hours. The spread of the data detected in the total of 8 segments obtained from the 4 wound edge biopsies is graphically displayed in figure 4.20.1. In general, low levels of MMP-2 were detected in wound edge tissue and in some tissue segments levels were undetectable. Table 4.11 summarises the descriptive statistics used to outline the spread of the data graphically presented in figure 4.20.1.

Evidently from the values for the range and standard deviation the data at all the time points has a wide spread around the mean. There is also a wide confidence interval at each time point, which at 2, 4, and 8 hours include the mean value of 0. This ties up with the absence of MMP-2 production seen in some of the segments illustrated in figure 4.20.1. Figure 4.20.2 a-d is a graphical representation of the levels of MMP-2 produced by the 2 segments of edge tissue in each of the 4 individual wound edge biopsies previously depicted in figure 4.20.1. These graphs illustrate the substantial intra-biopsy variation in levels of MMP-2 which was present within wound edge biopsies. This is particularly clear in biopsy 2, figure 4.20.2 (b).

The large variation in the production of MMP-2 by tissue segments within the same biopsy is reflected in a marked inter-biopsy variation in mean MMP-2 and is illustrated in figure 4.20.3. Again a wide spread around the mean is seen at all time points with large values for the SD and range, summarised in table 4.12. At 4 hours MMP2 was not detected in biopsy 3 confirming the wide confidence intervals at the 95% level recorded in table 4.12

Analysis of variance was applied to the wound edge data and no statistical difference was found overall between tissue segments within biopsies ($p = 0.723$). The MMP-2

levels were observed to be consistent between segments within biopsies, particularly in biopsies 1, 3 and 4 (figure 4.20.2 (a) (c) and (d)). However, there was an observed interaction between segments and time in biopsy 2 (figure 4.20.2 (b)). Significant interaction between biopsies and time was also present whereby the MMP-2 expression between biopsies generally decreases over the 8 hours ($p = 0.001$), which is depicted by the mean biopsy profiles in figure 4.20.3. Variation between triplicate readings was low after 2 hours and therefore 3 readings were considered sufficient to obtain a good estimate of the measurement error (see table 4.13).

Table 4.11: *Descriptive statistics characterising the data spread around the mean MMP-2 levels present in 8 tissue segments taken from 4 wound edge biopsies. Data is recorded in units of pg/ml/mg of tissue.*

Edge	2hrs	4hrs	6hrs	8hrs
Mean	5.29	2.06	1.60	1.68
Median	1.93	0.17	1.18	0.44
SD	8.68	3.01	1.60	3.21
Range	25.95(0-25.95)	7.44(0-7.44)	4.11(0-4.11)	9.43(0-9.43)
CI (95%) ±	7.26	2.52	1.34	2.68

Figure 4.20.1: Scatter graph depicting the data spread for MMP-2 levels detected in 8 tissue segments from 4 wound edge biopsies

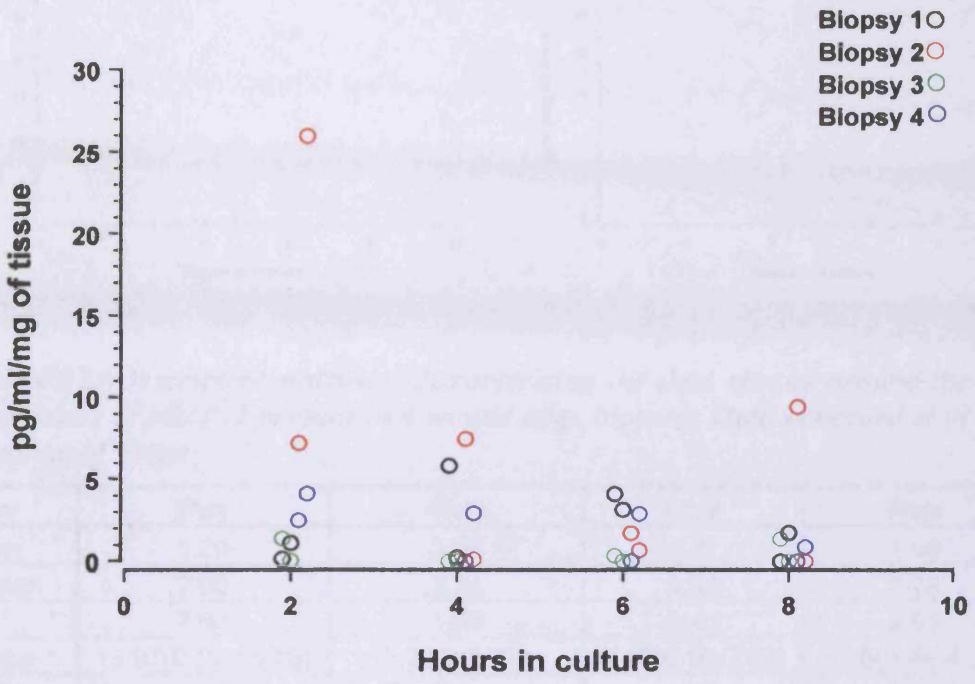

Figure 4.20.2: Line graphs depicting MMP 2 levels detected in tissue segments taken from 4 wound edge biopsies

(a) Biopsy 1

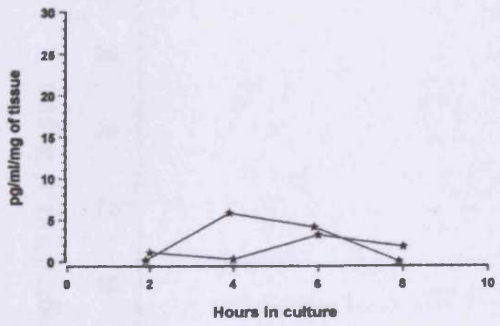

(b) Biopsy 2

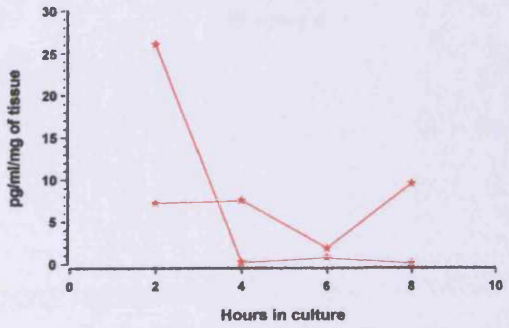

(c) Biopsy 3

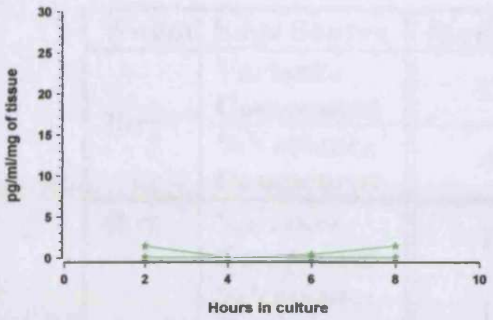

(d) Biopsy 4

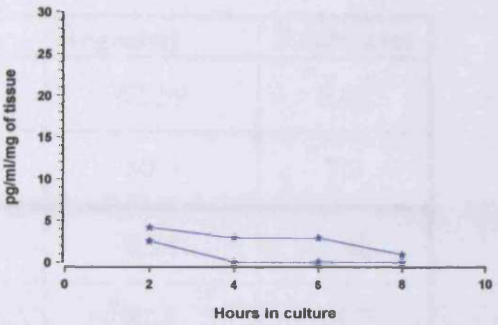

Table 4.12: *Descriptive statistics characterising the data spread around the overall mean levels of MMP-2 present in 4 wound edge biopsies Data is recorded in units of pg/ml/mg of tissue.*

Edge	2hrs	4hrs	6hrs	8hrs
Mean	5.29	2.06	1.6	1.68
Median	2.00	2.24	1.31	0.78
SD	7.62	1.68	1.46	2.03
Range	15.97(0.59-16.56)	3.78(0-3.78)	3.46(0.16-3.62)	4.28(0.44-4.72)
CI(95%)	12.13	2.67	2.32	3.24

Figure 4.20.3: *Line graph depicting mean MMP 2 levels present in 4 individual wound edge biopsies*

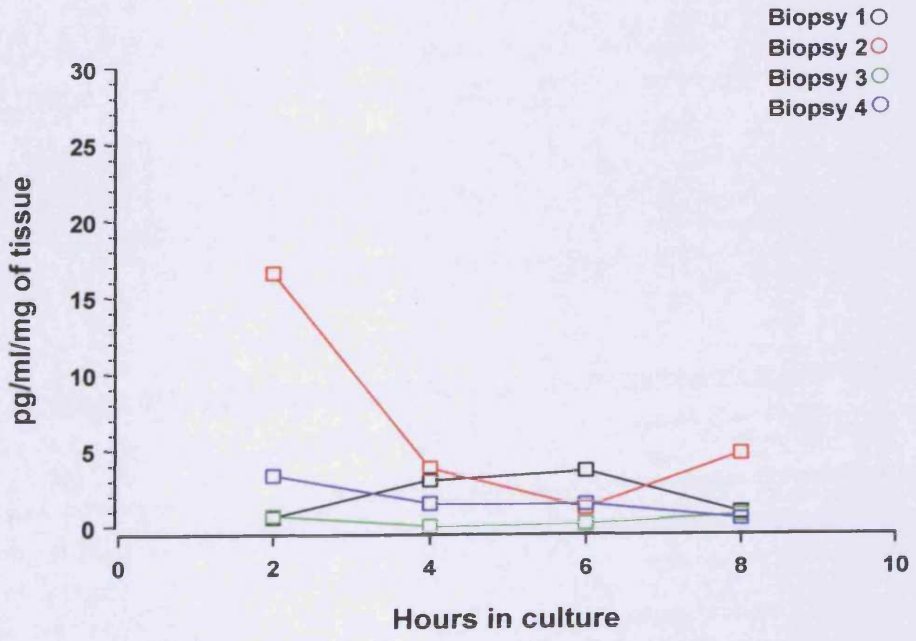

Table 4.13: *Analysis of variance (ANOVA) on MMP-2 levels detected in 4 wound edge biopsies.*

Wound Edge Source		Biopsy	Segment	Replicates
2hrs	**Variance Component**	35.72	42.59	6.42
	%Variance Component	42.2	50.3	7.3
4hrs	**Variance Component**	DM	8.58	1.48
	%Variance Component	DM	85.3	14.7
6hrs	**Variance Component**	1.47	0.90	1.24
	%Variance Component	40.8	24.9	34.3
8hrs	**Variance Component**	DM	9.62	2.04
	%Variance Component	DM	82.5	17.5

MMP-2 Levels in 12 Segments from 4 Wound Bed Biopsies

The spread of the data obtained from the total of 12 segments obtained from 4 wound bed biopsies is graphically displayed in figure 4.20.4. Overall, the levels of MMP-2 appeared to be higher in the wound bed tissue than that previously described in wound edge tissue and is depicted in figure 4.20.8. However levels of MMP2 were again undetectable in some of the wound bed tissue segments. Table 4.14 summarises the descriptive statistics used to outline the spread of the data graphically presented in figure 4.20.4.

Evidently from the values for the range the levels of MMP-2 present in each wound bed tissue segment vary widely at all time points suggesting a large intra-biopsy variation and even a similarly large inter-biopsy variation. Large standard deviation values and wide CI indicate the data at all time points had a wide spread around the mean. In contrast to wound edge tissue, the CI does not include mean levels of 0 suggesting that in a larger sample or the true population the majority of wound bed tissue would contain detectable levels of MMP-2. The minimum values for the range at 4, 6 and 8 hours does include 0 and can be attributed to one of the tissue segments from biopsy 2. This is seen more clearly in figure 4.20.5 (b) where one of the tissue segments from biopsy 2 does not contain any detectable MMP-2 at 4, 6 and 8 hours. The values for the median are generally smaller than the mean suggesting the distribution of the data may have a slight positive skew.

Figure 4.20.5 a-d is a graphical representation of the levels of MMP-2 produced by the 3 segments of tissue in each of the 4 individual wound bed biopsies shown in figure 18. These graphs illustrate the wide variation in the levels of MMP-2, which can occur between segments of bed tissue from the same biopsy. This is particularly

clear in figure 4.20.5 (a) and (b) and reflects the contribution of the large intra-biopsy variation to the overall wide spread of the data illustrated in figure 4.20.4.

Table 4.14: *Descriptive statistics characterising the data spread around mean MMP-2 levels present in 8 tissue segments taken from 4 wound edge biopsies Data is recorded in units of pg/ml/mg of tissue.*

Bed	2hrs	4hrs	6hrs	8hrs
Mean	37.83	17.42	21.52	19.49
Median	25.65	8.51	13.72	5.37
SD	40.13	17.50	22.11	24.37
Range	141.46 (0.84-142.30)	47.30 (0-47.30)	62.99 (0-62.99)	63.68 (0-63.68)
CI(95%)	25.50	11.12	14.05	15.49

Figure 4.20.4*: Scatter graph depicting MMP2 levels detected in 12 segments from 4 wound bed biopsies*

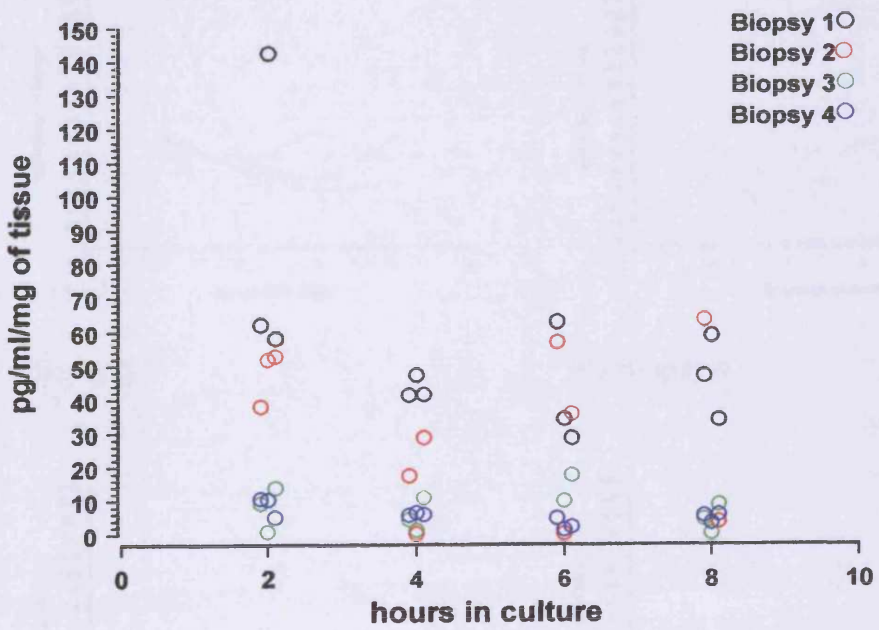

The large intra-biopsy variation in levels of MMP-2, is reflected in the large inter-biopsy variation in mean MMP-2 levels calculated for each wound bed biopsy, illustrated in figure 4.200.6. In figure 4.20.6 a wide spread around the mean is seen at

all time points, represented by large SDs with associated wide CIs, summarised in table 4.15. It is worth noting that the confidence interval at 4, 6 and 8 hours now include a mean value of 0. This is explained by the pooling of the MMP-2 levels for the individual segments to give a mean value for each of the 4 wound bed biopsies. The confidence interval in table 4.15 is therefore based on a smaller sample number of 4 and is inevitably larger than that given in table 4.14. The large values for the range at all time points reflect the large inter-biopsy variation illustrated in figure 4.20.6. Large values for the mean compared with the median recorded in table 4.15 suggest the data is distributed with a positive skew.

Figure 4.20.5: *Line graphs depicting MMP-2 levels in tissue segments from each of the 4 individual wound bed biopsies*

(a) Biopsy 1

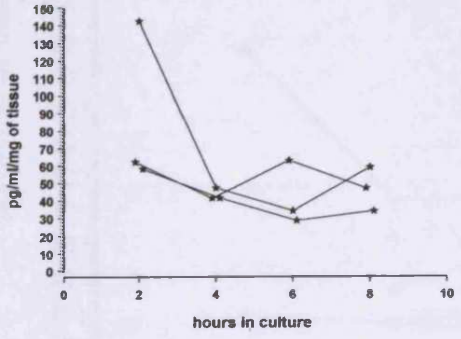

(b) Biopsy 2

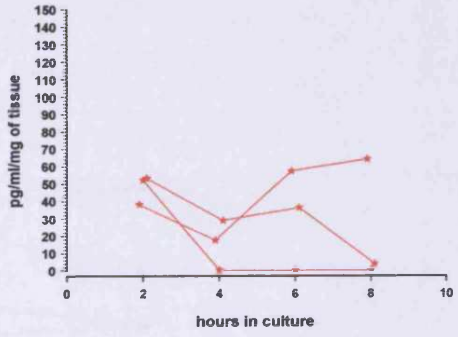

(c) Biopsy 3

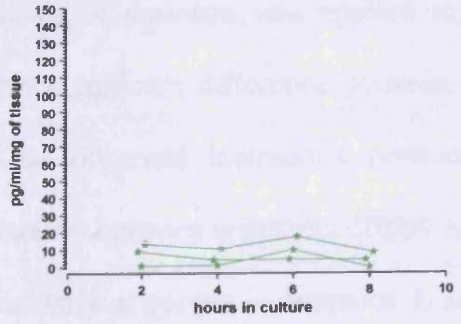

(d) Biopsy 4

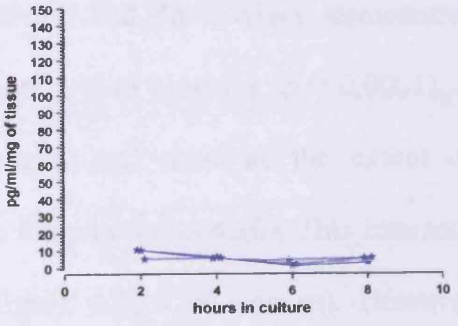

Table 4.15: Descriptive statistics characterising the data spread around the mean MMP-2 levels present in each of the 4 wound bed biopsies. Data is recorded in units of pg/ml/mg of tissue.

Bed	2hrs	4hrs	6hrs	8hrs
Mean	37.83	17.42	21.52	19.49
Median	27.98	10.49	20.81	13.47
SD	37.95	17.90	18.10	20.05
Range	79.68 (7.84-87.52)	38.06 (5.33-43.39)	39.39 (2.54-41.93)	42.49 (4.26-46.75)
CI(95%)	60.38	28.49	27.06	31.89

***Figure 4.20.6:** Line graph depicting mean MMP-2 levels present in 4 individual wound bed biopsies*

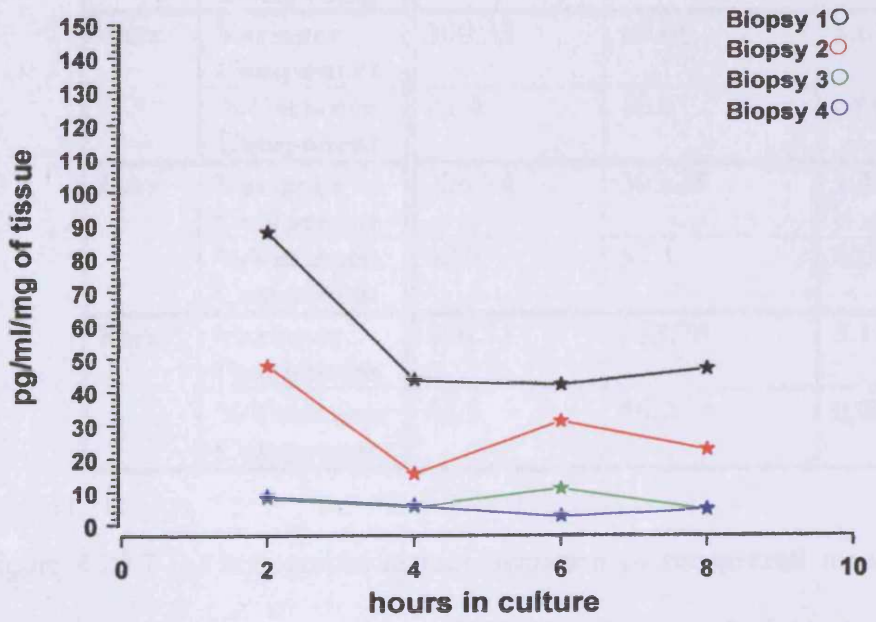

Analysis of variance was applied to the wound bed data, which demonstrated a highly significant difference between segments within biopsies ($p = 0.0001$). There was an observed interaction between segments and time, as the extent of the variability between segments differs over the 8 hours (table 4.16). This interaction is particularly apparent in biopsies 1 and 2 figure 4.20.5 (a) and (b). However the expression of MMP-2 is consistent between segments in biopsies 3 and 4. There was

a highly statistically significant interaction between biopsies and time (p = 0.001), whereby the variation between biopsies generally decreases over time (table 4.16). This is apparent in figure 4.20.6, which depicts larger differences in MMP-2 expression at 2 hours relative to later time points. Again there was low variation between triplicate readings of each segment therefore making a good estimate of measurement error.

Table 4.16: Analysis of variance on MMP-2 levels present in 4 wound bed biopsies

Wound Edge Source		Biopsy	Segment	Replicates
2hrs	Variance Component	1241.99	592.36	5.53
	%Variance Component	67.5	32.2	0.03
4hrs	Variance Component	300.33	60.06	1.67
	%Variance Component	83.0	16.6	0.005
6hrs	Variance Component	226.34	303.36	1.26
	%Variance Component	42.6	57.1	0.002
8hrs	Variance Component	280.31	363.76	3.11
	%Variance Component	43.3	56.2	0.004

Figure 4.20.7 (a) is a graphical representation of the overall mean MMP-2 levels detected in all wound edge or wound bed biopsies over the 8 hour culture period and previously recorded in table 4.12 and 4.15 respectively. The data spread around these mean values at each time point is also recorded in table 4.11 for wound edge and table 4.14 for wound bed tissue. It appears that overall there is a higher mean level of MMP-2 detected in the wound bed biopsies over the 8 hour culture period. However the wide data spread around the mean for both wound edge and bed tissue makes a statistical comparison difficult. Median values are not affected by extreme values and

in this case the values recorded in tables 4.11 and 4.14 indicate a higher level of MMP-2 to be present in wound bed tissue. This is further characterised in figure 4.20.7 (b) in which mean MMP-2 levels detected at all time points for all the wound edge or bed biopsies are depicted in a boxplot along with the associate range and median values for each dataset. Large values for the range and SD (edge SD = 4.0 bed SD = 23.8), indicate that the data was not normally distributed. Median values lower than the mean indicate a positive skew to the data distribution. Since the mean is affected by extreme values the median is recognised as a better comparison for these 2 datasets and again indicate modestly higher levels of MMP-2 to be present in wound bed tissue.

By pooling the data obtained for wound edge and bed tissue, a mean level of MMP2 production by chronic wound tissue over an 8 hour culture period is obtained and is an indication of the MMP-2 levels likely to be detected by this explant culture system. This mean level is also depicted in figure 4.20.7 (a) and had a range of 86.93 (0.59-87.52), 43.39 (0-43.39), 41.77 (0.16-41.93) and 46.32 (0.44-46.75) at 2, 4, 6 and 8 hours respectively.

Figure 4.20.7(a): Bar graph depicting overall mean MMP-2 levels present in n = 4 wound bed or n = 4 wound edge biopsies. A plot of overall mean levels present in both wound edge and bed biopsies is also included.

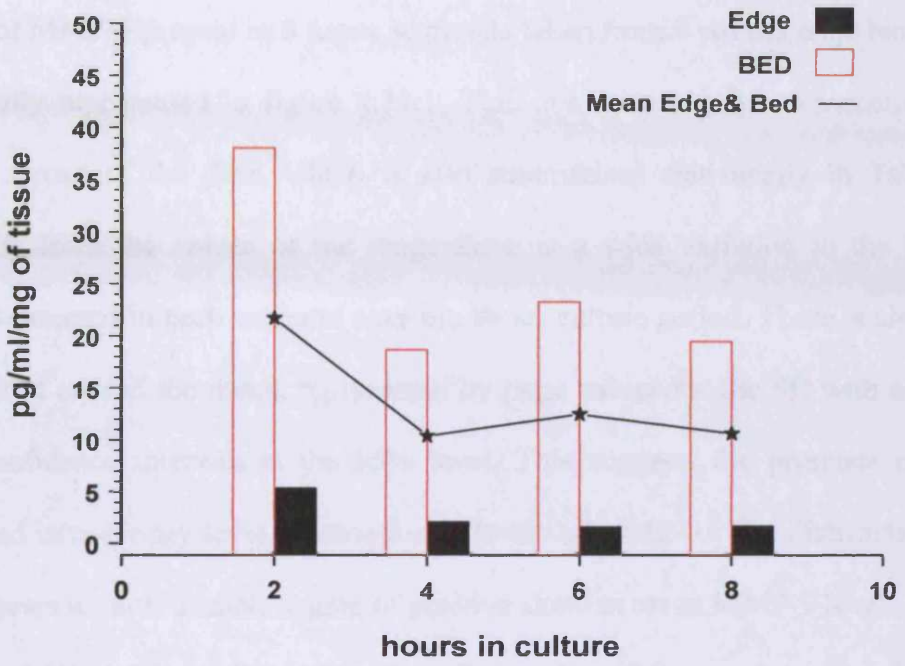

Figure 4.20.7(b): Box plot representing overall levels of MMP-2 present in wound edge or bed tissue at all the time points during the 8 hour culture. MMP-2 levels are depicted as mean median values along with the associated range for each dataset

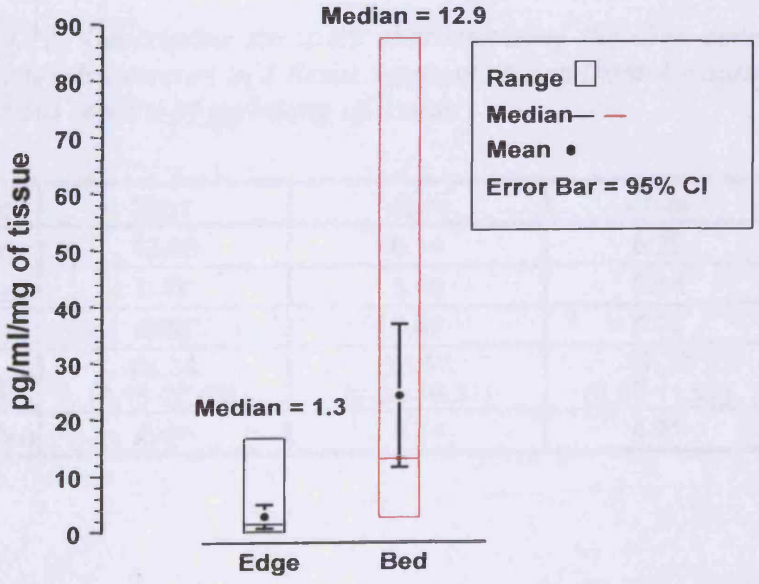

4.4.1.4: METALLOPROTEINASE 9 (MMP-9)

Determination of MMP-9 Levels in 8 Segments from 4 Wound Edge Biopsies

Levels of MMP-9 present in 8 tissue segments taken from 4 wound edge biopsies are graphically represented in figure 4.21.1. This is a scatter graph demonstrating the overall spread of the data, which is also summarised statistically in Table 4.17. Evidently from the values of the range there is a wide variation in the levels of MMP-9 detected in each segment over the 8hour culture period. There is also a wide data spread around the mean, represented by large values for the SD with associated wide confidence intervals at the 95% level. This suggests the presence of a high inter- and intra-biopsy level of variation in levels of MMP-9. The distribution of the data appears to have a small degree of positive skew as mean MMP-9 levels recorded in table 4.17 are generally higher than the median. Mean and median Levels of MMP-9 detected in wound edge tissue also decreased over the 8 hour culture period. In addition, some tissue segments at 4, 6 and 8 hours produce very little MMP-9 with levels detected under 1pg/ml/mg of tissue.

***Table 4.17**: Descriptive statistics characterising the data spread around the mean MMP-9 levels detected in 8 tissue segments taken from 4 wound edge biopsies. Data is recorded in units of pg/ml/mg of tissue.*

Edge	2hrs	4hrs	6hrs	8hrs
Mean	12.63	6.14	5.20	3.32
Median	9.32	5.46	2.36	2.09
SD	8.86	5.07	5.03	3.08
Range	24.38 (3.15-27.53)	15.67 (0.64-16.31)	11.23 (0.69-11.92)	8.44 (0.34-8.77)
CI(95%)	7.41	4.24	4.21	2.57

Figure 4.21.1: Scatter graph of MMP-9 levels detected in 8 tissue segments taken from 4 wound edge biopsies.

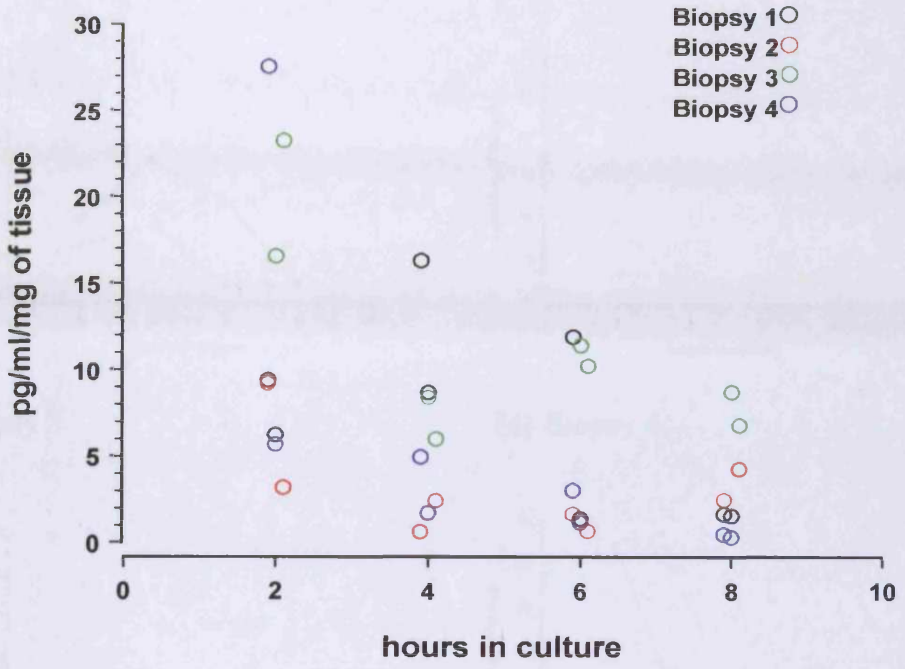

Figure 4.21.2 (a) to (d) graphically represents the levels of MMP-9 in the tissue segments from each of the 4 individual wound edge biopsies. It illustrates more clearly the wide intra-biopsy variation in MMP-9 levels described in figure 4.21.1 and which was evident in the large range and SD values recorded in table 4.17. This is particularly clear in biopsy 1 and 4 seen in figure 4.21.2 (a) and (d) respectively. An overall decrease in the levels of MMP-9 over the culture period is also more clearly seen in figure 4.21.2 (a) to (d).

Figure 4.21.2: *Line graph depicting MMP-9 levels present in tissue segments taken from 4 wound edge biopsies*

(a) Biopsy 1

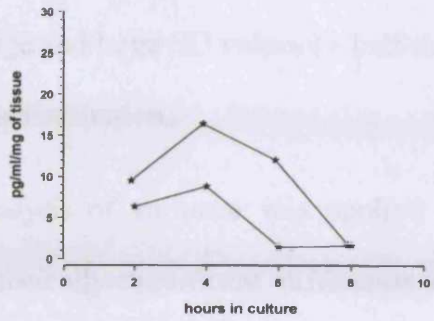

(b) Biopsy 2

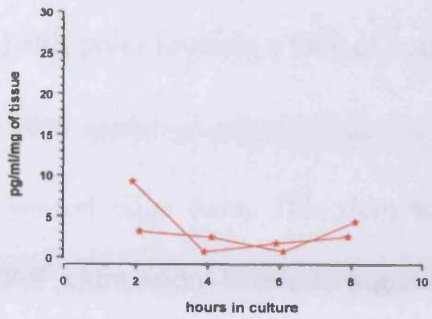

(c) Biopsy 3

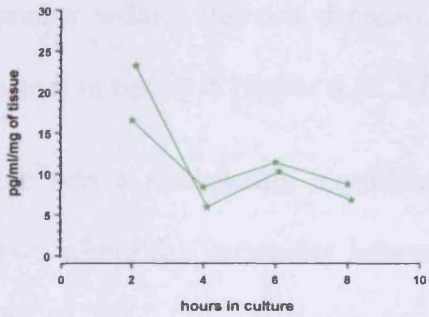

(d) Biopsy 4

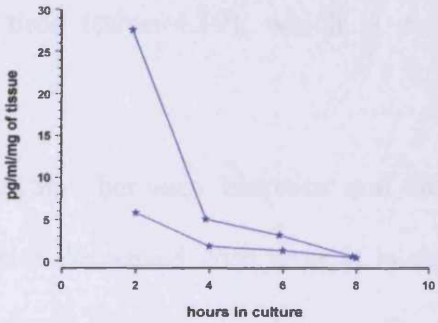

The large intra-biopsy variation in MMP-9 levels described above is reflected in the large inter-biopsy variation in MMP-9 levels calculated for each individual wound edge biopsy. This is illustrated in figure 4.21.3 and the variation in MMP-9 levels at each time point is summarised statistically in table 4.18.

Again there are large values for the range at each time point and the data is widely spread around the mean reflected by large SD values and wide confidence intervals at the 95% level. This would indicate that there is a large inter-biopsy variation present in addition to the intra-biopsy variation previously described. At 4, 6 and 8 hours the confidence intervals now include 0. This is because a wider confidence interval is obtained when taking a smaller sample number by pooling the segment data within a biopsy to give mean values for the 4 individual wound edge biopsies.

Again mean and median levels of MMP-9 present in wound edge tissue decreased over the 8 hour culture period. The small difference between mean and median values suggest that the data distribution does not have a positive skew but the wide range and large SD values (> half the mean) still point towards a lack of normality in this distribution.

Analysis of variance was applied to the wound edge data. This demonstrated a statistically significant difference in MMP-9 expression between segments ($p = 0.0002$), with marked differences between segments in biopsy 1. There was an observed interaction between segments and time. Generally, the variability between segments within biopsies decreased over time (table 4.19), which is particularly apparent in biopsy 4 (figure 4.21.2 (d))

There was a statistically significant interaction between biopsies and time ($p = 0.004$), where the variability between biopsies decreased with time. It is clear from MMP-9 levels plotted in figure 4.21.2 that after 2 hours the levels generally decrease over time. The variation between triplicate readings recorded in table 19 is low over time and therefore the readings were sufficient to obtain a good estimate of the measurement error.

Table 4.18: *Descriptive statistics characterising data spread around mean MMP-9 levels present in 4 wound edge biopsies. Data is recorded in units of pg/ml/mg of tissue.*

Edge	2hrs	4hrs	6hrs	8hrs
Mean	12.63	6.14	5.20	3.32
Median	12.23	5.26	4.39	2.52
SD	6.66	4.86	4.46	3.23
Range	13.69 (6.19-19.87)	10.97 (1.53-12.51)	9.65 (1.19-10.84)	7.39 (0.42-7.80)
CI(95%)	10.59	7.73	7.09	5.15

Figure 4.21.3: Line graph depicting mean MMP-9 levels present in each of the 4 individual wound edge biopsies.

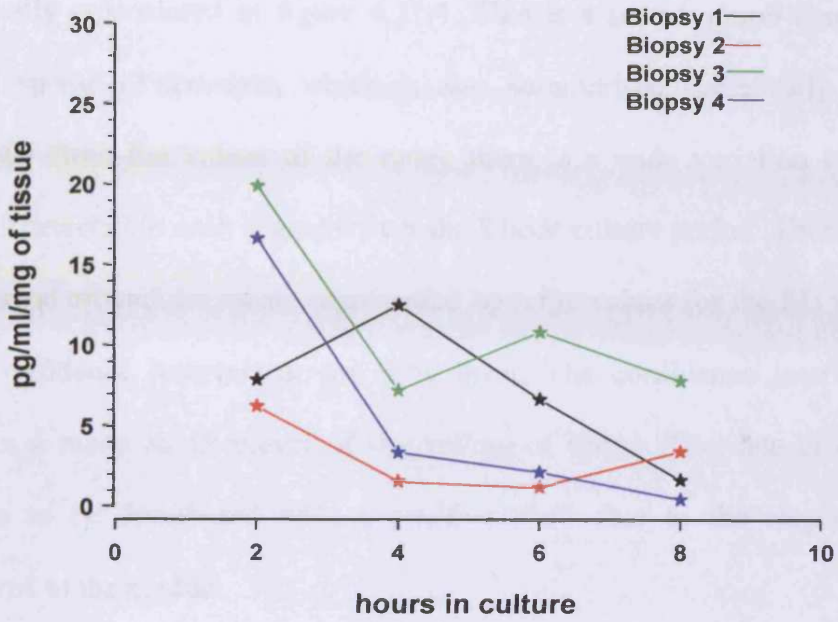

***Table 4.19:** Analysis of variance of MMP-9 levels detected in 4 wound edge biopsies.*

Wound Edge Source		Biopsy	Segment	Replicates
2hrs	Variance Component	8.79	70.62	1.14
	%Variance Component	13.0	87.7	1.4
4hrs	Variance Component	18.76	9.64	0.09
	%Variance Component	65.9	33.8	0.03
6hrs	Variance Component	12.58	14.44	0.30
	%Variance Component	46.1	52.9	1.1
8hrs	Variance Component	10.02	0.80	0.22
	%Variance Component	90.8	7.3	2.0

Determination of MMP-9 Levels in 12 Segments from 4 Wound Bed Biopsies

Levels of MMP-9 present in 12 tissue segments taken from 4 wound bed biopsies are graphically represented in figure 4.21.4. This is a scatter graph demonstrating the overall spread of the data, which is also summarised statistically in table 4.20. Evidently from the values of the range there is a wide variation in the levels of MMP-9 detected in each segment over the 8 hour culture period. There is also a wide data spread around the mean, represented by large values for the SD with associated wide confidence intervals at the 95% level. The confidence interval at 4 hours includes a mean MMP-9level of 0pg/ml/mg of tissue. The data at all time points appears to be distributed with a positive skew due to the larger mean values compared to the median.

Levels of MMP-9 detected in wound bed tissue appear to decrease over the 8 hour culture period. In addition some tissue segments at 4 and 6 hours produce very little MMP-9 with levels detected under 1pg/ml/mg of tissue. There is a particularly wide variation at 2 and 4 hours, which appears to be due in part to the high levels of MMP-9 produced by tissue segments from biopsies 1 and 2. This is more clearly evident in figure 4.21.5 where each biopsy is represented individually

Figure 4.21.5 (a) to (d) graphically represents the levels of MMP-9 in the tissue segments from each of the 4 individual wound bed biopsies. It illustrates more clearly the presence of a substantial intra-biopsy variation particularly within biopsies 1 and 2, figure 4.21.5 (a) and (b). Two tissue segments in biopsies 1 and 2 seem to behave differently to the remaining third tissue segment. The remaining third tissue segment in each biopsy appear to produce MMP-9 levels closer to that of the tissue segments from biopsies 3 and 4 suggesting a confounding factor may be present in biopsies 1 and 2.

Table 4.20: *Descriptive statistic characterising data spread around mean MMP-9 levels present in 12 tissue segments from 4 wound bed biopsies. Data is recorded in units of pg/ml/mg of tissue.*

Bed	2hrs	4hrs	6hrs	8hrs
Mean	115.46	55.88	23.74	21.98
Median	51.18	12.46	12.14	9.05
SD	129.77	99.15	27.73	34.18
Range	362.29 (3.99-366.29)	268.91 (0.78-269.70)	93.53 (0.53-94.06)	111.66 (1.61-113.26)
CI(95%) ±	82.45	63.00	17.62	21.72

Figure 4.21.4*: Scatter graph depicting MMP-9 levels present in 12 tissue segments taken from 4 wound bed biopsies.*

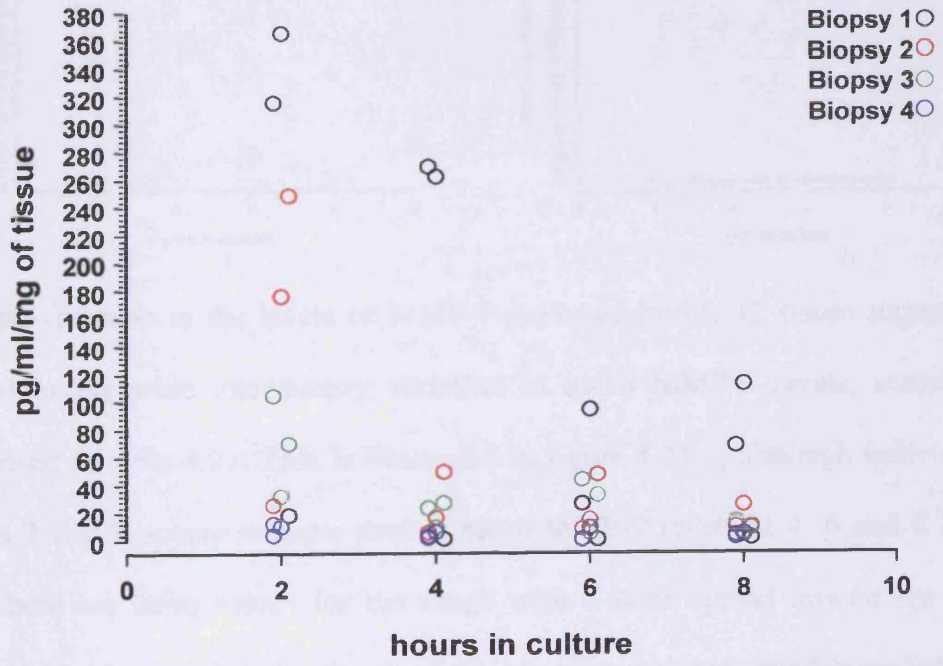

Figure 4.21.5: *Line graphs depicting MMP-9 levels present in tissue segments obtained from 4 individual wound bed biopsies*

(a) Biopsy 1

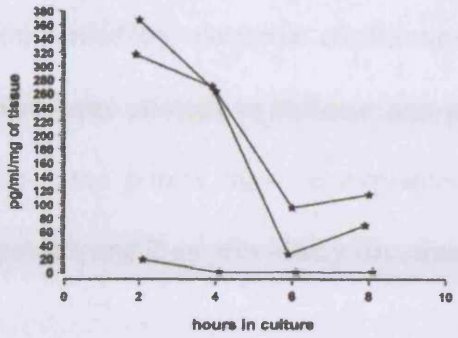

(b) Biopsy 2

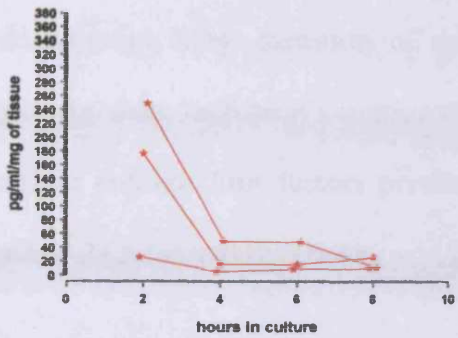

(c) Biopsy 3

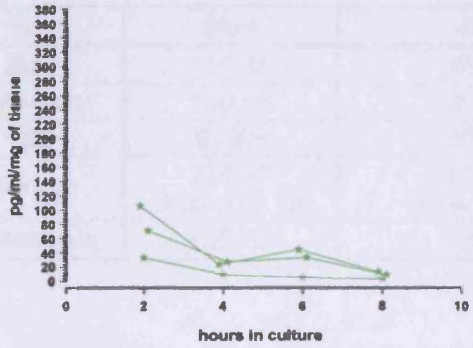

(d) Biopsy 4

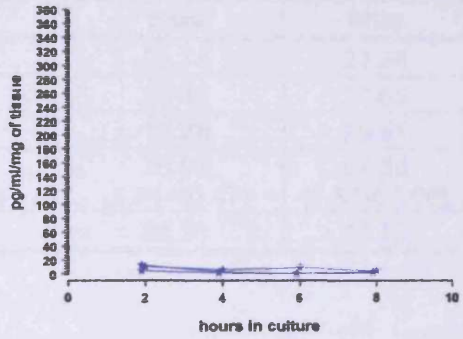

The wide variation in the levels of MMP-9 produced by the 12 tissue segments is reflected in the wide inter-biopsy variation in mean MMP-9 levels, statistically summarised in table 4.21. This is illustrated in figure 4.21.6, although individually biopsies 2 and 3 appear to have similar mean MMP-9 levels at 4, 6 and 8 hours. Again there are large values for the range with a wide spread around the mean represented by large values for the standard deviation and wide confidence intervals at the 95% level. The confidence interval at all time points includes a mean MMP-9 level of 0pg/ml/mg of tissue. This again is an effect of reducing the sample number from 12 to 4, when calculating the mean level of MMP-9 for each individual biopsy.

There is an overall trend for a decrease in mean and median levels of MMP-9 over the 8hour culture period and the degree of variation is also decreased at 6 and 8 hours. This is seen in the smaller values for the range and standard deviation accompanied by narrower confidence intervals although these measures of spread remain large enough to indicate non-normality of the data. Increased variation at the earlier time points may be explained by possible confounding factors present in biopsies 1 and 2 as previously illustrated in figure 4.21.5 (a) and (b) above.

Table 4.21: *Descriptive statistic characterising data spread around mean MMP-9 levels present in 4 wound bed biopsies. Data is recorded in units of pg/ml/mg of tissue.*

Bed	2hrs	4hrs	6hrs	8hrs
Mean	115.46	55.88	23.74	21.98
Median	109.56	21.38	25.48	11.65
SD	97.83	81.64	15.28	26.51
Range	224.87 (8.92-233.79)	174.50 (3.14-177.63)	36.93 (3.54-40.47)	57.58 (3.51-61.09)
CI(95%) ±	155.66	129.90	24.31	42.18

Figure 4.21.6*: Line graph depicting mean MMP-9 levels present in each of the 4 wound bed biopsies*

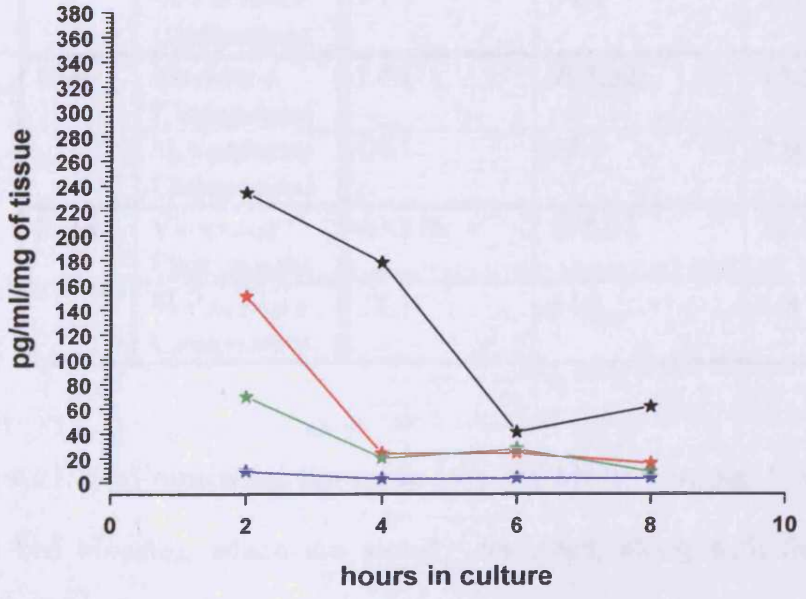

Analysis of variance was applied to the wound bed data. A highly statistically significant difference in MMP-9 expression between segments was present (p = <0.0001). There was an observed interaction between segments and time whereby the variability between segments generally decreases over time, table 4.22. This decrease in MMP-9 expression between segments is observed to be consistent between segments within biopsies 3 and 4. There was also a statistically significant interaction between biopsies and time (p = <0.001) whereby the difference in MMP-9 levels between biopsies decreases over time figure 4.21.6 table 4.22. In addition overall the level of MMP-9 decreases over time. Low variation between triplicate readings within segments indicated that measurement error associated with densitometry readings was very low.

Table 4.22: *Analysis of variance on MMP-9 levels present in 4 wound bed biopsies.*

Wound Edge Source		Biopsy	Segment	Replicates
2hrs	Variance Component	5439.89	12132.55	773.24
	%Variance Component	29.7	66.1	4.2
4hrs	Variance Component	4673.38	5910.21	281.09
	%Variance Component	43.0	54.4	2.6
6hrs	Variance Component	DM	763.32	15.57
	%Variance Component	DM	98.0	2.0
8hrs	Variance Component	430.76	808.31	22.60
	%Variance Component	34.1	64.1	1.8

Figure 4.21.7 (a) represents the mean level of MMP-9 in the 4 wound edge or 4 wound bed biopsies, which are already described, along with their data spreads

around these means, in tables 4.18 and 4.21 respectively. A mean level for the amount of MMP-9 detected in both wound edge and bed biopsies is also displayed as an indication of the overall level of MMP-9 likely to be detected in wound tissue by this explant culture system. This mean level had a range of 227.60(6.19-233.79), 176.63(1.53-177.63), 39.28(1.19-40.47) and 60.67(0.42-61.09) at 2, 4, 6 and 8 hours respectively.

Figure 4.21.7 (a) clearly demonstrates the overall trend for a decrease in mean MMP-9 levels over the 8 hour culture period. Presence of higher levels in the wound bed tissue compared with wound edge tissue is also observed. However the wide data spread around the mean for both wound edge and bed tissue makes a statistical comparison difficult. As median values are unaffected by extreme values the values recorded in tables 4.18 and 4.21 provide some initial evidence for the presence of a higher level of MMP-9 in wound bed tissue. This is further characterised in figure 4.21.7 (b) in which mean MMP-9 levels detected at all time points for all the wound edge or bed biopsies are depicted in a boxplot along with the associate range, 95% CI and median values for each dataset. Large values for the range and SD (edge SD = 5.7 bed SD = 70.4), indicate that the data was not normally distributed. Median values lower than the mean indicate a positive skew to the data distribution for the wound bed tissue. The median values also indicate levels of MMP-9 to be higher in wound bed tissue and are a more reliable comparison than the mean. It is also observed that the 95% CIs do not overlap, indicating that in the true population there may be a real difference between wound bed and edge tissue in terms of mean MMP-9 levels. However this is not a reliable observation, since both datasets are not normally distributed.

Figure 4.21.7(a): Bar graph depicting mean MMP-9 levels present in 4 wound edge or wound bed biopsies. A plot of mean MMP-9 levels present in both biopsy tissue types is also displayed

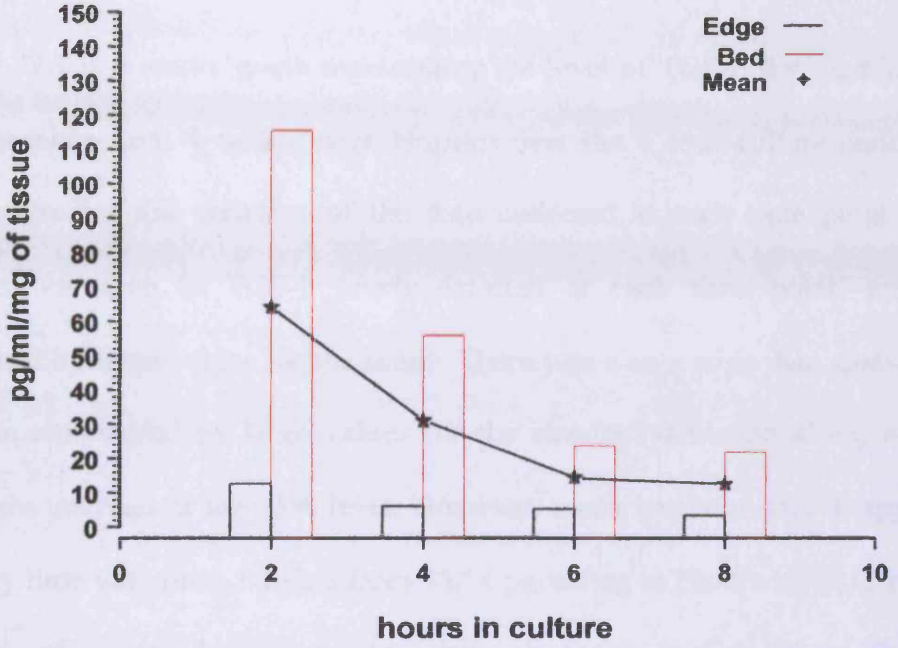

Figure 4.21.7(b): Overall levels of MMP-9 present in wound edge or bed tissue at all the time points during the 8 hour culture. Mean MMP-9 levels are plotted with their 95% CIs. Box plots represent the range and median values for each dataset

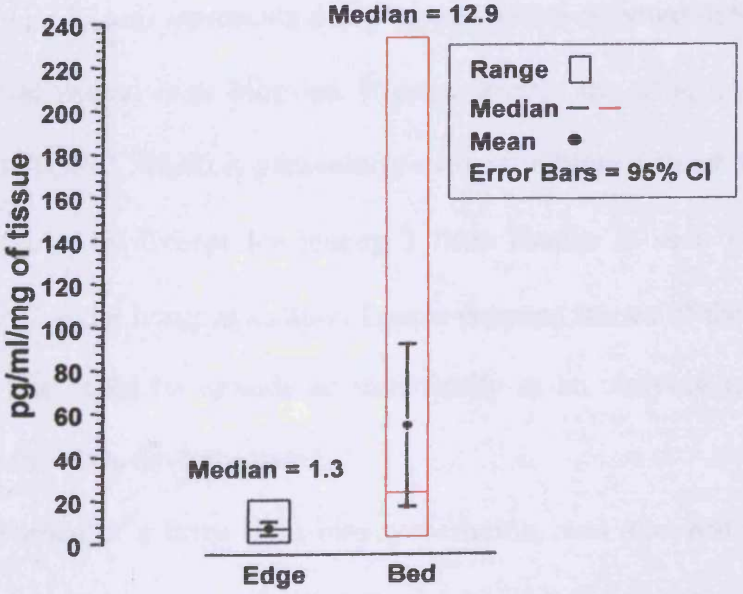

4.4.1.5 TRANSFORMING GROWTH FACTOR-β

TGF-β levels in wound edge tissue

Figure 4.22.1 is a scatter graph representing the level of TGF-β detected in 8 tissue segments taken from 4 wound edge biopsies over the 8 hour culture period. Table 4.23 summarises the variation of the data collected at each time point. A wide variation was seen in TGF-β levels detected at each time point, which was represented by large values for the range. There was also a wide data spread around the mean represented by large values for the standard deviation along with wide confidence intervals at the 95% level. However, mean levels of TGF-β appeared to vary very little with time, ranging from 33.54 pg/ml/mg at 2hours to 49.12 pg/ml/mg at 8 hours, which was also mirrored by similar changes in median values. This can be seen more clearly in figure 4.22.2 (a-d) and figure 4.22.3. Based on smaller median values compared with the mean the data distribution was also found to have a small degree of positive skew

Figure 4.22.2 (a-d) represents the levels of TGF-β detected in tissue segments from 4 individual wound edge biopsies. It demonstrates the wide intra-biopsy variation in levels of TGF-β, which is particularly evident in biopsy 1 and 3, figure 4.22.2 (a) and (c) respectively. Except for biopsy 1 little change is seen in the level of TGF-β between 2 and 8 hours in culture. Levels detected in one of the tissue segments from biopsy one could be considered statistically as an outlying result since the data is more than 3 SDs from the mean.

The presence of a large intra-biopsy variation, was also reflected in a large inter-biopsy variation in mean TGF-β levels calculated for each individual wound edge

biopsy. This is illustrated in figure 4.22.3 and statistically summarised in table 4.24. Mean TGF-β values calculated for each biopsy are seen to range widely during the 8 hour culture period. This wide range is also characterised by a wide data spread around the mean at each time point, represented by large values for the SD along with wide confidence intervals at the 95% level. Again except for biopsy 1, the mean TGF-β levels in each individual wound edge biopsy does not vary greatly between 2 and 8 hours in culture. The confidence interval at 2 hours includes a mean TGF-β level of 0pg/ml/mg of tissue, but this again is explained by the wider CI obtained when the mean levels in a smaller sample 4 biopsies is calculated from the levels in their corresponding tissue segments. Similar mean and median values at all time points indicate an approximately normal data distribution.

The level of inter and intra-biopsy variation as well as variation with time was investigated by analysis of variance. A large intra-biopsy variation was found which can be seen in the variance values recorded in table 4.27. This variation accounted for most of the variability in TGF-β levels within wound edge tissue across all time points. In addition the extent of intra-biopsy variation recorded in table 4.27 varied across the time points. Measurement variability between replicate samples of ELISA assay standards used to construct standard curves was found to be low relative to the variation between segments. Thus one replicate of culture supernatant was thought to be sufficient to reliably represent TGF-β.

Table 4.23: Descriptive statistic characterising data spread around mean TGFβ levels present in 8 tissue segments taken from 4 wound edge biopsies. Data is recorded in units of pg/ml/mg of tissue.

Edge	2hrs	4hrs	6hrs	8hrs
Mean	33.54	44.15	44.12	49.12
Median	28.97	29.91	31.19	36.38
SD	33.37	36.46	34.19	39.56
Range	95.26 (0-95.26)	105.97 (10.08-116.05)	92.69 (11.42-104.10)	115.43 (14.84-130.27)
CI (95%) ±	27.90	30.48	28.58	33.07

Figure 4.22.1: Scatter graph depicting TGFβ levels present in 8 tissue segments taken from 4 wound edge biopsies.

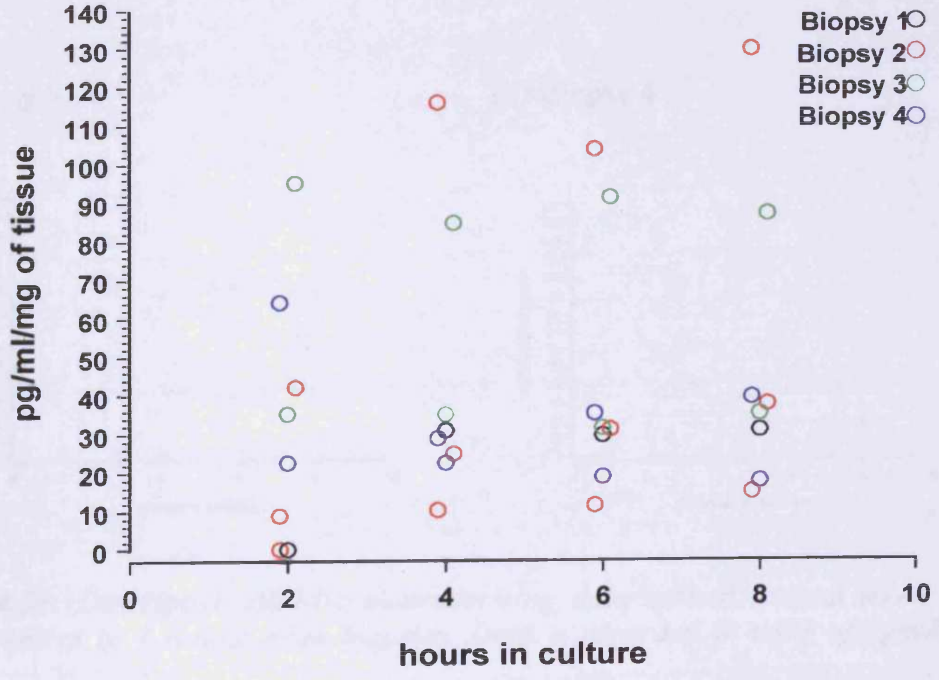

Figure 4.22.2: Line graph depicting TGFβ levels present in tissue segments from 4 individual wound edge biopsies

(a) Biopsy 1

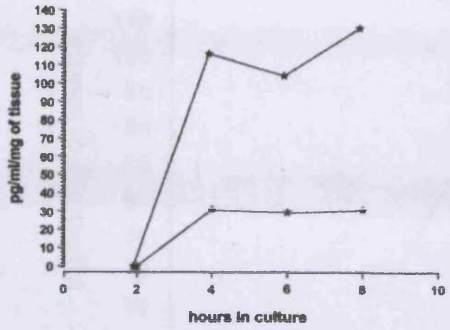

(b) Biopsy 2

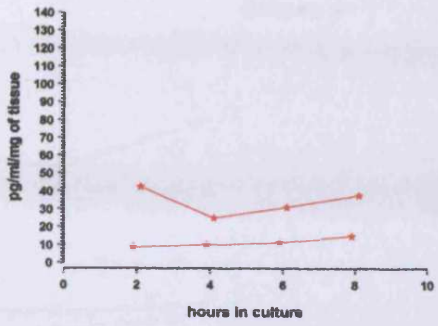

(c) Biopsy 3

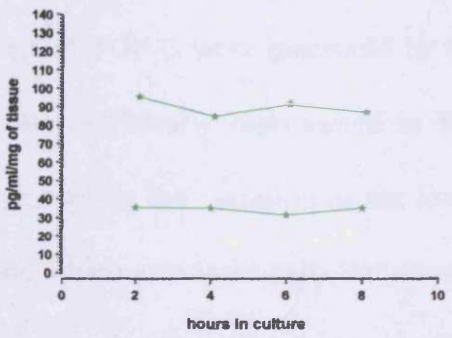

(d) Biopsy 4

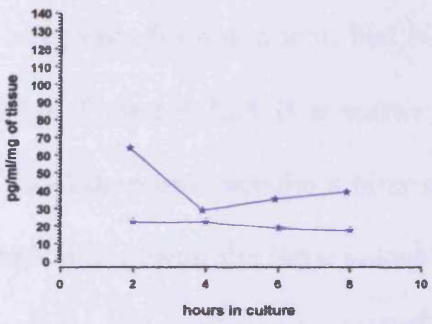

***Table 4.23:** Descriptive statistic characterising data spread around mean TGFβ levels present in 4 wound edge biopsies. Data is recorded in units of pg/ml/mg of tissue.*

Edge	2hrs	4hrs	6hrs	8hrs
Mean	33.54	44.15	44.12	49.12
Median	34.44	42.80	44.23	44.85
SD	27.65	26.84	23.33	26.33
Range	65.29(0-65.29)	56.01(17.49-73.50)	45.60(21.21-66.82)	54.31(26.24-80.56)
CI (95%) ±	43.99	42.71	37.12	41.90

Figure 4.22.3: Line graph depicting mean TGFβ levels present in 4 individual wound edge biopsies

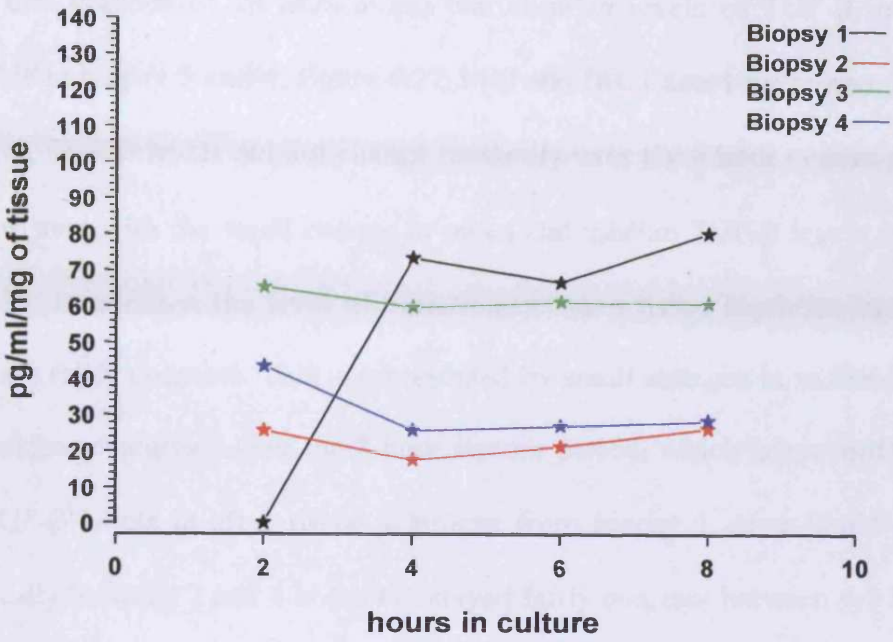

TGF-β Levels in wound bed biopsy tissue

Levels of TGF-β were measured in 12 tissue segments from 4 wound bed biopsies and are graphically represented in figure 4.22.4. Figure 4.22.4 is a scatter graph demonstrating the variation in the levels of TGF-β detected over the 8 hour culture period which are statistically summarised in table 4.25. From the large values of the range at each time point it is evident that there is a wide variation in TGF-β levels present in wound bed tissue segments. This is also characterised by a wide data spread around the mean at each 2 hour time point, represented by large values for the standard deviation along with wide confidence intervals at the 95% level. The mean level of TGF-β does not appear to vary greatly between 4 and 8 hours in culture. In addition the data at 2, 6 and 8 hours had smaller median values compared to the mean, indicating a positive skew to the data distribution.

Figure 4.22.5 is a graphical representation of TGF-β levels in the three tissue segments present in each of the 4 wound bed biopsies. This demonstrates more clearly the presence of an intra-biopsy variation in levels of TGF-β, particularly noticeable in biopsy 3 and 4, figure 4.22.5 (c) and (d). Except for biopsy 1 in figure 4.22.5 (a), TGF-β levels did not change markedly over the 8 hour culture period and was consistent with the small change in mean and median TGF-β levels recorded in table 4.25. In addition the level of variation between tissue segments at each time point stays fairly constant. This is represented by small changes in values for the SD and confidence intervals over the 8 hour culture period, which are recorded in table 4.25. TGF-β levels in all 3 tissue segments from biopsy 1 were found to change dramatically between 2 and 4 hours but stayed fairly constant between 4-8 hours (see figure 4.22.5 (a)). However the extent of the change between 2-4 hours is probably a reflection of the lack of TGF-β in all these tissue segments at 2 hours.

The intra-biopsy variation in TGF-β levels is also reflected in the large inter-biopsy variation in mean TGF-β values present in each of the 4 wound bed biopsies over the 8 hour culture period. This is graphically represented in figure 4.22.6 and statistically summarised in table 4.26. Mean TGF-β values calculated for each biopsy are seen to range widely at each of the 2 hour time points. This wide range is also characterised by a wide data spread around the mean at each of the time points, represented by large values for the SD along with wide confidence intervals at the 95% level. The data at 2 hours is approximately normally distributed but at 4, 6 and 8 hours has a small degree of positive skew reflected by the smaller median values compared to the mean

Again except for biopsy 1, the mean and median TGF-β levels in each individual wound bed biopsy, does not vary greatly between 2 and 8 hours in culture. This is also reflected in similar values for the SD and confidence intervals suggesting that the level of variability between biopsies stays fairly constant over the study period. However, biopsy 1 shows a much larger change in TGF-β levels between 2 and 4 hours. This is a direct result of the dramatic change in TGF-β levels between 2-4 hours in all the tissue segments from biopsy 1 and may suggest the presence of a confounding factor within this biopsy. The confidence intervals at 2 and 6 hours includes a mean TGF-β level of 0pg/ml/mg of tissue but this again is explained by the smaller sample number of 4 obtained when calculating mean levels for each individual biopsy.

The level of inter and intra-biopsy variation as well as variation with time was investigated by analysis of variance. Statistically significant inter-biopsy variation relative to intra-biopsy variation was found ($p=0.024$) and is characterised by the variance values recorded in table 4.27 Intra-biopsy variation was also found to vary with time whereby individual tissue segments behaved differently in terms of the level of TGF-β detected within them during the 8 hour culture period. Measurement variability between replicate samples of ELISA assay standards used to construct standard curves was found to be low relative to the variation between segments. Thus one replicate of culture supernatant was thought to be sufficient to reliably represent TGF-β values.

Table 4.25: *Descriptive statistics characterising data spread around mean TGFβ levels present in 8 tissue segments taken from 4 wound bed biopsies. Data is recorded in units of pg/ml/mg of tissue.*

Bed	2hrs	4hrs	6hrs	8hrs
Mean	20.91	41.97	40.86	33.39
Median	16.04	41.63	28.85	27.36
SD	19.74	24.55	26.86	20.31
Range	59.53(0-59.53)	71.59(5.24-76.83)	74.91(11.29-86.20)	63.96(8.31-72.28)
CI (95%) ±	12.54	15.60	17.07	12.90

Figure 4.22.4: *Scatter graph depicting data spread of TGFβ levels present in 12 tissue segments taken from 4 wound bed biopsies*

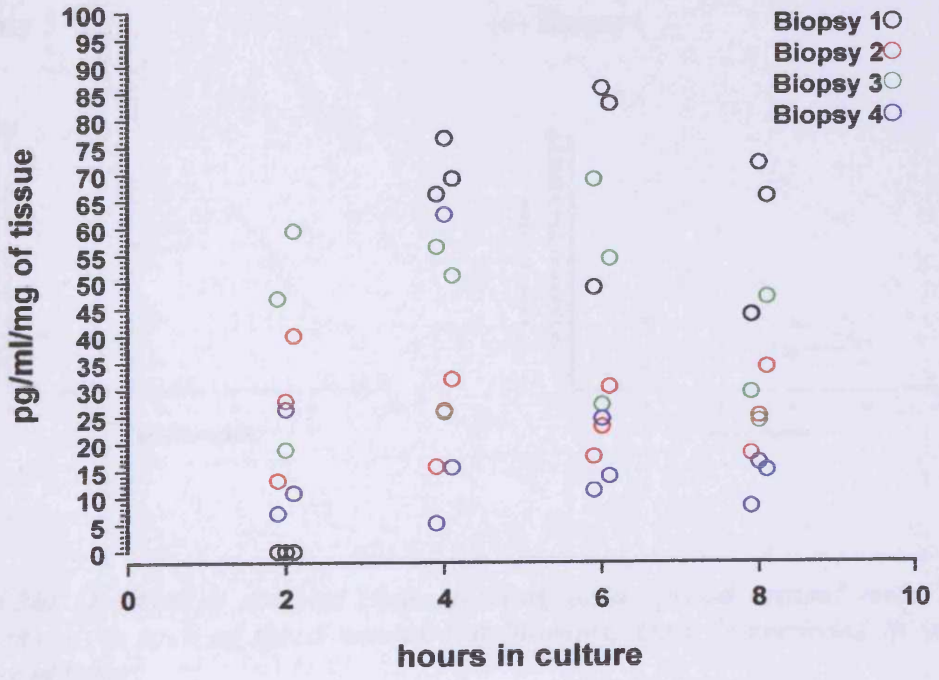

Figure 4.22.5: *Line graphs depicting TGFβ levels present in tissue segments taken from 4 individual wound bed biopsies*

(a) Biopsy 1

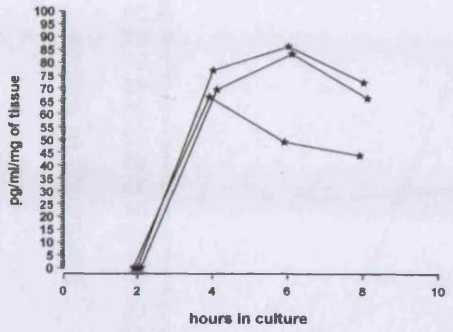

(b) Biopsy 2

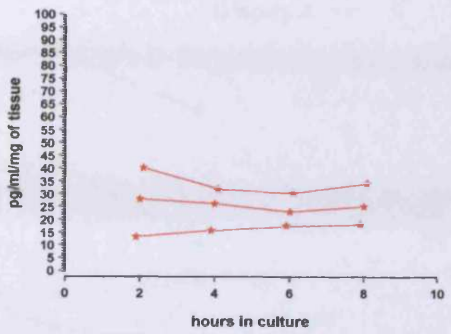

(c) Biopsy 3

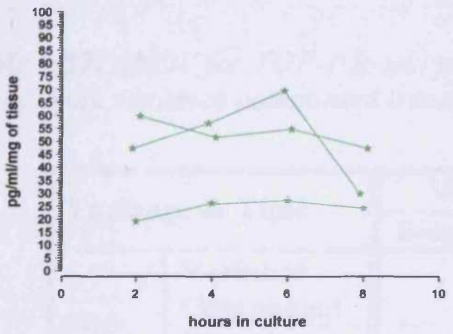

(d) Biopsy4

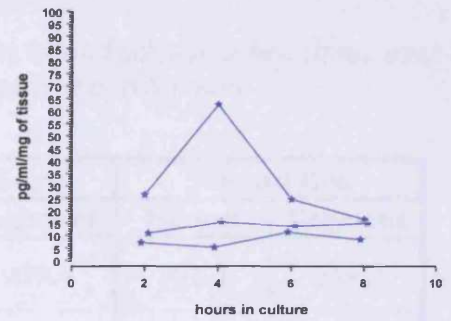

Table 4.26: *Descriptive statistic characterising data spread around mean TGFβ levels present in each of the 4 wound bed biopsies. Data is recorded in units of pg/ml/mg of tissue.*

Bed	2hrs	4hrs	6hrs	8hrs
Mean	20.91	41.97	40.86	33.39
Median	20.92	36.19	36.99	29.76
SD	17.79	21.15	25.79	20.09
Range	41.80(0-41.80)	46.22(24.64-70.85)	56.30(16.57-72.87)	47.49(13.28-60.77)
CI (95%) ±	28.31	33.65	41.04	31.97

Figure 4.22.6: Line graph depicting mean TGFβ levels present in each of the 4 wound bed biopsies

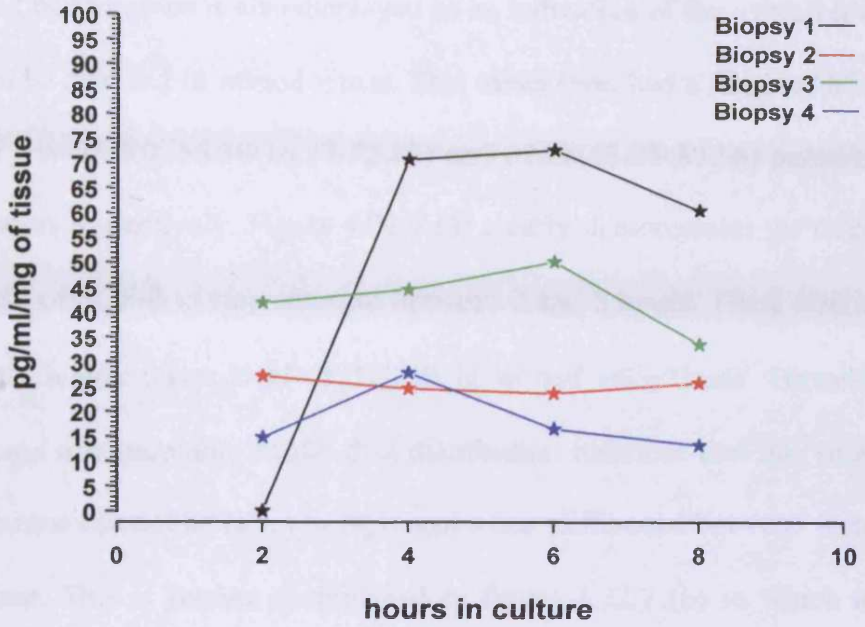

Table 4.27: ANOV for TGF-β levels present in wound edge and bed tissue over 8 hours. Note variance component inestimable at 2, 6 and 8 hours

Variance & Time		Wound Edge		Wound Bed	
		Biopsy	Segment	Biopsy	Segment
2hrs	Variance Component	-	959.4	103.3	239.7
	%Variance Component	-	100.0	30.1	69.9
4hrs	Variance Component	97.82	1245.18	338.7	325.7
	%Variance Component	7.3	92.7	51.0	49.0
6hrs	Variance Component	-	1168.9	584.1	243.5
	%Variance Component	-	100.0	70.6	29.4
8hrs	Variance Component	-	1564.7	366.0	112.9
	%Variance Component	-	100.0	76.4	23.6

Figure 4.22.7 (a) represents the mean level of TGF-β in the 4 wound edge or 4 wound bed biopsies. A mean level for the amount of TGF-β detected in both wound edge and bed biopsies is also displayed as an indication of the overall level of TGF-β likely to be detected in wound tissue. This mean level had a range of 65.29(0-65.29), 56.01(17.49-73.50), 56.30(16.57-72.87) and 67.28(13.28-80.56) pg/ml/mg at 2, 4, 6 and 8 hours respectively. Figure 4.22.7 (a) clearly demonstrates the overall trend for the levels of TGF-β to stay constant between 2 and 8 hours. There also appears to be a slightly higher mean level of TGF-β in wound edge tissue. However, the wide spread and non normality of the data distribution indicates that this small difference in the means can not be taken to represent a true difference between wound edge and bed tissue. This is further exemplified in figure 4.22.7 (b) in which mean TGF-β levels detected at all time points for all the wound edge or bed biopsies are depicted in a boxplot along with the associated range, 95% CI and median values for each dataset. Large values for the range and SD (edge SD = 24.1 bed SD = 21.1), indicate that the data was not normally distributed and median values lower than the mean indicate a positive skew to the data distribution. The median values also indicate levels of TGF-β to be slightly lower in wound bed tissue and are a more reliable comparison than the mean. However, this is only a small difference within a small sample number. When the wide overlapping CIs are considered this does not provide any evidence for a true difference in TGF-β levels between wound edge and bed tissue.

Figure 4.22.7: *Bar graph depicting overall mean TGFβ levels present in 4 wound edge or wound bed biopsies. A plot of the mean value present in both types of tissue is also displayed*

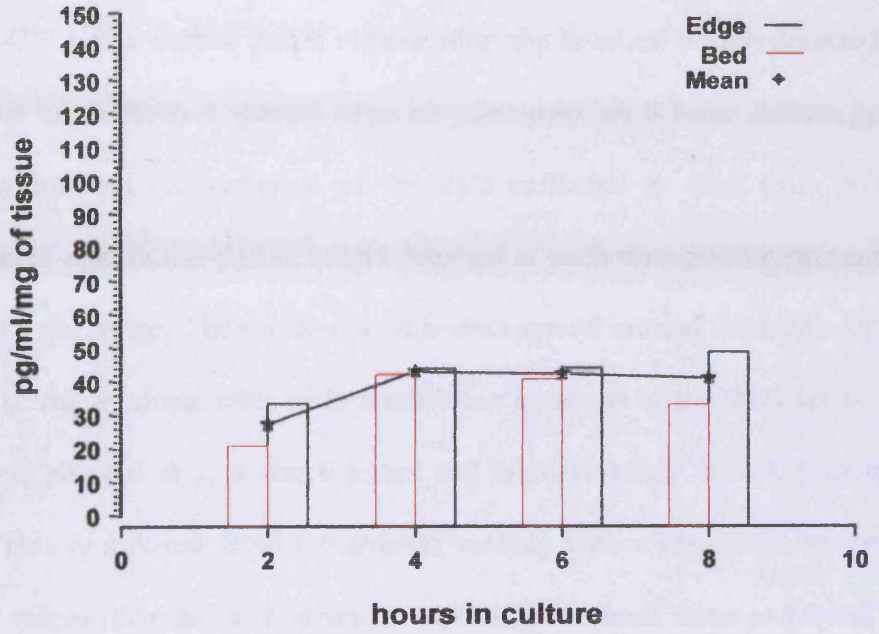

Figure 4.22.7 (b): *Overall levels of TGFβ present in wound edge or bed tissue at all the time points during the 8 hour culture. Mean TGFβ levels are plotted with their 95% CIs. Box plots represent the range and median values for each dataset*

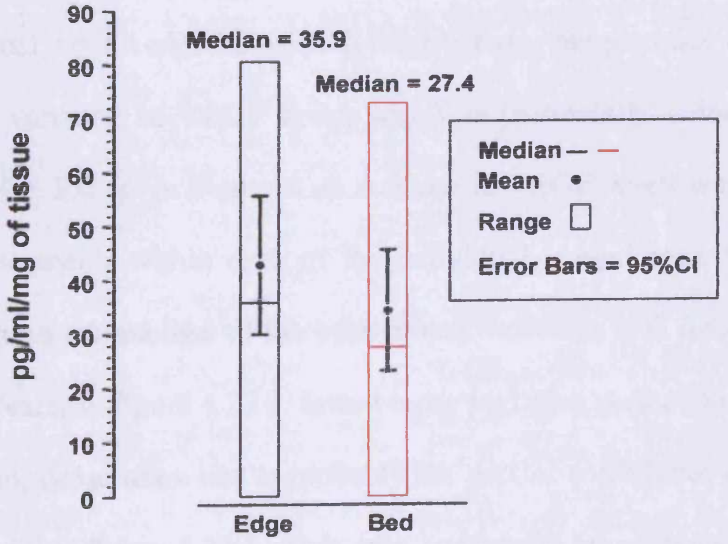

4.4.1.6 VASCULAR ENDOTHELIAL GROWTH FACTOR

VEGF levels in wound edge tissue

Figure 4.23.1 is a scatter graph representing the level of VEGF detected in 8 tissue segments taken from 4 wound edge biopsies over an 8 hour culture period. Table 4.28 summarises the variation of the data collected at each time point. A wide variation is seen in the VEGF levels detected at each time point represented by large values for the range. There is also a wide data spread around the mean represented by large SD values along with wide confidence intervals at the 95% level. The data is positively skewed at 2, 4 and 6 hours and approximately normally distributed at 8 hours. This is inferred from the smaller median values compared to the mean with similar values recorded at 8 hours in table 4.28. Overall there is a trend towards an increase in mean VEGF levels over the 8 hour culture period which is mirrored by a similar increase in median values. This trend is more clearly observed in figure 4.23.2

Figure 4.23.2 (a-d) represents the levels of VEGF detected in tissue segments from 4 individual wound edge biopsies. It demonstrates the presence of a considerable intra-biopsy variation in VEGF level, which is particularly evident in biopsy 4 figure 4.23.2 (d). Except in biopsy 1 an increase in VEGF levels was observed in all of the tissue segments within each of the individual wound edge biopsies. Figure 4.23.2 also allows comparison of the intra-biopsy variation with inter-biopsy variation seen more clearly in figure 4.23.3. Inter-biopsy variation seems to be relatively larger than intra-biopsy variation and is probably the greater contributor to the wide data spread described in figure 4.23.1. This was confirmed by analysis of variance described below.

Table 4.28: Descriptive statistics characterising data spread around mean VEGF levels present in 8 tissue segments taken from 4 wound edge biopsies. Data is recorded in units of pg/ml/mg of tissue.

Edge	2hrs	4hrs	6hrs	8hrs
Mean	22.22	29.89	44.95	50.71
Median	13.66	18.66	27.69	49.72
SD	24.23	31.96	44.84	39.75
Range	71.52 (5.05-76.57)	94.65 (4.01-98.66)	130.80 (2.02-132.82)	124.66 (1.67-126.33)
CI (95%)	20.26	26.72	37.49	33.24

***Figure 4.23.1:** Scatter graph depicting data spread of VEGF levels present in 8 tissue segments taken from 4 wound edge biopsies*

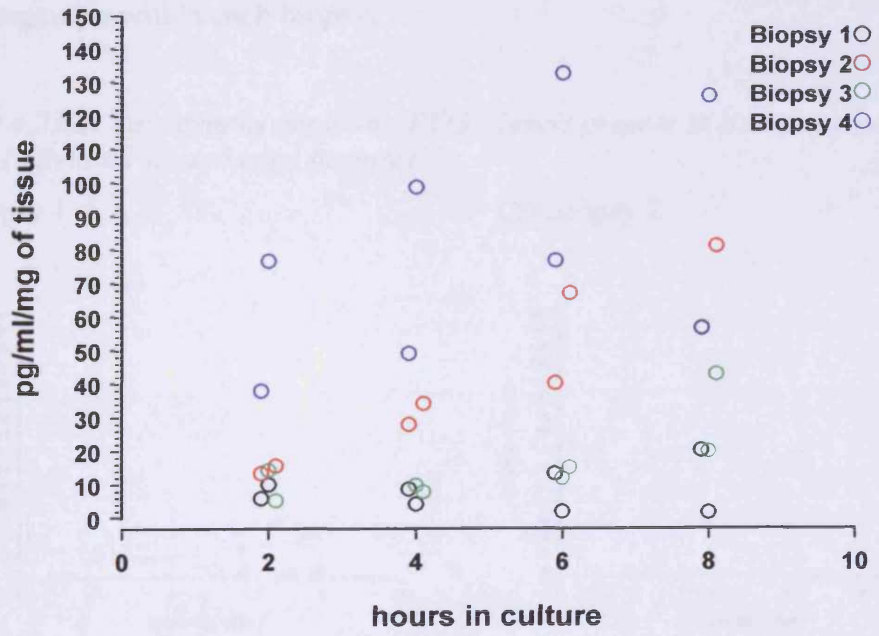

Inter-biopsy variation in levels of VEGF is more clearly shown in figure 4.23.3. Figure 4.23.3 represents the mean VEGF levels present in the two tissue segments taken from each of the 4 individual wound edge biopsies and therefore the mean levels in each biopsy. The inter-biopsy variation in VEGF levels is statistically summarised in table 4.29. Large values for the range seen in table 4.29 indicate that the overall mean levels of VEGF in each biopsy varies widely at each of the 2 hour

time points. This wide range is also represented by a wide data spread around the mean at each 2 hour time point, characterised by large SD values and wide confidence intervals at the 95% level. Again at 2 4 and 6 hours the data has a positive skew but is approximately normally distributed at 8 hours. The overall mean VEGF levels for the 4 wound edge biopsies increases from 22.22 at 2 hours to 50.71 pg/ml/mg at 8 hours with a similar increase in median values being observed. Wide confidence intervals are seen in all of the time points and include a mean VEGF level of 0pg/ml/mg of tissue. Again this is explained by the decrease in sample number occurring when calculating mean levels for the 4 wound edge biopsies from the 2 tissue segments within each biopsy.

Figure 4.23.2: *Line graphs depicting VEGF levels present in tissue segments taken from 4 individual wound edge biopsies*

(a) Biopsy 1

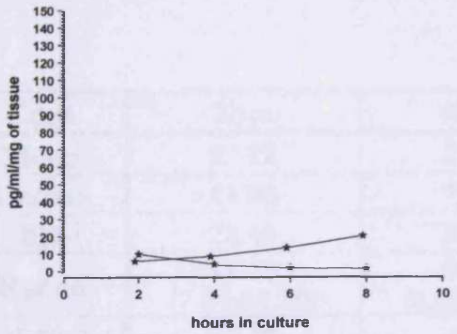

(b) Biopsy 2

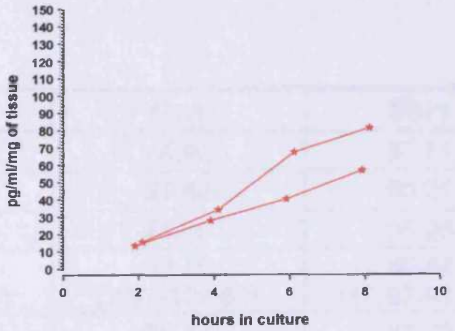

(c) Biopsy 3

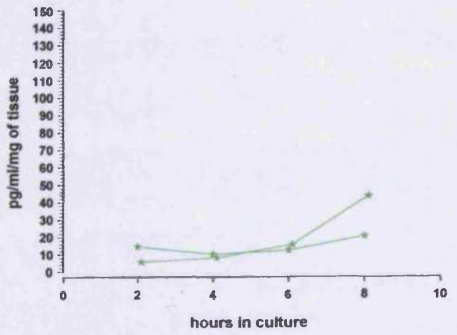

(d) Biopsy 4

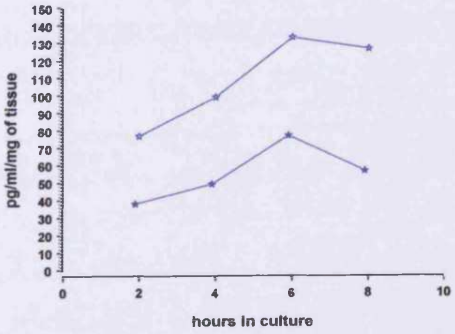

Table 4.32 summarises the results of analysis of variance carried out on the data for levels of VEGF present in wound edge tissue. A marginally non-significant difference (0.095) in VEGF levels between individual biopsies was found. This inter-biopsy variation was greater than intra-biopsy variation throughout the 8 hour culture period. There was also an observed interaction between tissue segments and time whereby intra-biopsy variation increased with time. Measurement variability between replicate samples of ELISA assay standards used to construct standard curves was found to be low relative to the variation between segments. Thus one replicate of culture supernatant was thought to be sufficient to reliably represent VEGF values.

Table 4.29 *Descriptive statistic characterising data spread around mean VEGF levels present in each of the 4 wound edge biopsies. Data is recorded in units of pg/ml/mg of tissue.*

Edge	2hrs	4hrs	6hrs	8hrs
Mean	22.22	29.89	44.95	50.71
Median	11.95	19.74	33.66	50.21
SD	23.48	31.32	44.85	36.26
Range	49.39 (7.81-57.20)	67.57 (6.25-73.83)	97.15 (7.67-104.82)	80.47 (10.97-91.44)
CI (95%) ±	37.36	49.84	71.37	57.70

Figure 4.23.3: Line graphs depicting VEGF levels present in tissue segments taken from 4 individual wound edge biopsies

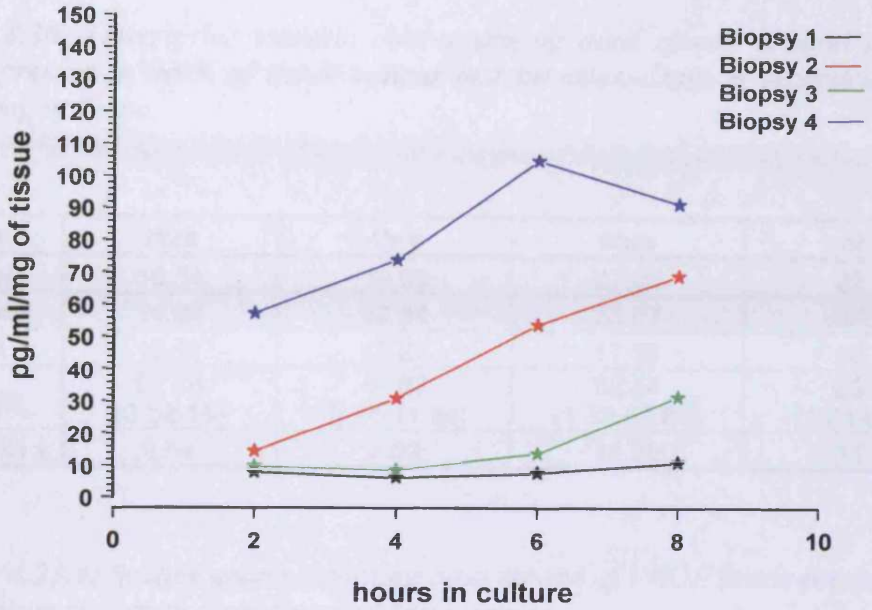

VEGF levels in wound bed tissue

Figure 4.23.4 is a scatter graph representing the level of VEGF detected in 12 tissue segments taken from 4 wound bed biopsies studied over an 8 hour culture period. Table 4.30 summarises the variation in levels of VEGF collected at each time point. A wide variation is seen in VEGF levels represented by large values for the range. There is also a wide data spread around the mean represented by large SD values along with wide confidence intervals at the 95% level. The data appears to be approximately normally distributed at all time points based on similar values recorded for the mean and median in table 4.30. Overall there appears to be a trend towards an increase in VEGF levels over the 8 hour culture period with mean levels increasing from 16.34 at 2 hours to 32.13 pg/ml/mg of tissue at 8 hours with a similar increase in median values observed. This trend is graphically represented in figure 4.23.2. In general there is not a great difference in the level of variation observed at

each of the 2 hour time points which is evident in the small changes in SD values and confidence intervals over the 8 hour culture period.

Table 4.30: *Descriptive statistic characterising data spread around mean VEGF levels present in each of the 4 wound bed biopsies. Data is recorded in units of pg/ml/mg of tissue.*

Bed	2hrs	4hrs	6hrs	8hrs
Mean	16.34	19.80	27.00	32.13
Median	14.94	22.54	33.07	34.22
SD	15.17	12.27	17.39	18.13
Range	52.18 (0-52.18)	40.60 (0.64-41.24)	52.54 (1.32-53.86)	63.50 (1.21-64.71)
CI (95%) ±	9.64	7.80	11.05	11.52

Figure 4.23.4*: Scatter graph depicting data spread of VEGF levels present in 12 tissue segments taken from 4 wound bed biopsies*

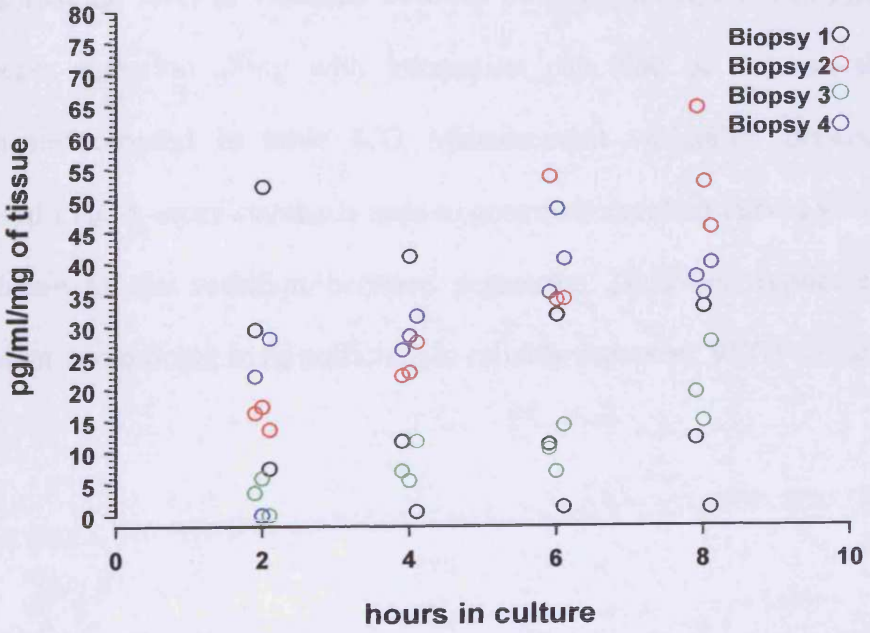

Figure 4.23.5 (a-d) represents the levels of VEGF detected in tissue segments from 4 individual wound bed biopsies. It demonstrates a marked intra-biopsy variation in VEGF levels, which is particularly evident in biopsy 1 figure 4.23.5(a). Except in biopsy 1 an overall increase in VEGF levels is observed in all of the tissue segments within each of the individual wound edge biopsies. Figure 4.23.5 also allows comparison of intra-biopsy variation with inter-biopsy variation which is more clearly illustrated in figure 4.23.6.

It appears that inter-biopsy variation in VEGF levels is greater than intra-biopsy variation and is probably the greater contributor to the wide variation in levels of VEGF described in figure 4.23.4. This was confirmed by analysis of variance detailed in table 4.32. A statistically significant level of inter-biopsy variation relative to intra-biopsy variation was found ($p=0.009$). In addition a highly statistically significant interaction ($p<0.001$) between biopsies and time was found showing that the level of variation between biopsies increased with time. Inter and intra-biopsy variation along with interaction can also be seen in the variance components recorded in table 4.32 Measurement variability between replicate samples of ELISA assay standards used to construct standard curves was found to be low relative to the variation between segments. Thus one replicate of culture supernatant was thought to be sufficient to reliably represent VEGF values.

Figure 4.23.5: *Line graphs depicting VEGF levels present in tissue segments taken from 4 individual wound bed biopsies*

(a) Biopsy 1

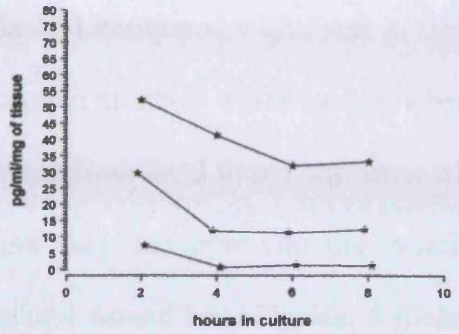

(b) Biopsy 2

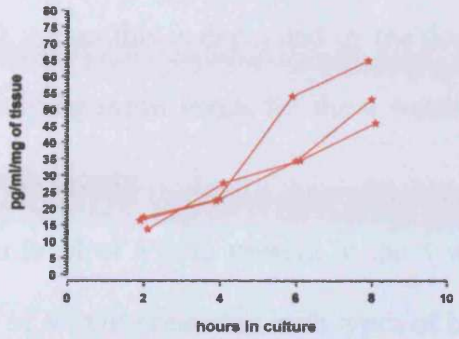

(c) Biopsy 3

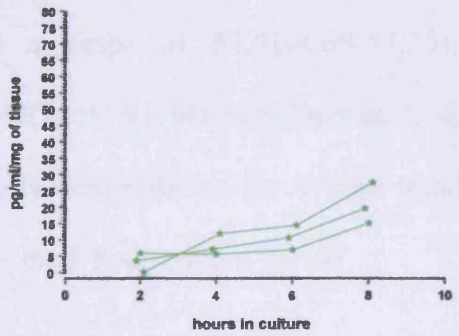

(d) Biopsy 4

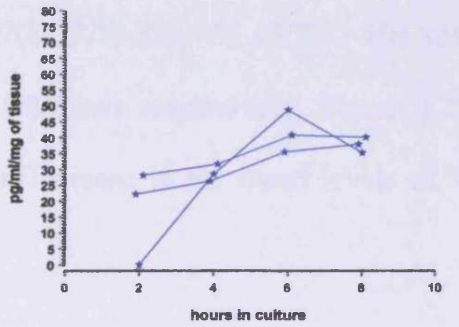

Inter-biopsy variation is more clearly shown in figure 4.23.6. Figure 4.23.6 represents the mean VEGF levels present in the two tissue segments taken from each of the 4 individual wound edge biopsies and therefore the mean levels in each biopsy. The variation in VEGF levels between biopsies is statistically summarised in table 4.31.

Large values for the range seen in table 4.31 indicate that the mean levels of VEGF in each biopsy varies widely at each of the 2 hour time points. This wide range is also represented by a wide data spread around the mean characterised by large SD

values and wide confidence intervals at the 95% level. The data is normally distributed at all time points based on similar mean and median values recorded in table 4.31. The mean VEGF levels for the 4 wound edge biopsies increases from 18.83 at 2 hours to 32.13 pg/ml/mg at 8 hours. Wider confidence intervals are seen in table 4.31 compared with those in table 4.30. Again this is explained by the decrease in sample number, which occurs when calculating mean levels for the 4 wound bed biopsies from the 3 tissue segments within each biopsy.

Figure 4.23.7(a) represents the overall mean level of VEGF present in the 4 wound edge or 4 wound bed biopsies. A mean level of VEGF present in both types of biopsy tissue is also displayed as an indication of the overall level of VEGF likely to be detected in wound tissue biopsies using this explant culture method. This mean level had a range of 52.51(4.69-57.20), 67.57(6.25-73.83), 97.15(7.67-104.82) and 80.47(10.97-91.44) pg/ml/mg at 2, 4, 6 and 8 hours respectively. Figure 4.23.7(a) clearly demonstrates the overall trend for an increase in the mean levels of VEGF over the 8 hour culture period

Table 4.31: *Descriptive statistic characterising data spread around mean VEGF levels present in each of the 4 wound bed biopsies. Data is recorded in units of pg/ml/mg of tissue.*

Bed	2hrs	4hrs	6hrs	8hrs
Mean	18.83	19.80	27.00	32.13
Median	20.45	21.07	27.85	29.24
SD	11.08	8.97	16.57	17.68
Range	25.03(4.69-29.72)	20.73(8.15-28.89)	31.07(10.60-41.67)	38.94(15.56-54.50)
CI (95%) ±	17.64	14.27	26.37	28.13

Figure 4.23.6: Line graph depicting mean VEGF levels present in each of the 4 wound bed biopsies

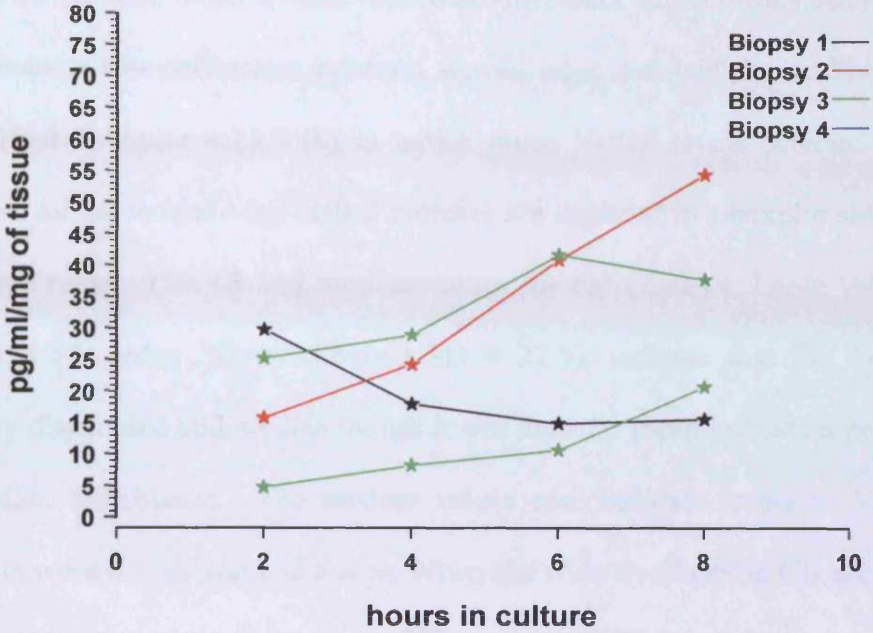

Table 4.32: Analysis of variance for VEGF levels present in wound edge and bed tissue over 8 hours.

Variance & Time		Wound Edge		Wound Bed	
		Biopsy	Segment	Biopsy	Segment
2hrs	Variance Component	450.8	200.6	44.5	173.9
	%Variance Component	69.2	30.8	20.4	79.6
4hrs	Variance Component	822.9	316.4	41.6	116.5
	%Variance Component	72.2	27.8	26.3	73.7
6hrs	Variance Component	1761.1	501.2	239.0	106.9
	%Variance Component	77.8	22.1	69.1	30.9
8hrs	Variance Component	918.6	793.0	279.1	100.2
	%Variance Component	53.7	46.3	73.6	26.4

There also appears to be a higher level of VEGF detected in the wound edge tissue particularly in the later time points. However, the wide spread and non normality of the data distribution indicates that this small difference in the means can not be taken to represent a true difference between wound edge and bed tissue. This is further exemplified in figure 4.23.7 (b) in which mean VEGF levels detected at all time points for all the wound edge or bed biopsies are depicted in a boxplot along with the associated range, 95% CI and median values for each dataset. Large values for the range and SD (edge SD = 22.6 bed SD = 22.5), indicate that the data was not normally distributed and median values lower than the mean indicate a positive skew to the data distribution. The median values also indicate levels of VEGF to be similar in wound edge and bed tissue. When the wide overlapping CIs are considered there is very little evidence for a true difference in VEGF levels between wound edge and bed tissue.

Figure 4.23.7(a): *Bar graph depicting overall mean VEGF levels present in 4 wound edge or wound bed biopsies. A plot of the mean value present in both types of tissue is also displayed*

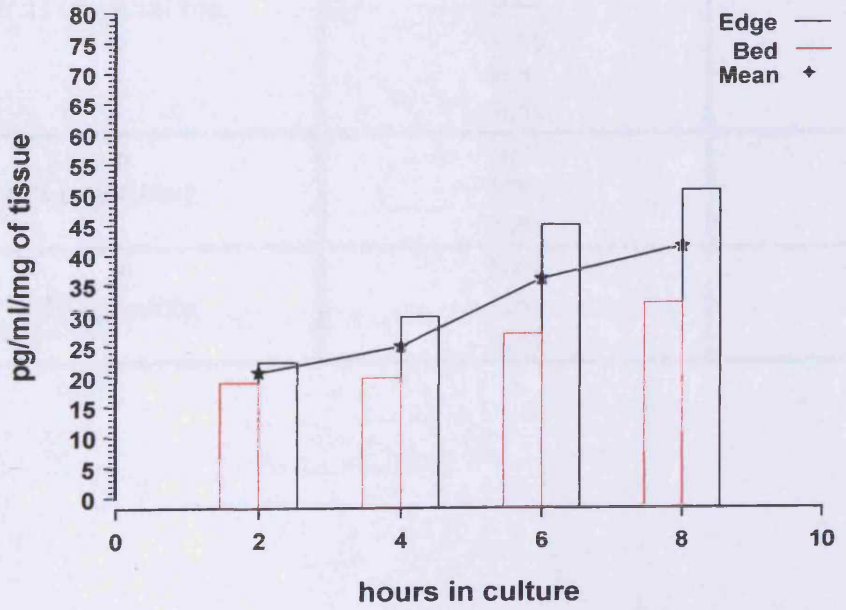

Figure 4.23.7(b): Overall levels of VEGF present in wound edge or bed tissue at all the time points during the 8 hour culture. Mean VEGF levels are plotted with their 95% CIs. Box plots represent the range and median values for each dataset

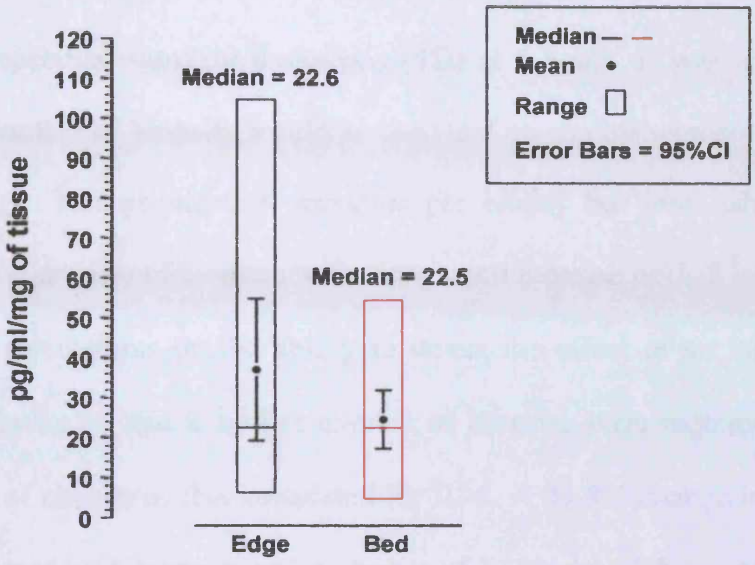

Table 4.33: Power calculations of number of biopsy required for further investigation

No. Segments/biopsy	% difference to detect	No. of biopsies
4	10%	80
	15%	37
SD = 1116 pg/ml/mg	20%	22
	30%	11
	40%	7
	50%	5
6	10%	54
SD = 911pg/ml/mg	15%	25
	20%	15
8	10%	41
SD = 789 pg/ml/ng	15%	20
	20%	12

Table 4.33 shows the power calculations based on 80% power of detecting a specified increase in IL-8 levels using a 2-sided test at the 5% level of significance. These calculations assumed a mean IL-8 expression of 3559.04 pg/ml/mg and the above specified standard deviations (SD) at 6 hours. It was agreed that for future experiments bed biopsies would be used and no control segments would be taken for histology. This provided 4 segments per biopsy but from table 33 it would still require a large no of biopsies to detect a small increase in IL-8 levels.

Power calculations on the ability to detect the effect of an intervention on TGFβ levels indicated that a similar number of biopsies were required to detect a similar degree of change as that calculated for IL-8. A 41.8% change in TGFβ levels could be detected by 8 biopsies and a change of 32.5% by 12 biopsies. These calculations were based on 80% power of detecting a change in TGFβ levels using a 2 sided test at the 5% level of significance, assuming a mean of 33.39 pg/ml/mg and a SD of 10.63 at 8 hours

4.4.1.7: Histology of control (time 0 hours) and 8hour explant culture tissue

Time 0 control tissue segments from each of the wound edge and bed biopsies were snap frozen and stored in liquid nitrogen. Frozen sections (6μm) were then cut and immunohistochemically stained with a panel of antibodies against CD markers expressed on inflammatory cells present in the wound edge or bed tissue. Having been cultured for 8 hours in normal medium, the remaining tissue segments from each biopsy were also snap frozen and prepared for staining with the same antibody panel. Wound edge and bed biopsies were taken as a matched pair from each of the 4 chronic venous leg ulcer wounds studied. Inflammatory cells expressing each

specific CD antigen were identified within the frozen sections by light microscopy and the numbers counted using the procedures outlined in the methodology.

Cell numbers detected in each tissue segment are recorded in tables 4.34-4.37 as mean number of cells per field of view (x 40 lens magnification) in each tissue section. CD68 and CD35 positive cells were present in too high a number to allow visualisation of individual cells and therefore were not suitable for counting. Instead, tissue sections stained with anti-CD68 and CD35 antibodies were graded for the degree of immunoreactivity present. This was done using a visual analogue grading scale of 1 to 5, where 1 represented minimal degree of staining and 5 represented the maximal degree of staining. This data is again recorded in tables 4.34-4.37.

Biopsies 1-4 in tables 4.34-4.37 refer to the same biopsies 1-4 described in previous sections on measurement of IL-8 and IL-1 levels present in wound edge and bed tissue. However, biopsies 1-4 only refer to the same biopsies used in the measurement of MMP-9 and MMP-2 in wound bed tissue. In addition, wound edge biopsies 4 and 3 refer to the same biopsies recorded as wound edge biopsies 2 and 3 respectively in the analysis of MMP-9 and 2 levels described in section 4.4.1.3 and 4.4.1.4. The cell type identified by each CD surface antigen is listed in table 3.2 recorded in the methodology.

It is clear from tables 4.34-4.37 that marked differences in leucocyte cell numbers can exist between tissue segments from the same biopsy in both wound edge and wound bed tissue. This was particularly noticeable in wound edge biopsy 1 and 2 in which tissue segments time 0 hours and wound edge segment 2 respectively, were found to contain markedly greater leucocyte cell numbers compared to the other tissue segments within the same biopsies. However, when the tissue segments

producing the highest cytokine levels within each of the biopsies studied in sections 4.4.1.1, 4.4.1.2, 4.4.1.5 and 4.4.1.6 were compared with those found to contain the greatest leucocyte numbers, they did not correspond. Similarly, the biopsies containing the highest mean number of leucocytes recorded in tables 4.34 – 4.37 did not correspond to those found in sections 4.4.1.1, 4.4.1.2, 4.4.1.5 and 4.4.1.6 to produce the highest level of each of the cytokines analysed.

The mean number of CD68 positive macrophages present in all the tissue sections from each wound edge and bed biopsy are also recorded in tables 4.34 – 4.37. It is evident from these mean values that 3 out of the 4 wound bed biopsies contained higher numbers of macrophages than the wound edge biopsies taken from the same wound. This was reflected in a median value of 3.5 CD68 positive cells in all the wound bed tissue segments compared to 2.9 in the wound edge tissue segments as graded by the visual analogue scale. Similarly, moderately higher numbers of CD35 positive cells were found in the wound bed biopsies, again using the visual analogue scale, and was reflected by a median value of 2.75 in all the wound bed tissue segments compared to a median value of 2 in the wound edge tissue segments.

The numbers of CD3, CD4 positive and CD8 positive lymphocytes present in wound edge and bed tissue taken from each wound are recorded in tables 4.34 – 4.37 and graphically represented in figure 4.24.1 and 4.24.2. The mean number of CD3 positive lymphocytes, were found to be higher in the wound edge tissue of 3 out of the 4 wounds studied as demonstrated in figure 4.24.1. This was reflected by a median value of 8.4 for all the wound edge tissue studied compared with a median value of 7.4 for the wound bed tissue studied. The median value is a better indicator of the difference between the two tissue locations, as unlike the mean it is not influenced by the large data spread represented by the large SD values recorded in

tables 4.34 – 4.37. Overall, numbers of CD4 positive lymphocytes were higher than CD8 lymphocyte numbers in the majority of the wound edge and bed biopsies, which is evident from the mean numbers graphically depicted in figure 4.24.2. Furthermore, the mean numbers of CD4 and CD8 positive lymphocytes was higher in wound edge tissue in 3 out of the 4 wounds studied. As there was a wide spread around the mean indicated by the large SD values recorded in tables 4.34 – 4.37 the median values of 4.1 for wound edge tissue compared to 3.3 for wound bed tissue are a better measure of this difference. CD8 positive lymphocytes were also present in higher numbers in the wound edge tissue of 3 out of the 4 wounds studied, which can be seen graphically in figure 4.24.2 and represented by a median value of 2.1 for wound bed tissue and 3.1 for wound edge tissue. However, the CD4/CD8 ratio was found to be higher in wound bed tissue with a median value of 1.8 compared to 1.3 in wound edge tissue.

Table 4.34: *Leucocyte cell numbers in chronic wound edge and bed biopsies recorded as mean number of cells per x40 field of view. Figures in parantheses represent the* range (R) and standard deviation (SD). *NS = not stained*

Cell marker	Edge Biopsy 1				Bed Biopsy 1				
	ETO (R)	E1 (R)	E2 (R)	Mean (SD)	BTO (R)	B1 (R)	B2 (R)	B3 (R)	Mean (SD)
CD68	4	3	4	3.7	5.0	4	2	3	3.5
CD35	NS	NS	NS	NS	3	3-4	3	2	2.9
CD3	53.3 (2-260)	24.6 (0-101)	18.1 (2-56)	32.0 (18.8)	12.1 (0-57)	7.9 (2-23)	13.0 (0-58)	13.1 (2-23)	11.5 (2.4)
CD4	55.0 (6-29)	7.4 (0-64)	14.3 (4-34)	25.6 (25.7)	9.1 (0-45)	7.1 (0-21)	7.0 (0-24)	10.5 (1-36)	8.4 (1.7)
CD8	38.5 (7-176)	10.2 (0-53)	11.7 (0-35)	20.1 (15.9)	4.6 (0-20)	3.9 (0-11)	3.6 (0-13)	4.3 (0-12)	4.1 (0.4)
CD4/8	1.4	0.7	1.2	1.1	2.0	1.8	1.9	27.9	2.0

Table 4.35: *Leucocyte cell numbers in chronic wound edge and bed biopsies recorded as mean number of cells per x40 field of view. Figures in parantheses represent the* range (R) and standard deviation (SD). *NS = not stained*

Cell marker	Edge Biopsy 2				Bed Biopsy 2				
	ETO (R)	E1 (R)	E2 (R)	Mean (SD)	BTO (R)	B1 (R)	B2 (R)	B3 (R)	Mean (SD)
CD68	2	3	3	2.7	2	3	4	3	3
CD35	1	1	2	1.3	3	1	3-4	2	2.4
CD3	3.8 (0-24)	14.8 (0-103)	68.5 (6-169)	29.0 (34.6)	0.0	7.5 (0-58)	4.9 (0-12)	1.5 (0-6)	3.5 (3.4)
CD4	4.5 (0-17)	5.4 (0-42)	32.6 (2-90)	14.2 (16.0)	0.0	2.6 (0-18)	1.8 (0-8)	1.3 (0-8)	4.4 (5.1)
CD8	2.7 (0-26)	6.9 (0-75)	16.1 (0-48)	8.5 (6.8)	0.0	1.6 (0-8)	1.3 (0.5)	3.0 (1-5)	1.5 (1.2)
CD4/8	1.7	0.8	2.0	1.5	0.0	1.6	1.5	0.4	1.2

Table 4.36 *Leucocyte cell numbers in chronic wound edge and bed biopsies recorded as mean number of cells per x40 field of view. Figures in parantheses represent the range (R) and standard deviation (SD). NS = not stained*

Cell marker	Edge Biopsy 3				Bed Biopsy 3				
	ETO (R)	E1 (R)	E2 (R)	Mean (SD)	BTO (R)	B1 (R)	B2 (R)	B3 (R)	Mean (SD)
CD68	1	3	3	2.3	4	3	3	3	3.3
CD35	1	2	2	1.7	3	1	2	2	2
CD3	6.9 (0-24)	7.3 (0-28)	9.4 (1-35)	7.9 (1.3)	6.7 (0-42)	4.7 (0-26)	0.0	7.3 (0-27)	4.6 (3.3)
CD4	2.2 (0-17)	3.0 (0-14)	3.8 (0-19)	3.0 (0.8)	4.3 (0-22)	2.0 (0-10)	0.0	2.0 (0-10)	2.1 (1.7)
CD8	1.9 (0-11)	3.5 (0-9)	2.6 (0-9)	2.7 (0.8)	2.2 (0-18)	1.3 (0-5)	0.0	2.1 (0-6)	1.4 (1.1)
CD4/8	1.1	0.9	1.5	1.2	1.9	1.6	0.0	1.0	1.5

Table 4.37 *Leucocyte cell numbers in chronic wound edge and bed biopsies recorded as mean number of cells per x40 field of view. Figures in parantheses represent the range (R) and standard deviation (SD). NS = not stained*

Cell marker	Edge Biopsy 4				Bed Biopsy 4				
	ETO (R)	E1 (R)	E2 (R)	Mean (SD)	BTO (R)	B1 (R)	B2 (R)	B3 (R)	Mean (SD)
CD68	4	1-2	3	2.8	4	5	4	4-5	4.4
CD35	2	1-2	2	1.8	2-3	3	3	2	2.6
CD3	6.7 (0-26)	5.0 (0-18)	3.1 (0-7)	4.9 (1.8)	8.4 (0-52)	14.1 (0-131)	0.4 (0-2)	8.0 (0-75)	7.7 (5.6)
CD4	2.6 (0-20)	2.8 (0-11)	2.1 (0-6)	2.5 (0.4)	4.1 (0-23)	4.4 (0-19)	0.0	4.5 (0-28)	3.3 (2.2)
CD8	1.9 (0-6)	2.2 (0-10)	1.0 (0-1)	1.7 (0.6)	2.1 (0-30)	4.0 (0-30)	0.0	1.1 (0-13)	1.8 (1.7)
CD4/8	1.3	1.3	2.1	1.6	1.9	1.1	0.0	4.2	2.4

Figure 4.24.1: Mean T lymphocyte numbers present in chronic wound edge and bed biopsies identified by their expression of the CD3 surface marker. Cell numbers are recorded as mean number of cells per x40 field of view

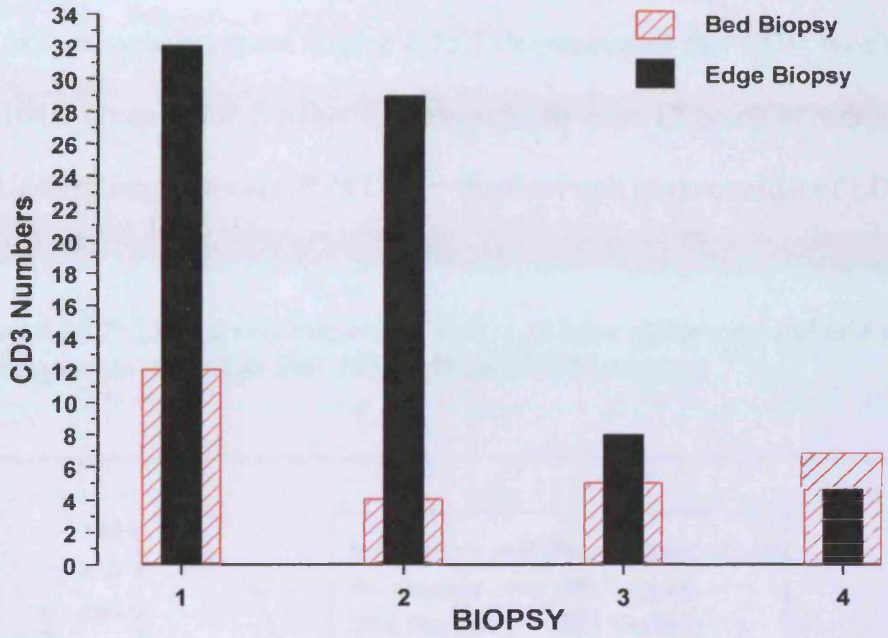

Figure 4.24.2: CD4 expressing T helper cell numbers and CD8 expressing T suppressor cell numbers present in chronic wound edge and bed biopsies. . Cell numbers are recorded as mean number of cells per x40 field of view. CD4/CD8 ratios are also recorded above each edge or bed biopsy (RT=Ratio).

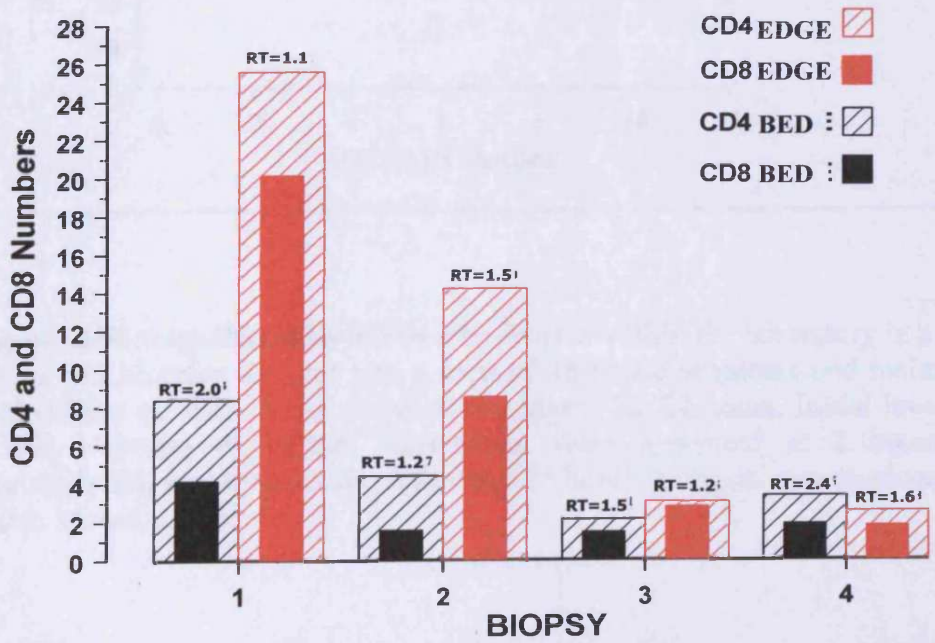

4.4.1.8 ANALYSIS OF LDH LEVELS AS A MARKER OF CELL DEATH

LDH levels detected within culture supernantants was used as a marker of cell death occurring within each tissue segment cultured over 12 hours in 0%, 10%, 20% or 95% oxygen concentration. Figure 4.25.1 demonstrated that LDH levels of between 73.9-104.9 measured at 2 hours fell dramatically over 12 hours to between 15.4-33.3 B-B Units/ml/mg of tissue (B-B Unit = standard unit measurement of LDH activity).

Figure 4.25.1: *LDH levels measured over a 12 hour culture period in 4 wound bed tissue segments placed in 0%, 10%, 20% and 95% oxygen.*

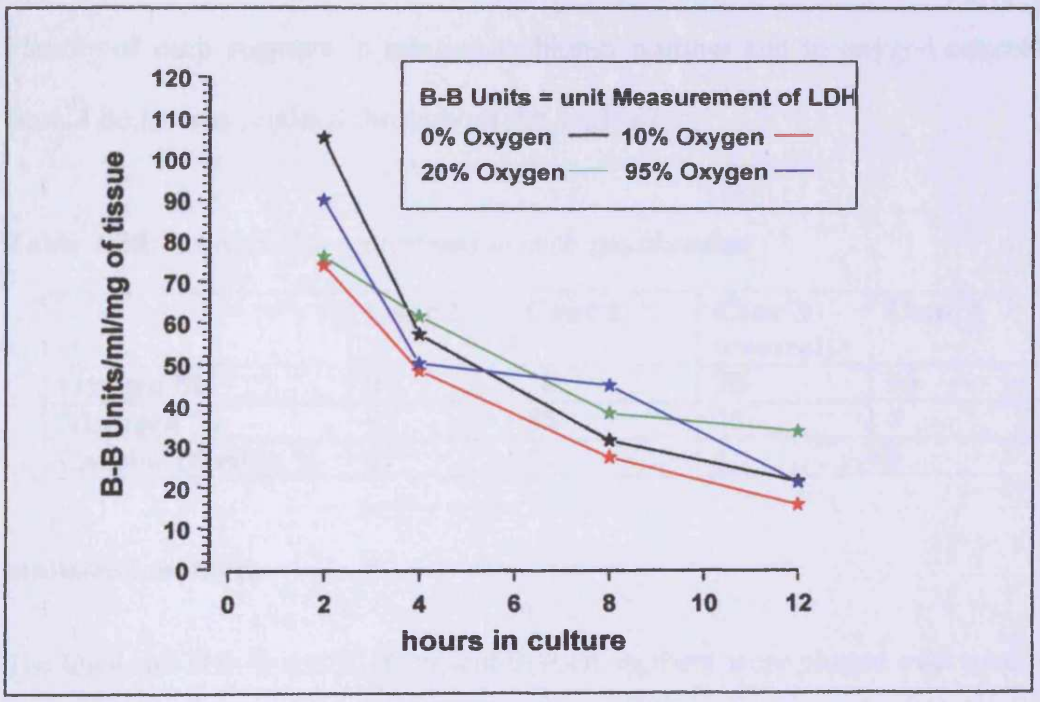

Levels of LDH were also analysed by a co-worker within the laboratory in a series of 6 wound bed biopsies divided into a total of 18 tissue segments and maintained in normal culture medium under standard conditions for 24 hours. Initial levels of 25-310 B-B Units/ml of culture supernatant were measured at 2 hours, which subsequently fell rapidly over the following 24 hours (personal communication from Dr Keith Moore).

4.4.2.0 Effect of changing oxygenation levels on IL-8 and TGF-β levels in wound bed tissue.

A study of wound bed biopsies taken from patients with chronic venous leg ulcers was undertaken. Each biopsy was dissected into 4 segments. The culture media from each segment was assayed at 2 and 4 hours for the levels of IL-8 (6 biopsies studied) and TGF-β (8 biopsies studied). At 4 hours, the four individual segments from each biopsy were placed in different oxygen chambers, each chamber containing different percentage concentrations of oxygen, which are shown below in table 4.38. The culture media from each segment was then assayed again at 8 and 12 hours. The identity of each segment in relation to biopsy number and to oxygen concentration from 4 hours was retained throughout the analysis.

Table 4.38: Oxygen Concentrations in each gas chamber

	Conc 1	**Conc 2**	**Conc 3 (control)**	**Conc 4**
Oxygen %	0	10	20	95
Nitrogen %	95	85	75	0
Carbon Dioxide %	5	5	5	5

Statistical methods

The levels of TGF-β and IL-8 present in each segment were plotted over time, shown in figures 4.26.1 and 4.27.1 respectively. The design was to analyse within biopsy levels of TGF-β and IL-8, whereby the variability between biopsies was removed.

Firstly, *analysis of variance* models were fitted to the responses of IL-8 and TGF-β levels with terms entered for biopsy and oxygen concentration at each time point. This was to determine the extent of the difference between segments and oxygen concentrations at each time point on a within biopsy basis.

Primary Analysis

The 4-hour time point was taken to represent the baseline IL-8 and TGF-β levels present in untreated segments. The extent of the change in levels between 4 and 8 hours and also between 4 and 12 hours was assessed. This was to determine if there was a statistically significant change in levels in response to treatment with different oxygen concentrations at 4 hours, after adjusting for the control levels present up until 4 hours. Analysis of variance models were fitted to both these responses with terms entered for biopsy, levels at 4 hours and oxygen concentration.

In addition, the extent of change in levels at different oxygen concentrations over time, without adjusting for the baseline levels was determined. Again, an analysis of variance was conducted on both these responses with terms entered for biopsy and oxygen concentration.

4.4.2.1 EFFECT OF CHANGING OXYGEN CONCENTRATIONS ON TGF-β LEVELS

TGF-β levels decreased over time in all biopsies regardless of surrounding oxygen concentration. This is graphically depicted in figure 4.26.1 and table 4.39 shows the mean TGF-β levels at each concentration also graphically depicted in figure 4.1.58. The extent of the difference in TGF-β levels between segments cultured in different oxygen concentrations also reduced over time (table 4.38). The mean TGF-β levels along with the data spread at each time point and at each %oxygen concentration is displayed in figure 4.26.2. This again demonstrates a general decrease in TGF-β levels in segments cultured in any of 4 different oxygen concentrations over a 12 hour culture period.

There was a high significant difference in levels of TGF-β between segments within biopsies at 2 and 4 hours ($p<0.001$), indicating a chance imbalance present in the segments allocated to each oxygen concentration group before entering the test period between 4 and 12 hours. This is related to the inherent intra-biopsy variation in TGF-β levels characterised in the previous section. It was apparent from the plot of TGF-β levels over time displayed in figure 4.26.1, that the extent of reduction in TGF-β levels in segments cultured in different oxygen concentration varied over time. The greatest reduction generally occurred in the segment that had the highest 4 hour levels of TGF-β.

Change in TGF-β expression between 4 and 8 hours

When taking into account the TGFβ levels at 4 hours and then looking at the effect of oxygen concentration, there was no statistically significant difference in TGF-β levels detected in segments cultured in different oxygen concentrations. ($p=0.206$) (table 4.40). The mean change in TGF-β expression was comparable across all oxygen concentrations. This suggests that when comparing the extent of reduction in TGF-β levels between different oxygen concentrations, any difference was attributable to the baseline level of TGF-β at 4 hours and not to the effect of oxygen concentration itself.

The mean decrease in TGF-β levels was greater in 20% oxygen concentration than in 0%, 10% and 95% oxygen (table 4.41). The decrease in levels from 4 to 8 hours was statistically significant for 0%, 10% and 20% oxygen but not for 95% oxygen. When studying the absolute change between 4 and 8 hours (i.e. without adjusting for baseline TGF-β levels), there was a statistically significant effect of oxygen on TGF-β levels ($p=0.048$). However, this significant change can be attributed to the inherent

imbalance in TGF-β levels and not to the effect of oxygen concentration itself. The inherent imbalance meant that variation in TGF-β levels was initially present before comparison between the oxygen concentration groups.

Change in TGFβ expression between 4 and 12 hours

Again, when taking into account the TGF-β levels present in all segments at 4 hours and then looking at the effect of changing oxygen concentration, there was no statistically significant difference between levels of TGF-β present in segments cultured in differing oxygen concentrations (p=0.676) (table 4.42). Therefore, the size of the reduction in TGF-β levels present in segments cultured in any of the oxygen concentrations, can be explained by the TGF-β level present at 4 hours.

The mean decrease in TGFβ concentration. was greatest in 20% oxygen concentration compared to 0%, 10% and 95% oxygen (table 4.43). Again, the change in levels from 4 hours to 12 hours was statistically significant for 0%, 10% and 20% oxygen concentrations but no for 95% oxygen.

There was a statistically significant difference in the extent of the absolute change in TGFβ levels in tissue cultured in different oxygen concentrations between 4 and 12 hours (p=0.028). However, again this significant change can be attributed to the inherent imbalance in TGFβ levels initially present in the tissue segments and not to the effect of oxygen concentration itself.

In biopsy 3 depicted in figure 4.26.1 (c) it was possible to dissect an extra tissue segment which was then cultured in room air over the same time course as the other tissue segments placed in the different oxygen concentrations. The TGF-β levels

detected in this tissue segment had a similar profile to those detected in the 20% oxygenated tissue segment and were quantitatively closer to the 20% oxygenated tissue segment than those segments cultured in 0, 10 and 95% oxygen. As this was the only biopsy where an extra segment was available, this could not be statistically tested but the raw data suggests that culturing in oxygenated chambers does not in itself have an effect on the tissue.

Figure 4.26.1: *TGF-β levels in 8 individual wound bed biopsies with 4 segments from each allocated for culture in 0%, 10%, 20% and 95% oxygen after 4 hours. In biopsy 3 an extra segment is included providing data on culture in atmospheric air.*

(a) Biopsy 1

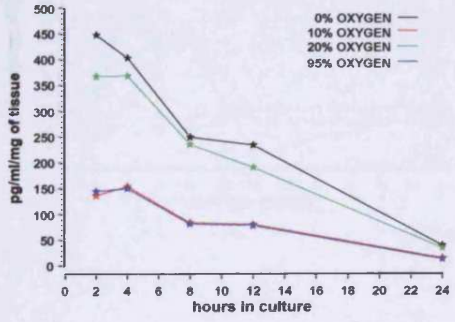

(b) Biopsy 2

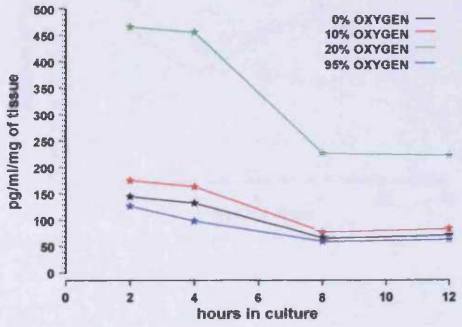

(c) Biopsy 3

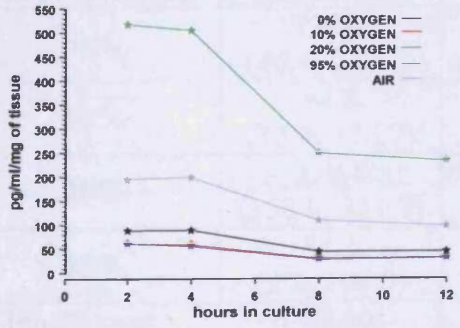

(d) Biopsy 4

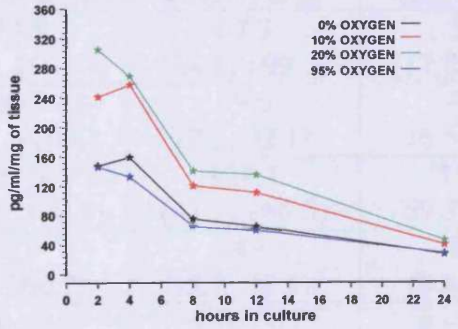

(e) Biopsy 5

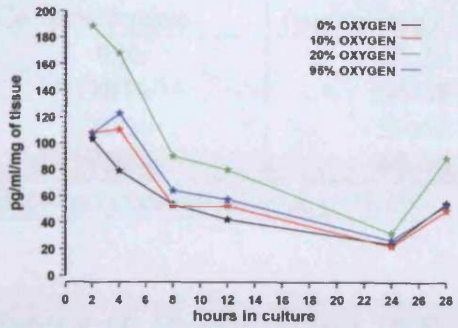

(f) Biopsy 6

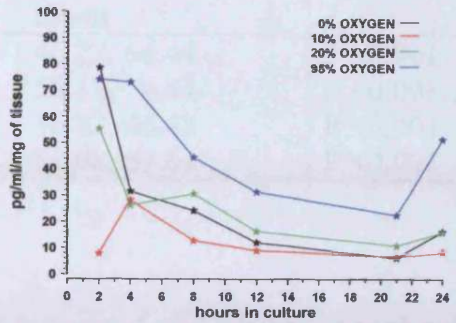

(g) Biopsy 7

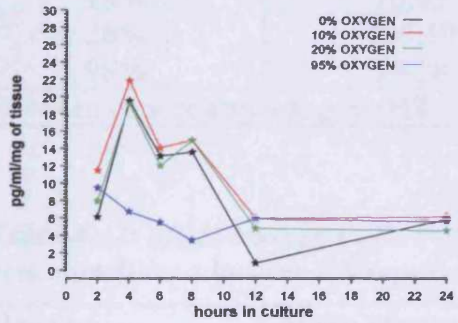

(h) Biopsy 8

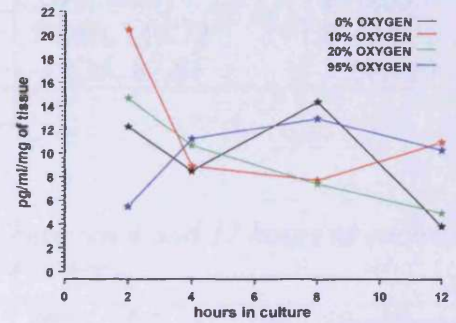

Table 4.39: *Mean TGF-β levels at all Oxygen concentrations (95% CIs of the mean).*

Oxygen Concentration	2 hours (pg/ml/mg)	4 hours (pg/ml/mg)	8 hours (pg/ml/mg)	12 hours (pg/ml/mg)
0%	128.2 (46.4, 210.1)	114.9 (35.2, 194.7)	67.3 (24.8, 109.7)	59.0 (17.8, 100.2)
10%	94.8 (12.9, 176.7)	100.1 (20.3, 179.8)	49.6 (7.2, 92.1)	47.7 (6.5, 88.9)
20%	239.8 (158.0, 321.7)	227.3 (147.5, 307.1)	124.1 (81.7, 166.5)	110.7 (69.5, 151.9)
95%	84.1 (2.2, 166.0)	80.9 (1.1, 160.7)	44.6 (2.2, 87.1)	41.8 (0.6, 83.0)
Significance	p <0.001	p <0.001	p <0.001	p <0.001

Table 4.40: *Mean change in TGF-β levels between 4 and 8 hours for each oxygen concentration adjusting for expression at 4 hours.*

Oxygen Concentration	Mean change (pg/ml/mg)	95% CI of the mean	Significance
0%	55.33	46.22, 64.44	P <0.001
10%	65.28	56.11, 74.44	P <0.001
20%	56.62	46.82, 66.43	P <0.001
95%	60.36	51.08, 69.64	P <0.001
Between concentrations, p=0.206			

Table 4.41: *Mean change in TGF-β levels between 4 and 8 hours at each oxygen concentration.*

Oxygen Concentration	Mean change (pg/ml/mg)	95% CI of the mean	Significance
0%	47.67	1.14, 94.20	P=0.045
10%	50.45	3.92, 96.97	P=0.035
20%	103.19	56.66, 149.72	P <0.001
95%	36.28	-10.25, 82.81	P =0.120
Between concentrations, p=0.048			

Table 4.42: *Mean change in TGF-β levels between 4 and 12 hours at each oxygen concentration, adjusting for expression at 4 hours*

Oxygen Concentration	Mean change (pg/ml/mg)	95% CI of the mean	Significance
0%	63.96	56.79, 171.12	P <0.001
10%	67.85	60.64, 75.06	P <0.001
20%	67.86	60.12, 75.61	P <0.001
95%	64.34	57.02, 71.65	P <0.001
Between concentrations, p=0.676			

Table 4.43: *Mean change in TGF-β levels between 4 and 12 hours at each oxygen concentration, without adjusting for expression at 4 hours*

Oxygen Concentration	Mean change (pg/ml/mg)	95% CI of the mean	Significance
0%	55.95	8.14, 103.75	P=0.024
10%	52.34	4.53, 100.14	P=0.033
20%	116.57	68.77, 164.38	P <0.001
95%	39.15	-8.66, 86.95	P=0.103
Between concentrations, p=0.028			

***Figure 4.26.2**: Scatter graph depicting the spread of TGF-β levels present in 32 segments taken from 8 biopsies cultured over 12 hours. One tissue segment from each biopsy was allocated for culture with either 0%, 10%, 20% or 95% oxygen after the 4 hour control period*

(a) 0% oxygen

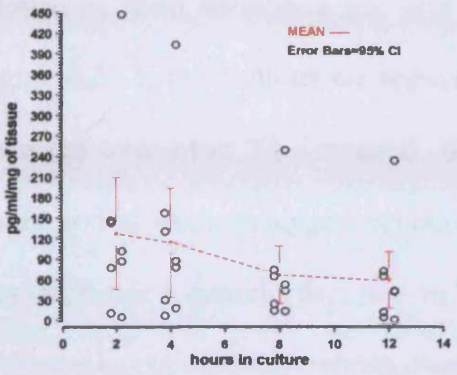

(b) 10% oxygen

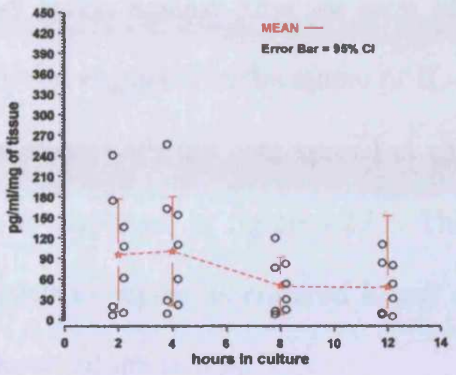

(c) 20% oxygen

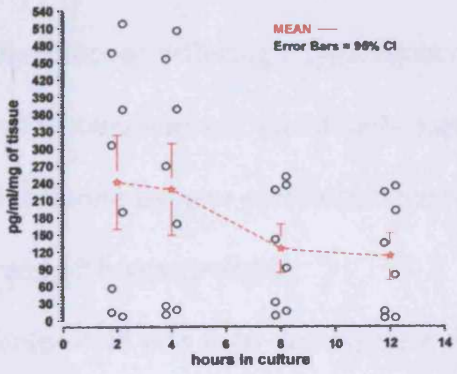

(d) 95% oxygen

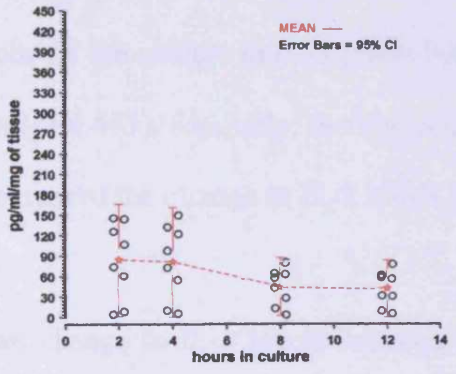

4.4.2.2 Effect of changing oxygen concentrations on IL-8 levels

The mean IL-8 levels generally decreased over time at all oxygen concentrations, with a marked decrease within biopsies occurring between 4 and 8 hours (table 4.44). However, from observing the plot of IL-8 levels against time for each biopsy in figure 4.27.1, fluctuations are apparent between segments in the extent of IL-8 levels detected over time. The mean IL-8 levels along with the data spread at each time point and at each %oxygen concentration is displayed in figure 4.27.2. This again demonstrates a general decrease in IL-8 levels in segments cultured in any of the 4 different oxygen concentrations over a 12 hour culture period.

Change in IL8 expression between 4-8 hours and 4-12 hours

The effect of differing oxygen concentrations on the change in IL-8 levels between 4 and 8 hours was not statistically significant ($p=0.633$). Similarly, there was no effect of differing oxygen concentrations on the extent of the change in IL-8 levels between 4 and 12 hours ($p=0.60$).

Tables 4.45 and 4.46 demonstrate the mean change in IL-8 levels between 4 and 8 hours, and between 4 and 12 hours for each oxygen concentration. At each concentration the extent of the change in mean levels was not significant either between 4 and 8 hours or between 4 and 12 hours. Figure 4.27.1 shows that the extent of the change in IL-8 levels over time at each oxygen concentration varied between biopsies. However, this is again related to the high inter-biopsy variation demonstrated to be present in this culture system and which was described in the previous section

In biopsy 2 and 3 depicted in figure 4.27.1 (b and c) it was possible to dissect extra tissue segments which were then cultured in room air over the same time course as

the other segments placed in differing oxygen concentrations. The IL-8 levels detected in these 2 tissue segments have a similar profile to those detected in the 20% oxygenated segments from within their own biopsies. In biopsy 2 the values were quantitatively closer to those detected in the segment cultured in 20% oxygen than segments cultured in 0, 10 and 95% oxygen. As there were only two biopsies where an extra tissue segment was available, this data could not be statistically tested. However, the raw data itself suggested that culturing in oxygenated chambers did not in itself have an effect on the tissue in terms of IL-8 production.

Figure 4.27.1: *IL-8 levels in 6 individual wound bed biopsies with 4 segments from each allocated for culture in 0%, 10%, 20% and 95% oxygen after 4 hours. In biopsy 2 & 3 an extra segment is included providing data on culture in atmospheric air.*

(a) Biopsy 1

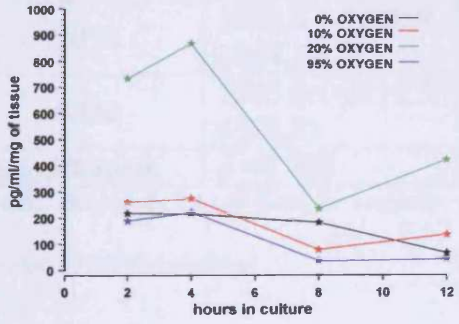

(b) Biopsy 2

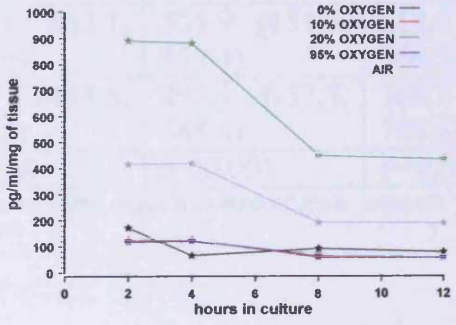

(c) Biopsy 3

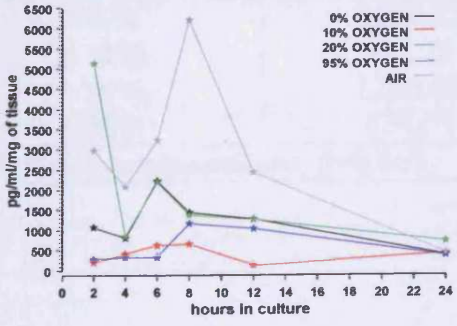

(d) Biopsy 4

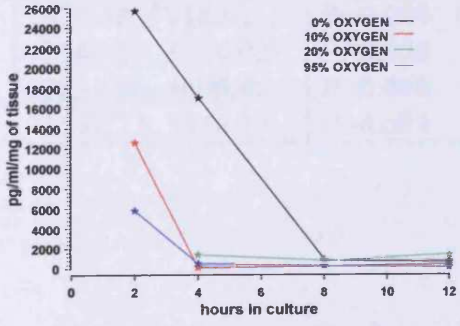

(e) Biopsy 5

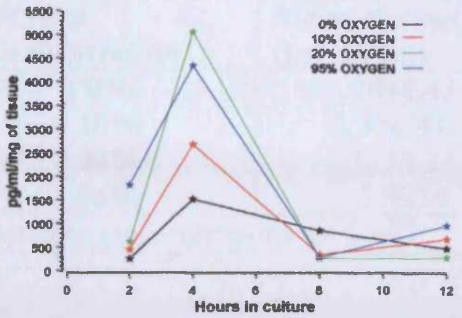

(f) Biopsy 6

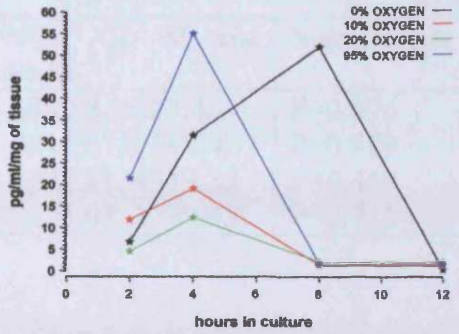

Table 4.44: *Mean IL-8 levels at all Oxygen concentrations (95% CIs of the mean).*

Oxygen Conc.	2 hours (pg/ml/mg)	4 hours (pg/ml/mg)	8 hours (pg/ml/mg)	12 hours (pg/ml/mg)
0%	455.9 (-610.5, 9722.2)	3264.2 (910.7, 5617.8)	566.6 (215.2, 918.1)	419.8 (73.1, 766.5)
10%	2253.9 (-2912.4, 7420.3)	592.6 (-1760.9, 2946.1	219.9 (-131.6, 571.3)	226.2 (-120.5, 572.9)
20%	3662.8 (-1638.9, 8964.5)	1491.1 (-862.1, 3844.9)	505.9 (154.5, 857.4)	618.0 (271.3, 964.7)
95%	1355.0 (-3811.3, 6521.3)	918.0 (-1435.5, 3271.5)	293.9 (-57.5, 645.4)	361.7 (15.0, 708.4)
Significance	p =0.226	P=0.228	p <0.001	P=0.096

Note: Biopsy 4, 2 hour data for segment allocated to 20% oxygen removed from analysis (very high value ≈50,000pg/ml/mg)

Table 4.45: *Mean change in IL-8 levels between 4 and 8 hours at each oxygen concentration*

Oxygen Concentration	Mean change (pg/ml/mg)	95% CI of the mean	Significance
0%	2697.62	-523.68, 5918.91	P=0.094
10%	372.73	-2848.57, 3594.02	P=0.808
20%	1286.03	-2234.38, 4806.45	P=0.446
95%	624.08	-2597.22, 3845.37	P=0.684
Between concentrations, p=0.663			

Table 4.46: *Mean change in IL-8 levels between 4 and 12 hours at each oxygen concentration*

Oxygen Concentration	Mean change (pg/ml/mg)	95% CI of the mean	Significance
0%	2844.43	-338.58, 6027.45	P=0.076
10%	366.41	-2816.61, 3549.42	P=0.809
20%	1238.25	-2242.81, 4719.32	P=0.458
95%	556.34	-2626.68, 3739.35	P=0.713
Between concentrations, p=0.607			

Figure 4.27.2*: Scatter graph depicting the spread of IL-8 levels present in 24 segments taken from 6 biopsies cultured over 12 hours. One tissue segment from each biopsy was allocated for culture in either 0%, 10%, 20% or 95% oxygen after the 4 hour control period.*

(a) 0% oxygen

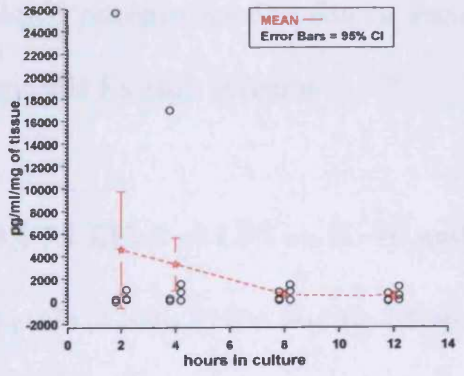

(b) 10% oxygen

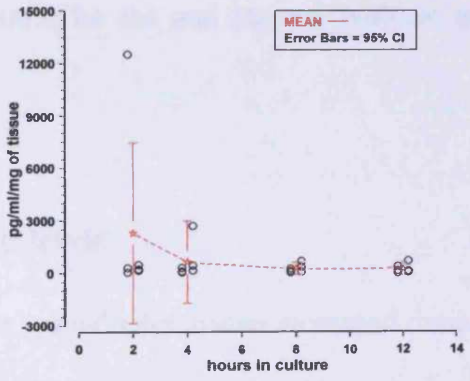

(c) 20% oxygen

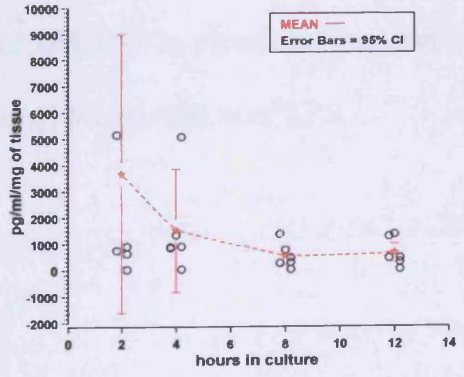

(d) 95% oxygen

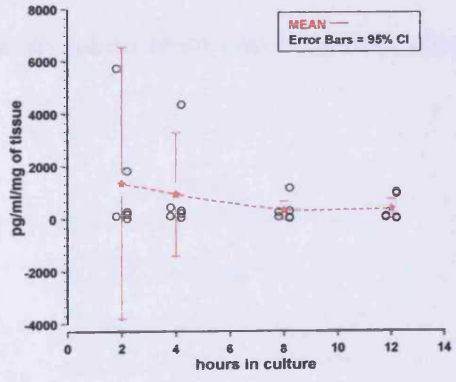

4.4.3.0 Stimulation of edge biopsies with LPS

Two wound edge biopsy taken from chronic venous leg ulcers were divided into a time 0 tissue segment a control tissue segment and a test tissue segment. The time 0 was frozen in liquid nitrogen and subsequently stained with an antibody specific for the $\alpha_5\beta_1$ integrin. The remaining biopsy tissue was split into a control segment to be cultured for 24 hours in normal culture medium and a segment to be cultured for 22 hours in medium containing LPS after initial 2 hour culture in normal medium. At 2 and 24 hours culture supernatant was removed to measure by ELISA the levels of IL-1β and TNFα present. At 2 hours LPS was added to the culture medium containing the test segment and after 24 hours in culture both tissue segments were frozen in liquid nitrogen so that frozen sections could be cut and stained with an antibody specific for $\alpha_5\beta_1$ integrin.

4.4.3.1 Effect of LPS on IL-1β and TNFα levels

Levels of both TNFα and IL-1β present in wound edge tissue increased dramatically after culture for 24hours in medium containing LPS compared with tissue cultured in normal medium. This can be seen in table 4.47 which records the mean levels of IL-1β and TNF-α present in two tissue segments taken from two biopsies cultured with or without addition of LPS.

Table 4.47: *Levels of IL-1β and TNFα present in a wound edge biopsy split into a control T0 histology tissue segment a T24hr tissue segment cultured in normal medium and T24hr tissue segment cultured in medium containing LPS. The level of $\alpha_5\beta_1$ integrin expression in the wound edge epidermis was also recorded. + = limited expression +++ = marked expression ± = no change*

Culture Conditions	**TNFα Production μg/10mg tissue**	**IL-1β Production μg/10mg tissue**	**$\alpha_5\beta_1$ Expression**
Time 0	Tissue Histology	Tissue Histology	+
24h Control	336	40.7	±
24h 10ng/ml LPS	1440	141.06	+++

4.4.3.2 Effect of LPS on $\alpha_5\beta_1$ integrin expression.

Increases in levels of TNFα and IL-1β present in wound edge tissue stimulated with LPS were mirrored by an observed increase in expression of α5β1 integrin on basal layer keratinocytes within the same wound edge tissue. In figure 4.28.1 (a) the weak expression of $\alpha_5\beta_1$ is evident (red arrows) in the zero time control segment of wound edge tissue taken from a biopsy of a chronic VLU. Another wound edge segment taken from the same biopsy and placed in normal culture medium for 24 hours is seen in figure 4.28.1 (b). Expression of $\alpha_5\beta_1$ in the epidermis of this tissue segment has not been affected by culture in normal medium and remains at the same level as that observed in the time 0 control (red arrow). These observations are consistent with the weak expression of $\alpha_5\beta_1$ found to be decreased on basal keratinocytes at the edge of chronic venous leg ulcers compared with surgically induced acute wounds (see sections 4.1.1 and 4.3.1). Figure 4.28.1 (c) demonstrates an observable increase in expression of $\alpha_5\beta_1$ in a third tissue segment taken from the same biopsy but cultured for 22 hours in medium containing LPS. A marked increase in expression is seen on the basal keratinocytes located towards the tip of the wound edge epidermis (red arrows).

Figure 4.28.1: *$\alpha_5\beta_1$ immunoreactivity within wound edge tissue taken from chronic VLU (reactivity indicated by arrows). a) T0hr control (scale bar = 100μm). b) T24hr placed in normal culture medium (scale bar =50μm) c) T24hr stimulated with LPS (scale bar = 25μm)*

(a)

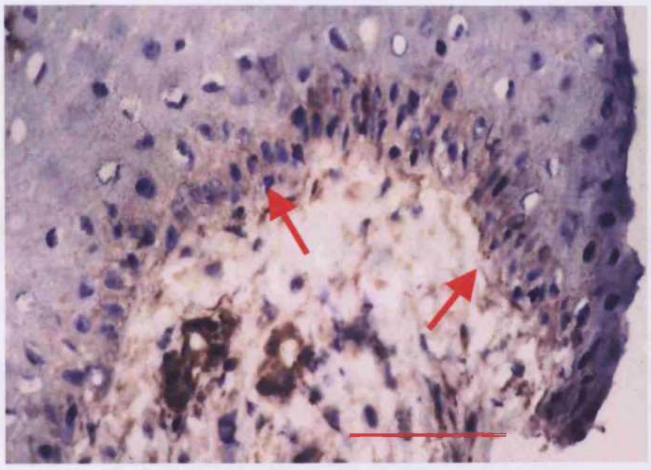

(b)

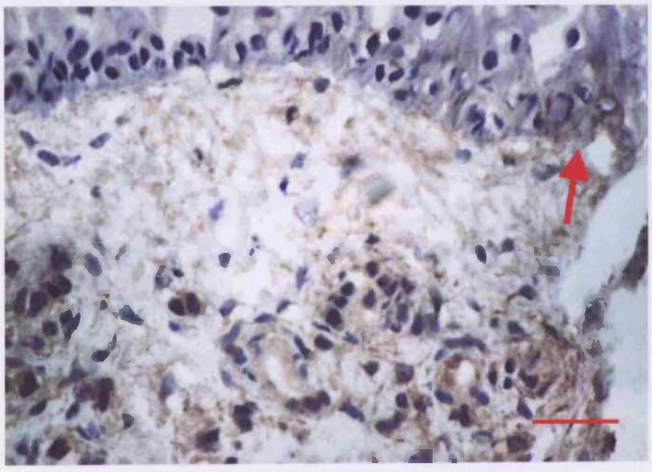

(c)

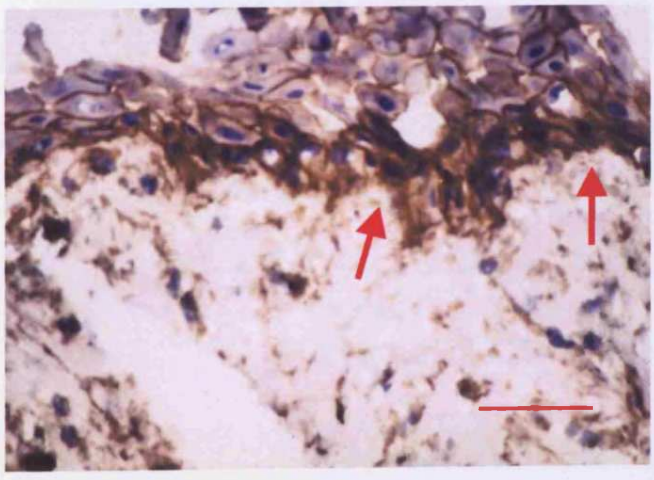

5.0 DISCUSSION

Epidermal Adhesion molecules: Acute and Chronic wound healing

This study used an *in vivo* human cutaneous wound model allowing a 96 hour time course study of the rapid healing response to acute dermal injury. In addition a limited number of biopsies were taken from the margin of healing pilonidal-excision wound tissue to allow extension of the original study in the cutaneous wound model. It is one of only a small number of studies to investigate the expression of keratinocyte integrins and extracellular matrix proteins after full thickness wounding of normal adult human skin (165-168). The difficulty in obtaining human tissue for this kind of investigation is reflected in the small number of studies to date and the small number of subjects/volunteers included in the current study (n = 8 for the cutaneous wound model). Related studies have used diverse tissue sources including the paravertebral area of pigs (31), normal human foreskin transplanted on SCID mice (261), human skin blisters (293) and human foetal skin (294). In this context, the author feels the *in vivo* model used in this study and the source of acute wound tissue were both a close representation of true events occurring in the human response to acute wounding.

The identity of keratinocyte integrins expressed by normal epidermal cells in this study was comparable to previous reports demonstrating $\alpha_2\beta_1$ $\alpha_3\beta_1$ $\alpha_v\beta_5$ $\alpha6\beta_4$ to be the main integrins present in normal epidermis (165;166;260;261;293;295). However, conflicting results have been presented with regard to the distribution of these integrins within normal epidermis along with the presence or absence of $\alpha_5\beta_1$ integrin. In this study a strong basolateral expression of $\alpha_3\beta_1$ was present on basal keratinocytes with expression also present on cells of the adjacent suprabasal layers.

This basolateral expression has not been consistently found in previous studies, with some investigators reporting $\alpha_3\beta_1$ to be specifically located at cell-to-cell contact sites (166;260;293;296). Demonstrating the basolateral expression of $\alpha_3\beta_1$ may be significant, since work by Hodivala-Dilke suggested that interaction of $\alpha_3\beta_1$ with its ligand laminin 5 may regulate the proliferative and migratory activity of resting epidermal cells by inhibiting the activity of $\alpha_5\beta_1$ and $\alpha_2\beta_1$ integrins (171). In the current study $\alpha_2\beta_1$ expression was found in the lower 2 suprabasal layers of normal epidermis, whereas previous studies have shown conflicting reports on the presence of $\alpha_2\beta_1$ on suprabasal cells (166;260;295).

The β_4 integrin subunit combines exclusively with the α_6 subunit on human keratinocytes (297;298). It is well established that the $\alpha_6\beta_4$ heterodimer forms part of the unique hemidesmosome adhesive structures, which are present in the basement membrane zone of normal epidermis (299). In this context, localisation and concentration of the β_4 subunit expression in this study on the basal pole of basal layer keratinocytes, is in agreement with previous studies of normal adult human skin (166;293).

The unavailability of an antibody towards the $\alpha_V\beta_5$ or $\alpha_V\beta_6$ hetrodimers at the time of study does not allow the investigator to comment on the identity of the β subunit associated with the α_V subunit identified in this study. The $\alpha_V\beta_5$ and $\alpha_V\beta_6$ are however the major α_V hetrodimers known to be expressed by keratinocytes, apart from the more recently characterised $\alpha_V\beta_8$ heterodimer found exclusively in the suprabasal layers of adult epidermis (296;300). Clark and co-workers in 1996 demonstrated the α_V hetorodimer present in normal skin to be $\alpha_V\beta_5$ with a switch to $\alpha_V\beta_6$ occurring on migrating keratinocytes as they encounter increasing amounts of

its ligand tenascin in the wound matrix (165). Weak or no expression of α_V has previously been reported in normal skin (165-167;260;261) but in the current study strong pericellular staining was demonstrated on basal keratinocytes along with weak expression on adjacent suprabasal cells. The suprabasal expression noted in this study may reflect the more recently discovered expression of $\alpha_V\beta_8$ exclusively in the suprabasal layers of adult epidermis since the antibody was directed against the α_V subunit (300).

Using the monoclonal antibody PID6 this study consistently failed to demonstrate the presence of $\alpha_5\beta_1$ expression in normal epidermis. Previous reports on the presence of this integrin on resting keratinocytes have depended on the antibody and type of tissue investigated (31;165;166;260;261;293). In light of the reported differences in distribution of $\alpha_5\beta_1$ and $\alpha_2\beta_1$ expression, it is worth noting that skin location (i.e. sun exposed vs non exposed), differences between aged and younger skin as well as differences between animal and human skin may all have a bearing on the observed distribution of integrin expression.

In this study, as previously reported by Cavani and co-workers (166), wounded epidermis underwent a characteristic change in integrin expression pattern, in particular upregulating the expression of $\alpha_5\beta_1$ and α_V integrin subunits. Although it is well established that $\alpha_5\beta_1$ is expressed by wound keratinocytes, the distribution and timing of this expression has not been confirmed. Cavani and Clark along with their co-workers both reported expression on migrating basal keratinocytes beyond 48 hours post wounding (165;166). In addition Clark reported $\alpha_5\beta_1$ expression on the basal surface of migrating keratinocytes and a patchy distribution around the perimeter of epidermal cells at the migrating tip (165). Both groups of investigators

reported disappearance of expression after epidermal wound closure. However Cass and co-workers reported neo-expression of $\alpha_5\beta_1$ at 4 hours post-wounding in foetal tissue which again disappeared after epidermal wound closure (294). In this study $\alpha_5\beta_1$ expression was present from 24 hours up to 96 hours post wounding but displayed a moderate decrease towards 96 hours, which coincided with epidermal closure in some of the wounds studied. Expression was limited to basal keratinocytes in contact with the provisional wound matrix with a pericellular distribution that was concentrated on their basolateral membranes. The timing of this expression contradicts the suggestion by Cass (294) that the faster induction of $\alpha_5\beta_1$ expression by wounded foetal skin compared to adult wounded skin, contributes to the scarless healing seen in foetal skin. The results of this study indicate that a rapid induction of $\alpha_5\beta_1$ expression can occur in adult human epidermis and suggests that future studies should incorporate the analysis of earlier time points post cutaneous injury (<24 hours) as confirmation of this. In this and previous studies, the wound matrix was demonstrated to contain the $\alpha_5\beta_1$ ligand fibronectin which in this study, was concentrated directly underneath the newly migrated tongue of keratinocytes (166).

In light of previous reports by Clark of a switch to $\alpha_V\beta_6$ expression on wound keratinocytes, expression of $\alpha_V\beta_5$ concomitantly with increasing amounts of $\alpha_V\beta_6$ may explain the marked increase in α_V subunit expression observed in this study (165). Furthermore, in this study there was a distinct localisation of αv subunit expression to the basal membranes of migrating keratinocytes suggesting a specific ligand interaction with the underlying matrix. Concentration of vitronectin, an established ligand for $\alpha v\beta_5$, was observed underneath the tongue of epidermis migrating over the provisional wound matrix. It may be possible that $\alpha_V\beta_5$ plays a

co-migratory role with $\alpha_5\beta_1$ and the switch to expression of $\alpha_V\beta_6$ signals the keratinocytes to limit their lateral migration as tenascin, a basment membrane component and ligand for $\alpha_V\beta_6$, accumulates in the wound matrix.

Previous investigations have reported decreasing expression of $\alpha_2\beta_1$ on migrating basal keratinocytes but increasing expression on suprabasal wound keratinocytes with expression being restored after epidermal closure (166;260;261;295). $\alpha_2\beta_1$ expression was found to be decreased on migrating basal keratinocytes in this study, after an initial increase at 24 hours, with no change in expression on suprabasal keratinocytes in the wound compared with normal epidermis. The increased staining intensity at 24 hours was observed as a concentration of expression on keratinocytes at the leading edge of the migrating epidermis directly in contact with provisional wound matrix. This intense staining was seen to persist on a small number of cells at the tip of the migrating epidermis, throughout the healing time course. This agrees with recent work by Pilcher which suggests that $\alpha_2\beta_1$ may be controling the direction of keratinocyte migration by its interaction with collagen I, inducing collagenase I production by basal keratinocytes which allows these cells to clear a path along the matrix of the wound (204).

The distribution of β_4 integrin subunit expression on migrating epidermis observed in this study is comparable to previous *in vivo* studies in human mucosal and mouse corneal tissue (260;301) as well as to *in vitro* migration studies (172;302). This is characterised by a relocation of β_4 expression to lateral and apical membranes of both basal keratinocyte and an increased number of suprabasal keratinocytes within migrating epithelia. This would be consistent with a downregulation of hemidesmosome attachment to the underlying basement membrane allowing lateral

migration of wounded epidermis. However, this is somewhat contradicted by Cavani and co-workers in a previous study of human adult skin where they found the β_4 expression to be polarised to the basal pole of basal keratinocytes along the whole length of migrating epidermis (166). In the current study, expression was found to be concentrated on the basolateral membranes of basal keratinocytes within the migrating epidermis but the characteristic linear labelling of the dermo epidermal junction seen in normal skin did not extend to the advancing tip. It is difficult to see, given the role of β_4 in hemidesmosome assembly, how this could occur at the leading edge of migrating epidermis.

The function of syndecan-1 in developing tissues has been extensively studied. However, to date this is only one of two studies to characterise its expression in human adult wounded epidermis, the other being a recent study by Lundqvist and Schmidtchen on normal skin and chronic leg ulcers (303). A limited number of studies have been carried out in animal tissue and human mucosal tissue (304;305). The results of this study are comparable with those of Lundqvist and Schmidtchen in terms of the expression pattern in normal skin. In addition, the expression found in acutely wounded epidermis is comparable with those published in a previous study on human acute mucosal wounds. In the current study, syndecan-1 expression was observed throughout the stratified layers of normal epidermis and in the non wounded epidermis of acute wounds, but expression was slightly weaker in the basal layer of both tissues. In the migrating epidermis, this was reversed. Syndecan-1 was slightly weaker in the suprabasal layers towards the advancing tip and appeared to be stronger on the basal keratinocytes in contact with wound matrix. Unfortunately, tissue from the onset of healing and at wound closure was not available for this study and thus a comment cannot be made about the temporal nature of these changes.

However, the previous study in human mucosal wounds described a loss of syndecan-1 expression at one day, regaining of basal layer expression at 3 days and return of suprabasal expression at seven days post wounding (time of wound closure) but without complete recovery in upper epidermal layers (304). These spatiotemporal changes in syndecan-1 expression suggest that it plays a specific role in keratinocyte migration in response to injury. This would not be surprising considering the functional diversity possessed by this molecule, which include binding and activation of growth factors, regulating epithelial proliferation and differentiation, modulating cell adhesion events and modulating proteolytic activity (reviewed in (41;306)). Interestingly, this is further supported by a study on wounded transgenic mice, demonstrating selective activation in migrating but not proliferating keratinocytes, of a response element within the syndecan-1 gene known as the far upstream AP-1-driven, FGF-inducible response element (FiRE) (307).

The expression pattern of E-cadherin was similar to that of syndecan-1 in both normal and acutely wounded epidermis. This was particularly evident in the migrating epidermis of acute wounds as the loss of suprabasal E-cadherin expression mirrored that of syndecan-1. In view of previous evidence indicating that these molecules are co-expressed (308;309), this is not an unexpected finding. The associated loss of these molecules from migrating epidermis would herald the switch to a motile phenotype as was seen when epithelial cells were transfected with antisense mRNA for syndecan-1, activating them to invade collagen gels (41). Similarly, work has focused on the role of E-cadherin in tumour biology, where loss of E-cadherin expression and therefore cell-to-cell adhesiveness, heralds the onset of an invasive phenotype (310). However, it was interesting to find that the downregulation of E-cadherin in migrating epidermis was greater than that of

syndecan-1 and may suggest a different functional co-operation between these two molecules in the biology of wound healing and tumours.

To date very little work has been done to investigate the effect of chronic wounding on epidermal adhesion molecules. A well established human model of wound chronicity, the chronic venous leg ulcer, was used as a source of tissue for investigating epidermal adhesion molecule expression in this cutaneous pathological setting. Distinct differences were found in the expression of integrins between acute and chronic wound epidermis. In particular, a decrease in the expression of $\alpha_5\beta_1$ was frequently found in the epidermis of chronic wound margin epidermis when compared to acute wound epidermis. In addition, expression of $\alpha_5\beta_1$ was found in chronic wound epidermis distal to the wound edge. It is difficult to account for this since the keratinocytes observed to be expressing this integrin were in contact with intact epidermal basement membrane. This is normally associated with a resting phenotype as opposed to the migratory phenotype characterised by keratinocyte $\alpha_5\beta_1$ expression. One possible explanation was that the inflammatory milieu of the chronic wound may have been providing positive signals to these keratinocytes through cytokines such as TGFβ_1 and PDGF (311;312). This may be supported by evidence that $\alpha_5\beta_1$ expression can be induced in inflammatory epidermis such as that seen in psoriasis (313). Furthermore, transgenic mice induced to express this integrin showed inflammatory changes in their epidermis which took on the hyperproliferative appearance of psoriatic skin (314). It was the observed expression of $\alpha_5\beta_1$ in hyperproliferative chronic wound epidermis that lead the author to investigate the possibility of modifying its expression directly by cytokine or growth factor action. The ultimate test of this hypothesis would be to modify expression on

chronic wound keratinocytes. The development of the tissue explant culture system was undertaken with this in mind and is discussed in more detail later.

The expression of the α_V integrin subunit was found to have a similar distribution in chronic wound edge epidermis when compared to the same area in acute wounds. However, the specific concentration of α_V expression on the basal pole of migrating basal keratinocytes in acute wounds was often not present in the chronic wound epidermis. In general, there was also a greater number of suprabasal cells expressing α_V in the chronic wound edge epidermis, which extended a long way into the non-wounded epidermis when compared to acute wounds.

An increase in suprabasal expression extending into the non-wounded epidermis of chronic wounds was also seen for $\alpha_2\beta_1$, $\alpha_3\beta_1$ and β_4 integrin subunits. This increase in suprabasal expression is probably a reflection of the hyperproliferative nature of the epidermis at the margin of chronic venous leg ulcers. A similar suprabasal expression has been observed in other diseases such as psoriasis, eczema and lichen planus, also characterised by a hyperproliferative epidermis (293;315). A number of explanations have been suggested for this increased suprabasal expression including *de novo* synthesis by differentiating keratinocytes, increased half-life of basal keratinocyte integrin heterodimers or modulation by cytokines and growth factors (316;317). However, it is currently unclear which of these are true and whether integrin suprabasal expression is a cause or consequence of hyperproliferation. Hertle *et al* in 1995 showed no effect of IFNγ or TNFα on suprabasal integrin expression when injected intradermally into healthy volunteers but did demonstrate suprabasal expression of keratinocytes grown on a dermal equivalent consisting of fibroblasts in a collagen gel (316). This suggests that suprabasal expression is not induced by these

inflammatory cytokines and merely reflects the proliferation/differentiation status of the epidermis. Work by Hakkinen *et al* lends further support to this as topical application of retinoic acid, an agent used in treatment of skin disorders (e.g. acne and actinic keratoses) and known to cause epidermal hyperplasia, induced suprabasal expression of $\alpha_2\beta_1$ and $\alpha_3\beta_1$ (318).

Expression of the β_4 subunit was again similar in both acute and chronic wound epidermis except for the increased suprabasal expression described above. There was also an extension of the continuous labelling of the dermo-epidermal junction towards the tip of the migrating epidermis in some of the chronic wounds. This may indicate that at the edge of chronic wounds, the epidermis can be in a static phase and does not undergo the necessary transformation to a migratory phenotype. Lateral migration requires disassembly of the hemidesmosome adhesive interaction with the basement membrane and upregulation of other integrins such as $\alpha_5\beta_1$ allowing adhesion to new matrix proteins encountered in the provisional wound matrix. Further studies will be required to elucidate the nature of the basement membrane at the leading edge of chronic wound epidermis and to determine the functional state of the hemidesmosome structures on the basal keratinocytes.

As this was the first study to look at the expression of E-cadherin in human adult epidermis and only the second to look at syndecan-1 expression it was particularly interesting to be able to compare their expression in acute and chronic wounds. Syndecan –1 was strongly expressed in all layers of the epidermis at the margin of chronic wounds but did not show a decrease on suprabasal keratinocytes within the leading edge epidermis as seen in acute wounds. Furthermore, in contrast to acute wounds, there was not a consistent increase in expression on basal keratinocytes at the leading edge. A similar trend was seen with E-cadherin, for which a marked

decrease in its suprabasal expression within the leading edge epidermis was observed in some wounds, while in others this suprabasal expression was maintained. Based on studies of these molecules in developmental and tumour biology, the down regulation of their expression would be consistent with a migratory phenotype, a prerequisite for initiation of epidermal re-epithelialisation. The data presented here suggests that keratinocytes at the margin of chronic wounds are not in the process of down regulating their stationary cell-to-cell contacts in which E-cadherin plays a major role, along with possibly co-regulation from syndecan-1. This downregulation which was evident in the acute wounds, may indicate that the signals for active migration are absent in chronic wound epidermis.

In addition to the findings already described for adhesion molecule expression within chronic wound epidermis, an overall impression was gained by the investigator that their pattern of expression may have been related to the healing phase of these wounds. A small number of chronic venous leg ulcers were observed to have a pattern of epidermal adhesion molecule expression similar to that seen in acute wounds and appeared to be consistent with a transit to a migratory phase. Most notable of these changes was an increase in leading edge basal keratinocyte expression of $\alpha_5\beta_1$ and α_V integrin subunits, accompanied by a concomitant decrease in β_4 subunit expression and a decrease in suprabasal E-cadherin expression. Unfortunately, clinical data was not collected as part of the current study and the time between investigation and presentation of the results in this thesis was too long to allow retrospective acquisition of the data. It is thus difficult for the investigator to confirm whether the tissue investigated here could have been clinically assessed to be undergoing an active phase of healing.

Since completing this study, a greater understanding of the role of epidermal integrins as regulators of epidermal homeostasis has emerged. The results of this study can now be discussed in light of this new evidence, and will allow speculation on future approaches to understanding the role of these molecules in the re-epithelialisation of human wounds.

In recent years the $\alpha_3\beta_1$ molecule has emerged as an important molecule in regulating the proliferation and differentiation of resting epidermis and in the switch to a migratory phenotype when the capacity for epidermal renewal is called upon. It is the interaction of $\alpha_3\beta_1$ with laminin 5, an important ECM protein and a key component of the basement membrane, which is a significant factor in its ability to carry out this role. Laminin 5 is composed of the heterodimeric association of $\alpha3$, $\beta3$ and $\gamma2$ laminin chains and supports cell adhesion via interaction of its $\alpha3$ C-Terminal extremity (G-domain), with both $\alpha_3\beta_1$ and $\alpha_6\beta_4$ (172;319). Its induction in migrating keratinocytes during wound healing has been shown in immunohistochemical and *in situ* hybridization studies (320). Efficient migration of normal human keratinocytes has also been shown in several studies to be dependent on endogenously deposited laminin 5 (172;321). In fact the primary mediator of motility on laminin in normal keratinocytes has been shown to be $\alpha_3\beta_1$ whereas interaction with $\alpha_6\beta_4$ is known to induce formation of hemidesmosomes that stabilise interaction with the underlying matrix (322-324). Furthermore deposition of laminin 5 onto an exposed collagen and fibronectin matrix, as found in human wounds, is also required for the repair of the basement membrane and re-establishement of its epithelial anchoring functions.

In 1999 Goldfinger and co-workers suggested a mechanism by which $\alpha_3\beta_1$ could regulate the dynamics of epithelial adhesion during re-epithelialisation based on the

proteolytic processing of laminin 5 (172). Laminin 5 is synthesised and secreted by cultured keratinocytes in a precursor form containing a 200-kDa $\alpha3$ chain and a 140-kDa $\gamma2$ chain (325). This precursor form is deposited into the provisional basement membrane of wounds but is absent from fully formed basement membranes (172). The precursor form was shown by Goldfinger *et al* to ligate the integrin $\alpha_3\beta_1$ with high affinity, promoting cell motility, and led them to suggest that its synthesis and deposition was increased by keratinocytes at the leading edge of wound epidermis. Interaction of $\alpha_3\beta_1$ with this precursor form would promote cell migration while proteolytic cleavage of the $\alpha3$ subunit of laminin 5 would lead to a higher affinity interaction with $\alpha_6\beta_4$ in the cells following behind the leading edge. The interaction with $\alpha_6\beta_4$ was then proposed to induce the assembly of immature hemidesmosomes, similar to type II hemidesmosomes seen in gut epithelial cells. These are thought to have a more dynamic nature allowing cell migration to occur while maintaining stable interaction with the underlying matrix.

In addition to the above model epithelial adhesive interactions regulated by $\alpha_3\beta_1$, Hodivala-Dilke and co-workers have proposed a role for $\alpha_3\beta_1$ as a trans-dominant inhibitor of fibronectin and collagen type IV integrin receptors in keratinocytes (171). By analysing skin and isolated keratinocytes from α_3 integrin-deficient mice, they demonstrated a change in filamentous actin (F-actin) bundling and a higher concentration of actin-associated proteins at focal contact sites, thus pointing to a role in regulating the actin cytoskeleton focal contact composition. This was allied to an increase in fibronectin ($\alpha_5\beta_1$) and collagen type IV ($\alpha_2\beta_1$) receptor activity. Focal contacts (also termed focal adhesions) have been described as clusters of integrins ligated to their matrix ligands while their cytoplasmic tails are linked to a

concentration of actin-associated proteins (e.g. talin, vinculin and α-actinin), that in turn link to actin filament bundles (145;326-328). A role in regulating these focal adhesions therefore represents a significant function for $\alpha_3\beta_1$ in directing cell-to-matrix interactions.

More recently $\alpha_3\beta_1$ has also been implicated in the integrin-mediated assembly of the sub-cortical cytoskeleton and the subsequent association of the cytoskeleton with the cadherin:catenin complex. Association of the cytoskeleton with cadherin:catenin complexes is important in areas of cell-to-cell adhesion. Wang and co-workers demonstrated that cells derived from kidney collecting ducts of $\alpha_3\beta_1$ integrin deficient mice were able to maintain cadherin mediated cell-to-cell adhesions but failed to organise the subcortical cytoskeleton and instead assembled actin stress fibers (170). In addition, they showed that association of the cadherin:catenin complex with α-actinin was greatly decreased in an immortalised cell line from these $\alpha_3\beta_1$ integrin deficient mice. They proposed this as direct evidence for integrin:cadherin cross regulation, in which cadherin function is dependent on the presence of an integrin. Evidence from other studies seems to suggest that this is a general property of β_1 integrins (295;329). This work lends support to the findings in the current study of increased suprabasal expression of β_1 integrins within migrating epidermis concomitantly with decreased expression of E-cadherin. It is possible to suggest that increased β_1 integrin expression maintains the organisation of the subcortical cytoskeleton at areas of cell-to-cell adhesion in the absence of E-cadherin during times when loosening of cell attachments is required (e.g. during the process of re-epithelialisation).

In light of this new evidence, the findings of the current study can now be used to propose a possible sequence of dynamic changes in cell adhesion molecule interactions during the process of epidermal re-epithelialisation. When cutaneous injury occurs, epidermal cells at the edge of the wound have to contend with loss of both cell-to-cell and cell to matrix adhesion. Basal layer keratinocytes are no longer in contact with intact basement membrane and are faced with a provisional matrix consisting of type V collagen, fibrin, fibronectin, tenascin, vitronectin and type I collagen (1). Pilcher *et al*, after demonstrating collagen induction of collagenase-1 and blocking of primary keratinocyte migration on collagen by antibodies against the α_2 integrin subunit, proposed that at this early stage interaction of $\alpha_2\beta_1$ with dermal collagen mediates the induction of collagenase-1 in keratinocytes (204). This supports the finding in the current study of $\alpha_2\beta_1$ expression by keratinocytes at the leading edge of acute wound epidermis. As discussed earlier, this may be enhanced by the release of trans-dominant inhibition of $\alpha_2\beta_1$ by $\alpha_3\beta_1$ as it would now have lost its ligation to processed (mature) laminin-5 within the basement membrane. In addition, this would also release the inhibition of $\alpha_5\beta_1$, thus allowing its expression to be upregulated and so enhancing its ability to promote migration on fibronectin present in the wound matrix. Loss of binding to processed laminin-5 by $\alpha_6\beta_4$ would also signal the dissasembly of the hemidesmosomal attachment to the basement membrane releasing the keratinocytes to initiate lateral movement. As the keratinocytes then undertake lateral migration, they will deposit unprocessed (immature) laminin-5 to enhance their migration on the provisional wound matrix, which again has been shown to be enhanced by $\alpha_3\beta_1$ (172). Proteolytic cleaving of laminin-5 during the process of migration would enable ligation of the processed laminin-5 with $\alpha_6\beta_4$ behind the leading edge, stabilising attachment to the underlying

matrix by inducing the assembly of hemidesmosomes. Cleavage of the G-domain of the laminin-5 $\alpha 3$ subunit has been shown to induce cell attachment and hemidesmosome assembly (330). Ligation of processed laminin-5 by $\alpha_3\beta_1$ would reinstate the trans-dominant inhibition of $\alpha_2\beta_1$ and $\alpha_5\beta_1$ integrins and thus limit the degree of lateral migration.

In addition to the upregulation of $\alpha_5\beta_1$, demonstrated in this study on migrating keratinocytes directly in contact with wound matrix, the α_V integrin subunit was also upregulated with a similar cellular distribution. This agreed with previous studies where dynamic changes in $\alpha_V\beta_5$ and $\alpha_V\beta_6$ expression were demonstrated during re-epithelialisation. In particular, a switch was shown to occur in the heterodimeric association of α_V subunit, from $\beta 5$ in the initial stages of re-epithelialisation to $\beta 6$ around the time of neo-epidermal fusion in human adult epidermis. Furthermore, the appearance of $\alpha_V\beta_6$ expression has been shown to coincide with maximal deposition of tenascin in the wound matrix (331). The matrix ligand for $\alpha_V\beta_5$ is vitronectin which was shown in this and other studies to be deposited under the migrating epidermis during re-epithelialisation (332). This may therefore indicate a co-migratory role with $\alpha_5\beta_1$ during the early stages of re-epithelialisation. In contrast, binding of $\alpha_V\beta_6$ to its matrix ligand tenascin, may be acting to limit the degree of lateral migration at the time of neo-epidermal fusion. Interestingly, $\alpha_9\beta_1$ a more recently characterised integrin heterodimer, also binds tenascin but recognises the Ile-Asp-Gly (IDG) adhesion sequence motif as apposed to the common integrin sequence motif Arg-Gly-Asp (RGD) recognised by $\alpha_V\beta_6$. This may be significant since tenascin has been shown to induce cell proliferation, an effect which can be mediated by $\alpha_9\beta_1$. Morover, a study in human oral mucosal wounds demonstrated

expression of $\alpha_9\beta_1$ to coincide with tenascin deposition early on in wound repair (333-335). This suggests that ligation of $\alpha_9\beta_1$ to tenascin by keratinocytes at the migrating front may be involved in the induction of the proliferative burst required to provide a pool of cells from which wounded epidermis can be rebiult.

An additional function of $\alpha_V\beta_6$ has been shown to be activation of TGF-β during injury to airway epithelium (336). Interestingly, a more recently identified integrin $\alpha_V\beta_8$ has also been shown to be involved in activation of TGF-β in airway epithelium (337). Moreover, its expression has been shown to be lost during malignant transformation of airway epithelial cells and reconstitution of lung cancer cells with $\alpha_V\beta_8$ restored growth inhibition by TGF-β (337). Given the importance of TGF-β to the healing of human wounds, it is evident that the role of $\alpha_V\beta_8$ and $\alpha_V\beta_6$ in regulating its activity during the process of re-epithelialisation requires further investigation. It is possible, given the late timing of its appearance during epidermal re-epithelialisation, $\alpha_V\beta_6$ serves to localise activation of TGF-β to keratinocytes at the migrating front of wounded epidermis. This could act as an autocrine signalling loop, since TGF-β is known to be synthesised and secreted by keratinocytes at the front of migrating epidermis (338). It is possible that this signals the stabilisation of lateral migration as epidermal closure becomes imminent, in addition to down regulation of proliferation, known to be a direct effect of TGF-β, and the initiation of keratinocyte differentiation (339). This would ultimately lead to stratification of the neo-epidermis and restoration of the barrier function of normal skin.

This is a very simplified version of a truly complex and highly regulated process but uses the most recent evidence to give a valuable snapshot of what will undoubtedly be a much bigger picture. The continuing advance in understanding the molecular

underpinnings of the intracellular signalling and extracellular adhesive interactions of cell adhesion molecules will pave the way to visualising the complete process of epidermal wound closure. It is becoming increasingly obvious that the matrix proteins involved in this process do not purely function as structural scaffolds for cell adhesion and movement Evidently they are seen as the source of a complex set of instructions, holding cues not just for directional movement but also for cell proliferation and differentiation. These instructions are then read by cell adhesion molecules of which the integrins appear to be the main players, but may well be aided by molecules such as the syndecans and cadherins.

Future recommendations

As more of the normal processes involved in epidermal repair are uncovered, the challenge ahead lies in identifying those processes which are missing or not functioning in chronic wounds. The results of the current study already suggest that the spatiotemporal regulation of adhesion events is lacking in epidermis at the margin of chronic venous leg ulcers. Further immunohistochemical studies would provide a better understanding of the miss-regulation of these events in chronic wounds.

The difficulty in obtaining normal human volunteers to provide cutaneous tissue for the study of epidermal repair is a significant impediment to understanding this process in human tissue. However, the current study has demonstrated the possibility of utilising a readily available human source of rapidly healing acute wound tissue due to the clinical practices within the University Department of Surgery, University of Wales College of Medicine. The practice of excising widely around an affected pilonidal sinus site and allowing it to heal by secondary intention, provides an acute

wound setting in fit young individuals where epidermal cells migrate across a granulating wound bed. In the current study, biopsy tissue was not available for the complete healing time course of around 42 weeks normally seen in these wounds. Future studies could rectify this and allow the study of some of the more recently discovered adhesion molecules in human acute wound tissue. The investigator would seek to include $\alpha_V\beta_8$, $\alpha_9\beta_1$, syndecan-1 and syndecan-4 in such a study. This would allow investigation of the role of $\alpha_9\beta_1$ in inducing keratinocyte proliferation and a better characterisation of the spatiotemporal modification of syndecan expression at the margin of acute human wounds. Simultaneous study of these molecules with the cadherin molecules may reveal the nature of their co-regulation in human epidermis. To date, the expression of $\alpha_V\beta_8$ has not been characterised in human epidermis but as previously discussed, its expression has been demonstrated in airway epithelium where it was also shown to be an activator of TGF-β (169). Double labelling immunohistochemical staining procedures carried out on pilonidal excision tissue could elucidate whether $\alpha_V\beta_6$ (also demonstrated to activate TGF-β) or indeed $\alpha_V\beta_8$ was involved in activating TGF-β at the leading edge of migrating epidermis.

The chronic venous leg ulcer is already recognised as a good model of the chronic wound process and is a readily available source of this tissue. The investigations highlighted above in pilonidal excision tissue could also be carried out in chronic venous leg ulcer tissue as a comparison between adhesive events in the chronic and acute wound setting. However, the investigator would also like to propose a novel approach to the use of this chronic wound tissue. The current study has demonstrated the value of taking a biopsy to create an acute wound within forearm skin of normal adult volunteers and taking a second biopsy from this original site to incoporate the healing tissue. It is possible that this approach could be taken in chronic venous leg

ulcer tissue. Anecdotal evidence personally communicated to the investigator by Professor Harding at the Wound Healing Research Unit, suggested that biopsy sites taken for clinical histology investigations subsequently heal successfully, while the surrounding ulcer remains dormant. This may indicate that the laying down of new matrix within the chronic wound bed provides the adhesive signals required to initiate cellular migration. In the context of the epidermal wound margin it would be useful to compare the new basement membrane components laid down by keratinocytes migrating over a biopsy site with that laid down by keratinocytes in contact with the original chronic wound bed. The deposition of laminin-5 and the nature of its proteolytic cleavage in both settings would be of particular interest as its interaction with $\alpha_6\beta_4$ and $\alpha_3\beta_1$ is known to be affected by its level of processing. In addition, it would be interesting to see if the healing pattern of adhesion molecule expression is induced in the biopsy site epidermis as compared to the surrounding chronic wound margin epidermis.

The creation of an acute wound within the margin of a chronic venous leg ulcer would therefore provide an invaluable insight into the biology of chronic wound repair. The investigator feels that this is a feasible approach since the chronic venous leg ulcer patient regularly attends clinics at the Wound Healing Research Unit and is therefore familiar with the procedures of taking biopsy tissue for research and clinical histopathology purposes. In addition, the patient would be unlikely to suffer any detrimental effects from the procedure as the biopsy sites commonly heal successfully.

Tissue Explant Culture System

The development of the tissue explant culture system was seen as the closest approximation to the *in vivo* conditions facing the cellular constituents of chronic wound tissue whilst allowing the control of the *in vitro* environment for the investigative process. The investigator believes this explant culture model provides a viable system for the study and further biological characterisation of chronic wound tissue. This is based on:-

a) Ability to study cytokine/growth factor production and immunohistological aspects within the same tissue over time.

b) Ability to histologically characterise modulation of functionally important molecules (e.g. $\alpha_5\beta_1$ integrin) in response to a stimulus such as LPS

However based on the results of this study the tissue explant culture system is not yet viable as a test bed for the application of potential therapeutic agents. This is due to the high level of variability within chronic venous leg ulcer tissue coupled with the small number of samples studied.

<u>Specific findings</u>

IL-1β

A high variability in IL-1β levels was detected. This consisted of both intra and inter-biopsy variation in wound edge and bed tissue. Detectable levels were also low, which resulted in large amounts of supernatant being required for each analysis, making it unsuitable as part of a panel of analytes for simultaneous study. Levels of IL-1β detected in wound edge biopsy 3 segment 2, displayed a wide departure from

other tissue segments within the same biopsy. It is possible that this represents outlying data (as it was > 3SDs from the mean) to be ignored, or alternatively it could represent the presence of an important confounding factor within this particular tissue segment. Possible confounding factors include the presence of an increased bacterial load or increased numbers of activated subpopulations of leucocytes (i.e. macrophages or lymphocytes) within this tissue segment. The same consideration can be made for wound bed biopsy 2 which contained a segment with levels >3SDs from the mean.

Comparison of median values for the wound edge and bed showed higher levels to be present in wound bed tissue. This was a small difference of 8.24pg/ml/mg of tissue, but it is unclear whether this would be a functional clinically important difference.

IL-8

A wide inter and intra-biopsy variation for levels of IL-8 was detected in both wound bed and edge tissue . Both segments from wound edge biopsy 1 showed a large departure from mean values in other biopsies at 6 and 8 hours. This biopsy had a substantial effect on overall mean levels at 6 and 8 hours (mean = 11579.50 but decreased to 1601pg/ml/mg when outlying data was removed at 6 hours). Again this could be considered as outlying data or indicate the presence of a biological confounding factor such as an increased bacterial load. The above was also true for wound bed biopsy 2. No real difference between levels of IL-8 present in wound bed or edge tissue was found in this small sample.

MMP-2

Some wound edge segments had undetectable levels of MMP-2. Overall levels were low in terms of pg/ml/mg of tissue when compared to other analytes. However, the absolute values may not be important, as this study did not differentiate between activated and latent levels of protease enzymes or measure levels of their natural inhibitors the tissue inhibitors of metalloproteinases (TIMP). It is most likely that it is the overall proteolytic balance that is the important consideration in tissue remodelling i.e. low levels of TIMP would allow lower levels of MMP to have more activity. Both wound edge and wound bed tissue showed large intra and inter-biopsy variation in levels of MMP-2. In addition, the median levels were higher in wound bed compared to wound edge tissue. This may be a reflection of its cellular source as Bullen in 1995 demonstrated fibroblasts to be a major source of MMP-2 (209).

MMP-9

There was a high inter and intra-biopsy variation in levels of MMP-9 present in wound edge and bed tissue. Similar pg levels to those of MMP-2 were detected but in general were observed to be slightly higher. MMP-9 levels generally decreased with time which may be a function of its storage in neutrophil granules (340;341). Release from these granules in the first 2-4 hours of culture may herald a steady decrease over the remaining culture period. This could also contribute to the inter/intra-biopsy variation observed as different tissue segments may have differing numbers of neutrophils present within them. The neutrophils themselves could also contain varying levels of MMP-9 stored in their granules. This could be dependent on the nature of the healing response at the time of biopsy, which would influence the activity levels of the neutrophils prior to entry into culture. Overall, median levels

were higher in wound bed tissue and the 95% CI's around the means did not overlap indicating that this may have been a true difference in the mean levels present in wound bed compared to edge tissue. Again this could reflect the fact that neutrophils are a major cellular source of MMP-9, although it is not clear whether increased neutrophil numbers would be expected to be present in the wound bed compared to the edge

TGF-β

Inter and intra-biopsy variation in TGFβ levels was found to be high in both wound edge and bed tissue. Overall, no difference in levels was found between wound edge or bed tissue. Undetectable levels were found in wound edge and bed biopsies 1 at 2 hours but they both responded to the culture conditions producing higher overall values than other biopsies. As these biopsies originated from the same wound, this may again indicate a biological confounding factor to be present within the wound related to the nature of the healing response occuring at the time of biopsy. However, the possibility of measurement error having occurred cannot be ruled out.

VEGF

Large inter and intra-biopsy variation in levels of VEGF were detected but in relative terms, inter-biopsy variation was found to be greater. There was a trend for an increase in levels of VEGF between 2 and 8 hours for wound edge and bed tissue. However the level of variability and small sample number make this an unreliable observation. No difference was found in the levels of VEGF present in wound edge or bed tissue.

Related histology of four wound edge and bed biopsies

Four wound edge and wound bed biopsies, taken as matched pairs from the same wounds, were studied immunohistologically in addition to the analysis of specific analytes present in their culture supernatant when they were placed in the tissue explant system. This was carried out to investigate whether the inter- or intra-biopsy variation in levels of cytokines or proteases could be related to the immune cell profile of each tissue segment.

Marked differences in leucocyte cell numbers were found between some biopsies and even between some tissue segments within the same biopsy. Overall, wound bed and edge biopsy 1 had the greater number of immune cells present. However, no clear association was seen between the levels any of the cytokines measured and immune cell numbers present in any of the wound edge or bed biopsies (inter-biopsy variation). Similarly there was no clear association between cytokine levels and immune cell numbers present in any of the tissue segments from the individual wound edge or bed biopsies.

Differences were found in the number of immune cells present in wound bed or wound edge tissue. This was represented by median values of 3.5 staining intensity for CD68 positive macrophages (measured using visual analogue scale grading 1-5) present in wound bed tissue compared to a median value of 2.9 in wound edge tissue. However, CD3 positive leucocytes were found to be present in higher numbers in wound edge tissue, which was represented by a median value of 8.4 mean cell number per x40 field of view in wound edge tissue compared with 7.4 mean cell number per x40 field of view for wound bed tissue. Similarly, a median value of 4.1 CD4 positive lymphocytes per x40 field of view was found in wound edge tissue

compared to a median value of 3.3 in wound bed tissue. CD8 positive lymphocytes were also found to be present in greater numbers within wound edge tissue as represented by a median value of 3.1 mean number of cells per x40 field of view in wound edge tissue compared with 2.1 in wound bed tissue. Interestingly however, the CD4/CD8 ratio was found to be higher in wound bed tissue with a median value of 1.8 compared to 1.3 in wound edge tissue.

This data can be related to published work from the WHRU laboratory indicating a lower CD4/CD8 ratio to be present in almost healed acute wounds compared to early healing acute wounds and paradoxically within non-healing chronic venous leg ulcer tissue (36;99). This may suggest that the inappropriate immune cell profile within the wound bed tissue of chronic venous leg ulcers may impair the inward healing of the ulcers from the wound edge tissue. Unfortunately the wide spread in the data indicated by large values for the range and SD in addition to the small number of biopsies studied make these observations unreliable.

Given the possible differences in immune cell profile between wound edge and bed tissue it is unfortunate that only four wounds could be studied in this way which inevitably contributed to the inability to relate cytokine levels to immune cell numbers within the tissue. There are however a number of other reasons why relating immune cell numbers to cytokine levels was difficult, including the ability of other cells within the wound such as fibroblasts and keratinocytes to poduce the cytokines being studied and the different activation status of the the immune cells present within the tissue at any given time. It may be possible to overcome this in future studies by using double labelling techniques to simultaneously identify the cellular source of a particular cytokine and its distribution within the tissue. However the most likely reason why a clear relationship between immune cell numbers and

cytokine levels could not be demonsted was the use of only one tissue section from each tissue segment to represent the rest of the tissue within that segment or biopsy. It may be possible to overcome this by cutting through the whole tissue segment or biopsy and analysing a representitive sample of tissue i.e. repeatedly discarding 10 sections and analysing the next lot of tissue sections throughout the tissue segment or biopsy. However, this would be very labour intensive and still may not be an accurate representation of the whole tissue. Alternatively it may be possible to extract the immune cells from the wound tissue and quantify them using flow cytometry. However, this would involve loosing the rest of the tissue and any other immunohistological information that could have been gained from it.

Investigation of oxygenation within tissue explant culture system

The reason for choosing oxygen to study the effect of external agents on chronic wound tissue was to try and further understand the changes that might occur within the tissue by the simple action of removing it from the wound environment. Tissue within chronic wounds is likely to be in a hypoxic environment and therefore by simply taking it out of this environment and into normal culture conditions, it would not be representative of the chronic wound environment. The intension was then to fully characterise this system by investigating other wound parameters such as pH and temperature. If this tissue explant system was to be a good representation of the chronic wound then the culture conditions would have to mirror as close as possible those in the true chronic wound environment.

Overall, no effect of differing concentrations of oxygen was seen on the levels of TGF-β or IL-8 detected within the explant culture tissue. A reduction in TGFβ levels was seen over time but this was related to the levels detected at 2 hours. Data on

wound tissue cultured in 20% oxygen and air suggested that the process of culturing within gas chambers in artificial gas mixtures did not in itself have an effect on this tissue. However only 1 of these control experiments was carried out for TGF-β and only 2 for IL-8 due to a lack of tissue.

Although no effect of oxygen was detected here, the number of samples were small. From the power calculations based on the earlier investigation of variability within the system, the sensitivity of this system to detect changes in IL-8 or TGF-β in response to an external stimulus was low (12 biopsies would only detect 32.5% change in TGF-β and 11 biopsies would only detect a 30% change in IL-8 levels). Future studies would have to ensure higher sample numbers or use an analyte with less variability in its expression. However, it is difficult to predict what level of oxygenation would be likely to activate cellular constituents within wound tissue as the PO_2 of both normal and wounded tissue can vary tremendously. Normally the tissues of an individual breathing atmospheric air at sea level can vary from 30 to 60 mmHg, depending on the degree of vascularisation. Likewise the pO_2 of the dead space in a soft tissue wound can vary from 20mmHg (≈3%) to near-anoxia (30). Culture of macrophages in 2% and 0% oxygen has previously been shown to stimulate the release of an angiogenic factor (33). The current study failed to show an effect of oxygen at similar hypoxic conditions (0%) but this may have been because a true effect was masked by the inherent variability within this culture system.

Evaluation and future recommendations for the tissue explant culture system

With the high intra and inter-biopsy variation, together with the limit on the number of biopsies and segments obtained from each biopsy, the value of this model in

screening out potential therapuetic agents is low. In this study, no effect of oxygen in either low or high concentrations was detected in relation to the levels of IL-8 and TGFβ detected in wound tissue. In addition, there is too much variation within this biological system as it currently stands to be a valid model for studying the expression of various analytes in relation to external stimuli.

The high level of inherent variability within this biological system may be a reflection of the heterogeneity of chronic venous leg ulcer wounds in general. Clinical observation has indicated that healing of venous leg ulcers often does not follow a uniform course (personal communication by Professor Harding). Clear improvements can be occurring in one region, while elsewhere in the same lesion intact epidermis is breaking down. Support for this observation was provided by an earlier study in which the investigator participated. Wound fluid samples were taken from multiple sites within the same wound and levels of analytes within it related to local changes in the healing profile of the corresponding region. This indeed demonstrated levels of MMP-2 and 9 to be differentially expressed at different sites within the same wound which was related to the severity of the wound at that site (342).

The results of the current study suggest that heterogeneity might not just exist at a macroscopic level but based on the levels of intra-biopsy variation, heterogeneity may also exist at a cellular level. If this is the case then it is possible to suggest that chronic wounds may contain microscopic areas of healing tissue which can either activate neighbouring cells to proceed in the same direction or be overwhelmed by the inhibitory conditions of the surrounding tissue. In this situation, ulcer healing would only progress when microscopic areas of healing join to form larger foci of healing tissue, which if the conditions are favourable for healing, could recruit more

neighbouring tissue in a wave of healing activity. It would be the overall balance of the amount of tissue proggressing towards healing and the amount of tissue breakdown that would determine the overall healing result.

In view of the heterogeneity of chronic venous leg ulcer tissue, it is possible that the current study was over ambitious in attempting to use this tissue to develop an explant culture system for the study of chronic wounding. The investigator believes that in future work, the use of more uniform tissue such as human acute wound tissue (e.g. pilonidal excision tissue) or even animal tissue where larger biopsy numbers can be obtained, may allow better characterisation of cellular behaviour within this system. This approach would enable a better evaluation of the number of biopsies required to demonstrate a biological effect and a better understanding of how cells respond to changing physical parameters such as oxygen pH and temperature within this system. Armed with this baseline knowledge, the investigator would understand more clearly the size of an expected response and therefore the number of biopsies required for its demonstration given the variability present within chronic wound tissue.

Upregulation of $\alpha_5\beta_1$ expression on chronic wound epidermis after stimulation with LPS

The observation that $\alpha_5\beta_1$ was expressed on basal keratinocytes in contact with intact basement membrane within chronic wound epidermis located away from the wound edge, indicated that expression of this integrin was not exclusively dependent on ligation to its ECM ligand fibronectin. One possibility for this aberrant expression given the inflammatory nature of tissue at the margins of chronic venous leg ulcers, was that this was the result of cytokine or growth factor activity. Previous studies in

keratinocyte cultures had shown a direct effect of TGFβ in upregulating expression of $\alpha_5\beta_1$ (167;312). The fact that basal keratinocytes in chronic wound epidermis were expressing $\alpha_5\beta_1$ indicated that they were capable of upregulating its expression in response to a stimulus. This raised the question of whether this stimulus was absent at the migrating front of epidermis where basal keratinocyte expression of this integrin was often very weak.

Although only two biopsies were used, a clear effect of an inflammatory stimulus on expression of $\alpha_5\beta_1$ by chronic wound epidermis within the tissue explant culture system was demonstrated. This is the first study therefore to demonstrate upregulation of $\alpha_5\beta_1$ expression by the action of biochemical mediators in human tissue. These were preliminary experiments, and unfortunately an assay for TGFβ was not available in the laboratory at that time. However, the effect of LPS in inciting an inflammatory stimulus in this tissue was demonstrated by increased levels of IL-1β and TNFα measured in the culture supernatant.

It is difficult to claim that this was a true result as it was based on only two biopsies. In addition, the variability subsequently shown to exist within this tissue when placed in the explant culture system indicates that a larger number of biopsies would have to be studied before any significance could be attributed to this observation. One of the aims of this study was to characterise the tissue explant system further so that a better understanding could be gained of the variables influencing any observations made in this tissue. It was unfortunate, that having gained a better understanding of the variability within the system, time was not available to repeat these initial experiments and carry them further. However the investigator believes that an important observation was made with regard to the presence of weak $\alpha_5\beta_1$ expression

on keratinocytes in contact with chronic wound matrix and the ability of these same keratinocytes to upregulate their expression in response to an inflammatory stimulus. It suggests that these positive stimuli are missing in chronic venous leg ulcer tissue and that future work should aim to elucidate their identity. This would hold the prospect of replacing the missing signals in this tissue, which may hold the key to enhancing the delayed re-epithelialisation characteristic of venous leg ulcer wounds.

Despite the evidence that TGFβ can upregulate $\alpha_5\beta_1$ expression directly, it would be interesting to know if there are other potential mediators of this effect present in wound fluid. Moreover, the possibility that chronic wound fluid either lacks the positive signals required for migration or holds inhibitory signals to this process needs to be investigated. Some simple experiments using this explant culture system could yield valuable information about the nature of the signals supplied by chronic wound fluid to the epidermis. These would involve doing a series of experiments where chronic wound fluid was added to acute wound tissue and acute wound fluid was added to chronic wound tissue within the explant system. Initially the effect of each type of fluid on each type of tissue could be assessed immunohistologically for changes in expression of epidermal adhesion molecules. The application of molecular biology could then further expand this line of investigation to evaluate the effects on intracellular signalling pathways and processes involved in cytoskeletal organisation essential for the co-ordinated process of epithelial migration. More specifically TGF-β and any other biochemical mediators known to affect adhesion molecule expression (e.g. PDGF), could be added to the culture system, allowing their effects to be monitored in explant tissue, which itself represents a good approximation of the *in vivo* tissue organisation within chronic venous leg ulcers.

Concluding Remarks

The application of molecular biology to the study of adhesive interactions is fast providing a better understanding of the molecules involved and the intracellular signalling pathways used by them to co-ordinate complex biological processes such as epidermal wound repair. However, difficulty in obtaining human tissue is a barrier to extending this understanding to the actual interactive processes occurring *in vivo* within human wounds. This study has demonstrated two approaches that could facilitate easier access to the information held within human tissue. The pilonidal sinus excision wound provides a readily available source of acute wound tissue (at the University of Wales College of Medicine), which can be studied over a complete healing time course while representing epidermal wound repair over a granulating wound bed. The chronic venous leg ulcer provides a readily available source of chronic wound tissue, which can be studied over time. This study has shown the possibility of taking this further by creating an *in vitro* model of chronic wound tissue by development of the tissue explant culture system.

To date there is no good animal model of the overall process of chronic wounding. Therefore the ability to study cellular interactions within the three dimensional architecture of their original tissue surroundings provides a valuable bridge between animal and human *in vivo* studies. The tissue explant culture system is the closest approximation to the human *in vivo* setting that is currently available and its further development could provide a more accurate model in which to study the complex process of human chronic wound healing.

A wealth of knowledge is now available on the adhesive interactions occurring during epidermal wound repair. However, we are still a long way from understanding

the specific signals that direct these interactions, in addition to the level of cross-regulation and co-operative intracellular signalling between the individual adhesive molecules that is important in co-ordinating such an immensely complex process. The last 20 years has seen an explosion of interest in this thoroughly fascinating area of human biology. Expansion of the knowledge already gained in the next 20 years holds an exciting prospect for the treatment of human wounds. In particular understanding the adhesive interaction of keratinocytes with the matrix of the wound could literally pave the way to the epidermal repair, which is evidently part of the cutaneous pathogenesis of chronic venous leg ulcers.

7.0 APPENDICES

Appendix I: Record of Biopsies

Tables I.I-I.5 below hold a record of the dates on which each biopsy referred to throughout previous sections were taken. Each date refers to a specific wound and where tissue was obtained from 2 wounds on the same day, the wounds are referred too as (a) and (b).

Table I.I

Wound Edge Tissue	IL-1	MMP-2	MMP-9	TGFβ	VEGF
Biopsy 1	19/05/98	24/06/98	24/06/98	23/09/98	25/05/99
Biopsy 2	20/05/98	10/06/98	10/06/98	14/10/98	02/06/99
Biopsy 3	03/06/98	03/06/98	03/06/98	27/10/98	08/06/99 (a)
Biopsy 4	10/06/98	02/06/98	02/06/98	11/01/98	08/06/99 (b)

Table I.II

Wound Bed Tissue	IL-1	MMP-2	MMP-9	TGFβ	VEGF
Biopsy 1	19/05/98	19/05/98	19/05/98	23/09/98	25/05/99
Biopsy 2	20/05/98	20/05/98	20/05/98	14/10/98	02/06/99
Biopsy 3	03/06/98	03/06/98	03/06/98	27/10/98	08/06/99 (a)
Biopsy 4	10/06/98	10/06/98	10/06/98	11/01/98	08/06/99 (b)

Table I.III

Wound Edge Tissue	IL-8	Wound Bed Tissue	IL-8
Biopsy 1	19/5/98	Biopsy 1 & 5	19/5/98 & 23/09/98
Biopsy 2	20/5/98	Biopsy 2 & 6	20/5/98 & 14/10/98
Biopsy 3	03/6/98	Biopsy 3 & 7	03/6/98 & 27/10/98
Biopsy 4	10/6/98	Biopsy 4 & 8	10/6/98 & 11/01/99
Biopsy 5	02/6/98		

Biopsy tissue utilised to investigate effect of changing tissue oxygenation

Table I.IV: IL-8

Biopsy No.	Wound Biopsy Date	Biopsy No.	Wound Biopsy Date
Biopsy 1	01/9/99	Biopsy 4	17/8/99
Biopsy 2	07/09/99	Biopsy 5	08/09/99
Biopsy 3	10/8/99	Biopsy 6	15/09/99 (a)

Table I.V: TGFβ

Biopsy No.	Wound Biopsy Date	Biopsy No.	Wound Biopsy Date
Biopsy 1	17/08/99	Biopsy 5	15/09/99 (a)
Biopsy 2	01/09/99	Biopsy 6	15/09/99 (b)
Biopsy 3	07/09/99	Biopsy 7	04/08/99
Biopsy 4	08/09/99	Biopsy 8	21/09/99

Pilonidal Sinus Excision Tissue

Patient 01

Age: 24

Sex: M

Medication: Nil

Significant PMH: Nil

Previous Surgery: Nil

Healed: Yes at 70 days

Patient 02

Age: 22

Sex: M

Medication: Nil

Significant PMH: Nil

Previous Surgery: Nil

Healed: Yes at 49 days

Patient 03

Age: 21 **Sex:** F

Medication: Nil **Significant PMH:** Nil

Previous Surgery: Yes Incision/Drainage of abscess 1 year previously

Healed: Yes at 56 days

Patient 04

Age: 18 **Sex:** M

Medication: Nil **Significant PMH:** Nil

Previous Surgery: Yes Pilonidal excision 10 months previously

Healed: Yes at 98 days

Appendix II: Reagent list for quantitation of MMPs by Zymography

Gelatin solution

20/mg/ml Porcine type A gelatin (Sigma G2625) in ddH2O (40mg + 2ml dd-water). Heat for 15 minutes at 70 degrees and mix well.

1.5M TRIS pH 8.8

181.65 g/L Tris-base in dd Water adjust to pH 8.8 w 1MHCl

1 **1.0M TRIS pH 6.8**
121.1 g/L Tris-base in dd Water adjust to pH 8.8 w 1MHCl

2 **8% resolving gel (10ml – sufficient for 2 gels in Biorad Protean II system)**

Sterile water	3.6ml
30% acrylamide*	2.7 ml
1.5M TRIS pH 8.8*	2.5 ml
10% SDS*	100 ul
10% ammonium persulphate APS*	100 ul
Gelatin solution	1.0 ml
TEMED (Biorad)	6 ul

APS and Temed chemically polymerise acrylamide – optimum temp 23-25°C. Gloves on with acrylamide neurotoxic

3 5% stacking gel (5ml – sufficient for 3 gels on Biorad Protean II system)

Sterile water	3.4 ml
30% acrylamide*	830 ul
1.5M TRIS pH 6.8*	630 ul
10% SDS*	50ul
10% ammonium persulphate APS*	50ul
TEMED (BIOrad)	5ul

4 Zymography sample loading buffer (non-reducing (SDS) buffer)

ddWater	4.4 ml
0.5M TRIS-HCL pH 6.8	1.0 ml
Glycerol	0.8 ml
10% (w/v) SDS	1.6 ml
0.05% (w/v) Bromophenol Blue	0.2 ml

Zymography Running (Electrode) Buffer (5x) 2 litres

TRIS base (Sigma T1503)	30.2 g
Glycine (Sigma G7126)	188 g
SDS (powder)	10 g

(pH should be 8.3 but is OK from 8.2 – 8.4. Dilute 1:4 for use with dd water).

5 Triton Exchange buffer

Triton	2.5 ml
ddH20	100 ml

2 gels require 400 mls

6 Incubation buffer (1x) usually made from (10x)

TRIS-HCL	**6.06 g**	
CaCL2	1.47 g	Made up to 1 litre with dH20
NaCl	2.92 g	Adjust to pH 7.6 with 1M HCL
Brij-35 (Sigma P-1254)	0.5 g	
10x incubation buffer.		
TRIS-HCL	30.3 g	
CaCl2	7.35g	
NaCl	14.6 g	
ddH2O	up to 500 ml	

200 ml 1x Incubation buffer (from 10x concentrate)

Incubation buffer (x10)	20 ml	
Water	130 ml	Adjust to pH 7.6 with 1M HCl

Brij-35 solubilised at 65 degrees in 50 ml of water.

7 Coomassie Blue Stock Stain:

Methanol	250 ml
Water	250 ml
Coomassie blue (Sigma BO149)	1.25 g

Coomassie Blue Stain

Coomassie Blue Stock Stain	25 ml
Methanol	44 ml
Glacial Acetic Acid	12 ml
Water	44 ml

Destain

Methanol	25 ml
Glacial	37.5 ml
Water (dd)	437.5 ml

Equipment

Biorad Mini Protean II System
Standard Power pack

8.0 REFERENCES

Reference List

(1) Clark RAF. Wound Repair: Overview and General Considerations. In: Clark RAF, editor. Plennum Press, 1996: 3-35.

(2) Mitchell C, Gilgenkrantz H. Transcriptional profiling of liver regeneration: new approaches to an old trick! J Hepatol 2003; 38(6):847-849.

(3) Martin P. Wound healing--aiming for perfect skin regeneration. Science 1997; 276(5309):75-81.

(4) Mehendale F, Martin P. The cellular and molecular events of wound healing. In: Falanga V, editor. Cutaneous Wound Healing. Martin Dunitz, 2001: 15-37.

(5) Schaffer M, Barbul A. Lymphocyte function in wound healing and following injury. Br J Surg 1998; 85(4):444-460.

(6) Hunt TK, Ehrlich HP, Garcia JA, Dunphy JE. Effect of vitamin A on reversing the inhibitory effect of cortisone on healing of open wounds in animals and man. Ann Surg 1969; 170(4):633-641.

(7) Karukonda SR, Flynn TC, Boh EE, McBurney EI, Russo GG, Millikan LE. The effects of drugs on wound healing--part II. Specific classes of drugs and their effect on healing wounds. Int J Dermatol 2000; 39(5):321-333.

(8) Karukonda SR, Flynn TC, Boh EE, McBurney EI, Russo GG, Millikan LE. The effects of drugs on wound healing: part 1. Int J Dermatol 2000; 39(4):250-257.

(9) Davis MH, Dunkley P, Harden RM, Harding K, Laidlaw JM, Morris AM et al. The Healing Process. The Wound Programme. Centre for Medical Education, University of Dundee, 1992: 89-108.

(10) Cunnion KM, Wagner E, Frank MM. Complement & Kinin. In: Parslow TG, Stites DP, Terr AI, Imboden JB, editors. Medical Immunology. McGraw-Hill Medical Publishing Division, 2001: 175-188.

(11) Terr AI. Inflammation. In: Parslow TG, Stites DP, Terr AI, Imboden JB, editors. Medical Immunology. McGraw-Hill Medical Publishing Division, 2001: 189-203.

(12) Singer AJ, Clark RA. Cutaneous wound healing. N Engl J Med 1999; 341(10):738-746.

(13) Engelhardt E, Toksoy A, Goebeler M, Debus S, Brocker EB, Gillitzer R. Chemokines IL-8, GROalpha, MCP-1, IP-10, and Mig are sequentially and differentially expressed during phase-specific infiltration of leukocyte subsets in human wound healing. Am J Pathol 1998; 153(6):1849-1860.

(14) Barbul A, Regan MC. Immune involvement in wound healing. Otolaryngol Clin North Am 1995; 28(5):955-968.

(15) Brown EJ. Phagocytosis. Bioessays 1995; 17(2):109-117.

(16) Leibovich SJ, Ross R. The role of the macrophage in wound repair. A study with hydrocortisone and antimacrophage serum. Am J Pathol 1975; 78(1):71-100.

(17) Rappolee DA, Mark D, Banda MJ, Werb Z. Wound macrophages express TGF-alpha and other growth factors in vivo: analysis by mRNA phenotyping. Science 1988; 241(4866):708-712.

(18) Rumalla VK, Borah GL. Cytokines, growth factors, and plastic surgery. Plast Reconstr Surg 2001; 108(3):719-733.

(19) Eckes B, Zigrino P, Kessler D, Holtkotter O, Shephard P, Mauch C et al. Fibroblast-matrix interactions in wound healing and fibrosis. Matrix Biol 2000; 19(4):325-332.

(20) Ross MH, Romrell LJ, Kaye GI. Connective Tissue. In: Ross MH, Romrell LJ, Kaye GI, editors. Histology:A Text and Atlas. Williams and Wilkins, 1995: 94-125.

(21) Greiling D, Clark RA. Fibronectin provides a conduit for fibroblast transmigration from collagenous stroma into fibrin clot provisional matrix. J Cell Sci 1997; 110 (Pt 7):861-870.

(22) Klinger MH. Platelets and inflammation. Anat Embryol (Berl) 1997; 196(1):1-11.

(23) Koopmann CF, Jr. Cutaneous wound healing. An overview. Otolaryngol Clin North Am 1995; 28(5):835-845.

(24) Robson M, Smith PD. Topical Use of Growth Factors to Enhance Healing. In: Falanga V, editor. Cutaneous Wound Healing. Martin Dunitz Ltd, 2001: 379-398.

(25) Fiddes JC, Hebda PA, Hayward P, Robson MC, Abraham JA, Klingbeil CK. Preclinical wound-healing studies with recombinant human basic fibroblast growth factor. Ann N Y Acad Sci 1991; 638:316-328.

(26) Steed DL. Clinical evaluation of recombinant human platelet-derived growth factor for the treatment of lower extremity diabetic ulcers. Diabetic Ulcer Study Group. J Vasc Surg 1995; 21(1):71-78.

(27) Grinnell F. Fibroblasts, myofibroblasts, and wound contraction. J Cell Biol 1994; 124(4):401-404.

(28) Lorena D, Uchio K, Costa AM, Desmouliere A. Normal scarring: importance of myofibroblasts. Wound Repair Regen 2002; 10(2):86-92.

(29) Compton CC, Gill JM, Bradford DA, Regauer S, Gallico GG, O'Connor NE. Skin regenerated from cultured epithelial autografts on full-thickness burn wounds from 6 days to 5 years after grafting. A light, electron microscopic and immunohistochemical study. Lab Invest 1989; 60(5):600-612.

(30) McNicol A, Israels SJ. Platelet dense granules: structure, function and implications for haemostasis. Thromb Res 1999; 95(1):1-18.

(31) Clark RA. Fibronectin matrix deposition and fibronectin receptor expression in healing and normal skin. J Invest Dermatol 1990; 94(6 Suppl):128S-134S.

(32) Broze GJ, Jr. Tissue factor pathway inhibitor and the revised theory of coagulation. Annu Rev Med 1995; 46:103-112.

(33) Furie B, Furie BC. Molecular and cellular biology of blood coagulation. N Engl J Med 1992; 326(12):800-806.

(34) Rang HP, Dale MM, Ritter JM. Haemostasis and Thrombosis. In: Rang HP, Dale MM, Ritter JM, editors. Pharmacology. Churchill Livingstone, 1999: 310-326.

(35) Salzman EW. Low-molecular-weight heparin and other new antithrombotic drugs. N Engl J Med 1992; 326(15):1017-1019.

(36) Boyce DE, Jones WD, Ruge F, Harding KG, Moore K. The role of lymphocytes in human dermal wound healing. Br J Dermatol 2000; 143(1):59-65.

(37) Trautmann A, Toksoy A, Engelhardt E, Brocker EB, Gillitzer R. Mast cell involvement in normal human skin wound healing: expression of monocyte chemoattractant protein-1 is correlated with recruitment of mast cells which synthesize interleukin-4 in vivo. J Pathol 2000; 190(1):100-106.

(38) Rutkow IM. Surgery: An Illustrated History. Mosby-Year Book Inc, 1993.

(39) Ansel JC, Armstrong CA, Song I, Quinlan KL, Olerud JE, Caughman SW et al. Interactions of the skin and nervous system. J Investig Dermatol Symp Proc 1997; 2(1):23-26.

(40) Schaffer M, Beiter T, Becker HD, Hunt TK. Neuropeptides: mediators of inflammation and tissue repair? Arch Surg 1998; 133(10):1107-1116.

(41) Lewis JS, Lee JA, Underwood JC, Harris AL, Lewis CE. Macrophage responses to hypoxia: relevance to disease mechanisms. J Leukoc Biol 1999; 66(6):889-900.

(42) Vaday GG, Lider O. Extracellular matrix moieties, cytokines, and enzymes: dynamic effects on immune cell behavior and inflammation. J Leukoc Biol 2000; 67(2):149-159.

(43) Gillitzer R, Goebeler M. Chemokines in cutaneous wound healing. J Leukoc Biol 2001; 69(4):513-521.

(44) Springer TA. Traffic signals on endothelium for lymphocyte recirculation and leukocyte emigration. Annu Rev Physiol 1995; 57:827-872.

(45) Butcher EC. Leukocyte-endothelial cell recognition: three (or more) steps to specificity and diversity. Cell 1991; 67(6):1033-1036.

(46) Muller WA, Randolph GJ. Migration of leukocytes across endothelium and beyond: molecules involved in the transmigration and fate of monocytes. J Leukoc Biol 1999; 66(5):698-704.

(47) Feng D, Nagy JA, Pyne K, Dvorak HF, Dvorak AM. Neutrophils emigrate from venules by a transendothelial cell pathway in response to FMLP. J Exp Med 1998; 187(6):903-915.

(48) Hubner G, Brauchle M, Smola H, Madlener M, Fassler R, Werner S. Differential regulation of pro-inflammatory cytokines during wound healing in normal and glucocorticoid-treated mice. Cytokine 1996; 8(7):548-556.

(49) Simpson DM, Ross R. Effects of heterologous antineutrophil serum in guinea pigs. Hematologic and ultrastructural observations. Am J Pathol 1971; 65(1):79-102.

(50) Simpson DM, Ross R. The neutrophilic leukocyte in wound repair a study with antineutrophil serum. J Clin Invest 1972; 51(8):2009-2023.

(51) Parslow TG, Bainton DF. Innate Immunity. In: Parslow TG, Stites DP, Terr AI, Imboden JB, editors. Medical Immunology. McGraw-Hill Medical Publishing Division, 2001: 19-39.

(52) Auger MJ, Ross JA. The Biology of the Macrophage. In: Lewis CE, McGee JO, editors. The Macrophage. Oxford, U.K.: Oxford University Press, 1993.

(53) Riches DWH. Macrophage Involvement in Wound Repair, Remodelling and Fibrosis. In: Clark RAF, editor. Plennum Press, 1996.

(54) Goud TJ, Van Furth R. Proliferative characteristics of monoblasts grown in vitro. J Exp Med 1975; 142(5):1200-1217.

(55) Van Furth R, Diesselhoff-den Dulk MC, Mattie H. Quantitative study on the production and kinetics of mononuclear phagocytes during an acute inflammatory reaction. J Exp Med 1973; 138(6):1314-1330.

(56) de Bakker JM, de Wit AW, Daems WT. The relation between monocytes and resident (tissue) macrophages. Haematol Blood Transfus 1981; 27:79-87.

(57) Haslett C, Henson P. Resolution of Inflammation. In: Clark RAF, editor. The Molecular and Cellular Biolgy of Wound Repair. Plennum Press, 1996: 143-167.

(58) Lasky LA. Selectin-carbohydrate interactions and the initiation of the inflammatory response. Annu Rev Biochem 1995; 64:113-139.

(59) Laszlo DJ, Henson PM, Remigio LK, Weinstein L, Sable C, Noble PW et al. Development of functional diversity in mouse macrophages. Mutual exclusion of two phenotypic states. Am J Pathol 1993; 143(2):587-597.

(60) De Whalley CV, Riches DW. Influence of the cytocidal macrophage phenotype on the degradation of acetylated low density lipoproteins: dual regulation of scavenger receptor activity and of intracellular degradation of endocytosed ligand. Exp Cell Res 1991; 192(2):460-468.

(61) Ding AH, Nathan CF, Stuehr DJ. Release of reactive nitrogen intermediates and reactive oxygen intermediates from mouse peritoneal macrophages. Comparison of activating cytokines and evidence for independent production. J Immunol 1988; 141(7):2407-2412.

(62) Riches DW, Underwood GA. Expression of interferon-beta during the triggering phase of macrophage cytocidal activation. Evidence for an autocrine/paracrine role in the regulation of this state. J Biol Chem 1991; 266(36):24785-24792.

(63) Lin E, Calvano SE, Lowry SF. Inflammatory cytokines and cell response in surgery. Surgery 2000; 127(2):117-126.

(64) Fanning NF, Kell MR, Shorten GD, Kirwan WO, Bouchier-Hayes D, Cotter TG et al. Circulating granulocyte macrophage colony-stimulating factor in plasma of patients with the systemic inflammatory response syndrome delays neutrophil apoptosis through inhibition of spontaneous reactive oxygen species generation. Shock 1999; 11(3):167-174.

(65) Welgus HG, Campbell EJ, Cury JD, Eisen AZ, Senior RM, Wilhelm SM et al. Neutral metalloproteinases produced by human mononuclear phagocytes. Enzyme profile, regulation, and expression during cellular development. J Clin Invest 1990; 86(5):1496-1502.

(66) Campbell EJ, Cury JD, Lazarus CJ, Welgus HG. Monocyte procollagenase and tissue inhibitor of metalloproteinases. Identification, characterization, and regulation of secretion. J Biol Chem 1987; 262(33):15862-15868.

(67) Shapiro SD, Campbell EJ, Welgus HG, Senior RM. Elastin degradation by mononuclear phagocytes. Ann N Y Acad Sci 1991; 624:69-80.

(68) Campbell EJ, Silverman EK, Campbell MA. Elastase and cathepsin G of human monocytes. Quantification of cellular content, release in response to stimuli, and heterogeneity in elastase-mediated proteolytic activity. J Immunol 1989; 143(9):2961-2968.

(69) Sandhaus RA, McCarthy KM, Musson RA, Henson PM. Elastolytic proteinases of the human macrophage. Chest 1983; 83(5 Suppl):60S-62S.

(70) Etherington DJ, Taylor MA, Henderson B. Elevation of cathepsin L levels in the synovial lining of rabbits with antigen-induced arthritis. Br J Exp Pathol 1988; 69(2):281-289.

(71) Huybrechts-Godin G, Hauser P, Vaes G. Macrophage-fibroblast interactions in collagenase production and cartilage degradation. Biochem J 1979; 184(3):643-650.

(72) Unemori EN, Ehsani N, Wang M, Lee S, McGuire J, Amento EP. Interleukin-1 and transforming growth factor-alpha: synergistic stimulation of metalloproteinases, PGE2, and proliferation in human fibroblasts. Exp Cell Res 1994; 210(2):166-171.

(73) Ito A, Goshowaki H, Sato T, Mori Y, Yamashita K, Hayakawa T et al. Human recombinant interleukin-1 alpha-mediated stimulation of procollagenase production and suppression of biosynthesis of tissue inhibitor of metalloproteinases in rabbit uterine cervical fibroblasts. FEBS Lett 1988; 234(2):326-330.

(74) Manthey CL, Allen JB, Ellingsworth LR, Wahl SM. In situ expression of transforming growth factor beta in streptococcal cell wall-induced granulomatous inflammation and hepatic fibrosis. Growth Factors 1990; 4(1):17-26.

(75) Lyons RM, Keski-Oja J, Moses HL. Proteolytic activation of latent transforming growth factor-beta from fibroblast-conditioned medium. J Cell Biol 1988; 106(5):1659-1665.

(76) Falcone DJ, McCaffrey TA, Haimovitz-Friedman A, Garcia M. Transforming growth factor-beta 1 stimulates macrophage urokinase expression and release of matrix-bound basic fibroblast growth factor. J Cell Physiol 1993; 155(3):595-605.

(77) Falcone DJ, McCaffrey TA, Haimovitz-Friedman A, Vergilio JA, Nicholson AC. Macrophage and foam cell release of matrix-bound growth factors. Role of plasminogen activation. J Biol Chem 1993; 268(16):11951-11958.

(78) Wahl SM, Hunt DA, Wakefield LM, McCartney-Francis N, Wahl LM, Roberts AB et al. Transforming growth factor type beta induces monocyte chemotaxis and growth factor production. Proc Natl Acad Sci U S A 1987; 84(16):5788-5792.

(79) Noble PW, Henson PM, Lucas C, Mora-Worms M, Carre PC, Riches DW. Transforming growth factor-beta primes macrophages to express inflammatory gene products in response to particulate stimuli by an autocrine/paracrine mechanism. J Immunol 1993; 151(2):979-989.

(80) Noble PW, Lake FR, Henson PM, Riches DW. Hyaluronate activation of CD44 induces insulin-like growth factor-1 expression by a tumor necrosis factor-alpha-dependent mechanism in murine macrophages. J Clin Invest 1993; 91(6):2368-2377.

(81) Lew DB, Leslie CC, Henson PM, Riches DW. Role of endogenously derived leukotrienes in the regulation of lysosomal enzyme expression in macrophages exposed to beta 1,3-glucan. J Leukoc Biol 1991; 49(3):266-276.

(82) Tsunawaki S, Sporn M, Ding A, Nathan C. Deactivation of macrophages by transforming growth factor-beta. Nature 1988; 334(6179):260-262.

(83) Appling WD, O'Brien WR, Johnston DA, Duvic M. Synergistic enhancement of type I and III collagen production in cultured fibroblasts by transforming growth factor-beta and ascorbate. FEBS Lett 1989; 250(2):541-544.

(84) Overall CM, Wrana JL, Sodek J. Transforming growth factor-beta regulation of collagenase, 72 kDa-progelatinase, TIMP and PAI-1 expression in rat bone cell populations and human fibroblasts. Connect Tissue Res 1989; 20(1-4):289-294.

(85) O'Kane S, Ferguson MW. Transforming growth factor beta s and wound healing. Int J Biochem Cell Biol 1997; 29(1):63-78.

(86) Reuterdahl C, Sundberg C, Rubin K, Funa K, Gerdin B. Tissue localization of beta receptors for platelet-derived growth factor and platelet-derived growth factor B chain during wound repair in humans. J Clin Invest 1993; 91(5):2065-2075.

(87) Blatti SP, Foster DN, Ranganathan G, Moses HL, Getz MJ. Induction of fibronectin gene transcription and mRNA is a primary response to growth-factor stimulation of AKR-2B cells. Proc Natl Acad Sci U S A 1988; 85(4):1119-1123.

(88) Heldin P, Laurent TC, Heldin CH. Effect of growth factors on hyaluronan synthesis in cultured human fibroblasts. Biochem J 1989; 258(3):919-922.

(89) Pierce GF, Mustoe TA, Senior RM, Reed J, Griffin GL, Thomason A et al. In vivo incisional wound healing augmented by platelet-derived growth factor and recombinant c-sis gene homodimeric proteins. J Exp Med 1988; 167(3):974-987.

(90) Pierce GF, Mustoe TA, Lingelbach J, Masakowski VR, Griffin GL, Senior RM et al. Platelet-derived growth factor and transforming growth factor-beta enhance tissue repair activities by unique mechanisms. J Cell Biol 1989; 109(1):429-440.

(91) Vlodavsky I, Folkman J, Sullivan R, Fridman R, Ishai-Michaeli R, Sasse J et al. Endothelial cell-derived basic fibroblast growth factor: synthesis and deposition into subendothelial extracellular matrix. Proc Natl Acad Sci U S A 1987; 84(8):2292-2296.

(92) Tonnesen MG, Feng X, Clark RA. Angiogenesis in wound healing. J Investig Dermatol Symp Proc 2000; 5(1):40-46.

(93) Hom DB. Growth factors in wound healing. Otolaryngol Clin North Am 1995; 28(5):933-953.

(94) Barbul A, Lazarou SA, Efron DT, Wasserkrug HL, Efron G. Arginine enhances wound healing and lymphocyte immune responses in humans. Surgery 1990; 108(2):331-336.

(95) Fishel R, Barbul A, Wasserkrug HL, Penberthy LT, Rettura G, Efron G. Cyclosporine A impairs wound healing in rats. J Surg Res 1983; 34(6):572-575.

(96) Peterson JM, Barbul A, Breslin RJ, Wasserkrug HL, Efron G. Significance of T-lymphocytes in wound healing. Surgery 1987; 102(2):300-305.

(97) Barbul A. Immune aspects of wound repair. Clin Plast Surg 1990; 17(3):433-442.

(98) Agaiby AD, Dyson M. Immuno-inflammatory cell dynamics during cutaneous wound healing. J Anat 1999; 195 (Pt 4):531-542.

(99) Moore K, Ruge F, Harding KG. T lymphocytes and the lack of activated macrophages in wound margin biopsies from chronic leg ulcers. Br J Dermatol 1997; 137(2):188-194.

(100) van Neerven RJ, Ebner C, Yssel H, Kapsenberg ML, Lamb JR. T-cell responses to allergens: epitope-specificity and clinical relevance. Immunol Today 1996; 17(11):526-532.

(101) Abbas AK, Murphy KM, Sher A. Functional diversity of helper T lymphocytes. Nature 1996; 383(6603):787-793.

(102) Seder RA, Paul WE. Acquisition of lymphokine-producing phenotype by CD4+ T cells. Annu Rev Immunol 1994; 12:635-673.

(103) Kemeny DM, Noble A, Holmes BJ, Diaz-Sanchez D. Immune regulation: a new role for the CD8+ T cell. Immunol Today 1994; 15(3):107-110.

(104) Nicholson LB, Kuchroo VK. Manipulation of the Th1/Th2 balance in autoimmune disease. Curr Opin Immunol 1996; 8(6):837-842.

(105) Trinchieri G, Gerosa F. Immunoregulation by interleukin-12. J Leukoc Biol 1996; 59(4):505-511.

(106) Folkman J. Angiogenesis in cancer, vascular, rheumatoid and other disease. Nat Med 1995; 1(1):27-31.

(107) Folkman J. Tumor angiogenesis: therapeutic implications. N Engl J Med 1971; 285(21):1182-1186.

(108) Carmeliet P. Angiogenesis in health and disease. Nat Med 2003; 9(6):653-660.

(109) Yang GP, Lim IJ, Phan TT, Lorenz HP, Longaker MT. From scarless fetal wounds to keloids: molecular studies in wound healing. Wound Repair Regen 2003; 11(6):411-418.

(110) Nguyen M, Arkell J, Jackson CJ. Human endothelial gelatinases and angiogenesis. Int J Biochem Cell Biol 2001; 33(10):960-970.

(111) Carmeliet P. Angiogenesis in health and disease. Nat Med 2003; 9(6):653-660.

(112) Rundhaug JE. Matrix metalloproteinases, angiogenesis, and cancer: commentary re: A. C. Lockhart et al., Reduction of wound angiogenesis in patients treated with BMS-275291, a broad spectrum matrix metalloproteinase inhibitor. Clin. Cancer Res., 9: 00-00, 2003. Clin Cancer Res 2003; 9(2):551-554.

(113) Eliceiri BP, Cheresh DA. Adhesion events in angiogenesis. Curr Opin Cell Biol 2001; 13(5):563-568.

(114) Forsythe JA, Jiang BH, Iyer NV, Agani F, Leung SW, Koos RD et al. Activation of vascular endothelial growth factor gene transcription by hypoxia-inducible factor 1. Mol Cell Biol 1996; 16(9):4604-4613.

(115) Pugh CW, Ratcliffe PJ. Regulation of angiogenesis by hypoxia: role of the HIF system. Nat Med 2003; 9(6):677-684.

(116) Semenza GL, Wang GL. A nuclear factor induced by hypoxia via de novo protein synthesis binds to the human erythropoietin gene enhancer at a site required for transcriptional activation. Mol Cell Biol 1992; 12(12):5447-5454.

(117) Wang GL, Jiang BH, Rue EA, Semenza GL. Hypoxia-inducible factor 1 is a basic-helix-loop-helix-PAS heterodimer regulated by cellular O2 tension. Proc Natl Acad Sci U S A 1995; 92(12):5510-5514.

(118) Liu Y, Cox SR, Morita T, Kourembanas S. Hypoxia regulates vascular endothelial growth factor gene expression in endothelial cells. Identification of a 5' enhancer. Circ Res 1995; 77(3):638-643.

(119) Wenger RH. Cellular adaptation to hypoxia: O2-sensing protein hydroxylases, hypoxia-inducible transcription factors, and O2-regulated gene expression. FASEB J 2002; 16(10):1151-1162.

(120) Brown LF, Yeo KT, Berse B, Yeo TK, Senger DR, Dvorak HF et al. Expression of vascular permeability factor (vascular endothelial growth factor) by epidermal keratinocytes during wound healing. J Exp Med 1992; 176(5):1375-1379.

(121) Lau LF, Lam SC. The CCN family of angiogenic regulators: the integrin connection. Exp Cell Res 1999; 248(1):44-57.

(122) Fassett JT, Nilsen-Hamilton M. Mrp3, a mitogen-regulated protein/proliferin gene expressed in wound healing and in hair follicles. Endocrinology 2001; 142(5):2129-2137.

(123) Dvorak HF. Vascular permeability factor/vascular endothelial growth factor: a critical cytokine in tumor angiogenesis and a potential target for diagnosis and therapy. J Clin Oncol 2002; 20(21):4368-4380.

(124) Clark RA, Tonnesen MG, Gailit J, Cheresh DA. Transient functional expression of alphaVbeta 3 on vascular cells during wound repair. Am J Pathol 1996; 148(5):1407-1421.

(125) Brooks PC, Clark RA, Cheresh DA. Requirement of vascular integrin alpha v beta 3 for angiogenesis. Science 1994; 264(5158):569-571.

(126) Friedlander M, Brooks PC, Shaffer RW, Kincaid CM, Varner JA, Cheresh DA. Definition of two angiogenic pathways by distinct alpha v integrins. Science 1995; 270(5241):1500-1502.

(127) Eliceiri BP, Paul R, Schwartzberg PL, Hood JD, Leng J, Cheresh DA. Selective requirement for Src kinases during VEGF-induced angiogenesis and vascular permeability. Mol Cell 1999; 4(6):915-924.

(128) Kim S, Harris M, Varner JA. Regulation of integrin alpha vbeta 3-mediated endothelial cell migration and angiogenesis by integrin alpha5beta1 and protein kinase A. J Biol Chem 2000; 275(43):33920-33928.

(129) Hynes RO. A reevaluation of integrins as regulators of angiogenesis. Nat Med 2002; 8(9):918-921.

(130) O'Reilly MS, Boehm T, Shing Y, Fukai N, Vasios G, Lane WS et al. Endostatin: an endogenous inhibitor of angiogenesis and tumor growth. Cell 1997; 88(2):277-285.

(131) Petitclerc E, Boutaud A, Prestayko A, Xu J, Sado Y, Ninomiya Y et al. New functions for non-collagenous domains of human collagen type IV. Novel integrin ligands inhibiting angiogenesis and tumor growth in vivo. J Biol Chem 2000; 275(11):8051-8061.

(132) Rehn M, Veikkola T, Kukk-Valdre E, Nakamura H, Ilmonen M, Lombardo C et al. Interaction of endostatin with integrins implicated in angiogenesis. Proc Natl Acad Sci U S A 2001; 98(3):1024-1029.

(133) Pepper MS. Manipulating angiogenesis. From basic science to the bedside. Arterioscler Thromb Vasc Biol 1997; 17(4):605-619.

(134) Ailawadi M, Lee JM, Lee S, Hackett N, Crystal RG, Korst RJ. Adenovirus vector-mediated transfer of the vascular endothelial growth factor cDNA to healing abdominal fascia enhances vascularity and bursting strength in mice with normal and impaired wound healing. Surgery 2002; 131(2):219-227.

(135) Romano DP, Mangoni A, Zambruno G, Spinetti G, Melillo G, Napolitano M et al. Adenovirus-mediated VEGF(165) gene transfer enhances wound healing by promoting angiogenesis in CD1 diabetic mice. Gene Ther 2002; 9(19):1271-1277.

(136) Bosman FT. Integrins: cell adhesives and modulators of cell function. Histochem J 1993; 25(7):469-477.

(137) English D, Garcia JG, Brindley DN. Platelet-released phospholipids link haemostasis and angiogenesis. Cardiovasc Res 2001; 49(3):588-599.

(138) Giancotti FG, Ruoslahti E. Integrin signaling. Science 1999; 285(5430):1028-1032.

(139) Juliano RL. Signal transduction by cell adhesion receptors and the cytoskeleton: functions of integrins, cadherins, selectins, and immunoglobulin-superfamily members. Annu Rev Pharmacol Toxicol 2002; 42:283-323.

(140) Eckes B, Aumailley M, Krieg T. Collagens and the Reestablishment of Dermal Integrity. In: Clark RAF, editor. The Molecular and Cellular Biology of Wound Repair. Plennum Press, 1996: 493-512.

(141) Bosman FT. Integrins: cell adhesives and modulators of cell function. Histochem J 1993; 25(7):469-477.

(142) Hynes RO. Integrins: a family of cell surface receptors. Cell 1987; 48(4):549-554.

(143) Loftus JC, Liddington RC. Cell adhesion in vascular biology. New insights into integrin-ligand interaction. J Clin Invest 1997; 99(10):2302-2306.

(144) Humphries MJ, Newham P. The structure of cell-adhesion molecules. Trends Cell Biol 1998; 8(2):78-83.

(145) Clark EA, Brugge JS. Integrins and signal transduction pathways: the road taken. Science 1995; 268(5208):233-239.

(146) Ryynanen J, Jaakkola S, Engvall E, Peltonen J, Uitto J. Expression of beta 4 integrins in human skin: comparison of epidermal distribution with beta 1-integrin epitopes, and modulation by calcium and vitamin D3 in cultured keratinocytes. J Invest Dermatol 1991; 97(3):562-567.

(147) Bosman FT. Integrins: cell adhesives and modulators of cell function. Histochem J 1993; 25(7):469-477.

(148) Rahilly MA, Fleming S. Differential expression of integrin alpha chains by renal epithelial cells. J Pathol 1992; 167(3):327-334.

(149) Gould VE, Koukoulis GK, Virtanen I. Extracellular matrix proteins and their receptors in the normal, hyperplastic and neoplastic breast. Cell Differ Dev 1990; 32(3):409-416.

(150) Jutila MA. Leukocyte traffic to sites of inflammation. APMIS 1992; 100(3):191-201.

(151) Shimizu Y, Van Seventer GA, Horgan KJ, Shaw S. Regulated expression and binding of three VLA (beta 1) integrin receptors on T cells. Nature 1990; 345(6272):250-253.

(152) Yong K, Khwaja A. Leucocyte cellular adhesion molecules. Blood Rev 1990; 4(4):211-225.

(153) Kurzinger K, Reynolds T, Germain RN, Davignon D, Martz E, Springer TA. A novel lymphocyte function-associated antigen (LFA-1): cellular distribution, quantitative expression, and structure. J Immunol 1981; 127(2):596-602.

(154) Horton M. Vitronectin receptor: tissue specific expression or adaptation to culture? Int J Exp Pathol 1990; 71(5):741-759.

(155) Cooper DR. The Physiology of Wound Healing: An Overview. In: Diane Krasner, editor. Chronic Wound Care: A clinical Source Book For Health Care Professionals. Health Management Publishers, 1995.

(156) Sastry SK, Horwitz AF. Integrin cytoplasmic domains: mediators of cytoskeletal linkages and extra- and intracellular initiated transmembrane signaling. Curr Opin Cell Biol 1993; 5(5):819-831.

(157) Ginsberg MH. Integrins: dynamic regulation of ligand binding. Biochem Soc Trans 1995; 23(3):439-446.

(158) Horwitz AF, Thiery JP. Cell-to-cell contact and extracellular matrix. Curr Opin Cell Biol 1994; 6(5):645-647.

(159) Hynes RO. The impact of molecular biology on models for cell adhesion. Bioessays 1994; 16(9):663-669.

(160) Calderwood DA, Shattil SJ, Ginsberg MH. Integrins and actin filaments: reciprocal regulation of cell adhesion and signaling. J Biol Chem 2000; 275(30):22607-22610.

(161) Sundberg C, Rubin K. Stimulation of beta1 integrins on fibroblasts induces PDGF independent tyrosine phosphorylation of PDGF beta-receptors. J Cell Biol 1996; 132(4):741-752.

(162) Miyamoto S, Teramoto H, Gutkind JS, Yamada KM. Integrins can collaborate with growth factors for phosphorylation of receptor tyrosine kinases and MAP kinase activation: roles of integrin aggregation and occupancy of receptors. J Cell Biol 1996; 135(6 Pt 1):1633-1642.

(163) Hynes RO. Cell adhesion: old and new questions. Trends Cell Biol 1999; 9(12):M33-M37.

(164) Clark RAF. Integrins in Wound Repair. In: Yamada KM, Gailit J, Clark RAF, editors. The Molecular and Cellular Biology of Wound Repair. Plennum Press, 1996: 311-338.

(165) Clark RA, Ashcroft GS, Spencer MJ, Larjava H, Ferguson MW. Re-epithelialization of normal human excisional wounds is associated with a switch from alpha v beta 5 to alpha v beta 6 integrins. Br J Dermatol 1996; 135(1):46-51.

(166) Cavani A, Zambruno G, Marconi A, Manca V, Marchetti M, Giannetti A. Distinctive integrin expression in the newly forming epidermis during wound healing in humans. J Invest Dermatol 1993; 101(4):600-604.

(167) Gailit J, Welch MP, Clark RA. TGF-beta 1 stimulates expression of keratinocyte integrins during re-epithelialization of cutaneous wounds. J Invest Dermatol 1994; 103(2):221-227.

(168) Kirchhofer D, Languino LR, Ruoslahti E, Pierschbacher MD. Alpha 2 beta 1 integrins from different cell types show different binding specificities. J Biol Chem 1990; 265(2):615-618.

(169) Mu D, Cambier S, Fjellbirkeland L, Baron JL, Munger JS, Kawakatsu H et al. The integrin alpha(v)beta8 mediates epithelial homeostasis through MT1-MMP-dependent activation of TGF-beta1. J Cell Biol 2002; 157(3):493-507.

(170) Wang Z, Symons JM, Goldstein SL, McDonald A, Miner JH, Kreidberg JA. (Alpha)3(beta)1 integrin regulates epithelial cytoskeletal organization. J Cell Sci 1999; 112 (Pt 17):2925-2935.

(171) Hodivala-Dilke KM, DiPersio CM, Kreidberg JA, Hynes RO. Novel roles for alpha3beta1 integrin as a regulator of cytoskeletal assembly and as a trans-dominant inhibitor of integrin receptor function in mouse keratinocytes. J Cell Biol 1998; 142(5):1357-1369.

(172) Goldfinger LE, Hopkinson SB, deHart GW, Collawn S, Couchman JR, Jones JC. The alpha3 laminin subunit, alpha6beta4 and alpha3beta1 integrin coordinately regulate wound healing in cultured epithelial cells and in the skin. J Cell Sci 1999; 112 (Pt 16):2615-2629.

(173) Somerville RP, Oblander SA, Apte SS. Matrix metalloproteinases: old dogs with new tricks. Genome Biol 2003; 4(6):216.

(174) Gross J, LAPIERE CM. Collagenolytic activity in amphibian tissues: a tissue culture assay. Proc Natl Acad Sci U S A 1962; 48:1014-1022.

(175) Stamenkovic I. Extracellular matrix remodelling: the role of matrix metalloproteinases. J Pathol 2003; 200(4):448-464.

(176) Bosman FT, Stamenkovic I. Functional structure and composition of the extracellular matrix. J Pathol 2003; 200(4):423-428.

(177) Visse R, Nagase H. Matrix metalloproteinases and tissue inhibitors of metalloproteinases: structure, function, and biochemistry. Circ Res 2003; 92(8):827-839.

(178) Stocker W, Grams F, Baumann U, Reinemer P, Gomis-Ruth FX, McKay DB et al. The metzincins--topological and sequential relations between the astacins, adamalysins, serralysins, and matrixins (collagenases) define a superfamily of zinc-peptidases. Protein Sci 1995; 4(5):823-840.

(179) Park HI, Ni J, Gerkema FE, Liu D, Belozerov VE, Sang QX. Identification and characterization of human endometase (Matrix metalloproteinase-26) from endometrial tumor. J Biol Chem 2000; 275(27):20540-20544.

(180) Wilson CL, Matrisian LM. Matrilysin: an epithelial matrix metalloproteinase with potentially novel functions. Int J Biochem Cell Biol 1996; 28(2):123-136.

(181) Sato H, Takino T, Okada Y, Cao J, Shinagawa A, Yamamoto E et al. A matrix metalloproteinase expressed on the surface of invasive tumour cells. Nature 1994; 370(6484):61-65.

(182) Velasco G, Pendas AM, Fueyo A, Knauper V, Murphy G, Lopez-Otin C. Cloning and characterization of human MMP-23, a new matrix metalloproteinase predominantly expressed in reproductive tissues and lacking conserved domains in other family members. J Biol Chem 1999; 274(8):4570-4576.

(183) Pei D. CA-MMP: a matrix metalloproteinase with a novel cysteine array, but without the classic cysteine switch. FEBS Lett 1999; 457(2):262-270.

(184) Itoh Y, Kajita M, Kinoh H, Mori H, Okada A, Seiki M. Membrane type 4 matrix metalloproteinase (MT4-MMP, MMP-17) is a glycosylphosphatidylinositol-anchored proteinase. J Biol Chem 1999; 274(48):34260-34266.

(185) Stamenkovic I. Matrix metalloproteinases in tumor invasion and metastasis. Semin Cancer Biol 2000; 10(6):415-433.

(186) Overall CM, Lopez-Otin C. Strategies for MMP inhibition in cancer: innovations for the post-trial era. Nat Rev Cancer 2002; 2(9):657-672.

(187) Lijnen HR. Plasmin and matrix metalloproteinases in vascular remodeling. Thromb Haemost 2001; 86(1):324-333.

(188) Baker AH, Edwards DR, Murphy G. Metalloproteinase inhibitors: biological actions and therapeutic opportunities. J Cell Sci 2002; 115(Pt 19):3719-3727.

(189) Oh J, Takahashi R, Kondo S, Mizoguchi A, Adachi E, Sasahara RM et al. The membrane-anchored MMP inhibitor RECK is a key regulator of extracellular matrix integrity and angiogenesis. Cell 2001; 107(6):789-800.

(190) Banyai L, Patthy L. The NTR module: domains of netrins, secreted frizzled related proteins, and type I procollagen C-proteinase enhancer protein are homologous with tissue inhibitors of metalloproteases. Protein Sci 1999; 8(8):1636-1642.

(191) Egeblad M, Werb Z. New functions for the matrix metalloproteinases in cancer progression. Nat Rev Cancer 2002; 2(3):161-174.

(192) Brew K, Dinakarpandian D, Nagase H. Tissue inhibitors of metalloproteinases: evolution, structure and function. Biochim Biophys Acta 2000; 1477(1-2):267-283.

(193) Gomez DE, Alonso DF, Yoshiji H, Thorgeirsson UP. Tissue inhibitors of metalloproteinases: structure, regulation and biological functions. Eur J Cell Biol 1997; 74(2):111-122.

(194) Martel-Pelletier J, McCollum R, Fujimoto N, Obata K, Cloutier JM, Pelletier JP. Excess of metalloproteases over tissue inhibitor of metalloprotease may contribute to cartilage degradation in osteoarthritis and rheumatoid arthritis. Lab Invest 1994; 70(6):807-815.

(195) Keyszer G, Redlich A, Haupl T, Zacher J, Sparmann M, Engethum U et al. Differential expression of cathepsins B and L compared with matrix metalloproteinases and their respective inhibitors in rheumatoid arthritis and osteoarthritis: a parallel investigation by semiquantitative reverse transcriptase-polymerase chain reaction and immunohistochemistry. Arthritis Rheum 1998; 41(8):1378-1387.

(196) Hayashi T, Stetler-Stevenson WG, Fleming MV, Fishback N, Koss MN, Liotta LA et al. Immunohistochemical study of metalloproteinases and their tissue inhibitors in the lungs of patients with diffuse alveolar damage and idiopathic pulmonary fibrosis. Am J Pathol 1996; 149(4):1241-1256.

(197) Reynolds JJ, Meikle MC. The functional balance of metalloproteinases and inhibitors in tissue degradation: relevance to oral pathologies. J R Coll Surg Edinb 1997; 42(3):154-160.

(198) Lovejoy B, Welch AR, Carr S, Luong C, Broka C, Hendricks RT et al. Crystal structures of MMP-1 and -13 reveal the structural basis for selectivity of collagenase inhibitors. Nat Struct Biol 1999; 6(3):217-221.

(199) Yu Q, Stamenkovic I. Cell surface-localized matrix metalloproteinase-9 proteolytically activates TGF-beta and promotes tumor invasion and angiogenesis. Genes Dev 2000; 14(2):163-176.

(200) Suzuki M, Raab G, Moses MA, Fernandez CA, Klagsbrun M. Matrix metalloproteinase-3 releases active heparin-binding EGF-like growth factor by cleavage at a specific juxtamembrane site. J Biol Chem 1997; 272(50):31730-31737.

(201) Noe V, Fingleton B, Jacobs K, Crawford HC, Vermeulen S, Steelant W et al. Release of an invasion promoter E-cadherin fragment by matrilysin and stromelysin-1. J Cell Sci 2001; 114(Pt 1):111-118.

(202) Kajita M, Itoh Y, Chiba T, Mori H, Okada A, Kinoh H et al. Membrane-type 1 matrix metalloproteinase cleaves CD44 and promotes cell migration. J Cell Biol 2001; 153(5):893-904.

(203) McCawley LJ, Matrisian LM. Matrix metalloproteinases: they're not just for matrix anymore! Curr Opin Cell Biol 2001; 13(5):534-540.

(204) Pilcher BK, Dumin JA, Sudbeck BD, Krane SM, Welgus HG, Parks WC. The activity of collagenase-1 is required for keratinocyte migration on a type I collagen matrix. J Cell Biol 1997; 137(6):1445-1457.

(205) Romer J, Bugge TH, Pyke C, Lund LR, Flick MJ, Degen JL et al. Impaired wound healing in mice with a disrupted plasminogen gene. Nat Med 1996; 2(3):287-292.

(206) Lund LR, Romer J, Bugge TH, Nielsen BS, Frandsen TL, Degen JL et al. Functional overlap between two classes of matrix-degrading proteases in wound healing. EMBO J 1999; 18(17):4645-4656.

(207) Naglich JG, Jure-Kunkel M, Gupta E, Fargnoli J, Henderson AJ, Lewin AC et al. Inhibition of angiogenesis and metastasis in two murine models by the matrix metalloproteinase inhibitor, BMS-275291. Cancer Res 2001; 61(23):8480-8485.

(208) Wysocki AB, Staiano-Coico L, Grinnell F. Wound fluid from chronic leg ulcers contains elevated levels of metalloproteinases MMP-2 and MMP-9. J Invest Dermatol 1993; 101(1):64-68.

(209) Bullen EC, Longaker MT, Updike DL, Benton R, Ladin D, Hou Z et al. Tissue inhibitor of metalloproteinases-1 is decreased and activated gelatinases are increased in chronic wounds. J Invest Dermatol 1995; 104(2):236-240.

(210) Vaalamo M, Weckroth M, Puolakkainen P, Kere J, Saarinen P, Lauharanta J et al. Patterns of matrix metalloproteinase and TIMP-1 expression in chronic and normally healing human cutaneous wounds. Br J Dermatol 1996; 135(1):52-59.

(211) Ravanti L, Kahari VM. Matrix metalloproteinases in wound repair (review). Int J Mol Med 2000; 6(4):391-407.

(212) Aimes RT, Quigley JP. Matrix metalloproteinase-2 is an interstitial collagenase. Inhibitor-free enzyme catalyzes the cleavage of collagen fibrils and soluble native type I collagen generating the specific 3/4- and 1/4-length fragments. J Biol Chem 1995; 270(11):5872-5876.

(213) Allan JA, Docherty AJ, Barker PJ, Huskisson NS, Reynolds JJ, Murphy G. Binding of gelatinases A and B to type-I collagen and other matrix components. Biochem J 1995; 309 (Pt 1):299-306.

(214) Salo T, Makela M, Kylmaniemi M, Autio-Harmainen H, Larjava H. Expression of matrix metalloproteinase-2 and -9 during early human wound healing. Lab Invest 1994; 70(2):176-182.

(215) Wang Z, Juttermann R, Soloway PD. TIMP-2 is required for efficient activation of proMMP-2 in vivo. J Biol Chem 2000; 275(34):26411-26415.

(216) Deryugina EI, Ratnikov B, Monosov E, Postnova TI, DiScipio R, Smith JW et al. MT1-MMP initiates activation of pro-MMP-2 and integrin alphavbeta3 promotes maturation of MMP-2 in breast carcinoma cells. Exp Cell Res 2001; 263(2):209-223.

(217) Templeton NS, Stetler-Stevenson WG. Identification of a basal promoter for the human Mr 72,000 type IV collagenase gene and enhanced expression in a highly metastatic cell line. Cancer Res 1991; 51(22):6190-6193.

(218) Nguyen M, Arkell J, Jackson CJ. Active and tissue inhibitor of matrix metalloproteinase-free gelatinase B accumulates within human microvascular endothelial vesicles. J Biol Chem 1998; 273(9):5400-5404.

(219) Stahle-Backdahl M, Parks WC. 92-kd gelatinase is actively expressed by eosinophils and stored by neutrophils in squamous cell carcinoma. Am J Pathol 1993; 142(4):995-1000.

(220) Matrisian LM. The matrix-degrading metalloproteinases. Bioessays 1992; 14(7):455-463.

(221) Wysocki AB, Kusakabe AO, Chang S, Tuan TL. Temporal expression of urokinase plasminogen activator, plasminogen activator inhibitor and gelatinase-B in chronic wound fluid switches from a chronic to acute wound profile with progression to healing. Wound Repair Regen 1999; 7(3):154-165.

(222) Mirastschijski U, Impola U, Jahkola T, Karlsmark T, AGren MS, Saarialho-Kere U. Ectopic localization of matrix metalloproteinase-9 in chronic cutaneous wounds. Hum Pathol 2002; 33(3):355-364.

(223) Mauviel A. Cytokine regulation of metalloproteinase gene expression. J Cell Biochem 1993; 53(4):288-295.

(224) Huhtala P, Tuuttila A, Chow LT, Lohi J, Keski-Oja J, Tryggvason K. Complete structure of the human gene for 92-kDa type IV collagenase. Divergent regulation of expression for the 92- and 72-kilodalton enzyme genes in HT-1080 cells. J Biol Chem 1991; 266(25):16485-16490.

(225) Han YP, Tuan TL, Hughes M, Wu H, Garner WL. Transforming growth factor-beta - and tumor necrosis factor-alpha -mediated induction and proteolytic activation of MMP-9 in human skin. J Biol Chem 2001; 276(25):22341-22350.

(226) Holvoet S, Vincent C, Schmitt D, Serres M. The inhibition of MAPK pathway is correlated with down-regulation of MMP-9 secretion induced by TNF-alpha in human keratinocytes. Exp Cell Res 2003; 290(1):108-119.

(227) Ellerbroek SM, Halbleib JM, Benavidez M, Warmka JK, Wattenberg EV, Stack MS et al. Phosphatidylinositol 3-kinase activity in epidermal growth factor-stimulated matrix metalloproteinase-9 production and cell surface association. Cancer Res 2001; 61(5):1855-1861.

(228) Eberhardt W, Huwiler A, Beck KF, Walpen S, Pfeilschifter J. Amplification of IL-1 beta-induced matrix metalloproteinase-9 expression by superoxide in rat glomerular mesangial cells is mediated by increased activities of NF-kappa B and activating protein-1 and involves activation of the mitogen-activated protein kinase pathways. J Immunol 2000; 165(10):5788-5797.

(229) Opdenakker G, Van den Steen PE, Van Damme J. Gelatinase B: a tuner and amplifier of immune functions. Trends Immunol 2001; 22(10):571-579.

(230) Fiore E, Fusco C, Romero P, Stamenkovic I. Matrix metalloproteinase 9 (MMP-9/gelatinase B) proteolytically cleaves ICAM-1 and participates in tumor cell resistance to natural killer cell-mediated cytotoxicity. Oncogene 2002; 21(34):5213-5223.

(231) Yu Q, Stamenkovic I. Localization of matrix metalloproteinase 9 to the cell surface provides a mechanism for CD44-mediated tumor invasion. Genes Dev 1999; 13(1):35-48.

(232) Olson MW, Toth M, Gervasi DC, Sado Y, Ninomiya Y, Fridman R. High affinity binding of latent matrix metalloproteinase-9 to the alpha2(IV) chain of collagen IV. J Biol Chem 1998; 273(17):10672-10681.

(233) Pepper MS. Role of the matrix metalloproteinase and plasminogen activator-plasmin systems in angiogenesis. Arterioscler Thromb Vasc Biol 2001; 21(7):1104-1117.

(234) Madlener M, Parks WC, Werner S. Matrix metalloproteinases (MMPs) and their physiological inhibitors (TIMPs) are differentially expressed during excisional skin wound repair. Exp Cell Res 1998; 242(1):201-210.

(235) Oikarinen A, Kylmaniemi M, Autio-Harmainen H, Autio P, Salo T. Demonstration of 72-kDa and 92-kDa forms of type IV collagenase in human skin: variable expression in various blistering diseases, induction during re-epithelialization, and decrease by topical glucocorticoids. J Invest Dermatol 1993; 101(2):205-210.

(236) Baker EA, Leaper DJ. Profiles of matrix metalloproteinases and their tissue inhibitors in intraperitoneal drainage fluid: relationship to wound healing. Wound Repair Regen 2003; 11(4):268-274.

(237) Young PK, Grinnell F. Metalloproteinase activation cascade after burn injury: a longitudinal analysis of the human wound environment. J Invest Dermatol 1994; 103(5):660-664.

(238) Matsubara M, Girard MT, Kublin CL, Cintron C, Fini ME. Differential roles for two gelatinolytic enzymes of the matrix metalloproteinase family in the remodelling cornea. Dev Biol 1991; 147(2):425-439.

(239) Yager DR, Zhang LY, Liang HX, Diegelmann RF, Cohen IK. Wound fluids from human pressure ulcers contain elevated matrix metalloproteinase levels and activity compared to surgical wound fluids. J Invest Dermatol 1996; 107(5):743-748.

(240) Trengove NJ, Stacey MC, MacAuley S, Bennett N, Gibson J, Burslem F et al. Analysis of the acute and chronic wound environments: the role of proteases and their inhibitors. Wound Repair Regen 1999; 7(6):442-452.

(241) Pai MP, Hunt TK. Effect of varying oxygen tensions on healing of open wounds. Surg Gynecol Obstet 1972; 135(5):756-758.

(242) Moon RE. Use of hyperbaric oxygen in the management of selected wounds. Adv Wound Care 1998; 11(7):332-334.

(243) Hunt TK, Pai MP. The effect of varying ambient oxygen tensions on wound metabolism and collagen synthesis. Surg Gynecol Obstet 1972; 135(4):561-567.

(244) Tibbles PM, Edelsberg JS. Hyperbaric-oxygen therapy. N Engl J Med 1996; 334(25):1642-1648.

(245) Hammarlund C, Sundberg T. Hyperbaric oxygen reduced size of chronic leg ulcers: a randomized double-blind study. Plast Reconstr Surg 1994; 93(4):829-833.

(246) Steed DL. Surgical Management of Difficult to heal Wounds: A Vascular Approach. In: Falanga V, editor. Cutaneous Wound Healing. Martin Dunitz, 2001: 369-378.

(247) Doctor N, Pandya S, Supe A. Hyperbaric oxygen therapy in diabetic foot. J Postgrad Med 1992; 38(3):112-4, 111.

(248) Leek RD, Landers RJ, Harris AL, Lewis CE. Necrosis correlates with high vascular density and focal macrophage infiltration in invasive carcinoma of the breast. Br J Cancer 1999; 79(5-6):991-995.

(249) Negus RP, Stamp GW, Hadley J, Balkwill FR. Quantitative assessment of the leukocyte infiltrate in ovarian cancer and its relationship to the expression of C-C chemokines. Am J Pathol 1997; 150(5):1723-1734.

(250) Hunt TK, Knighton DR, Thakral KK, Goodson WH, III, Andrews WS. Studies on inflammation and wound healing: angiogenesis and collagen synthesis stimulated in vivo by resident and activated wound macrophages. Surgery 1984; 96(1):48-54.

(251) Hansch A, Stiehl P, Geiler G. [Quantification of macrophages and granulocytes at the joint cartilage-pannus junction in rheumatoid arthritis]. Z Rheumatol 1996; 55(6):401-409.

(252) Esser P, Heimann K, Wiedemann P. Macrophages in proliferative vitreoretinopathy and proliferative diabetic retinopathy: differentiation of subpopulations. Br J Ophthalmol 1993; 77(11):731-733.

(253) Babior BM. The respiratory burst of phagocytes. J Clin Invest 1984; 73(3):599-601.

(254) Leeper-Woodford SK, Mills JW. Phagocytosis and ATP levels in alveolar macrophages during acute hypoxia. Am J Respir Cell Mol Biol 1992; 6(3):326-334.

(255) te Koppele JM, Keller BJ, Caldwell-Kenkel JC, Lemasters JJ, Thurman RG. Effect of hepatotoxic chemicals and hypoxia on hepatic nonparenchymal cells: impairment of phagocytosis by Kupffer cells and disruption of the endothelium in rat livers perfused with colloidal carbon. Toxicol Appl Pharmacol 1991; 110(1):20-30.

(256) Harris GD, Johanson WG, Jr., Pierce AK. Determinants of lung bacterial clearance in mice after acute hypoxia. Am Rev Respir Dis 1977; 116(4):671-677.

(257) Melillo G, Taylor LS, Brooks A, Cox GW, Varesio L. Regulation of inducible nitric oxide synthase expression in IFN-gamma-treated murine macrophages cultured under hypoxic conditions. J Immunol 1996; 157(6):2638-2644.

(258) West MA, Li MH, Seatter SC, Bubrick MP. Pre-exposure to hypoxia or septic stimuli differentially regulates endotoxin release of tumor necrosis factor, interleukin-6, interleukin-1, prostaglandin E2, nitric oxide, and superoxide by macrophages. J Trauma 1994; 37(1):82-89.

(259) Hempel SL, Monick MM, Hunninghake GW. Effect of hypoxia on release of IL-1 and TNF by human alveolar macrophages. Am J Respir Cell Mol Biol 1996; 14(2):170-176.

(260) Larjava H, Salo T, Haapasalmi K, Kramer RH, Heino J. Expression of integrins and basement membrane components by wound keratinocytes. J Clin Invest 1993; 92(3):1425-1435.

(261) Juhasz I, Murphy GF, Yan HC, Herlyn M, Albelda SM. Regulation of extracellular matrix proteins and integrin cell substratum adhesion receptors on epithelium during cutaneous human wound healing in vivo. Am J Pathol 1993; 143(5):1458-1469.

(262) Woodley DT, Bachmann PM, O'Keefe EJ. Laminin inhibits human keratinocyte migration. J Cell Physiol 1988; 136(1):140-146.

(263) Woodley DT, Bachmann PM, O'Keefe EJ. Laminin inhibits human keratinocyte migration. J Cell Physiol 1988; 136(1):140-146.

(264) Cheresh DA. Integrins in thrombosis, wound healing and cancer. Biochem Soc Trans 1991; 19(4):835-838.

(265) Mustoe TA, Cutler NR, Allman RM, Goode PS, Deuel TF, Prause JA et al. A phase II study to evaluate recombinant platelet-derived growth factor-BB in the treatment of stage 3 and 4 pressure ulcers. Arch Surg 1994; 129(2):213-219.

(266) Phillips TJ. Chronic cutaneous ulcers: etiology and epidemiology. J Invest Dermatol 1994; 102(6):38S-41S.

(267) Mogford JE, Mustoe TA. Experimental models of wound healing. In: Vincent Falanga, editor. Cutaneous Wound Healing. Martin Dunitz, 2001: 109-122.

(268) Goodson WH, III, Hunt TK. Wound healing and aging. J Invest Dermatol 1979; 73(1):88-91.

(269) Eaglstein WH. Wound healing and aging. Clin Geriatr Med 1989; 5(1):183-188.

(270) Chick LR, Walton RL, Reus W, Colen L, Sasmor M. Free flaps in the elderly. Plast Reconstr Surg 1992; 90(1):87-94.

(271) Mendoza CB, Jr., Postlethwait RW, Johnson WD. Veterans Administration cooperative study of surgery for duodenal ulcer. II. Incidence of wound disruption following operation. Arch Surg 1970; 101(3):396-398.

(272) Ashcroft GS, Horan MA, Ferguson MW. Aging is associated with reduced deposition of specific extracellular matrix components, an upregulation of angiogenesis, and an altered inflammatory response in a murine incisional wound healing model. J Invest Dermatol 1997; 108(4):430-437.

(273) Swift ME, Burns AL, Gray KL, DiPietro LA. Age-related alterations in the inflammatory response to dermal injury. J Invest Dermatol 2001; 117(5):1027-1035.

(274) Ashcroft GS, Horan MA, Ferguson MW. The effects of ageing on wound healing: immunolocalisation of growth factors and their receptors in a murine incisional model. J Anat 1997; 190 (Pt 3):351-365.

(275) Ashcroft GS, Horan MA, Ferguson MW. Aging alters the inflammatory and endothelial cell adhesion molecule profiles during human cutaneous wound healing. Lab Invest 1998; 78(1):47-58.

(276) Ashcroft GS, Horan MA, Herrick SE, Tarnuzzer RW, Schultz GS, Ferguson MW. Age-related differences in the temporal and spatial regulation of matrix metalloproteinases (MMPs) in normal skin and acute cutaneous wounds of healthy humans. Cell Tissue Res 1997; 290(3):581-591.

(277) Ashcroft GS, Dodsworth J, van Boxtel E, Tarnuzzer RW, Horan MA, Schultz GS et al. Estrogen accelerates cutaneous wound healing associated with an increase in TGF-beta1 levels. Nat Med 1997; 3(11):1209-1215.

(278) Ashcroft GS, Greenwell-Wild T, Horan MA, Wahl SM, Ferguson MW. Topical estrogen accelerates cutaneous wound healing in aged humans associated with an altered inflammatory response. Am J Pathol 1999; 155(4):1137-1146.

(279) Taylor RJ, Taylor AD, Smyth JV. Using an artificial neural network to predict healing times and risk factors for venous leg ulcers. J Wound Care 2002; 11(3):101-105.

(280) Jennings RW, Adzick NS, Longaker MT, Duncan BW, Scheuenstuhl H, Hunt TK. Ontogeny of fetal sheep polymorphonuclear leukocyte phagocytosis. J Pediatr Surg 1991; 26(7):853-855.

(281) Ghahary A, Shen YJ, Scott PG, Gong Y, Tredget EE. Enhanced expression of mRNA for transforming growth factor-beta, type I and type III procollagen in human post-burn hypertrophic scar tissues. J Lab Clin Med 1993; 122(4):465-473.

(282) Peltonen J, Hsiao LL, Jaakkola S, Sollberg S, Aumailley M, Timpl R et al. Activation of collagen gene expression in keloids: co-localization of type I and VI collagen and transforming growth factor-beta 1 mRNA. J Invest Dermatol 1991; 97(2):240-248.

(283) Border WA, Noble NA. Transforming growth factor beta in tissue fibrosis. N Engl J Med 1994; 331(19):1286-1292.

(284) Pierce GF, Tarpley JE, Yanagihara D, Mustoe TA, Fox GM, Thomason A. Platelet-derived growth factor (BB homodimer), transforming growth factor-beta 1, and basic fibroblast growth factor in dermal wound healing. Neovessel and matrix formation and cessation of repair. Am J Pathol 1992; 140(6):1375-1388.

(285) Overall CM, Wrana JL, Sodek J. Independent regulation of collagenase, 72-kDa progelatinase, and metalloendoproteinase inhibitor expression in human fibroblasts by transforming growth factor-beta. J Biol Chem 1989; 264(3):1860-1869.

(286) Shah M, Foreman DM, Ferguson MW. Neutralising antibody to TGF-beta 1,2 reduces cutaneous scarring in adult rodents. J Cell Sci 1994; 107 (Pt 5):1137-1157.

(287) Shah M, Foreman DM, Ferguson MW. Neutralisation of TGF-beta 1 and TGF-beta 2 or exogenous addition of TGF-beta 3 to cutaneous rat wounds reduces scarring. J Cell Sci 1995; 108 (Pt 3):985-1002.

(288) Igarashi A, Okochi H, Bradham DM, Grotendorst GR. Regulation of connective tissue growth factor gene expression in human skin fibroblasts and during wound repair. Mol Biol Cell 1993; 4(6):637-645.

(289) Leask A, Holmes A, Abraham DJ. Connective tissue growth factor: a new and important player in the pathogenesis of fibrosis. Curr Rheumatol Rep 2002; 4(2):136-142.

(290) Igarashi A, Nashiro K, Kikuchi K, Sato S, Ihn H, Fujimoto M et al. Connective tissue growth factor gene expression in tissue sections from localized scleroderma, keloid, and other fibrotic skin disorders. J Invest Dermatol 1996; 106(4):729-733.

(291) Adair HM. Epidermal repair in chronic venous ulcers. Br J Surg 1977; 64(11):800-804.

(292) Latijnhouwers MA, Bergers M, Van Bergen BH, Spruijt KI, Andriessen MP, Schalkwijk J. Tenascin expression during wound healing in human skin. J Pathol 1996; 178(1):30-35.

(293) Hertle MD, Kubler MD, Leigh IM, Watt FM. Aberrant integrin expression during epidermal wound healing and in psoriatic epidermis. J Clin Invest 1992; 89(6):1892-1901.

(294) Cass DL, Bullard KM, Sylvester KG, Yang EY, Sheppard D, Herlyn M et al. Epidermal integrin expression is upregulated rapidly in human fetal wound repair. J Pediatr Surg 1998; 33(2):312-316.

(295) Carter WG, Wayner EA, Bouchard TS, Kaur P. The role of integrins alpha 2 beta 1 and alpha 3 beta 1 in cell-cell and cell-substrate adhesion of human epidermal cells. J Cell Biol 1990; 110(4):1387-1404.

(296) Watt FM. Role of integrins in regulating epidermal adhesion, growth and differentiation. EMBO J 2002; 21(15):3919-3926.

(297) Adams JC, Watt FM. Expression of beta 1, beta 3, beta 4, and beta 5 integrins by human epidermal keratinocytes and non-differentiating keratinocytes. J Cell Biol 1991; 115(3):829-841.

(298) De Luca M, Tamura RN, Kajiji S, Bondanza S, Rossino P, Cancedda R et al. Polarized integrin mediates human keratinocyte adhesion to basal lamina. Proc Natl Acad Sci U S A 1990; 87(17):6888-6892.

(299) Mercurio AM, Rabinovitz I, Shaw LM. The alpha 6 beta 4 integrin and epithelial cell migration. Curr Opin Cell Biol 2001; 13(5):541-545.

(300) Stepp MA. Alpha9 and beta8 integrin expression correlates with the merger of the developing mouse eyelids. Dev Dyn 1999; 214(3):216-228.

(301) Kainulainen T, Hakkinen L, Hamidi S, Larjava K, Kallioinen M, Peltonen J et al. Laminin-5 expression is independent of the injury and the microenvironment during reepithelialization of wounds. J Histochem Cytochem 1998; 46(3):353-360.

(302) Kurpakus MA, Quaranta V, Jones JC. Surface relocation of alpha 6 beta 4 integrins and assembly of hemidesmosomes in an in vitro model of wound healing. J Cell Biol 1991; 115(6):1737-1750.

(303) Lundqvist K, Schmidtchen A. Immunohistochemical studies on proteoglycan expression in normal skin and chronic ulcers. Br J Dermatol 2001; 144(2):254-259.

(304) Oksala O, Salo T, Tammi R, Hakkinen L, Jalkanen M, Inki P et al. Expression of proteoglycans and hyaluronan during wound healing. J Histochem Cytochem 1995; 43(2):125-135.

(305) Elenius K, Vainio S, Laato M, Salmivirta M, Thesleff I, Jalkanen M. Induced expression of syndecan in healing wounds. J Cell Biol 1991; 114(3):585-595.

(306) Tumova S, Woods A, Couchman JR. Heparan sulfate proteoglycans on the cell surface: versatile coordinators of cellular functions. Int J Biochem Cell Biol 2000; 32(3):269-288.

(307) Jaakkola P, Kontusaari S, Kauppi T, Maata A, Jalkanen M. Wound reepithelialization activates a growth factor-responsive enhancer in migrating keratinocytes. FASEB J 1998; 12(11):959-969.

(308) Leppa S, Vleminckx K, Van Roy F, Jalkanen M. Syndecan-1 expression in mammary epithelial tumor cells is E-cadherin-dependent. J Cell Sci 1996; 109 (Pt 6):1393-1403.

(309) Sun D, Mcalmon KR, Davies JA, Bernfield M, Hay ED. Simultaneous loss of expression of syndecan-1 and E-cadherin in the embryonic palate during epithelial-mesenchymal transformation. Int J Dev Biol 1998; 42(5):733-736.

(310) Birchmeier W. E-cadherin as a tumor (invasion) suppressor gene. Bioessays 1995; 17(2):97-99.

(311) Gailit J, Xu J, Bueller H, Clark RA. Platelet-derived growth factor and inflammatory cytokines have differential effects on the expression of integrins alpha 1 beta 1 and alpha 5 beta 1 by human dermal fibroblasts in vitro. J Cell Physiol 1996; 169(2):281-289.

(312) Zambruno G, Marchisio PC, Marconi A, Vaschieri C, Melchiori A, Giannetti A et al. Transforming growth factor-beta 1 modulates beta 1 and beta 5 integrin receptors and induces the de novo expression of the alpha v beta 6 heterodimer in normal human keratinocytes: implications for wound healing. J Cell Biol 1995; 129(3):853-865.

(313) De Luca M, Pellegrini G, Zambruno G, Marchisio PC. Role of integrins in cell adhesion and polarity in normal keratinocytes and human skin pathologies. J Dermatol 1994; 21(11):821-828.

(314) Carroll JM, Romero MR, Watt FM. Suprabasal integrin expression in the epidermis of transgenic mice results in developmental defects and a phenotype resembling psoriasis. Cell 1995; 83(6):957-968.

(315) Ralfkiaer E, Thomsen K, Vejlsgaard GL. Expression of a cell adhesion protein (VLA beta) in normal and diseased skin. Br J Dermatol 1991; 124(6):527-532.

(316) Hertle MD, Jones PH, Groves RW, Hudson DL, Watt FM. Integrin expression by human epidermal keratinocytes can be modulated by interferon-gamma, transforming growth factor-beta, tumor necrosis factor-alpha, and culture on a dermal equivalent. J Invest Dermatol 1995; 104(2):260-265.

(317) Hotchin NA, Watt FM. Transcriptional and post-translational regulation of beta 1 integrin expression during keratinocyte terminal differentiation. J Biol Chem 1992; 267(21):14852-14858.

(318) Hakkinen L, Westermarck J, Johansson N, Aho H, Peltonen J, Heino J et al. Suprabasal expression of epidermal alpha 2 beta 1 and alpha 3 beta 1 integrins in skin treated with topical retinoic acid. Br J Dermatol 1998; 138(1):29-36.

(319) Rousselle P, Lunstrum GP, Keene DR, Burgeson RE. Kalinin: an epithelium-specific basement membrane adhesion molecule that is a component of anchoring filaments. J Cell Biol 1991; 114(3):567-576.

(320) Nguyen BP, Ryan MC, Gil SG, Carter WG. Deposition of laminin 5 in epidermal wounds regulates integrin signaling and adhesion. Curr Opin Cell Biol 2000; 12(5):554-562.

(321) Nguyen BP, Gil SG, Carter WG. Deposition of laminin 5 by keratinocytes regulates integrin adhesion and signaling. J Biol Chem 2000; 275(41):31896-31907.

(322) Baker SE, Hopkinson SB, Fitchmun M, Andreason GL, Frasier F, Plopper G et al. Laminin-5 and hemidesmosomes: role of the alpha 3 chain subunit in hemidesmosome stability and assembly. J Cell Sci 1996; 109 (Pt 10):2509-2520.

(323) Xia Y, Gil SG, Carter WG. Anchorage mediated by integrin alpha6beta4 to laminin 5 (epiligrin) regulates tyrosine phosphorylation of a membrane-associated 80-kD protein. J Cell Biol 1996; 132(4):727-740.

(324) Zhang K, Kramer RH. Laminin 5 deposition promotes keratinocyte motility. Exp Cell Res 1996; 227(2):309-322.

(325) Marinkovich MP, Lunstrum GP, Burgeson RE. The anchoring filament protein kalinin is synthesized and secreted as a high molecular weight precursor. J Biol Chem 1992; 267(25):17900-17906.

(326) Johnson RP, Craig SW. F-actin binding site masked by the intramolecular association of vinculin head and tail domains. Nature 1995; 373(6511):261-264.

(327) Burridge K, Fath K, Kelly T, Nuckolls G, Turner C. Focal adhesions: transmembrane junctions between the extracellular matrix and the cytoskeleton. Annu Rev Cell Biol 1988; 4:487-525.

(328) Burridge K, Chrzanowska-Wodnicka M. Focal adhesions, contractility, and signaling. Annu Rev Cell Dev Biol 1996; 12:463-518.

(329) Larjava H, Peltonen J, Akiyama SK, Yamada SS, Gralnick HR, Uitto J et al. Novel function for beta 1 integrins in keratinocyte cell-cell interactions. J Cell Biol 1990; 110(3):803-815.

(330) Goldfinger LE, Stack MS, Jones JC. Processing of laminin-5 and its functional consequences: role of plasmin and tissue-type plasminogen activator. J Cell Biol 1998; 141(1):255-265.

(331) Haapasalmi K, Zhang K, Tonnesen M, Olerud J, Sheppard D, Salo T et al. Keratinocytes in human wounds express alpha v beta 6 integrin. J Invest Dermatol 1996; 106(1):42-48.

(332) Kim JP, Zhang K, Chen JD, Kramer RH, Woodley DT. Vitronectin-driven human keratinocyte locomotion is mediated by the alpha v beta 5 integrin receptor. J Biol Chem 1994; 269(43):26926-26932.

(333) Hakkinen L, Hildebrand HC, Berndt A, Kosmehl H, Larjava H. Immunolocalization of tenascin-C, alpha9 integrin subunit, and alphavbeta6 integrin during wound healing in human oral mucosa. J Histochem Cytochem 2000; 48(7):985-998.

(334) End P, Panayotou G, Entwistle A, Waterfield MD, Chiquet M. Tenascin: a modulator of cell growth. Eur J Biochem 1992; 209(3):1041-1051.

(335) Yokosaki Y, Monis H, Chen J, Sheppard D. Differential effects of the integrins alpha9beta1, alphavbeta3, and alphavbeta6 on cell proliferative responses to tenascin.

Roles of the beta subunit extracellular and cytoplasmic domains. J Biol Chem 1996; 271(39):24144-24150.

(336) Munger JS, Huang X, Kawakatsu H, Griffiths MJ, Dalton SL, Wu J et al. The integrin alpha v beta 6 binds and activates latent TGF beta 1: a mechanism for regulating pulmonary inflammation and fibrosis. Cell 1999; 96(3):319-328.

(337) Cambier S, Mu DZ, O'Connell D, Boylen K, Travis W, Liu WH et al. A role for the integrin alphavbeta8 in the negative regulation of epithelial cell growth. Cancer Res 2000; 60(24):7084-7093.

(338) Kane CJ, Hebda PA, Mansbridge JN, Hanawalt PC. Direct evidence for spatial and temporal regulation of transforming growth factor beta 1 expression during cutaneous wound healing. J Cell Physiol 1991; 148(1):157-173.

(339) Moses HL, Yang EY, Pietenpol JA. TGF-beta stimulation and inhibition of cell proliferation: new mechanistic insights. Cell 1990; 63(2):245-247.

(340) Borregaard N, Lollike K, Kjeldsen L, Sengelov H, Bastholm L, Nielsen MH et al. Human neutrophil granules and secretory vesicles. Eur J Haematol 1993; 51(4):187-198.

(341) Kjeldsen L, Sengelov H, Lollike K, Nielsen MH, Borregaard N. Isolation and characterization of gelatinase granules from human neutrophils. Blood 1994; 83(6):1640-1649.

(342) Tarlton JF, Bailey AJ, Crawford E, Jones D, Moore K, Harding KD. Prognostic value of markers of collagen remodeling in venous ulcers. Wound Repair Regen 1999; 7(5):347-355.